

Control of hepatic fatty acid oxidation in suckling rats

Karen Jayne New

A thesis submitted for the degree of
Doctor of Philosophy (PhD): August 2000

Department of Paediatric Surgery, The Institute of Child Health
and Great Ormond Street Hospital for Sick Children NHS Trust
University College London

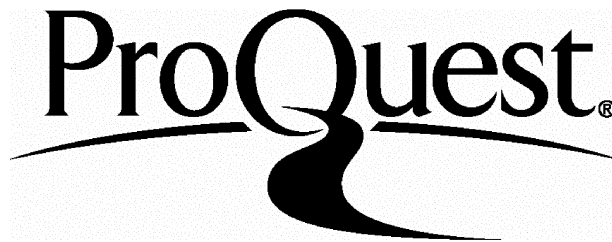
ProQuest Number: U145535

All rights reserved

INFORMATION TO ALL USERS

The quality of this reproduction is dependent upon the quality of the copy submitted.

In the unlikely event that the author did not send a complete manuscript and there are missing pages, these will be noted. Also, if material had to be removed, a note will indicate the deletion.



ProQuest U145535

Published by ProQuest LLC(2015). Copyright of the Dissertation is held by the Author.

All rights reserved.

This work is protected against unauthorized copying under Title 17, United States Code.
Microform Edition © ProQuest LLC.

ProQuest LLC
789 East Eisenhower Parkway
P.O. Box 1346
Ann Arbor, MI 48106-1346

Abstract

In this thesis, I use metabolic control analysis to investigate quantitatively, the control of neonatal hepatic fatty acid oxidation and ketogenesis. Specifically, I model, report and discuss the control of hepatic fatty acid oxidation, Krebs cycle and ketogenic fluxes by mitochondrial outer membrane carnitine palmitoyltransferase I (CPT I), in hepatocytes or mitochondria isolated from suckling rats, under physiological and (patho)physiological conditions, mimicking healthy and diseased states.

My work has:

- (a) provided the first quantitative assessment of the control exerted by CPT I over carbon fluxes from palmitate, octanoate and palmitate:octanoate mixtures, in hepatocytes isolated from suckling rats;
- (b) provided a quantitative assessment of the control exerted by CPT I over ketogenesis and total carbon flux from palmitate, in a re-defined system, in mitochondria isolated from suckling or adult rats (Krauss, *et al.*, 1996);
- (c) shown that the numerical value of the flux control coefficient for CPT I over ketogenesis changes with developmental stage and is lower in suckling rats than in adult rats in both hepatocyte and mitochondrial systems;
- (d) demonstrated that the numerical value of the flux control coefficient for CPT I over ketogenesis changes in response to different substrates;
- (e) indicated that whilst in adult rats, CPT I exerts a high level of control over ketogenesis in neonatal rats, CPT I is not 'rate-limiting' over ketogenesis, under physiological conditions;
- (f) provided the first quantitative assessment of the control exerted by CPT I over carbon fluxes from palmitate in an *in vitro* model of neonatal sepsis;
- (g) demonstrated that the potential of CPT I to control ketogenesis increases under certain (patho)physiological conditions;
- (h) provided an investigation into hepatocyte respiration under (patho)physiological conditions and has shown that in this *in vitro* model of neonatal sepsis, oxygen consumption is increased.

Publications arising from this work

New KJ, Eaton S, Elliott KRF, Spitz L and Quant PA. (accepted for publication, *J Paed Surg*)

Effect of lipopolysaccharide and cytokines on oxidative metabolism in neonatal hepatocytes.

New KJ, Eaton S, Spitz L, Elliott KRF and Quant PA. *Eur J Med Res.* **5**, 46-47. 2000.

Analysis of control exerted by CPT I over ketogenic flux in *in vitro* hepatocyte models designed to mimic the early stages of neonatal sepsis.

New KJ, Spitz L, Elliott KRF, Eaton S and Quant PA. (Poster/Abstract, *Biochemical Society, Cork Meeting*) 1999.

In vitro models of early stages of neonatal sepsis.

New KJ, Elliott KRF and Quant PA. *Eur J Biochem.* **259**, 684-691. 1999.

Comparisons of flux control exerted by mitochondrial outer membrane carnitine palmitoyltransferase over ketogenesis in hepatocytes and mitochondria isolated from suckling or adult rats.

New KJ, Eaton S, Elliott KRF and Quant PA. in *Advances in experimental medicine and biology: current views of fatty acid oxidation and ketogenesis, from organelles to point mutations*. Plenum Press. 227-232. 1999.

Is it time to reconsider the role of CPT I in control over ketogenesis?

Eaton S, Bartlett K, Pourfarzam M, Markley MA, New KJ and Quant PA. in *Advances in experimental medicine and biology: current views of fatty acid oxidation and ketogenesis, from organelles to point mutations*. Plenum Press. 155-160. 1999.

Production and export of acyl-carnitine esters by neonatal rat hepatocytes.

New KJ. *The Biochemist, October Issue.* **50**. 1999.

Communicating communication.

Quant PA, Lascelles CV, New KJ, Patil KK, Azzouzi N, Eaton S and Elliott KRF. *Biochem Soc Trans.* **26**, 125-130. 1998.

Impaired neonatal hepatic ketogenesis.

New KJ, Eaton S, Elliott KRF and Quant PA. in *BioThermoKinetics in the Post Genomic Era, Proceedings of the 8th International meeting on BioThermoKinetics* 113-116. 1998.

CPT I: a reassessment of its role in control over ketogenic flux.

New KJ, Elliott KRF and Quant PA. *Biochem Soc Trans.* **26**, S88. 1998.

Flux control exerted by mitochondrial outer membrane carnitine palmitoyltransferase over ketogenic flux in hepatocytes isolated from suckling rats.

New KJ, Elliott KRF and Quant PA. *Biochem Soc Trans.* **25**, 418S. 1997.

Quantitative analysis of control exerted by mitochondrial outer membrane carnitine palmitoyltransferase over carbon fluxes from palmitate in hepatocytes isolated from suckling rats.

Acknowledgements

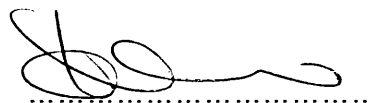
The research presented in this dissertation was performed in the Departments of Paediatric Surgery and Biochemistry, at the Institute of Child Health in London. My research was made possible by the financial support of the Sir Halley Stewart Trust, and Professor Spitz, within the Department of Paediatric Surgery, for which I remain and will always be grateful.

I would like to thank my supervisors, Dr P A Quant, Dr K R F Elliott, Dr S Eaton and Dr D Muller, for their support and guidance during these studies. Their patience and suggestions were truly appreciated.

My grateful thanks are also extended to my family, friends and colleagues, who have provided encouragement and entertainment, both inside and outside the laboratory.

Especially, Chris Newman, who provided support, love and Cherry Coke. Thank you.

This dissertation is the result of my own work and includes nothing which is the outcome of work done in collaboration, unless acknowledged in the text. No part of this thesis has been, or is currently being submitted to any other Board for any other purposes.



K J New

Table of Contents

Title page.....	1
Abstract.....	2
Publications arising from this work.....	3
Acknowledgements.....	4
Table of contents.....	5
List of tables / List of schemes.....	10
List of figures.....	11
List of abbreviations.....	13
List of enzymes.....	14
Chapter 1	
Literature Review and Aims	
1.1 Introduction.....	15
1.2 Biochemical perspectives on hepatic fatty acid oxidation, the Krebs cycle and ketogenesis.....	15
1.2.1 Plasma free fatty acids and their entry into hepatocytes.....	15
1.2.2 Formation of acyl-CoA esters.....	17
1.2.3 Site of β -oxidation: mitochondria <i>versus</i> peroxisomes.....	18
1.2.4 Entry into mitochondria.....	19
1.2.5 The reactions of mitochondrial β -oxidation.....	27
1.2.6 Transesterification.....	30
1.2.7 The reactions of the Krebs cycle.....	30
1.2.8 The reactions of the 3-hydroxy-3-methylglutaryl-CoA cycle.....	31
1.2.9 Ketone body utilization.....	33
1.2.10 Control distribution over the pathways of hepatic fatty acid oxidation and ketogenesis.....	35
1.3 Physiological and clinical significance of the pathways of fatty acid oxidation and ketogenesis.....	36
1.3.1 The role of ketone bodies.....	36
1.3.2 Fluctuation in ketone body concentrations.....	37
1.4 Metabolic control analysis (MCA).....	39
1.4.1 General introduction.....	39
1.4.2 Flux control coefficients.....	40
1.4.3 The summation theorem.....	43
1.4.4 Elasticity coefficients.....	45
1.4.5 The connectivity theorem.....	46
1.4.6 Bottom-up control analysis (BUCA).....	47
1.4.7 Top-down control analysis (TDCA).....	47
1.4.8 Assumptions underlying the application of MCA.....	48
1.5 Overall Aims.....	49
1.5.1 Aims and objectives of Chapter 3: Analysing the role of hepatic mitochondrial outer membrane carnitine palmitoyltransferase in the control of carbon fluxes from palmitate.....	49

1.5.2	Aims and objectives of Chapter 4: Application of top-down control analysis in hepatocytes to investigate the distribution of control over carbon fluxes in the pathways of fatty acid oxidation, ketogenesis and the Krebs cycle.....	50
1.5.3	Aims and objectives of Chapter 5: Analysing the role of CPT I in control of carbon flux from medium-chain fatty acids and mixtures of long- and medium-chain fatty acids	50
1.5.4	Aims and objectives of Chapter 6: Analysing the role of CPT I in control of ketogenic flux in <i>in vitro</i> models of neonatal sepsis.....	51
1.5.5	Aims and objectives of Chapter 7: Effects of lipopolysaccharide and/or cytokines on neonatal oxidative liver metabolism.....	52

Chapter 2

Materials and methods

2.1	Materials.....	53
2.1.1	Chemicals	53
2.1.2	Animals	53
2.2	Methods	53
2.2.1	Isolation of hepatocytes.....	53
2.2.2	Incubation of hepatocytes for the measurement of ¹⁴ C-ketone body production and ¹⁴ CO ₂ release.....	56
2.2.3	Assay of ¹⁴ CO ₂ release in hepatocytes	57
2.2.4	Assay of ¹⁴ C-ketone body production in hepatocytes.....	57
2.2.5	Permeabilization of hepatocytes and assay of mitochondrial outer membrane carnitine palmitoyltransferase (CPT I) activity	58
2.2.6	Hepatocyte oxygen consumption.....	60
2.2.7	Electron microscopy of hepatocytes	61
2.2.8	Statistical analysis	62

Chapter 3

Analysing the role of hepatic mitochondrial outer-membrane carnitine palmitoyltransferase in the control of carbon flux from palmitate

3.1	Introduction.....	63
3.1.1	Historical perspectives in the control of hepatic fatty acid oxidation and ketogenesis.....	63
3.1.2	Control analysis of hepatic fatty acid oxidation and ketogenesis	65
3.1.3	Aims of this section.....	67
3.2	Theory and approaches.....	67
3.2.1	Application of bottom-up control analysis in hepatocytes isolated from suckling rats	67
3.2.2	Application of bottom-up control analysis in mitochondrial systems	70
3.3	Results	74
3.3.1	Bottom-up control analysis in hepatocyte systems.....	74
3.3.2	Bottom-up control analysis in mitochondrial systems.....	81
3.4	Discussion.....	86
3.4.1	Validation of techniques	86
3.4.2	Tangents to inhibitor curves (where inhibitor tends to zero).....	87
3.4.3	Application of bottom-up control analysis in hepatocytes isolated from suckling rats	87

3.4.4	Application of bottom-up control analysis in mitochondria.....	91
3.4.5	Interpretation of bottom-up control analysis results.....	92
3.4.6	Factors effecting the values for flux control coefficients for CPT I over carbon fluxes.....	93
3.4.7	Conclusions.....	94

Chapter 4

Application of top-down control analysis in hepatocytes to investigate the distribution of control over carbon fluxes in the pathways of fatty acid oxidation, ketogenesis and the Krebs cycle

4.1	Introduction and aims	95
4.2	Theory and approaches.....	95
4.2.1	Application of top-down control analysis in hepatocytes	95
4.3	Results	99
4.3.1	Effects of manipulation of the Krebs block.....	99
4.3.2	Effects of manipulation of the β -oxidation block.....	99
4.3.3	Flux data from two independent manipulation experiments	104
4.3.4	Calculation of group flux control coefficients	105
4.4	Discussion and conclusions.....	106

Chapter 5

Analysing the role of mitochondrial outer membrane carnitine palmitoyltransferase in control of carbon flux from medium-chain fatty acids and mixtures of long- and medium-chain fatty acids

5.1	Introduction.....	107
5.1.1	<i>In utero</i> nutrition	107
5.1.2	Immediate <i>post-partum</i> nutrition	108
5.1.3	Neonatal nutrition	109
5.1.4	Metabolic fate of the fatty acid components of milk.....	110
5.1.5	Aims of this section.....	112
5.2	Theory and approaches.....	112
5.2.1	Application of bottom-up control analysis in hepatocytes.....	112
5.3	Results	114
5.3.1	Bottom-up control analysis in hepatocytes (octanoate as substrate).....	114
5.3.2	Bottom-up control analysis in hepatocytes ([1- ¹⁴ C]octanoate:unlabelled palmitate as substrate)	114
5.3.3	Bottom-up control analysis in hepatocytes ([1- ¹⁴ C]palmitate:unlabelled octanoate as substrate)	117
5.3.4	Bottom-up control analysis in hepatocytes ([1- ¹⁴ C]octanoate:[1- ¹⁴ C]palmitate as substrate)	117
5.4	Discussion.....	120
5.4.1	Control exerted by CPT I over flux from octanoate to ketone bodies.....	120
5.4.2	Control exerted by CPT I over flux from singly labelled mixed fats to ketone bodies.....	123
5.4.3	Control exerted by CPT I over flux to ketone bodies, where both substrates have been labelled	123
5.4.4	Potential implications for inborn errors of metabolism.....	125
5.4.5	Diet related changes in the ability of CPT I to control carbon fluxes	126
5.4.6	Conclusions.....	127

Chapter 6**Analysing the role of hepatic mitochondrial outer-membrane carnitine palmitoyltransferase in control of ketogenic flux in *in vitro* models of neonatal sepsis**

6.1	Introduction.....	128
6.1.1	Sepsis	128
6.1.2	Common causes of sepsis.....	129
6.1.3	Agents involved in the sepsis response	130
6.1.4	Fatty acid oxidation and ketogenesis during sepsis	134
6.1.5	Control of ketogenesis during sepsis: the role of CPT I	137
6.1.6	Aims of this section.....	140
6.2	Theory and approaches.....	141
6.2.1	Isolation of hepatocytes in the presence of lipopolysaccharide (LPS) and/or tumour necrosis factor (TNF α), interleukin 6(IL6)	141
6.2.2	Application of bottom-up control analysis in control and treated hepatocytes.....	142
6.3	Results	143
6.3.1	Effect on cell yield and viability of addition of LPS, TNF α and/or IL6 during the hepatocyte isolation procedure	143
6.3.2	Effect of addition of LPS+TNF α on hepatocyte gross morphology.....	146
6.3.3	Effect of addition of LPS+TNF α +IL6 on hepatocyte gross morphology.....	147
6.3.4	Effect of LPS, TNF α and/or IL6 on ketone body production	148
6.3.5	Effect of combinations of LPS, TNF α and/or IL6 on the role of CPT I in control of carbon flux from palmitate.....	150
6.4	Discussion.....	160
6.4.1	The addition of agents during the cell isolation procedure	160
6.4.2	Ketone body production in hepatocytes exposed to LPS and/or cytokines during isolation.....	162
6.4.3	Bottom-up control analysis of LPS+TNF α or LPS+TNF α +IL6 treated hepatocytes isolated from suckling rats	164
6.4.4	Factors affecting the capacity of CPT I to control flux in response to cytokines and LPS	166
6.4.5	Conclusions.....	167

Chapter 7**Effects of lipopolysaccharide and/or cytokines on neonatal oxidative liver metabolism**

7.1	Introduction.....	169
7.1.1	Mitochondrial oxygen consumption.....	170
7.1.2	Non-mitochondrial oxygen consumption	174
7.1.3	Total cellular oxygen consumption.....	176
7.1.4	Oxygen consumption during sepsis	177
7.1.5	Reye's Syndrome	179
7.1.6	Aims of this section.....	179
7.2	Results	180
7.2.1	Effect of LPS on hepatocyte respiration.....	180
7.2.2	Effect of TNF α on hepatocyte respiration	180

7.2.3	Effect of LPS+TNF α on hepatocyte respiration.....	183
7.2.4	Effect of half dose LPS+TNF α on hepatocyte respiration	184
7.2.5	Effect of LPS+TNF α +IL6 on hepatocyte respiration.....	184
7.2.6	Effect of half dose LPS+TNF α +IL6 on hepatocyte respiration	186
7.2.7	Effect of salicylic acid on total endogenous hepatocyte respiration in control and in LPS+TNF α +IL6 exposed hepatocytes.....	186
7.3	Discussion.....	189
7.3.1	The effect of LPS or individual cytokines on hepatocyte respiration	189
7.3.2	The effect of combinations of LPS and cytokines on hepatocyte respiration.....	190
7.3.3	Comparison of the effects of the different models of neonatal sepsis on oxygen consumption	194
7.3.4	Investigating the effects of salicylic acid on hepatocyte respiration in the LPS+TNF α +IL6 <i>in vitro</i> model of neonatal sepsis.....	197
7.3.5	Conclusions.....	198

Chapter 8

Conclusions and future research

8.1	The effects of development, substrate or clinical condition on the potential of CPT I to control carbon fluxes	199
8.2	Development and use of <i>in vitro</i> neonatal model of sepsis	201

Appendix

Derivation of generalised and specific forms of the equations used in the TDCA in Chapter 4

A1.1	Introduction.....	204
A1.2	Consideration of sign convention.....	204
A1.3	Derivation of generalised equations using the sign convention set out by Brand (1996).....	206
A1.4	Derivation of generalised equations for the calculation of group flux control coefficients as a function of fluxes alone.....	208
A1.5	Specific equations for the calculation of the first series of group flux control coefficients as a function of fluxes alone.....	210
A1.6	Calculation of relative elasticities.....	211
A1.7	Calculation of the remaining series of group flux control coefficients	214
A1.8	Summary of key equations used for the calculation of each group flux control coefficient	215

Reference list	217
----------------------	-----

List of tables

Table 3.1	Individual flux control coefficients for CPT I over rates of formation of ketone bodies (ASP), carbon dioxide or total carbon products (TCP) from palmitate in isolated hepatocytes	81
Table 4.1	Full series of flux control coefficients in hepatocyte TDCA system described in Section 4.1	97
Table 4.2	Data from each experimental manipulation expressed in terms of percent change in flux	104
Table 6.1	<i>In vitro</i> model of neonatal sepsis: agents added during cell preparation	141
Table 6.2	Absolute cell yields following addition of LPS and/or cytokines during hepatocyte isolation procedure	144
Table 6.3	Effect of addition of LPS and/or cytokines during hepatocyte isolation procedure on hepatocyte yield and viability.....	145
Table 6.4	Individual flux control coefficients for CPT I over rates of formation of ketone bodies (ASP) from palmitate in untreated control and treated hepatocytes	160
Table 7.1	Effect of LPS and/or various cytokines on hepatocyte respiration expressed in terms of cell number	181
Table 7.2	Effect of LPS and/or various cytokines on hepatocyte respiration expressed in terms of dry mass.....	182
Table 7.3	Absolute rates of total oxygen consumption in the absence or presence of sodium salicylate.....	187
Table 7.4	Possible factors resulting in increased total oxygen consumption	192
Table A1.1	Full series of generalised flux control coefficients in hepatocyte TDCA system.....	205
Table A1.2	(a) Equations used for series 1 flux control coefficients.....	215
Table A1.2	(b) Equations used for series 2 flux control coefficients.....	216
Table A1.2	(c) Equations used for series 3 flux control coefficients.....	216

List of schemes

Scheme 1.1	Long-chain fatty acid activation.....	17
Scheme 1.2	Formation of acyl-carnitine esters	20
Scheme 1.3	Reactions of β -oxidation.....	28
Scheme 1.4	Reactions of the 3-hydroxy-3-methylglutaryl-CoA cycle	32
Scheme 1.5	General linear pathway	41
Scheme 1.6	General branched pathway	44
Scheme 3.1	Hepatocyte BUCA system.....	68
Scheme 3.2	Original TDCA mitochondrial system.....	71
Scheme 3.3	Re-defined BUCA mitochondrial system	71
Scheme 4.1	Conceptually simplified system used for TDCA in hepatocytes ...	96
Scheme 5.1	Hepatocyte BUCA system.....	112
Scheme 6.1	Hepatocyte BUCA system.....	142

List of figures

Figure 1.1	Schematic representation of long-chain fatty acid activation, transport and oxidation	23
Figure 1.2	Summary of reactions of ketone body utilization in extrahepatic tissues	34
Figure 3.1	Schematic grid for calculation of individual flux control coefficients for CPT I over ketogenesis and total carbon flux in isolated mitochondria	73
Figure 3.2	Effect of etomoxir on CPT I activity	75
Figure 3.3	Effect of etomoxir on CPT I activity and ketogenic flux.....	76
Figure 3.4	Scatter of points from individual data sets	77
Figure 3.5	Effect of etomoxir on CPT I activity and flux to carbon dioxide	79
Figure 3.6	Effects of etomoxir on CPT I activity and total carbon flux	80
Figure 3.7	Effect of malonyl-CoA concentration and respiratory rate on external palmitoyl-carnitine levels and carbon fluxes from palmitoyl-CoA in mitochondria isolated from adult rats.....	83
Figure 3.8	Effect of malonyl-CoA concentration and respiratory rate on external palmitoyl-carnitine levels and carbon fluxes from palmitoyl-CoA in mitochondria isolated from suckling rats.....	84
Figure 3.9	Effect of malonyl-CoA concentration on flux control coefficients for CPT I over carbon fluxes from palmitoyl-CoA in mitochondria isolated from (a) adult or (b) suckling rats	85
Figure 3.10	Comparison of distribution of control exerted by CPT I over ketogenic flux in (a) adult and (b) suckling rats.....	88
Figure 3.11	Comparison of distribution of control exerted by CPT I over flux to CO ₂ in adults and suckling rats.....	89
Figure 3.12	Comparison of distribution of control over total carbon flux observed in (a) adult and (b) suckling rats	90
Figure 4.1	Effects of malonate on flux through the Krebs cycle block of reactions.....	100
Figure 4.2	Effects of malonate on flux through the KB and β ox blocks of reactions	101
Figure 4.3	Effect of etomoxir on flux through the β ox block of reactions.....	102
Figure 4.4	Effect of etomoxir on flux through the KB and Krebs cycle blocks of reactions.....	103
Figure 5.1	Effect of etomoxir on CPT I activity and ketogenic flux in the presence of octanoate as substrate	115
Figure 5.2	Effect of etomoxir on CPT I activity and ketogenic flux in the presence of ([1- ¹⁴ C]octanoate:unlabelled palmitate.....	116
Figure 5.3	Effect of etomoxir on CPT I activity and ketogenic flux in the presence of ([1- ¹⁴ C]palmitate:unlabelled octanoate	118
Figure 5.4	Effect of etomoxir on CPT I activity and ketogenic flux in the presence of ([1- ¹⁴ C]palmitate:[1- ¹⁴ C]octanoate	119
Figure 5.5	Ketogenic flux as a function of CPT I inhibition	120
Figure 5.6	Comparison of flux control coefficients from adult rats and from suckling rats	122
Figure 5.7	Comparison of flux control coefficients calculated from suckling rats in mixed fatty acid experiments	124

List of figures (continued)

Figure 6.1	Schematic representation detailing the time course of cytokine appearance in plasma	132
Figure 6.2	Effect of addition of LPS+TNF α during hepatocyte isolation on the ultrastructure of isolated hepatocytes	146
Figure 6.3	Effect of addition of LPS+TNF α +IL6 during hepatocyte isolation on the ultrastructure of isolated hepatocytes	147
Figure 6.4	Formation of [14 C]ASP over time	149
Figure 6.5	Effect of etomoxir on CPT I activity in control and LPS+TNF α treated groups	151
Figure 6.6	Effect of etomoxir on ketogenic flux in control and LPS+TNF α treated groups	152
Figure 6.7	Data used for the calculation of individual flux control coefficients for CPT I over ketogenic flux in control groups	153
Figure 6.8	Data used for the calculation of individual flux control coefficients for CPT I over ketogenic flux in LPS+TNF α treated groups	154
Figure 6.9	Effect of etomoxir on CPT I activity in control and LPS+TNF α +IL6 treated groups	156
Figure 6.10	Effect of etomoxir on ketogenic flux in control and LPS+TNF α +IL6 treated groups	157
Figure 6.11	Data used for the calculation of individual flux control coefficients for CPT I over ketogenic flux in control groups	158
Figure 6.12	Data used for the calculation of individual flux control coefficients for CPT I over ketogenic flux in LPS+TNF α +IL6 treated groups	159
Figure 6.13	Comparison of flux control coefficients for CPT I over ketogenesis in untreated control, LPS+TNF α - or LPS+TNF α +IL6-treated hepatocytes isolated from suckling rats	165
Figure 7.1	Schematic arrangement of the ATPase, the complexes of the respiratory chain and association of proton pumping	171
Figure 7.2	Hydroxylation by cytochrome P ₄₅₀	175
Figure 7.3	Schematic representation of peroxisomal respiration	176
Figure 7.4	Summary of total oxygen consumption	177
Figure 7.5	Total endogenous, non-mitochondrial and/or mitochondrial respiration of isolated hepatocytes from control and LPS+TNF α +IL6 treated groups	185
Figure 7.6	Total oxygen consumption: Control or LPS+TNF α +IL6-exposed cells in absence or presence of salicylic acid	188
Figure 7.7	Comparison of the distribution of oxygen consumption in isolated hepatocytes from (a) control and (b) LPS+TNF α +IL6 treated groups	193
Figure 7.8	Percentage change in total endogenous respiration in hepatocytes	194
Figure 7.9	Changes in the contribution of the non-mitochondrial fraction to total oxygen consumption	196
Figure 7.10	Comparison of total oxygen consumption in control and LPS+TNF α +IL6 exposed hepatocytes in response to two different doses of salicylic acid	197

List of abbreviations

ACBP	acyl-CoA binding protein
APP	acute phase proteins
ASP	acid soluble products
BSA	bovine serum albumin
BUCA	bottom-up control analysis
C_E^J or C_{Blk}^J	individual or group flux control coefficients respectively
CLP	caecal ligation and puncture
ε_x^a	generalised elasticity coefficient for the effector, X on enzyme/step a
ETC	electron transport chain / mitochondrial respiratory chain
ex-pc	external palmitoylcarnitine
FAD	flavin adenine dinucleotide (oxidized form)
FADH ₂	flavin adenine dinucleotide (reduced form)
FAT	fatty acid translocase
FATP	fatty acid transport protein
FABP	fatty acid binding protein
FCCP	p-trifluoromethoxyphenylhydrazone
IL1	interleukin-1
IL6	interleukin-6
J_{ASP}	carbon flux to acid soluble products \approx ketogenic flux in isolated hepatocytes
J_{TCP}	total carbon flux in isolated hepatocytes
J_{CO_2}	Krebs cycle flux in isolated hepatocytes
$J_{\beta ox}$	β -oxidation flux in isolated hepatocytes
$J_{ketogenesis}$	carbon flux to ketone bodies (acetoacetate and β -hydroxybutate in isolated mitochondria)
J_{carbon}	total carbon flux ($J_{ASP} + J_{CO_2}$) in isolated mitochondria
KRB	Krebs Ringer bicarbonate
KRP	Krebs Ringer phosphate
LPS	lipopolysaccharide
L-CPTI	liver isoform CPT I
M-CPTI	muscle isoform CPT I
MCA	metabolic control analysis
MCoA	malonyl-CoA
MYX	myxothiazol
NEFA	non-esterified fatty acids
PCA	perchloric acid
P-CoA	palmitoyl-CoA
PMF	proton motive force
R_x^J	generalised response coefficient for effector X on flux J
ROS	reactive oxygen species
RS	Reye's Syndrome
SIDS	Sudden Infant Death Syndrome
SIRS	systemic inflammatory response syndrome
SGA	small-for-gestational-age
TCP	total carbon products
TDCA	top-down control analysis
TNF α	tumour necrosis factor alpha
TPN	total parenteral nutrition

List of enzymes

acetoacetyl-CoA thiolase, (E.C. 2.3.1.9)	
acetoacetyl-CoA synthase	
acetyl-CoA carboxylase, (E.C. 6.4.1.2)	ACC
acyl-CoA synthases, (E.C. 6.2.1.3)	ACS
camitine acetyltransferase, (E.C. 2.3.1.7)	CAT
Clostridopeptidase A, type IV, (E.C.3.4.24.3)	collagenase
DNAaseI, (E.C.3.1.21.1)	
mitochondrial outer membrane camitine palmitoyltransferase, (E.C.2.3.1.21)	CPT I
mitochondrial inner membrane camitine palmitoyltransferase, (E.C.2.3.1.21)	CPT II
2-enoyl-CoA hydratases, (E.C. 4.2.1.17)	
3-hydroxybutyrate dehydrogenase, (E.C. 1.1.1.30)	
3-hydroxyacyl-CoA dehydrogenases, (E.C. 1.1.1.35)	
3-hydroxy-3-methylglutaryl-CoA synthase, (E.C.4.1.3.5)	HMG-CoA synthase
3-hydroxy-3-methylglutaryl-CoA lyase, (E.C. 4.1.3.4)	HMG-CoA lyase
3-oxoacid-CoA transferase, (E.C. 2.8.3.5)	
3-oxoacyl-CoA thiolases, (E.C. 2.3.1.9 and E.C. 2.3.1.16)	
Short-; medium-; long- very-long- chain acyl-CoA dehydrogenases, (E.C. 1.3.99.2 and E.C. 1.3.99.3)	
succinate dehydrogenase, (E.C. 1.3.5.1)	SDH

Chapter 1

Literature review and aims

1.1 Introduction

Although the pathways involved in the metabolism of fatty acids are well mapped, the regulation and control of hepatic fatty acid oxidation fluxes under different physiological/clinical situations are poorly understood. In this study, I have investigated control over hepatic fatty acid oxidation and ketogenesis in the suckling rat, in response to different substrates and the clinical condition of sepsis, using the approaches of metabolic control analysis (MCA). In this introduction, I shall briefly consider hepatic fatty acid metabolism, the role of ketone bodies and introduce the central themes of MCA.

1.2 Biochemical perspectives on hepatic fatty acid oxidation, the Krebs cycle and ketogenesis

1.2.1 Plasma free fatty acids and their entry into hepatocytes

Fatty acids may be defined as monocarboxylic acids and are named on the basis of the number of carbon atoms and locus of double bonds. For example, the C₁₆ saturated fatty acid has a systematic name of n-hexadecanoate, since its parent hydrocarbon is hexadecane. The C₁₆ fatty acid with a double bond is known as *cis*- Δ^9 -hexadecenoate, where the *cis*- Δ^9 indicates the presence of a double bond between carbons 9 and 10. Fatty acids in paediatric nutrition have been reviewed by Girard (1992) and Giovannini (1995) and are discussed in more detail in relation to neonatal diet in later chapters of this thesis. In summary, in the neonate, medium-chain fatty acids (chain length C₆-C₁₀) and long-chain fatty acids (chain length C₁₂-C₂₂) are present in variable proportions as the acyl chains of the triacylglycerols in maternal milk. Short-chain (chain length \leq C₄) fatty acids are derived mainly from anaerobic bacterial fermentation of undigested lactose. In addition to providing energy following oxidation, fatty acids (and their derivatives) have many physiological roles. These include, for example, components of phospholipids, lipophilic modifiers of proteins, in the control of cell proliferation and transmembrane signalling. The following sections, however, will consider their oxidation as metabolic fuels during the neonatal period.

In the immediate post-natal period, the concentration of plasma free fatty acids (non-esterified fatty acids; NEFA) increases. Depending on the species considered, this

is due to increased hydrolysis of triacylglycerol derived either from white adipose tissue or from the absorption of triacylglycerols from maternal milk (Novak *et al.*, 1964, Persson *et al.*, 1966; Blazquez *et al.*, 1974; Ferré *et al.*, 1978; Pégorier *et al.*, 1981). NEFA are transported between organs as unesterified fatty acids complexed with serum albumin (Spector, 1975) or in the form of triacylglycerols associated with lipoproteins.

Situated in the right upper quadrant of the abdominal cavity and receiving blood from the hepatic portal vein, the liver is the first organ to be exposed to blood from the digestive system. It encounters a wide variety of nutrients, including the fatty acid-serum complexes, in addition to xenobiotics, toxins and gut-derived micro-organisms. The liver is involved in a large number of metabolic activities, from the anabolism and catabolism of fats, proteins, carbohydrates and vitamins, to detoxification processes and metabolism of hormones. The work reported here is concerned with the role of the liver in the oxidation of fatty acids and in particular, focuses on fatty acid oxidation in hepatocytes. In its broadest sense, the term hepatocyte refers to all resident liver cells but is most commonly used to refer to liver parenchymal cells and this is the convention used throughout this thesis. Hepatocytes represent approximately 60-65% of all liver cells by number but, owing to their large size, they occupy approximately 80-90% of the volume of the organ (reviewed in Berry, 1991). The non-parenchymal cells consist of 25-30% Kupffer cells, 10% endothelial cells, while the fat storing cells form less than 5% of the remaining liver cells.

Circulating triacylglycerols are hydrolysed outside cells by lipoprotein lipase bound to the capillary endothelium to yield free fatty acids. The mechanisms involved in the transport of long-chain fatty acids (LCFA) across biological membranes are still poorly understood, however, at low concentrations, LCFA enter cells by a carrier mechanism (Weisiger *et al.*, 1981; Ockner *et al.*, 1983). Relatively recently, several fatty acid transport proteins (FATPs) and a fatty acid translocase (FAT) have been identified (reviewed in Memon *et al.*, 1999). At higher concentrations, LCFA may cross the plasma membrane by direct diffusion (Zammit, 1984; Schulz, 1991; Guzmán *et al.*, 1993). Once inside cells, LCFA can be bound to fatty acid binding proteins (FABP) within the cytosol (Glatz *et al.*, 1985; Clarke *et al.*, 1989). These small soluble proteins, between 14-16kDa (Færgeman *et al.*, 1997) facilitate the diffusion of fatty acids through the aqueous medium of the cytosol to membrane-bound enzymes (acyl-CoA binding proteins). This is believed to help protect the cell

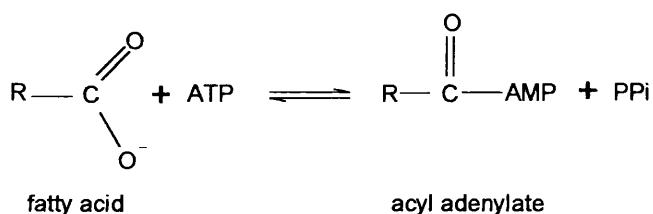
from the adverse detergent effects of fatty acids (Ockner *et al.*, 1992). During the fetal-neonatal transition, both the expression and content of liver FABP increase markedly (Gordon *et al.*, 1985; Paulussen *et al.*, 1986, 1989).

1.2.2 Formation of acyl-CoA esters

Inside the cell, LCFA (e.g. C₁₄, C₁₆ and C₁₈) are converted to their corresponding CoA-esters by long-chain acyl-CoA synthases (lc-ACS, EC 6.2.1.3). Mitochondria, microsomes, endoplasmic reticulum and peroxisomes all contain membrane bound ATP-dependent lc-ACS activity (Shindo *et al.*, 1978; Krisans *et al.*, 1980; Singh *et al.*, 1985). The mitochondrial enzyme forms an integral part of the outer membrane, with its CoA-binding site exposed to the cytosol (Hesler *et al.*, 1990). The activity of lc-ACS increases following birth (Warshaw *et al.*, 1972; Foster *et al.*, 1976; Chalk *et al.*, 1983).

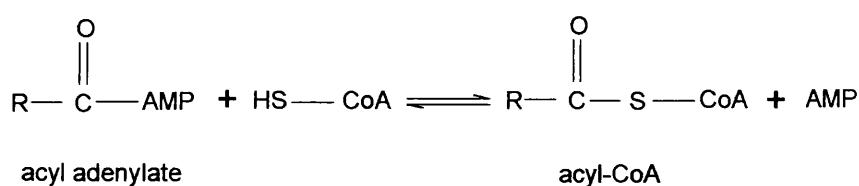
The long-chain fatty acid activation process occurs in two-steps (Scheme 1.1):

- (i) the first step (Scheme 1.1(a)) involves the reaction of the fatty acid with ATP forming an acyl adenylate and releasing pyrophosphate,



Scheme 1.1 (a)

- (ii) in the second step (Scheme 1.1(b)), the sulfhydryl group of CoA reacts with the acyl adenylate to form acyl-CoA and AMP.



Scheme 1.1 (b)

Whilst these partial reactions are readily reversible, the reaction is pulled forward since pyrophosphate is rapidly hydrolysed in a reaction catalysed by a pyrophosphatase.

The accumulation of acyl-CoA esters would have deleterious effects on cellular structures, for example, due to interactions with mitochondrial membranes (Shug *et al.*, 1971). This build up is prevented by the action of acyl-CoA binding protein (ACBP), which is present in concentrations near-equimolar with those of acyl-CoA within the liver cytosol (Rasmussen *et al.*, 1993). ACBP binds medium- and long-chain acyl-CoA esters with very high affinity, but shows only low affinity for CoA and does not bind fatty acids, acyl-carnitines or cholesterol (Færgeman *et al.*, 1997). Since this protein sequesters long-chain acyl-CoA esters, it also has the effect of removing product inhibition of the lc-ACS synthases (Pande, 1973). Additionally, Bhuiyan *et al.*, (1994) has shown that acyl-CoA esters are also able to bind with FABP.

Following activation, there are several possible fates for the fatty acids, which can for example, be incorporated into phospholipids and triacylglycerols or undergo desaturation and chain elongation in the endoplasmic reticulum. Alternatively, activated long-chain fatty acids may undergo the reactions of β -oxidation within peroxisomes or mitochondria (reviewed in Bremer *et al.*, 1984).

1.2.3 Site of β -oxidation: mitochondria versus peroxisomes

Fatty acid oxidation occurs within mitochondria and peroxisomes (Lazarow *et al.*, 1976). The studies reported and discussed in this thesis, were concerned primarily with mitochondrial-based processes. There are several justifications for this, firstly, despite an increase in the number of peroxisomes and in the activities of specific enzymes during the fetal/neonatal transition, the non-mitochondrial contribution to overall β -oxidation is less than 15% in both neonatal and adult rats (Mannaerts *et al.*, 1979; Krahling *et al.*, 1979; Horie *et al.*, 1981; Duée *et al.*, 1985). Secondly, although the volume of individual mitochondria decreases by 30-50% in the early neonatal period (Rohr *et al.*, 1971; Valcarce *et al.*, 1988), there is a substantial increase in the number of mitochondria per hepatocyte (Rohr *et al.*, 1971; Herzfeld *et al.*, 1973; reviewed in Aprille *et al.*, 1986). The net result of these processes is an increase in the size of the mitochondrial compartment relative to the volume of the hepatocyte (Rohr *et al.*, 1971; Herzfeld *et al.*, 1973; Aprille *et al.*, 1986). Thirdly,

during the first hours of extra-uterine life, pre-existing mitochondria demonstrate an increase in functional capacity brought about, at least in part, by an increase in the concentration of F_1 -ATPase, which is needed for efficient coupling between respiration and oxidative phosphorylation (Valcarce *et al.*, 1988). Finally, mitochondria are the primary site of oxidation of short-, medium- and long-chain fatty acids. Very-long chain fatty acids ($>C_{22}$) and *trans*-fatty acids are preferentially oxidized in hepatic peroxisomes (Vandenbosch *et al.*, 1992; Guzmán *et al.*, 1999). Thus the major physiological substrates, such as $C_{16:0}$ are oxidized mainly in mitochondria, both in the absence and in the presence of peroxisome proliferation (Skorin *et al.*, 1992).

In addition to their role in the breakdown of very-long chain fatty acids, peroxisomes can degrade a variety of other lipophilic carboxylates and physiological substrates include polyunsaturated fatty acids, dicarboxylic fatty acids, pristanic acid, bile acid intermediates and certain xenobiotics (van Veldhoven *et al.*, 1999). It has also been established that peroxisomes are involved in the biosynthesis of cholesterol and other isoprenoids (Wanders, 1999).

1.2.4 Entry into mitochondria

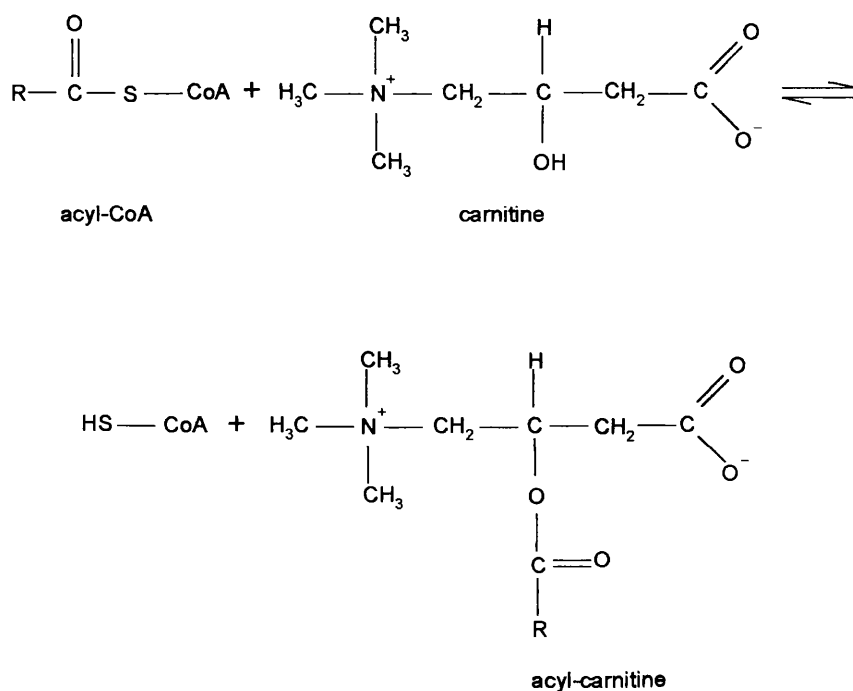
The mitochondrial membranes act as a barrier to long-chain CoA-esters, which are transported across the membranes in a three-step system comprising:

- (i) mitochondrial outer membrane carnitine palmitoyltransferase (CPT I);
- (ii) acyl-carnitine/carnitine translocase; and
- (iii) mitochondrial inner membrane carnitine palmitoyltransferase (CPT II).

Medium- and short-chain fatty acids ($<C_{10}$) are thought to be metabolised independently of this three-step system, crossing the mitochondrial membranes independently of CPT I (Smith *et al.*, 1968; McGarry *et al.*, 1980; Bremer *et al.*, 1984). They are activated to CoA esters by medium- or short-chain acyl-CoA synthases located in the mitochondrial matrix (Killenberg *et al.*, 1971).

Historically, there has been some controversy regarding the topographical, functional and regulatory relationships between the different components of the long-chain fatty acid transport system. However, many of the questions on this transport system have now been resolved, (recently reviewed in McGarry *et al.*, 1997 and Zammit, 1999) and this three-step system will now be considered.

(i) The initial step in this transport system, which is catalysed by CPT I (E.C. 2.3.1.21), generates free CoA and extra-mitochondrial acyl-carnitines (Scheme 1.2). The formation of the acyl-carnitines is the first committed step of mitochondrial β -oxidation.



Scheme 1.2 Formation of acyl-carnitine esters

It has recently been found that CPT I also recognises acyl-CoA-ACBP complexes and acyl-CoA substrates bound to FABP, rather than only the free acyl-CoAs as their substrate (Bhuiyan *et al.*, 1994; Abo-Hashema *et al.*, 1999).

Through cell and mitochondrial fractionation techniques, CPT I has been localised to the mitochondrial outer membrane (Murthy *et al.*, 1987; Fraser *et al.*, 1997). Recent work has also shown that CPT I is highly enriched in contact sites that occur between the outer and inner membranes of mitochondria (Fraser *et al.*, 1998). Contact sites, defined as areas where outer and inner membranes are in such stable and close contact that they cannot be separated by mechanical forces (for example, sonication protocols), are believed to have key roles in energy metabolism (Moynagh, 1995) rather than merely being morphological features where the

mitochondrial membranes are brought into close proximity. Zammit (1999) suggests that the increase in density of CPT I at contact sites may reflect the importance of acyl-carnitine transfer in the energetics of mitochondria.

Different isoforms of CPT I have been identified in the rat. The L isoform (L-CPT I) is the major form expressed in liver, kidney, pancreatic islets, ovary, spleen, intestine and brain (McGarry *et al.*, 1997), whilst the M isoform (M-CPT I) is expressed in cardiac and skeletal muscle and adipose tissue (Yamazaki *et al.*, 1995), although there may be some inter-species variation (Kolodziej *et al.*, 1992; McGarry *et al.*, 1997; Zammit, 1999). Additionally, tissue distribution of isoforms may change with development. For example, whilst both L-CPT I and M-CPT I are present in neonatal and adult rat heart mitochondria, in the late fetal/neonatal period, L-CPT I levels are higher than at later stages of development (McGarry *et al.*, 1997). This is potentially important, since although the two CPT I isoforms catalyse identical reactions, they differ in their Michaelis constant for the substrate carnitine (β -hydroxy- γ -trimethylaminobutyric acid) and in sensitivity to malonyl-CoA (McGarry *et al.*, 1997). A change in the ratios of the different isoforms, therefore, provides a potential means of regulation of the system at different stages of development.

Carnitine, a zwitterionic compound, can be synthesised in human liver and kidney from trimethyllysine derived from the essential amino acids lysine and methionine (Rebouche *et al.*, 1980). Neonates and particularly preterm infants, however, have low synthetic capabilities and are dependent on exogenous sources, such as maternal milk (Linz *et al.*, 1995). In the liver of suckling rats, the concentration of carnitine increases rapidly after birth (Ferré *et al.*, 1978) due to increased transfer of carnitine from the mothers milk to the pups (Robles-Valdes *et al.*, 1976). After 20 days of lactation, milk still provides almost half of the total carnitine in neonatal rats (Davis, 1989). The apparent K_m for carnitine is dependent on the palmitoyl-CoA concentration, since, as well as being a substrate, palmitoyl-CoA acts as a competitive inhibitor to carnitine, the second substrate for CPT I (Bremer *et al.*, 1967(a)(b)).

Two structural genes, α and β , encode CPT I. These are differentially expressed in tissues that utilise fatty acids as fuel: the α -gene mRNAs (encoding L-CPT I) are expressed with greatest abundance in liver, pancreatic beta cells and heart,

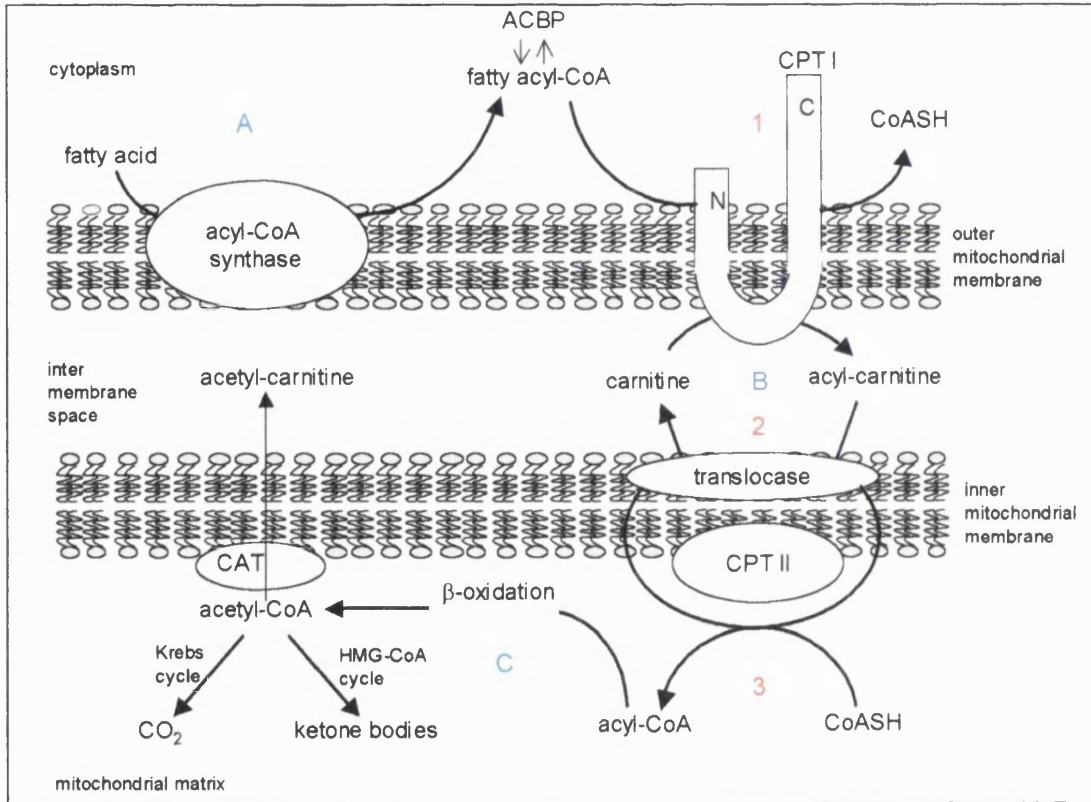
whereas β -gene products (encoding M-CPT I) predominate in skeletal muscle, adipose tissue, heart and testis (Yu *et al.*, 1998). In addition, there are also splice variants for M-CPT I (Yu *et al.*, 1998).

It is now known that L-CPT I consists of a single polypeptide of M_r 88,150 (Esser *et al.*, 1993(a)(b)) containing both the catalytic and regulatory domains and adopts a "hair-pin" topology within the mitochondrial outer membrane (Kolodziej *et al.*, 1993; Fraser *et al.*, 1997). Both the short (≈ 47 -residue) N-terminal domain and the longer (≈ 650 -residue) C-domain are exposed on the cytosolic side of the membrane (Fraser *et al.*, 1997). Two transmembrane domains "anchor" the molecule within the membrane, whilst a linker region between the transmembrane domains protrudes into the inner membrane space (Jackson *et al.*, 1999). This topology is illustrated in Figure 1.1, which also summarises the components of the three-step long-chain fatty acid transport system. Interestingly, one of the products from the splice variants mentioned previously, is predicted to have radically different membrane topology (Zammit, 1999) and altered malonyl-CoA regulatory domains (Yu *et al.*, 1998). Potentially, therefore, proteins translated from the splice variants may provide further regulation and control of the system, although the physiological significance is yet to be established.

Both the catalytic and malonyl-CoA binding sites are believed to reside in the C-domain of CPT I (Zammit *et al.*, 1997). However, since both the N- and C-domains are exposed on the outer face of the outer mitochondrial membrane (Fraser *et al.*, 1997), in addition to interacting with the cytosolic pool of long-chain acyl-CoA/ACBP and malonyl-CoA (Van der Leij *et al.*, 1999), the two domains are also able to interact with each other (Zammit *et al.*, 1997) subject to the constraints imposed by the linker region and transmembrane domains. The two transmembrane domains are themselves able to interact (Shai *et al.*, 1995).

The N-terminal domain in particular, is essential for the maintenance of an optimal conformation for both catalytic function and malonyl-CoA sensitivity and binding (Cohen *et al.*, 1998; Shi *et al.*, 1998). Furthermore, Swanson *et al.*, (1998) have proposed that the differences in the kinetics of the two isoforms of CPT I are determined by the nature of the interaction between the N- and C-terminal regions. Additionally, it has recently been demonstrated that the N-terminal residues critical for activity and malonyl-CoA sensitivity in M-CPT I are different from those of L-CPT I (Shi *et al.*, 2000)

(a)



(b)

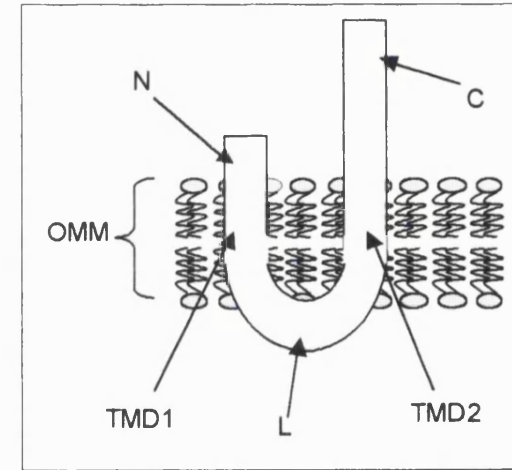


Figure 1.1 (b) Key:

- OMM (outer mitochondrial membrane)
- N (N-terminal domain, NH₂)
- C (C-terminal domain, COO')
- TMD1 (transmembrane domain 1)
- TMD2 (transmembrane domain 2)
- L (linker region protruding into intermembrane space)

Figure 1.1 Schematic representation of long-chain fatty acid activation, transport and oxidation

Figure (a) **A**: long-chain fatty acids are activated by long-chain acyl-CoA synthases located in the outer mitochondrial membrane. **B**: transport of the resulting CoA-esters across mitochondrial membranes occurs via the three-step system, comprising CPT I (1), the acyl-carnitine/carnitine exchange carrier (2) and CPT II (3). **C**: fatty acid oxidation, Krebs cycle and HMG-CoA cycle. Carnitine acyltransferase (CAT), which acts with acetyl-CoA as substrate, is also shown on this figure.

Figure (b) The "hair-pin" topology of CPT I (discussed in the main text) is emphasised in this scheme.

As already noted, malonyl-CoA, the product of the reaction catalysed by acetyl-CoA carboxylase (ACC, EC 6.4.1.2) which commits cytosolic acetyl-CoA to the synthesis of fatty acids, interacts with CPT I. Malonyl-CoA is a potent, physiological reversible inhibitor of CPT I (McGarry *et al.*, 1977; Saggerson *et al.*, 1981(a),(b),(c)). However, the malonyl-CoA/CPT I interaction is complex, since both the inhibitory effects of malonyl-CoA (Kashfi *et al.*, 1988; Kolodziej *et al.*, 1990) and sensitivity of CPT I to this inhibitor (Cook *et al.*, 1980; Robinson *et al.*, 1982; Zammit *et al.*, 1984; Herbin *et al.*, 1987) may be altered in response to certain (patho)physiological conditions. Zammit and co-workers (1990, 1998) have suggested that alterations in malonyl-CoA sensitivity may arise through changes in the interaction of the transmembrane domains with the membrane lipids as well as between the domains themselves.

Cook *et al.*, (1980) proposed that variations in the concentration of malonyl-CoA provide a potential method of co-ordinating the opposing pathways of fatty acid synthesis and fatty acid oxidation and prevent the potential futile cycling of oxidation of newly synthesised fatty acids. For example, during episodes of high carbohydrate feeding, circulating glucose levels are high, while non-esterified fatty acid levels are low. Under such conditions, i.e. high insulin to glucagon ratios and higher citrate efflux, mechanisms exist which raise the tissue concentration of malonyl-CoA. Citrate, for example, is cleaved by ATP-citrate lyase, forming acetyl-CoA, which may be used to form malonyl-CoA. Additionally, citrate is an allosteric activator of ACC, which would also result in raised concentration of malonyl-CoA. Under such conditions, CPT I itself becomes more sensitive to malonyl-CoA inhibition (Ontko *et al.*, 1980). Thus, under conditions where glucose is readily available, CPT I is inhibited, the rate of fatty acid oxidation is lowered and the liver switches to fatty acid biosynthesis. It is interesting, however, to consider this within the context of metabolic control analysis (MCA, Section 1.4) and specifically top down regulation analysis, which can be used to derive response coefficients that quantify the response of a system to an effector. The mechanism described here assumes a large and negative response coefficient for malonyl-CoA over fatty acid oxidation, $-R_{MCoA}^{J_{fao}}$. Since response coefficients may be defined as the product of a flux control coefficient and an elasticity, this in turn would imply a large value for the flux control coefficient for CPT I over fatty acid oxidation, $C_{CPTI}^{J_{fao}}$, and a large and negative elasticity for malonyl-CoA over CPT I, $-\varepsilon_{MCoA}^{CPTI}$. As discussed in later sections of this introduction, large flux control coefficients are rare.

In states of low insulin to glucagon ratios, such as during starvation or uncontrolled diabetes, gluconeogenesis has been shown to be stimulated in perfused liver (Heimberg *et al.*, 1969) and in isolated hepatocytes (Christiansen, 1977). Under such conditions, ACC is phosphorylated by AMP-dependent kinase to its inactive form (Hardie *et al.*, 1992). ACC, which is located in the cytoplasm, also requires a hydroxytricarboxylic acid activator such as citrate or isocitrate for its catalytic activity (Matsushashi *et al.*, 1962, 1964). Thus, the concentration of malonyl-CoA falls due to both slower efflux of citrate from the mitochondrion and to the inactivation of ACC. Additionally, CPT I is desensitised to the inhibitor, fatty acids are oxidized and there is an acceleration in ketone body production (McGarry *et al.*, 1989). The rise in glucagon also de-inhibits mitochondrial 3-hydroxy-3-methylglutaryl-CoA (mHMG-CoA) synthase and increases the expression of enzymes involved in the HMG-CoA cycle. This also results in an increase in ketone body production. Again, considered in the context of control analysis, this suggests that there are multiple steps involved in the control of ketogenic flux, rather than a single step/enzyme.

The activity of CPT I can also be inhibited through interaction with CoA esters of synthetic substrate analogues that contain a 2-oxirane ring moiety, for example, etomoxir (ethyl-2-[6-(4-chlorophenoxy)hexyl]oxirane-2-carboxylate), which binds to the C-domain in both L- and M-isoforms (Swanson *et al.*, 1998). This agent has been used to manipulate CPT I activity in the studies reported and discussed in this thesis. Etomoxir is converted *in situ* to etomoxir-CoA, an irreversible inhibitor of CPT I and it has been demonstrated that the R-enantiomer of etomoxir is esterified to its CoA-ester more readily than the S-enantiomer (Agius *et al.*, 1991(a)). Inhibition of CPT I is enantiomer specific, with only the R-enantiomer of etomoxir, a potent hypoglycaemic compound, inhibiting fatty acid oxidation in hepatocytes (Agius *et al.*, 1991(b)).

(ii) The second step in the transport of CoA esters across mitochondrial membranes involves an acyl-carnitine/carnitine translocase, situated in the inner mitochondrial membrane (Ramsay *et al.*, 1975; Pande, 1975; Indiveri *et al.*, 1990; Sherratt *et al.*, 1994, Ramsay *et al.*, 1994). The relationship of this translocase with the other steps in the transport system is illustrated in Figure 1.1. This translocase returns carnitine to the cytosolic side, in exchange for an incoming acyl-carnitine. In addition to its translocase activity, the carnitine acyl-carnitine translocase also has the capacity for slow unidirectional carnitine transport (Ramsay *et al.*, 1976; Pande *et al.*, 1980; Indiveri *et al.*, 1991).

The K_m for external carnitine is approximately 0.5-1.5mM, the same range as the concentration of carnitine in the tissue, and is lower for acyl-carnitines (Idell-Wenger, 1981) indicating that acyl-carnitines are preferentially transported into mitochondria. In addition, the K_m decreases with the chain-length of the fatty acid. The rate of exchange depends on the intramitochondrial concentration of carnitine (reviewed in Bremer *et al.*, 1984). However, chain-shortened carnitine esters can accumulate extramitochondrially (Eaton *et al.*, 1999(a)).

The acyl-carnitine/carnitine exchange carrier is similar, both in size (apparent molecular mass of 32.5kDa, Indiveri *et al.*, 1990) and in sequence, to other mitochondrial carrier proteins that transfer substrates between the cytosol and the mitochondrial matrix (Palmieri *et al.*, 1996). It is enriched within the contact sites of mitochondria, although to a lesser extent than CPT I and CPT II (Fraser *et al.*, 1998). The exchange activity of the translocase is strongly influenced by cardiolipin, a phospholipid specific to the mitochondrial membrane (Noel *et al.*, 1986; Indiveri *et al.*, 1991).

(iii) The final step in the CoA-ester transport system involves CPT II, which is loosely associated with the inner face of the inner membrane (Woeltje *et al.*, 1987) and particularly the contact sites between inner membrane cristae and outer membranes in liver mitochondria (Fraser *et al.*, 1998). In this final step, acyl-carnitines are reconverted back to acyl-CoA esters by CPT II. These acyl-CoA esters may then undergo β -oxidation, the carnitine being returned as described previously. Since the mitochondrial CoA pool is limited (approximately 3-5mM) depletion of free CoASH will inhibit CPT II and it has been suggested that β -oxidation flux may be partially controlled by either lack of intramitochondrial CoASH or an elevated [acetyl-CoA]/[CoA] ratio (reviewed in Eaton *et al.*, 1999(b)).

The relationship of CPT II to the other components of this transport system is illustrated in Figure 1.1. Since its active site faces the matrix space (McGarry *et al.*, 1992), CPT II is not accessible to cytosolic acyl-CoA esters in intact mitochondria (Fraser *et al.*, 1998). It is also insensitive to malonyl-CoA (McGarry *et al.*, 1978; Declercq *et al.*, 1987). CPT II has a M_r of approximately 69,000 (Kolodziej *et al.*, 1992). It is immunologically distinct from CPT I and the two enzymes are encoded by different genes (Kolodziej *et al.*, 1992, Esser *et al.*, 1993(a)(b)). Furthermore, CPT II mRNAs from a variety of rat tissues are identical in size and result in an

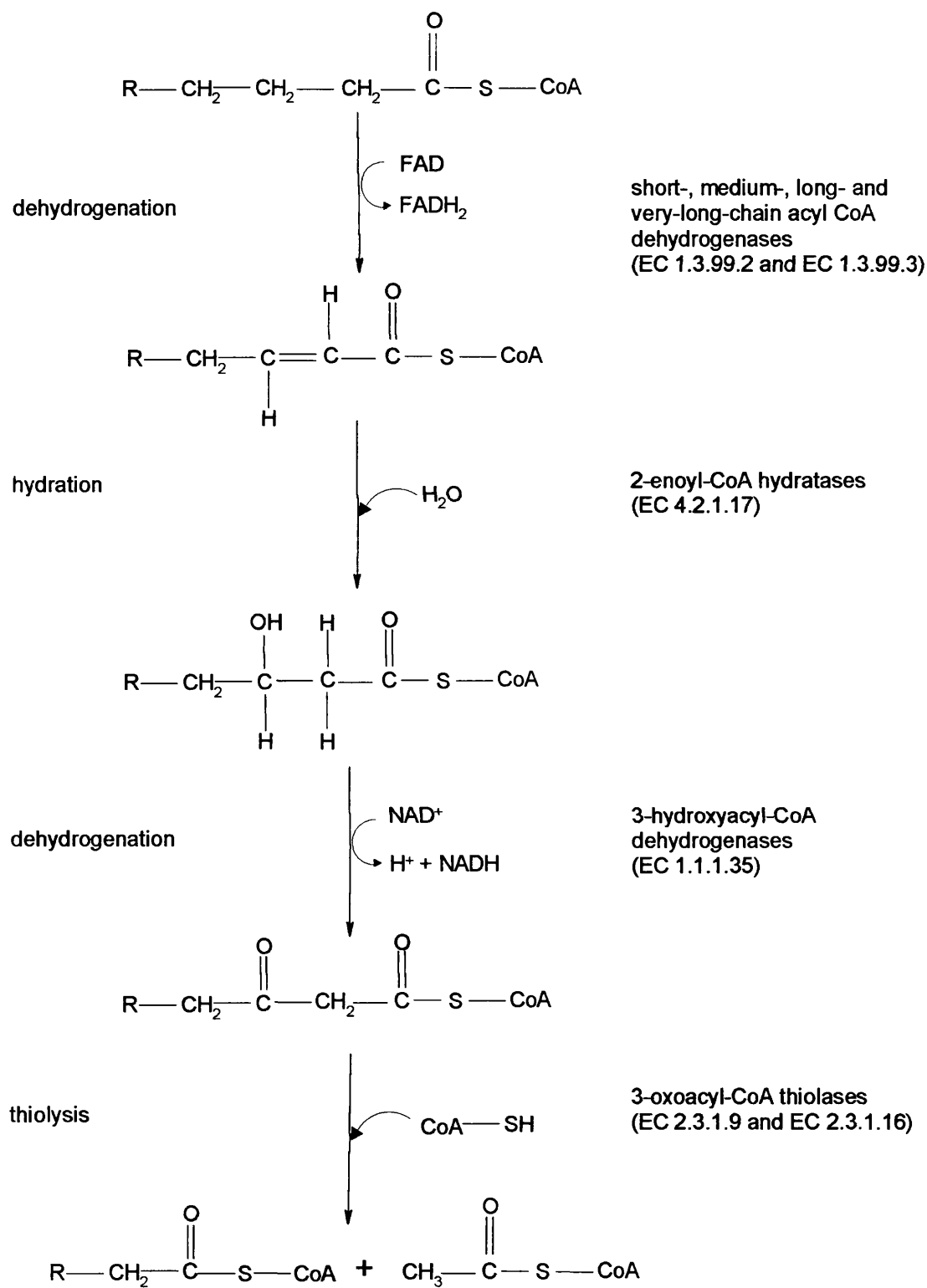
immunologically indistinguishable product, which implies that, unlike CPT I, CPT II appears not to have tissue specific isoforms (Woeltje *et al.*, 1990; McGarry *et al.*, 1991). Others, however, have found evidence which suggests that although CPT II in all rat tissues may be of approximately the same M_r , there may actually be immunologically distinct isoforms in different tissues (Kolodziej *et al.*, 1992).

Defects have been reported for each of the stages of transport of fatty acids into mitochondria, recently reviewed by Bonnefont *et al.*, (1999) and Brivet *et al.*, (1999). In brief, for CPT I deficiencies, only defects of L-CPT I have been documented. These are characterized by recurrent episodes of Reye's-like Syndrome (considered in more detail in Chapter 7). Severe muscular and cardiac problems are associated with episodes of fasting hypoglycaemia in defects of carnitine transport and translocase. CPT II deficiency has several clinical presentations. In adults, CPT II deficiency presents as exercise intolerance, whilst the infantile-type CPT II deficiency presents as severe attacks of hypoketotic hypoglycemia, occasionally associated with cardiac damage commonly responsible for sudden death before one year of age (Bonnefont *et al.*, 1996; Wieser *et al.*, 1999). Brain and kidney dysorganogenesis are frequently seen in the neonatal-onset CPT II deficiency and are usually fatal early in life.

1.2.5 The reactions of mitochondrial β -oxidation

Acyl-CoA molecules are progressively degraded by the reactions of the β -oxidation spiral. Each turn through the spiral produces two-carbon fragments of acetyl-CoA, while the parent acyl-CoAs are progressively shortened and undergo further β -oxidation (Knoop, 1905). The series of four types of enzyme-catalysed reactions, with multiple enzymes, each specific for different fatty acid chain-lengths, for each of the steps, is summarised in Scheme 1.3.

The first reaction in each round of degradation is the oxidation of acyl-CoA. This step is catalysed by short-, medium-, long- and very-long-chain acyl-CoA dehydrogenases (EC 1.3.99.2 and EC 1.3.99.3), which are active with fatty acids of chain lengths C_4 and C_6 ; C_4 to C_{12} ; C_8 to C_{20} and C_{12} to C_{22} respectively. The enzymes are all tetramers, with similar molecular weights and similar amino acid compositions (Furuta *et al.*, 1981; Finocchiaro *et al.*, 1987; Ikeda *et al.*, 1985;

Scheme 1.3 Reactions of β -oxidation

Izai *et al.*, 1992). FAD is bound to the enzymes and is reduced to FADH₂ at the same time as a 2-enoyl-CoA is formed from the corresponding saturated ester. The reduced enzyme is reoxidised by a second flavoprotein, the electron transfer flavoprotein (Crane *et al.*, 1956). This flavoprotein then feeds electrons into the electron transport (respiratory) chain, donating electrons to ETF:ubiquinone oxidoreductase and hence to ubiquinone (Ramsay *et al.*, 1987). Ubiquinone is thereby reduced to ubiquinol, which delivers its reducing equivalents to Complex III of the respiratory chain. The reactions of the respiratory chain are considered in more detail in Chapter 7 and Figure 7.1.

The hydration of the 2-enoyl CoA by two 2-enoyl-CoA hydratases (EC 4.2.1.17) is the second reaction in the β -oxidation series (Hass *et al.*, 1969). These hydratases have overlapping chain-length specificities. The third reaction is a second dehydrogenation/oxidation step, and generates NADH and 3-oxo-acyl-CoA. This reaction is catalysed by 3-hydroxyacyl-CoA dehydrogenases (EC 1.1.1.35), which, again, have overlapping chain length specificities (Uchida *et al.*, 1992). The final step of the pathway involves a thiolysis of 3-oxoacyl CoA by a second molecule of CoA. This reaction is catalysed by 3-oxoacyl-CoA thiolases (EC 2.3.1.9 and EC 2.3.1.16) and produces an acyl-CoA shortened by two carbons and a corresponding acetyl-CoA (Gehring *et al.*, 1968).

Whilst the individual reactions of β -oxidation, as detailed above, have been known for some time, their structural and functional relationships are still incompletely understood. The enzymes of the β -oxidation series of reactions are, however, believed to be organised in a loose complex (Stanley *et al.*, 1975). Indeed, relatively recently, a trifunctional protein complex has been described, which comprises long-chain 2-enoyl-CoA hydratase, long-chain 3-hydroxyacyl-CoA dehydrogenase and 3-oxoacyl-CoA thiolase activities (Carpenter *et al.*, 1992; Luo *et al.*, 1993; Eaton *et al.*, 1996). Trifunctional protein deficiency, a potentially fatal disorder, may be one of the most common β -oxidation disorders (cases reviewed in Jackson *et al.*, 1992; Wanders *et al.*, 1992).

The activities of acyl-CoA dehydrogenases have been shown to exhibit some changes during development (Bailey *et al.*, 1973; Chalk *et al.*, 1983; Carroll *et al.*, 1989). In addition, enoyl-CoA hydratase, 3-hydroxyacyl-CoA dehydrogenase, and oxoacyl-CoA thiolase also show increased activity following birth. These changes,

however, are probably not as significant as those seen for CPT I or mHMG-CoA synthase (Bailey *et al.*, 1973; Chalk *et al.*, 1983; Quant *et al.*, 1989,1990,1991; Lascelles *et al.*, 1997,1998).

Polyunsaturated fatty acids require auxiliary enzymes systems to undergo β -oxidation due to the specificities of the enoyl-CoA hydratases, which do not act on 3-enoyl-CoA esters and of hydroxyacyl dehydrogenases, which are stereospecific for the L-3-hydroxyacyl CoA isomer. These auxiliary isomerases and reductases exist in several isoforms, which are still to be fully identified and characterised at the molecular level.

In the final step of the β -oxidation spiral, fatty acids with an odd number of carbons yield the three-carbon molecule, propionyl-CoA (which enters the Krebs cycle following its conversion to succinyl-CoA) and the two-carbon molecule, acetyl-CoA. Fatty acids with even chain numbers produce two acetyl-CoA molecules (Lipmann, 1953). The acetyl-CoA molecules have three potential metabolic fates, transesterification to acetyl-carnitine, the Krebs cycle or the 3-hydroxy-3-methylglutaryl-CoA cycle (HMG-CoA cycle). Under conditions of high oxaloacetate concentrations, acetyl-CoA is condensed to citrate and thus enters the Krebs cycle. When the oxaloacetate concentration is low, acetyl-CoA is directed towards the formation of ketone bodies, *via* the reactions of the HMG-CoA cycle. These different metabolic fates of acetyl-CoA will now be considered.

1.2.6 Transesterification

Acetyl-CoA may undergo transesterification to acetyl-carnitine by carnitine acetyltransferase (CAT) (E.C. 2.3.1.7) (Figure 1.1). Intramitochondrial acetyl-carnitine leaves mitochondria *via* the carnitine acyl-carnitine translocase and the cell *via* the plasma membrane carnitine transporter. Acetyl-carnitine can be taken up and utilized in muscle (Bartlett *et al.*, 1989) and brain (Kuratsune *et al.*, 1997). However, in neonatal rats this may not be quantitatively important as a circulatory product of hepatic β -oxidation (Eaton *et al.*, 1999(a)).

1.2.7 The reactions of the Krebs cycle

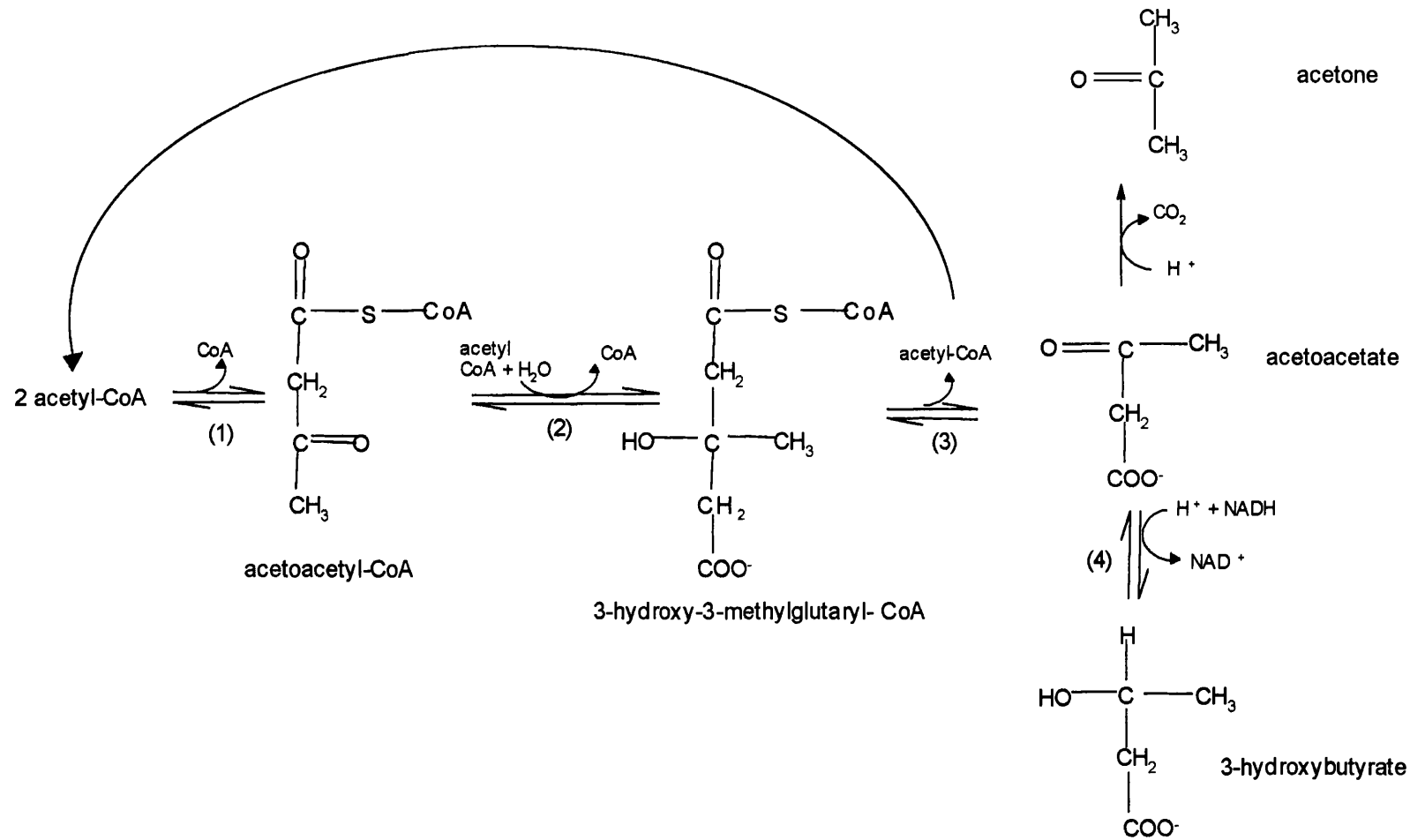
The reactions of the Krebs or tricarboxylic acid cycle (TCA cycle) were first proposed by Krebs (1937) under the name "citric acid cycle", and described the

intermediary stages of the oxidation of carbohydrate in pigeon breast muscle. The essential features of this original scheme remain unchanged. The cycle produces reducing equivalents to be delivered to the respiratory chain and supplies a series of precursor molecules that may be used in biosynthetic pathways.

The reactions of the Krebs cycle may be summarised as follows: in a reaction catalysed by citrate synthase, the acetyl group produced by β -oxidation may enter the Krebs cycle and condense with oxaloacetate, forming the six-carbon molecule citrate. Isomerisation of citrate by aconitase, forms isocitrate, which is then oxidized and decarboxylated to α -oxoglutarate by isocitrate dehydrogenase. α -oxoglutarate undergoes oxidative decarboxylation by the α -oxoglutarate dehydrogenase complex, forming succinyl-CoA. Succinyl-CoA synthetase catalyses the cleavage of the thioester bond of succinyl-CoA, thus generating succinate and one GTP or ATP. Succinate is oxidized to fumarate by succinate dehydrogenase, which is imbedded in the inner mitochondrial membrane and is directly linked to the respiratory chain. This reaction also generates FADH_2 . Malate is formed by the hydration of fumarate by fumarase. Finally, malate is oxidized by malate dehydrogenase, regenerating oxaloacetate. Overall, the two carbons of acetyl-CoA enter the cycle as an acetyl unit and two carbons leave the cycle in the form of two molecules of CO_2 . In addition, three moles of NADH and one of FADH_2 are produced. When the electrons from these carriers are donated to molecular oxygen in the electron transport chain, a large amount of free energy is liberated, which can be used to generate ATP.

1.2.8 The reactions of the 3-hydroxy-3-methylglutaryl-CoA cycle

Alternatively, acetyl-CoA may enter the HMG-CoA cycle to form the short-chain (4-carbon) organic acids, acetoacetate and 3-hydroxybutyrate, and the 3-carbon acetone (Scheme 1.4). Collectively (although not entirely chemically correct) these entities are known as ketone bodies. As indicated in Scheme 1.4, two molecules of acetyl-CoA can condense to form acetoacetyl-CoA in a reaction catalysed by acetoacetyl-CoA thiolase (EC 2.3.1.9). Acetoacetyl-CoA reacts with a further acetyl-CoA (catalysed by HMG-CoA synthase (EC 4.1.3.5)) to form 3-hydroxy-3-methylglutaryl-CoA (HMG-CoA). This condensation reaction has a favourable equilibrium owing to the hydrolysis of a thioester linkage. Cleavage of the HMG-CoA, catalysed by HMG-CoA lyase, (EC 4.1.3.4), results in the formation of acetyl-CoA and acetoacetate.



Scheme 1.4 Reactions of the 3-hydroxy-3-methylglutaryl-CoA cycle

Formation of the short-chain organic acids, acetoacetate and 3-hydroxybutyrate, and acetone. (1) acetoacetyl-CoA thiolase (2) HMG-CoA synthase (3) HMG-CoA lyase (4) 3-hydroxybutyrate dehydrogenase. Acetone is formed by the spontaneous decarboxylation of acetate.

An alternative route for the conversion of acetoacetyl-CoA into acetoacetate is by deacylation, which, as in the reaction detailed above, also involves the enzyme acetoacetyl-CoA thiolase. However, only a small proportion of ketone bodies are formed from this pathway in neonatal rat liver (Lockwood *et al.*, 1971). Acetone can be formed by the slow spontaneous decarboxylation of acetoacetate (Guthrie *et al.*, 1972). However, it is not metabolised further, being excreted or exhaled, and its contribution to ketogenesis is not thought to be significant (Quant, 1994).

3-Hydroxybutyrate may be formed by the reduction of acetoacetate, which is catalysed by 3-hydroxybutyrate dehydrogenase (EC 1.1.1.30). In the course of this reaction, NADH is oxidized to NAD⁺. The ratio of 3-hydroxybutyrate to acetoacetate depends on the NADH/NAD⁺ ratio in mitochondria; the higher this ratio, the higher the ratio of 3-hydroxybutyrate to acetoacetate.

During the neonatal period, in addition to the liver, other tissues such as the intestine (Asins *et al.*, 1995) and kidney (Thumelin *et al.*, 1993) can contribute to ketone body production. However, these tissues also utilize ketone bodies, whereas the liver only produces and exports them. Overall, therefore, the liver contributes more to ketone body synthesis in suckling rats than other tissues (Arias *et al.*, 1997).

1.2.9 Ketone body utilization

Acetoacetate and 3-hydroxybutyrate formed in the mitochondrial matrix may be transferred to the cytosol by simple diffusion across the mitochondrial membranes. Some acetoacetate may leave the mitochondria in an exchange mechanism with pyruvate on the monocarboxylate carrier (Halestrap *et al.*, 1978; Robinson *et al.*, 1980). Ketone bodies diffuse readily into the blood and are carried to extra-hepatic tissues. Whilst oxidation to CO₂ is a major fate of ketone bodies in peripheral tissues, ketone bodies may also be used for lipid or sterol synthesis (Figure 1.2). The physiological roles of ketone bodies are considered further in Section 1.3.1.

The first step in the utilization of acetoacetate is its conversion into acetoacetyl-CoA. In the mitochondria, this reaction is catalysed by 3-oxoacid-CoA transferase (E.C. 2.8.3.5), the activity of which is 10-fold greater than the activity of acetoacetyl-CoA synthase, which catalyses this conversion in the cytosol (Robinson *et al.*, 1980).

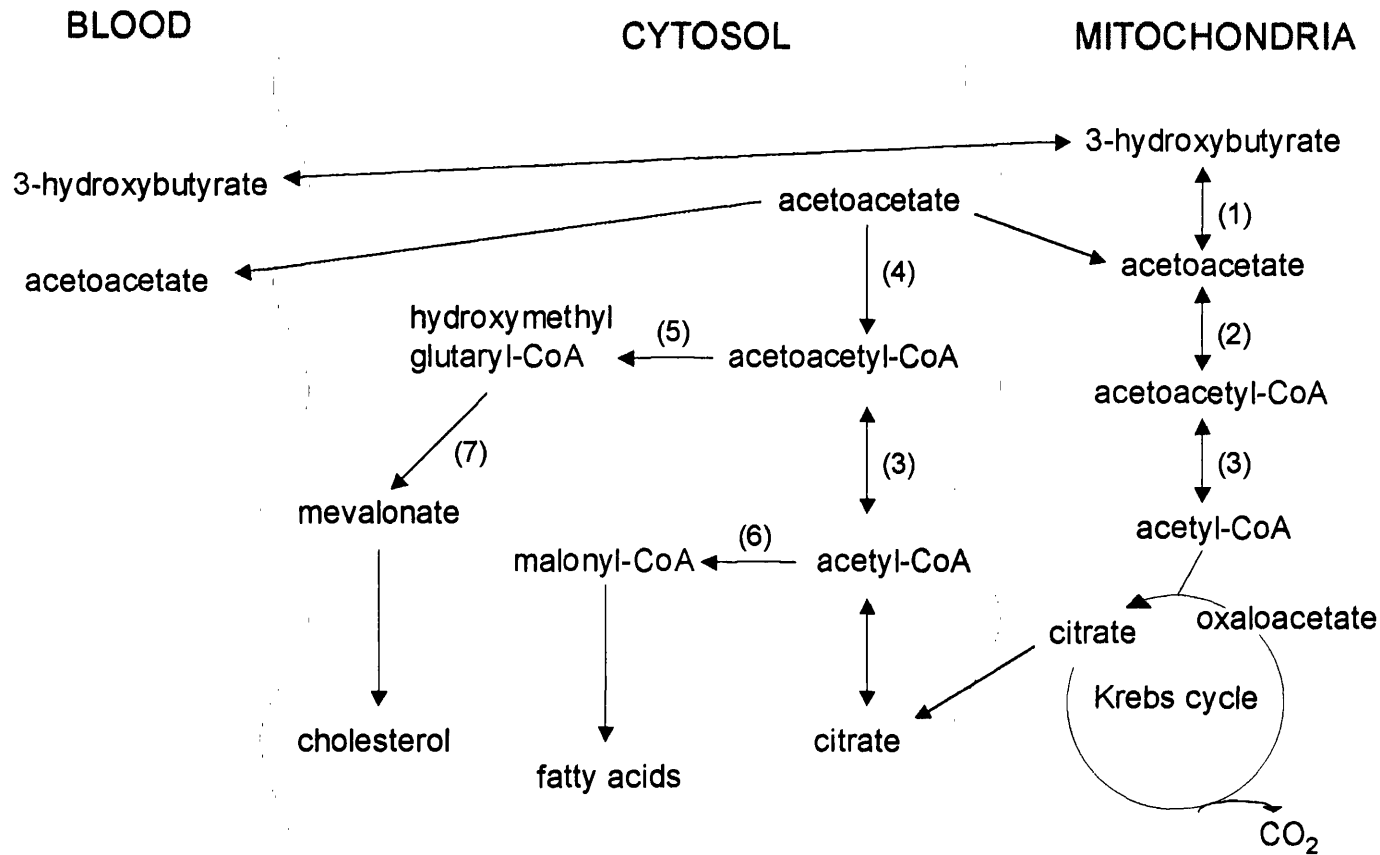


Figure 1.2 Summary of reactions of ketone body utilization in extrahepatic tissues

Adapted from Robinson *et al.*, (1980). Acetoacetate produced from the oxidation of fatty acids and ketogenesis in the liver is exported from mitochondria and then activated in the cytosol to acetoacetyl-CoA or exported in the blood. The acetoacetyl-CoA is available for sterol or fatty acid synthesis. (1) 3-hydroxybutyrate dehydrogenase (2) 3-oxoacid-CoA transferase (3) mitochondrial or cytosolic acetoacetyl-CoA thiolase (4) acetoacetyl-CoA synthase (5) cHMG-CoA synthase (6) acetyl-CoA carboxylase (7) HMG-CoA reductase.

In a reaction catalysed by either mitochondrial or cytosolic acetoacetyl-CoA thiolase, (E.C. 2.3.1.9) depending on the compartment, acetoacetyl-CoA is cleaved to form acetyl-CoA. Within the mitochondria, this is then condensed to form citrate and enters the Krebs cycle.

Alternatively, when citrate levels are high, it may be transported to the cytosol, where it is cleaved by ATP-citrate lyase (E.C. 4.1.3.8), to provide acetyl-CoA for lipid synthesis. In the cytosol, acetoacetyl-CoA combines with acetyl-CoA, in a reaction catalysed by cytosolic cHMG-CoA synthase (E.C. 4.1.3.5), to form HMG-CoA, which is used for sterol synthesis. Thus, HMG-CoA synthase is also present in two different compartments: the cytosol and the mitochondria.

Many tissues, for example the kidney, brain, mammary gland, skeletal muscle and heart are capable of oxidizing ketone bodies at appreciable rates (Patel *et al.*, 1975; Robinson *et al.*, 1980). The liver, however, has low levels of 3-oxoacid CoA-transferase and thus ketone bodies produced by the liver are exported for oxidation by extra-hepatic tissues, rather than being metabolised within the liver itself (McGarry, 1980). In the mammary gland, ketone bodies are also involved in lipogenesis and in the brain they are used for myelin formation (reviewed in Robinson *et al.*, 1980). The physiological roles of ketone bodies are considered further in Section 1.3.1.

1.2.10 Control distribution over the pathways of hepatic fatty acid oxidation and ketogenesis

There are several potential sites for intra-hepatic control over the pathways of fatty acid oxidation and ketogenesis. These include the activation of long-chain fatty acids, the various steps of the transport system *via* which long-chain acyl-CoAs enter the mitochondria (i.e. CPT I, the acyl-carnitine/carnitine translocase, CPT II), the reactions of β -oxidation, the HMG-CoA cycle and/or the Krebs cycle, and the efflux of ketone bodies from mitochondria (Quant, 1994). Historically, however, intra-hepatic control over the pathways of fatty acid oxidation and ketogenesis has been considered to reside at the level of the entry of acyl groups into the mitochondrion, with CPT I being considered as the “rate-limiting” step at all developmental stages and (patho)physiological conditions (reviewed in Chapter 3). However, the role of CPT I in control over ketogenesis has recently been questioned (reviewed in Chapter 3). The work presented in this thesis further questions these

assumptions, and suggests that the level of control exerted by CPT I, over fatty acid oxidation and ketogenesis, changes with development, substrate and clinical status. This is considered in detail in Chapters 3 to 6.

1.3 Physiological and clinical significance of the pathways of hepatic fatty acid oxidation and ketogenesis

1.3.1 The role of ketone bodies

Geelmuyden (1897) showed that ketone bodies were formed from fatty acids and although ketone bodies were once considered only as metabolic degradation products associated with uncontrolled diabetes or starvation states, with uncertain physiological value to the whole organism, (Grenville *et al.*, 1968; reviewed in McGarry *et al.*, 1980), it is now known that they have important roles at some stages of development and in certain metabolic states.

Under “normal conditions” in the suckling rat, ketone bodies are a major metabolic fuel of extrahepatic tissues, including the brain (Hawkins *et al.*, 1971, Nehlig *et al.*, 1993, 1996). During the suckling period, the brain has a higher total activity of the enzymes of ketone body utilization than other peripheral tissues in rats (Robinson *et al.*, 1980; Cullingford *et al.*, 1997). Furthermore, the immature brain of the suckling rat is able to take up ketone bodies approximately three times more efficiently than the mature brain and a similar situation exists in humans (Robinson *et al.*, 1980). In the first few days of extrauterine life, ketone bodies can account for one quarter of the neonatal basal energy requirement (Hamosh, 1991). Ketone bodies are also an important energy source during fasting. For example, during periods of prolonged fasting in adult humans, almost two-thirds of the brain’s energy is supplied through the oxidation of ketone bodies, which, unlike the fatty acids from which they are derived, can cross the blood-brain barrier (Owen *et al.*, 1967; Hawkins *et al.*, 1971).

Ketone bodies are also important in amino acid and lipid biosynthesis (Nehlig *et al.*, 1993, 1996). For example, they provide the carbon precursors for myelin sheath synthesis, necessary for the human brain to continue to mature during the first two years of infant life (Robinson *et al.*, 1980; Clark, 1993). They also provide the carbon skeleton for phosphatidylcholine and act as precursors of surfactant lipids, both of which are essential for lung function in the newborn (Yeh *et al.*, 1985). In addition, ketone bodies have also been implicated in reducing the seizures in several forms of epilepsy (Lennox, 1928, Dodson *et al.*, 1976). Although the precise

mechanisms are unclear, ketogenic diets are thought to control certain types of seizures through a fundamental change in the brain's metabolism from that of a glucose-based energy metabolism to that which utilizes ketone bodies (Swink *et al.*, 1997). Additionally, raised concentrations of ketone body bodies alter the concentration of key amino acid neurotransmitters, which would effect seizure-susceptible neurons (Cullingford *et al.*, 1999).

1.3.2 Fluctuation in ketone body concentrations

The concentration of blood ketone bodies represents the balance between the rate of production and the rate of utilization by peripheral tissues. Normoketonaemia (acetoacetate plus 3-hydroxybutyrate) in the fed state has been defined as <0.2mM (Williamson, 1992). However, even this "normal" level varies considerably among individuals due, for example, to differences in basal metabolic rate, hepatic glycogen stores and differences in the mobilization of amino acids from muscle proteins (reviewed in Mitchell *et al.*, 1995). Diurnal variations in ketone body concentrations occur, for example, concentrations are low during the morning, increase later in the day and reach a maximum at midnight (Robinson *et al.*, 1980). Fluctuations in the concentration of ketone bodies in response to changes in physiological state are also normal. For example, ketosis (hyperketonemia), where levels are >0.2mM (Williamson, 1992) is normal during fasting (McGarry, 1980, 1995), after prolonged exercise (Koeslag *et al.*, 1980; Balasse *et al.*, 1989), when a high fat diet is consumed, or during the neonatal period (Hawdon *et al.*, 1992). In addition, there is a slight elevation of maternal ketone body levels during pregnancy (Paterson *et al.*, 1967). Typically, these raised concentrations indicate that fatty acid energy metabolism is active and that the pathways of fatty acid degradation are intact. In rare cases, however, raised concentrations may reflect defects in the pathways of ketone body utilization or, for example, overproduction of ketone bodies in juvenile-onset diabetes.

Extreme fluctuations in the concentration of ketone bodies, however, may result from abnormalities of ketone body metabolism (reviewed in Mitchell *et al.*, 1995). In brief, such abnormalities can present in three ways: (i) ketoacidosis, (ii) hypoketotic hypoglycaemia; or (iii) abnormal 3-hydroxybutyrate : acetoacetate ratio

(i) The extremely elevated concentrations of ketone bodies observed during ketoacidosis (>7mM, Williamson, 1992) may become life-threatening, since the blood cannot buffer against such a high acid load. Raised concentrations of ketone

bodies may be indicative of a range of medical conditions, including: diabetes, ketotic hypoglycemia of childhood, corticosteroid/growth hormone deficiency and intoxication with alcohol/salicylates (reviewed in Mitchell *et al.*, 1995).

(ii) Abnormally low concentrations of ketone bodies can also present a problem. Hypoketotic hypoglycaemia, a state in which ketone bodies are not elevated in response to hypoglycaemia, may be indicative of hyperinsulinism. This condition may be found in infants whose mothers have poorly controlled diabetes (Hawdon *et al.*, 1993). Alternatively, low concentrations of ketone bodies may be suggestive of one of several inborn errors of metabolism, where there may be a total or partial enzyme deficiency in the pathways of fatty acid oxidation and ketogenesis (Morris *et al.*, 1997, 1998; Mitchell, 1998). The presenting symptoms for inborn errors are rarely diagnostic and prior to identification of a specific defect, complex biochemical and genetic investigations are needed. For example, inborn errors of fatty acid oxidation result in metabolite build-up proximal to the enzyme defect and a defect at any stage of β -oxidation will increase formation of the corresponding acyl-carnitines (Saudubray *et al.*, 1992) thus acyl-carnitine profiles are of importance with regard to the diagnosis of inborn errors of β -oxidation. Fatty acids that accumulate in β -oxidation defects can be metabolic toxins due to their detergent properties, which, for example, may alter membrane fluidity. It has been suggested that in some cases this may be a cause of Sudden Infant Death Syndrome (Duran *et al.*, 1986, Emery *et al.*, 1988; Harpey *et al.*, 1990).

There are also groups of infants who may fail to produce the elevated concentrations of ketone bodies that are normally observed during the neonatal period (Hawdon *et al.*, 1992, 1993). These groups include pre-term infants, small-for-gestational-age (SGA) infants (Quant *et al.*, 1998), those who experience perinatal asphyxia and newborns who have undergone surgery and require intravenous feeding via total parenteral nutrition (TPN). A common surgical problem associated with infants on long-term TPN is sepsis (Pierro 1996, 1998) and abnormalities in ketone body metabolism are frequently observed during this clinical condition. For example, ketone body production during sepsis may be suppressed, despite raised concentrations of glucagon, cortisol and catecholamines. Furthermore, such suppression may not be explained by increased plasma insulin concentrations alone (Neufeld *et al.*, 1976; Kaminski *et al.*, 1979; Wannemacher *et al.*, 1979; Neufeld *et al.*, 1980; Vasconcelos *et al.*, 1987). The cytokines produced in response to septic shock are believed to have a direct antiketotic effect (Samra *et*

al., 1996). Sepsis is considered further in Chapters 6 and 7.

All of the groups of infants mentioned above may be at risk of neurological impairment and metabolic complications. Additional stress, in the form of fasting, cold exposure or infection could threaten the survival of these infants (Quant *et al.*, 1993). Furthermore, epidemiological and animal studies suggest that “at-risk groups” may be predisposed to certain diseases during childhood and adult life, such as persistent hyperinsulinaemia of infancy and maturity onset-diabetes (Barker, 1994; Desia *et al.*, 1995; Aynsley-Green *et al.*, 1997).

(iii) Changes in the 3-hydroxybutyrate : acetoacetate ratio may result from fasting or clinical situations, such as hypoxia-ischaemia, where the hepatic mitochondrial matrix is in a reduced state. The more reduced the matrix, (i.e. the higher the NADH:NAD⁺ ratio) the higher the 3-hydroxybutyrate : acetoacetate ratio. High ratios may indicate defects in the respiratory chain (reviewed in Mitchell *et al.*, 1995).

1.4 Metabolic Control Analysis

1.4.1 General introduction

Metabolic control analysis (MCA) was developed simultaneously by Kacser and Burns (1973) and Heinrich and Rapoport (1974(a),(b)). It has been reviewed both theoretically and experimentally by Westerhoff (1984) and Fell (1992). Metabolic control analysis provides both the framework and language to examine metabolic control in complex, dynamic systems, in a quantitative manner (Quant, 1993). Although aspects of MCA, like any experimental and/or theoretical tool, may have limitations, it does provide a foundation on which a better understanding may be developed than was previously provided by the more traditional, qualitative approaches (Fell, 1997). For example, Kell and Mendes (1999) proposed that MCA can be used to provide an “approximation” to a more complex reality.

Historically, descriptions of flux through specific pathways have been qualitative and have centred on the concept of single, rate-limiting steps (Blackman, 1905). This traditional approach considers that flux through successive steps in a pathway is limited by the pace of the slowest factor. Such rate-limiting steps, which have frequently been considered to control flux through a pathway under all conditions, have been characterised as detailed below (Thomas *et al.*, 1998(b)):

- an enzyme catalysing a far-from-equilibrium reaction;
- an enzyme with low activity compared to other enzymes in the pathway;
- an enzyme which is subject to regulation by metabolites other than substrates;
- an enzyme which is generally situated near the start of the pathway or at a branchpoint; and
- variations in the activity of a rate-limiting step would be expected to change pathway flux, whilst varying the activity of any other step would not be expected to change flux.

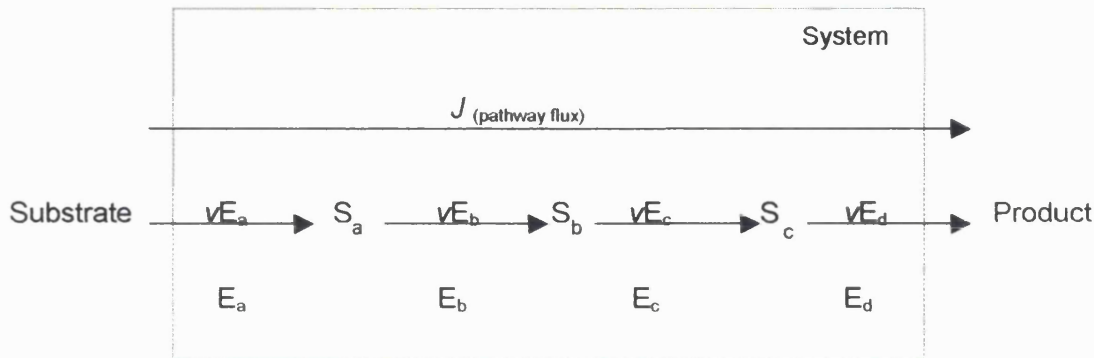
In this traditional model, the rate of the whole pathway could be altered by changing the activity of one particular enzyme in the pathway. It was considered, therefore, that identification of this rate-limiting step, could fully describe the control structure of the whole pathway. However, the defining statements considered above may not necessarily hold true during quantitative investigations into control distribution in pathways. For example, there is little evidence to date to support the idea that a significant proportion of control is always found at the beginning of a pathway (Fell *et al.*, 1995). Indeed, in contradiction to this idea, a high level of control over flux through the mammalian pathway of serine synthesis, is exerted by phosphoserine phosphatase, which is the last enzyme in the pathway (Fell *et al.*, 1988). Furthermore, a 3.5-fold increase in expression of the activity of phosphofructokinase, which is often cited as the rate-limiting enzyme of glycolysis in yeast and which should, according to these traditional views, lead to increases in the rate of the pathway, had no significant effect on the anaerobic glycolytic flux (Heinisch, 1986). The qualitative label of “rate-limiting enzyme”, which has been a central concept in traditional biochemistry, became one of the first “victims” of MCA, since this latter approach demonstrates both theoretically and experimentally that control over pathway flux is shared amongst all the steps in a pathway (Kacser, 1995; Thomas *et al.*, 1998(a),(b)). The following section will introduce some of the central themes of MCA.

1.4.2 Flux control coefficients

The qualitative nature of the traditional approaches makes comparisons of the relative contributions of specific steps in the control of pathway flux difficult to evaluate. In contrast, MCA enables the degree of control of any given step in a metabolic pathway over the rate (flux) of the pathway to be quantified by its flux control coefficient (originally termed *sensitivities* (Kacser & Burns, 1979)). Since this

provides a quantitative scale for the influence of an enzyme on a metabolic flux, it replaces the qualitative categories “rate-limiting” and “not rate-limiting” (Fell, 1997).

For simplicity, consider the following general linear pathway in Scheme 1.5:



Scheme 1.5 General linear pathway

The system is represented by the green box. Further detail is provided in the main text.

The importance of each step in the defined pathway (E_a, E_b etc.) in controlling pathway flux (*J*) in a steady state, is given its own flux control coefficient C_E^J . Therefore, in the simple system described in Scheme 1.5, the following flux control coefficients may be calculated: $C_{E_a}^J$, $C_{E_b}^J$, $C_{E_c}^J$ and $C_{E_d}^J$. It should be noted, however, that there are as many flux control coefficients as there are steps in a pathway, which may include transport processes and non-catalysed reactions in addition to enzymatic reactions (Salter *et al.*, 1994). Furthermore, ‘hidden’ branches can also have flux control, if the system has not been correctly described.

The flux control coefficient may be defined as a fractional change in flux as a consequence of a fractional change in enzyme/step activity, where the fractional changes are very small (i.e. tend to zero) and the defined system has been allowed to settle to a new steady state:

$$C_{E_a}^J = \frac{\delta J / J}{\delta vE_a / vE_a}$$

Equation 1.1:

- where: C_{Ea}^J describes the flux control coefficient of step E_a on steady-state flux J ;
- $\delta J/J$ stands for the fractional change in pathway flux;
- $\delta v_{Ea}/v_{Ea}$ stands for the fractional change in the activity of the enzyme/step under study, in this example, E_a (footnote¹);
- δ represents infinitesimal changes, where the fractional changes are very small (i.e. tend to zero).

Since control analysis deals with infinitesimal changes, flux control coefficients can not usually be used to describe or predict the effects of *large* changes, although this has been considered experimentally and theoretically (Small *et al.*, 1993).

Quantitative values for flux control coefficients can, therefore, be obtained from experimental access to appropriate flux assays and a procedure for manipulating enzyme/step activity, such as titration with specific inhibitors, to reduce the activity and/or effective concentration of the enzyme/step under study (Groen *et al.*, 1982; Duszynski *et al.*, 1982), whilst all the other conditions are kept constant. In practice, however, a means of specifically modulating enzyme/step activity and/or concentration is not always available (an example is considered in Section 1.4.7). Furthermore, measurement of flux is often complicated by the interconnection of metabolic processes. However, fluxes that produce a metabolic end-product can be measured relatively easily, for example, Krebs cycle carbon flux can be assessed by accumulation of CO_2 .

¹ Flux control coefficients may also be defined in terms of changes in the concentration of the enzyme, for example, by genetic manipulation.

$$C_{Ea}^J = \frac{\delta J}{J} \bigg/ \frac{\delta [Ea]}{[Ea]}$$

Where C_{Ea}^J describes the flux control coefficient of step E_a on steady-state flux J ; $\delta J/J$ stands for the fractional change in pathway flux; $\delta [Ea]/[Ea]$ stands for the fractional change in the concentration of the enzyme under study, in this example, E_a ; δ represents infinitesimal changes, where the fractional changes are very small (i.e. tend to zero).

Generally, enzyme activities are expected to be proportional to enzyme concentration, and thus this can be considered as equivalent to titrating with a specific inhibitor, which changes the effective concentration of the enzyme. In rare cases, however, the activity of the enzyme does not relate directly to its concentration (i.e. $v \neq [E]$). In such cases the equation defining the flux control coefficient requires modification (Fell, 1997). It is vital, therefore, to carefully consider the precise form of flux control coefficient used in an analysis.

The numerical value of most flux control coefficients lies between zero (which would signify no control) and one (which would signify high control). Experimental values of control coefficients are frequently much less than one (Fell, 1992) in confirmation of theoretical expectations. In branched pathways, however, values may occur outside this range, i.e. less than zero or greater than one (Mazat *et al.*, 1996). When interpreting values for flux control coefficients, it is important to realise that they are properties of the *defined system* rather than the enzyme(s) themselves, since the importance of each of the enzymes in determining flux through the pathway depends on the kinetic properties of all the enzymes in the system. Therefore, if the pathways under consideration, or the conditions of their measurement, are changed, the numerical values of the flux control coefficients may also change. The numerical values of flux control coefficients are subject to a number of constraints and inter-relationships, for example, the summation theorem (Fell, 1992) which is detailed in the following section.

Although the existence of single, rate-limiting steps is believed to be a rare occurrence, several groups, for example, Salter *et al.*, (1994) have used control analysis to identify candidate enzymes as targets for therapeutic intervention, on the assumption that enzymes with high flux control coefficients have greater potential as effective targets for inhibitory compounds *in vivo* than enzymes with low flux control coefficients. Others have shown experimentally, however, that it is often necessary to change more than one step to achieve an increase/decrease in flux and/or in product (Kacser *et al.*, 1993; Fell, 1998).

Although these are not considered in more detail in this thesis, in the same way that control coefficients express the dependence of a system variable (such as flux) on an internal parameter (such as enzyme activity) a *response coefficient*, R_z^J , can be used to express the dependence of a system variable on an external parameter (such as added inhibitor or hormone). An example relevant to the work presented in this thesis is provided by the work of Makins *et al.*, (1995), where the response of CPT I to malonyl-CoA is considered in a quantitative manner.

1.4.3 The summation theorem

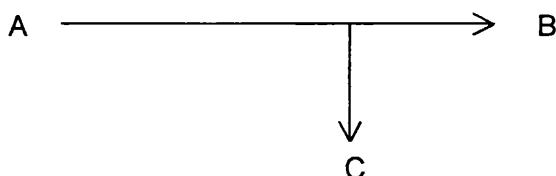
The summation theorem for flux control coefficients was originally derived by Kacser and Burns (1979). It states that the sum of all the flux control coefficients in a pathway is generally one, for example, in the pathway considered previously:

$$\text{Equation 1.2} \quad C_{Ea}^J + C_{Eb}^J + C_{Ec}^J + C_{Ed}^J = 1$$

Which can be written as:

$$\text{Equation 1.3} \quad \sum_{i=1}^n C_i^J = 1$$

The summation theorem allows flux control coefficient(s) to have a value greater than one, when other flux control coefficient(s) within the system are negative. Negative values can be more easily understood by consideration of a branched pathway, where a metabolite may form more than one end product. Consider Scheme 1.6:



Scheme 1.6 General branched pathway

In the above scheme, you may calculate flux control coefficients for pathway flux to product B, ($C_E^{J_B}$). However, in the flux from A there are two branches, one to product B, the other to product C. It can be seen that an increase in any step between A and B would increase flux J_B , giving a positive flux control coefficient, ($+C_E^{J_B}$). Whilst, an increase in any step along the branch to C would decrease J_B , giving a negative flux control coefficient, ($-C_E^{J_B}$).

There are two important consequences of summation theory. Firstly, it suggests that each step in the pathway has a contribution to control flux, i.e. control is multi-step, distributed across all of the steps in the pathway, rather than, as the more traditional views suggest, situated at one single, rate-limiting step. Secondly, this

control may not necessarily be distributed equally amongst the steps; each step may exert different degrees of control and there may be more than one step exerting significant control (Fell *et al.*, 1995).

The earlier example from serine biosynthesis demonstrates these points, since it has been shown that control of this pathway is not entirely at a single step, that it is distributed between the steps, and that the distribution can change with alterations in flux, metabolite and enzyme levels (Fell *et al.*, 1988). Drynan *et al.*, (1996) have also used MCA to show that the distribution of control over pathway flux may change with metabolic state, by applying control analysis on data obtained from hepatocytes isolated from adult rats which had been fed, starved, starved/refed, or starved/insulin treated. Krauss *et al.*, (1996) have also demonstrated changes in control distribution during development, using mitochondria isolated from adult and suckling rats. It was this work which prompted some of the initial investigations presented in this thesis (Chapters 3 and 4).

1.4.4 Elasticity coefficients

The potential of an enzyme to control flux is related to the kinetic property of the enzyme (its elasticity coefficient). Elasticities (or elasticity coefficients) offer a replacement for qualitative statements of “responsiveness” of an enzyme to a metabolite, providing instead quantitative indications of the sensitivity of an enzyme to changes in concentrations of the effector, where the effector might be a substrate, product of the enzyme or an internal or external metabolite (Heinrich & Rapoport, 1974(a),(b); Kacser & Burns, 1979).

Elasticities are defined as the fractional change in the flux through the enzyme caused by a fractional change in the concentration of the effector, with everything else in the system held constant:

Equation 1.4
$$\mathcal{E}_x^a = \frac{\delta v_a}{v_a} \cdot \frac{\delta [x]}{[x]}$$

Where: \mathcal{E}_x^a describes the elasticity coefficient for the effector, X on enzyme/step a;

$\delta v_a / v_a$ stands for the fractional change in local flux through the enzyme/step;

$\delta [x] / [x]$ stands for the fractional change in the concentration of the effector.

Therefore, in contrast to flux control coefficients, elasticities are local properties of the individual *step under consideration* and are not system properties. A positive value for an elasticity coefficient indicates that the effector stimulates the rate of reaction, whilst inhibitors which slow the reaction, have negative values. The magnitude of the numerical value indicates the potency of the effector. Thus, in Scheme 1.5, there will be sets of elasticities which describe the potency of each metabolite to affect each enzyme/step, for example: $\mathcal{E}_{S_a}^{E_a}$; $\mathcal{E}_{S_a}^{E_b}$; $\mathcal{E}_{S_a}^{E_c}$; $\mathcal{E}_{S_a}^{E_d}$; $\mathcal{E}_{S_b}^{E_a}$; $\mathcal{E}_{S_b}^{E_b}$ and so on, (where $E_a, E_b, \text{e.t.c.}$, indicates the step and $S_a, S_b, \text{e.t.c.}$, indicates the metabolite).

1.4.5 The connectivity theorem

The connectivity theorem (also known as the connectivity property) was originally derived by Kacser and Burns (1979). It provides the link between global/system flux control coefficients and local/individual elasticity coefficients. The theorem states that the sum of each flux control coefficient on a particular flux, J , multiplied by its elasticity with respect to X , equals zero (where X might represent $S_a; S_b; S_c, \text{e.t.c.}$), i.e.

$$(C_{E_a}^J \cdot \mathcal{E}_x^a) + (C_{E_b}^J \cdot \mathcal{E}_x^b) + (C_{E_c}^J \cdot \mathcal{E}_x^c) + (C_{E_d}^J \cdot \mathcal{E}_x^d) = 0$$

Equation 1.5

Or, alternatively:

$$\sum_{i=1}^n C_i^J \mathcal{E}_X^i = 0$$

It can be seen, therefore, that a complete set of elasticities (which can be calculated from enzyme kinetic equations or measured experimentally) can give flux control coefficients without experimental analysis, by substitution into the summation and connectivity theorems (Fell, 1997). Furthermore, the connectivity and summation

theorems provide a means of linking the (global) systemic properties of the pathway to the (local) properties of individual enzymes.

For the purposes of this thesis, two complementary approaches to MCA are considered: the “bottom-up” approach and the “top down” approach. As will be seen, the two approaches adopt different strategies for investigating control in complex systems and could potentially achieve the same end goal of complete understanding of the control structure of a defined pathway, if multiple applications of each method were to be carried out.

1.4.6 Bottom-up control analysis

Bottom-up control analysis (BUCA) aims to determine the control coefficients of individual steps (enzymes) over a pathway flux (i.e. individual flux control coefficients, C_{step}^J). Repeated application of BUCA to different enzymes in the pathway and subsequent summation of the contributions of all the individual components enables a full description of the control structure to be determined. It can be seen, therefore, that BUCA starts at the “bottom”, with the detail, and works up towards the behaviour of the whole system. Application of this approach is, however, restricted to the ability to manipulate individual enzyme activities.

1.4.7 Top-down control analysis

In contrast, top-down control analysis (TDCA, also known as ‘modular analysis’ Schuster *et al.*, 1993) starts at the level of the “intact system” and moves down into the detail (Brown *et al.*, 1990; Quant, 1993; Brand, 1996). It aims to determine the control coefficients of blocks of reactions over pathway flux (i.e. group flux control coefficients, $*C_{block}^J$).

In TDCA, the pathway under consideration is conceptually divided into blocks of reactions that produce a given intermediate and into blocks of reactions that consume the intermediate. In this way, complex systems can be simplified to a level that can be analysed and an overview of control structure determined. The system may be linear or branched. As the name implies, repeated application by further subdividing the system into different blocks, around different intermediates enables the control structure of the whole pathway to be determined, although in practice this

might be difficult to achieve (Kell *et al.*, 1999).

One of the main advantages of TDCA is that it can be used in complex physiological situations where the BUCA approach is not appropriate or feasible. BUCA requires a means of manipulating each step under investigation independently of other steps in the pathway. Thus, if there is no specific method of independent manipulation available, BUCA cannot be applied to that particular system. An example relevant to this thesis is mHMG-CoA synthase. At present, specific, independent manipulation of this enzyme is not possible and thus BUCA cannot be performed on this particular step in the pathway of ketogenesis. However, by considering the pathways of fatty acid oxidation, Krebs cycle and the HMG-CoA cycle as separate blocks of reactions, TDCA has been applied to the mitochondrial system (Makins *et al.*, 1994). Although in this instance the system comprises three blocks of reactions, only two perturbations to the system need to be made in order to calculate group flux control coefficients for the whole system. Independent manipulation can be made within the block relating to fatty acid oxidation and within the Krebs cycle block of reactions. In this way, no specific inhibitor for any step in the HMG-CoA cycle is required. This is considered in more detail in Chapter 4, where TDCA is applied to these pathways, in neonatal hepatocytes.

1.4.8 Assumptions underlying the application of MCA

Unless otherwise stated to the contrary and compensated for in the calculations, there are a number of assumptions underlying the application of MCA. They are considered in some depth by Fell (1992), but may be summarised as follows:

- the system under study is a single, connected unit;
- the system is in a stable, steady state;
- metabolites are distributed homogeneously over the enzymes that act on them;
- rates of enzyme action should be directly proportional to enzyme concentration and one enzyme should affect one reaction;
- enzymes do not appear in the analysis as variables but as parameters (i.e. as factors that influence the behaviour of the system, but that can be held constant after it has been altered while the system reaches a new steady state); and
- all metabolites are in the free (unbound) form.

It is also important to ensure that parameter changes are as small as possible to reduce the mathematical bias of the control coefficient estimate but should be large enough to allow detection of the changes in response to these modifications (Pettersson, 1996).

1.5 Overall Aims

By critically analysing the scientific, clinical and theoretical literature to date in earlier sections of this introduction I have shown that whilst the pathways hepatic fatty acid oxidation and ketogenesis are clearly mapped, current understanding of how these pathway fluxes are regulated by effectors or controlled by enzymes/steps is incomplete. Until there is a more complete understanding of the mechanisms of ketogenesis in "normal" infants, for example, it is difficult to understand how and why the mechanisms that regulate and control fatty acid oxidation and ketogenesis are altered in certain clinical conditions (Quant *et al.*, 1998). An investigation into the role of CPT I in controlling these pathways is of clinical significance, since, for example, it continues to attract attention as a potential target in the pharmacological management of clinical conditions such as diabetes (Foley, 1992; Anderson, 1995; Zammit, 1998).

In this thesis, I seek to begin to address these important issues. Specifically, I aim to model (using MCA), report and discuss the control of neonatal hepatic fatty acid oxidation, Krebs cycle and ketogenic fluxes by CPT I under physiological and (patho)physiological conditions, mimicking healthy and diseased states. For ethical and practical considerations it is not feasible to perform such investigations on liver samples from human infants, thus, in the investigations performed and reported in this thesis, rat pups at their peak of suckling (11-13d old) are used to model the human neonate (Girard *et al.*, 1992).

1.5.1 Aims and objectives of Chapter 3: Analysing the role of hepatic mitochondrial outer membrane carnitine palmitoyltransferase in the control of carbon fluxes from palmitate

Although quantitative analyses have been performed in hepatocytes isolated from adult rats to explore the control exerted by CPT I over carbon fluxes through the three pathways of fatty acid oxidation (Drynan *et al.*, 1996), no such studies have been performed in neonatal models. In Chapter 3, therefore, I aim to address the

following question:

- “How much control does CPT I exert over carbon fluxes from palmitate to ketone bodies, carbon dioxide and total carbon products, in suckling rats?”

My objectives are to calculate the relevant individual flux control coefficients from experimentally measured fluxes and activities.

1.5.2 Aims and objectives of Chapter 4: Application of top-down control analysis in hepatocytes to investigate the distribution of control over carbon fluxes in the pathways of fatty acid oxidation, ketogenesis and the Krebs cycle

Whilst quantitative analyses of control structure of fatty acid oxidation in model systems consisting of mitochondria isolated from neonatal rats have been performed (Krauss *et al.*, 1996) it is vital to consider control distribution over these pathways in more ‘physiological systems’, since isolated mitochondria may not necessarily reflect the control distribution in whole cells (Berry *et al.*, 2000). In this chapter, therefore, I aim to further characterise the distribution of control over the pathways of fatty acid oxidation, Krebs cycle, and ketogenesis, in intact hepatocytes isolated from neonatal rats. In contrast to the BUCA performed in the previous chapter, which enabled the control at a specific step to be investigated, in this chapter I perform TDCA, which provides an overview of control structure in these complex pathways. In this way I aim to answer the following question:

- “What control do sections of the pathway, for example, the Krebs cycle block of reactions, or the HMG-CoA cycle block, exert over pathway carbon fluxes?”

To perform such an investigation, I will define the system and equations and calculate the group flux control coefficients from experimentally measured fluxes and activities.

1.5.3 Aims and objectives of Chapter 5: Analysing the role of CPT I in control of carbon flux from medium-chain fatty acids and mixtures of long- and medium-chain fatty acids

In many species, including humans and rats, nutrition *in utero* and in adulthood is

high in carbohydrates and low in fats. In contrast, during the neonatal period, the reverse situation is seen: the neonate is exposed to a diet high in fats and low in carbohydrates. Furthermore, a significant proportion of the fats are of medium-chain length. In Chapter 5, therefore, I aim to investigate the control exerted by CPT I over carbon fluxes through the pathways of fatty acid oxidation and ketogenesis from fatty acid mixtures more relevant to neonates. In this way, I aim to address the following question:

- “How much control does CPT I exert over carbon flux to ketone bodies in a system using different substrates?”

As in Chapter 3, my objectives are to calculate the relevant individual flux control coefficients from experimentally measured fluxes and activities.

1.5.4 Aims and objectives of Chapter 6: Analysing the role of CPT I in control of ketogenic flux in *in vitro* models of neonatal sepsis

Sepsis is part of a broad-ranging clinical syndrome which may progress from bacteraemia to multiple-organ failure and death. Despite medical advances and considerable scientific research, sepsis remains a major clinical problem with a high mortality rate. In this chapter I aim to investigate and report on the development of *in vitro* neonatal hepatocyte models to study the onset and progression of neonatal sepsis, which may be used to answer the following question:

- “How much control does CPT I exert over pathway carbon fluxes in response to clinical conditions, for example, sepsis?”

To achieve this aim, agents known to be involved in the septic response, namely lipopolysaccharide (LPS), tumour necrosis factor (TNF α) and interleukin 6 (IL6), will be added to the hepatocyte isolation procedure. The effect of these agents on resulting cell yield and viability will be reported and discussed. Additionally, I aim to calculate the relevant individual flux control coefficients from experimentally measured fluxes and activities in control and treated hepatocytes.

1.5.5 Aims and objectives of Chapter 7: Effects of lipopolysaccharide and/or cytokines on neonatal oxidative liver metabolism

Historically, there has been controversy relating to the precise effects of sepsis on cellular respiration. Furthermore, there are few investigations into sepsis in the literature which specifically investigate the changes occurring during the early stage of sepsis in neonates. In Chapter 7, therefore, I aim to explore the effect of LPS, $\text{TNF}\alpha$, or a combination of agents, LPS+ $\text{TNF}\alpha$, LPS+ $\text{TNF}\alpha$ +IL6 on total hepatocyte respiration and on the relative contributions of mitochondrial and non-mitochondrial respiration. In addition, I aim to provide a preliminary investigation of the effects of salicylic acid, which has been implicated in the development of Reyes' Syndrome, in this chapter.

Chapter 2

Materials and methods

This chapter provides detail of the principal methods used during the course of the study. Details relating to specific experiments are given in the relevant chapter for ease of reference.

2.1 Materials

2.1.1 Chemicals

L-[*methyl*-³H]carnitine hydrochloride and [1-¹⁴C]palmitic acid were purchased from Amersham Life Sciences (Amersham, Bucks., U.K.) and [1-¹⁴C]octanoate from ICN Pharmaceuticals Limited (Thame, Oxfordshire, U.K.). Bovine serum albumin (BSA) (fatty acid free) was bought from First Link (UK) Limited and Optisorb 1 and Optisorb S from E. G. & G Wallac, Milton Keynes, U.K. Etomoxir (sodium salt) (2-[6-(4-chlorophenoxy)hexyl]oxirane-2-carboxylate) was a gift from Dr L. Agius, University of Newcastle, U.K. All other chemicals were purchased from Sigma Chemical Co. (Poole, Dorset, U.K.), Merck or Boehringer.

2.1.2 Animals

Suckling Wistar rat pups were used for the isolation of hepatocytes and were supplied by B & K Universal Limited (Hull, U.K.) or by Harlan (UK) Limited (Bicester, Oxon, U.K.). As rats open their eyes and start weaning at approximately 15 days (Henning, 1981), 11-13 day old pups were used to ensure the pups were at the peak of their suckling period. Litters were standardised to 10 and the pups were allowed to suckle milk *ad libitum*. Five pups were used per hepatocyte preparation.

2.2 Methods

2.2.1 Isolation of hepatocytes

Hepatocytes were isolated from the livers of 5 suckling rat pups per preparation by

the method of Lorenzo *et al.*, (1986), modified as described below.

Cell preparation solutions:

- (a) stock balanced salt solution
- (b) stock phosphate buffer
- (c) working Krebs Ringer phosphate buffer (KRP)
- (d) working Krebs Ringer bicarbonate buffer (KRB)

Cell preparation solutions comprise:

- (a) 10-fold concentrated stock balanced salt solutions comprising 80g NaCl, 4g KCl and 2g MgSO₄.7H₂O dissolved in 1 litre distilled H₂O and kept at 4°C;
- (b) 100-fold concentrated stock phosphate buffer comprising 2.4g Na₂HPO₄ and 0.4g KH₂PO₄ dissolved in 200ml distilled H₂O and kept at 4°C;
- (c) KRP (50ml stock salt solution, 5ml phosphate buffer in 500ml distilled water, pH 7.4) was prepared daily, and
- (d) KRB (50ml stock salt solution, 5ml phosphate buffer and 12.5ml 1M NaHCO₃ in 500ml distilled water, pH 7.4) was prepared daily. 95%O₂:5%CO₂ was bubbled through the KRB solution. The pH was checked to ensure adequate gas equilibration.

Rat pups were killed by cervical dislocation. Hepatocytes were isolated following a three stage incubation procedure:

- (a) Livers were rapidly excised and washed with approximately 10ml KRP, chopped finely and rapidly, into sections of approximately 2mm³ and transferred to a 100ml conical flask containing "isolation medium" (20ml KRB, 1% bovine serum albumin (BSA)) and 0.5mM ethylene glycol-bis(β-aminoethyl ether) N,N,N',N'-tetra-acetic acid (EGTA). The chopped liver was gassed with 95%O₂:5%CO₂, the flask sealed with a subaseal and placed in a reciprocating water bath at 120 strokes/min, at 37°C for 30min (with further gassing at 15 min).

- (b) At the end of the pre-incubation stage, 2mM CaCl₂, 0.05% collagenase (Clostridiopeptidase A, type IV, E.C. 3.4.2.4.3, from *Clostridium histolyticum*) and 0.0025% DNAase (from bovine pancreas, grade II) were added to the medium and the liver was incubated for a further 30min (regassing at 15min).

In the first stage of the isolation procedure, due to the addition of the chelating agent EGTA, the chopped liver was in a Ca²⁺-depleted environment (Berry *et al.*, 1969, 1983). Ca²⁺ has a complex role in cell adhesion and is essential for desmosomal integrity. A medium lacking Ca²⁺, therefore, results in irreversible cleavage of the desmosomes. In the second stage of the procedure, Ca²⁺ is added back into the medium. This is necessary since it is essential for collagenase activation. Collagenase binds Ca²⁺ tightly (Gallop *et al.*, 1957) and assists in liver disruption by breaking down the collagen-rich intercellular matrix. The presence of DNAase in the medium was essential as it minimized cell 'clumping' by digesting DNA from cells that have lost their integrity.

BSA was included in the "isolation" and "incubation" media since long-chain fatty acids, released during isolation, are bound by complexing with albumin, thus preventing their detergent properties.

- (c) At the end of the second stage, the supernatant was poured into two 15ml centrifuge tubes and centrifuged at 400rpm (34g) for 2 min. The supernatant was removed and the pellet resuspended in 20ml KRB and 1% BSA, CaCl₂, DNAase and collagenase as above and incubated for a further 40min, with regassing at 10min intervals.

During all the incubation stages, the gentle mechanical disruption supplied by incubating flasks in the shaking water bath also assisted cell separation.

The contents of the flask were then poured through a nylon mesh (150 micron), massaged gently with a spatula and washed with 60ml "washing medium" (KRB, 2mM CaCl₂). After approximately 4min the liver disintegrated and the suspension was poured into two 50ml conical centrifuge tubes and centrifuged at 400rpm (34g)

for 2min. After discarding the supernatants, the pellets were resuspended in 60ml washing medium and the centrifugation/resuspension process repeated a further three times. Finally, the two pellets were combined into one tube and resuspended in 30ml "incubation medium" (KRB, 2% (w/v) BSA, 2mM CaCl₂ and 1mM L-carnitine).

Cell yield was estimated using a haemocytometer and cell viability assessed by trypan blue dye exclusion. In this procedure, 0.1ml 0.4% trypan blue, 0.2ml KRB and 0.1ml cell suspension were gently mixed in an Eppendorf tube. This mixture (0.1ml) was added to the haemocytometer by capillary action and examined under a microscope with a 10x eyepiece and 10x objective. In order for the cell suspension to be considered suitable for experimental work, at least 85% of the cells needed to be viable, i.e. excluding trypan blue. Typical cell yields were in the range 30-40 (10⁶ cells) g (wet mass liver)⁻¹.

To assess approximate dry mass, 1ml of cells suspended in 'incubation' medium was added to a pre-weighed microcentrifuge tube. This was centrifuged for 2 min in a bench centrifuge, the supernatant discarded and the pellet dried in an oven 40°C for 4 hours and the tube re-weighed. The difference between the two measurements was taken as an estimate of the dry weight of the cellular material.

2.2.2 Incubation of hepatocytes for the measurement of ¹⁴C-ketone body production and ¹⁴CO₂ release

For the application of BUCA and for one of the manipulations required for TDCA the freshly prepared cells were incubated at a density of 3 x 10⁶ cells in 3ml incubation medium in 25ml conical flasks. These were gassed with 95%O₂:5%CO₂, sealed with subbaseals and placed in a reciprocating water bath for 30min at 37°C (with further regassing at 15min). At the end of this preincubation stage, appropriate etomoxir concentrations (0µM-100µM) were added to each flask. After 10min incubation with the inhibitor, 1ml of the appropriate substrate(s) were added, depending on the type of experiment ([1-¹⁴C]palmitate (0.5mM), [1-¹⁴C]octanoate (2mM), [1-¹⁴C]palmitate (0.5mM):[1-¹⁴C]octanoate (0.33mM), specific details provided in appropriate chapters). For experiments using [1-¹⁴C]palmitate as substrate, small wells containing fanned filter paper were

suspended in the flasks to collect CO₂ (see below). Flasks were regassed, resealed and the incubation continued for 60min. Incubations were terminated by the addition of 400µl of ice-cold 20% perchloric acid (PCA) delivered to the incubation medium via a syringe needle through the subbaseal.

For the manipulation of the Krebs block of reactions, required for the application of TDCA (Chapter 4), cells were incubated as described above, except that at the end of the preincubation stage, appropriate malonate concentrations (0mM-15mM) were added to each flask. After 10min incubation with this inhibitor, 1ml [1-¹⁴C]palmitate (0.5mM) was added to each flask.

2.2.3 Assay of ¹⁴CO₂ release in hepatocytes

After addition of PCA to the incubation medium, 200µl Optisorb-1 was added to the wells containing the fanned-filter paper, via a syringe needle through the subbaseal, to collect ¹⁴CO₂ formed during the incubation. The flasks were then cooled and left on ice for 1 hour. The wells (and filter paper) were then transferred to scintillation vials, and 10ml Optisorb S was then added to the vials. ¹⁴CO₂ was assessed from disintegrations per minute (dpm) measured using a Wallac 1410 Liquid Scintillation Counter with internal standardisation.

2.2.4 Assay of ¹⁴C-ketone body production in hepatocytes

The acidified incubation medium was centrifuged for 2min at 6000rpm (7600g) to remove precipitated protein.

The measurement of radiolabelled acid soluble products ([¹⁴C]ASP) formed from [1-¹⁴C]palmitate depends on the insolubility of palmitate in the deproteinized perchloric acid extracts. Therefore, where labelled palmitate (either in isolation, or in the presence of unlabelled octanoate) was used, 0.4ml deproteinised perchloric acid supernatant was added directly to 4ml Ecoscint and dpm measured as described previously. This procedure measures ¹⁴C-label in the ASP, which have been shown to primarily represent ketone body production, rather than Krebs cycle intermediates (Garland *et al.*, 1968; Drynan *et al.*, 1996) or acetyl-carnitine. Any

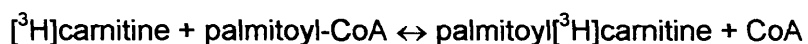
unprecipitated [1-¹⁴C]palmitate was corrected for by the subtraction of appropriate blanks.

The measurement of radiolabelled ASP formed from [1-¹⁴C]octanoate was complicated by the fact that octanoate is partly soluble in deproteinized perchloric acid extracts and only partly removed from perchloric acid extracts by centrifugation. Therefore, where labelled octanoate was used (either in isolation or in the presence of labelled/unlabelled palmitate) the supernatant could not be used directly to assess ketone body production. Unoxidized octanoate was extracted from the ASP using heptane, by a method modified from Fromenty *et al.*, (1989), which has been shown to extract 98% of octanoate into the heptane layer (Spurway, 1995). Several washes were performed to extract the unreacted [1-¹⁴C]octanoate into heptane: for the first wash, 1.5ml of the supernatant was added to 4.5ml heptane, mixed vigorously and centrifuged for 2min at 3000rpm (1900g). The upper heptane layer containing unreacted [1-¹⁴C]octanoate was discarded, and a further 4ml heptane added to each tube and recentrifuged. This washing procedure was repeated two more times. Ketone body production was estimated by adding 1ml of the aqueous layer to 4ml Ecoscint and measuring dpm as described previously. Any unreacted [1-¹⁴C]octanoate was corrected for by appropriate blanks.

In all studies, ketone body production (as assessed by the formation of [¹⁴C]ASP) was examined over 60min. In all cases, the rates of ketone body production were linear with time, indicating that under the experimental conditions employed in these studies, substrate did not become rate-limiting and that hepatocytes remained viable even though they remained ungasged in sealed flasks for 60 min.

2.2.5 Permeabilization of hepatocytes and assay of mitochondrial outer membrane carnitine palmitoyltransferase (CPT I) activity

The CPT I assay used in these studies assessed the activity of the enzyme by measuring the formation of palmitoyl[³H]carnitine from L-[*methyl*-³H]Carnitine and palmitoyl-CoA:



As the plasma membrane represents a barrier to palmitoyl-CoA, the cell membrane was permeabilized by digitonin (see below). The permeability protocol described here enabled access of palmitoyl-CoA to CPT I, but not CPT II, in intact isolated hepatocytes and allowed measurement of CPT I under physiological conditions (Guzmán *et al.*, 1988,1992; Zammit *et al.*, 1988). Although carnitine acyltransferase activity is also present in peroxisomes (Chatterjee *et al.*, 1988) and microsomes (Lilly *et al.*, 1990), the techniques used in the CPT I assay described here have been extensively validated elsewhere (Guzmán *et al.*, 1988,1992; Zammit *et al.*, 1988; Grantham *et al.*, 1988) and it has been shown by these groups, that in permeabilised cells, the carnitine palmitoyltransferase activity measured using palmitoyl-CoA as substrate, represents predominantly mitochondrial CPT I, despite the presence of carnitine acyl-transferase activity in peroxisomes and microsomes. Others, however, have found that the contribution of peroxisomal CPT to CPT activities measured using this approach cannot be excluded (Ramsay, 1993).

For these procedures, duplicate sets of intact hepatocyte incubations containing unlabelled palmitate (0.5mM) were performed to measure the effects of increasing etomoxir concentration on CPT I activity in each cell preparation. As before, freshly prepared hepatocytes were incubated at a density of 3×10^6 cells in 3ml incubation medium, in 25ml conical flasks, gassed and placed in a reciprocating water bath for 30min at 37°C (with further regassing at 15min). Appropriate etomoxir concentrations (0µM-100µM) were added to each flask and after 10min, either 1ml palmitate (0.5mM), 1ml octanoate (2mM) or 1ml palmitate:octanoate mixture (palmitate (0.5mM):octanoate, (0.33mM)) was added to each flask.

After 30min the plasma membranes of these cells were permeabilized by the addition of 1ml digitonin (1.5mg ml^{-1} in KRB). After exactly 10 seconds the suspension was diluted with 40ml ice-cold KCl buffer (150mM KCl; 1mM EGTA; 5mM Tris, pH 7.4) and centrifuged for 3min at 2100rpm (930g).

It has been shown elsewhere that this procedure:

- (i) causes minimal damage to intracellular membranes;
- (ii) retains cytosolic protein kinases and phosphatases that may be involved in mediating the effects of CPT I; and
- (iii) optimises the probability that CPT I, rather than CPT II, would be measured *in situ* in its membrane environment.

(Guzmán *et al.*, 1988, 1992; Zammit *et al.*, 1988)

The permeabilized cells were collected as a pellet and resuspended in 0.5ml KCl buffer. Each 0.5ml suspension was used to measure CPT I activity by total [³H]palmitoylcarnitine accumulation using 320µM L-[*methyl*-³H]carnitine (0.8µCi µmol⁻¹) and 135µM palmitoyl-CoA (1% BSA) as substrates in 1ml of "assay cocktail" (19.5ml KCl buffer, 0.2g BSA, 0.5ml MgCl₂/ATP solution (0.407g:1.204g in 10ml H₂O), 3.07mg DTT, 40µl antimycin A and rotenone solution (1mg antimycin A:2mg rotenone in ethanol)).

Reactions were terminated by the addition of 300µl of ice-cold 6M HCl. 1ml of H₂O (*n*-butanol saturated) and 4.5ml *n*-butanol (H₂O saturated) were added to each tube, which were then shaken and vortexed vigorously. After centrifugation for 5min at 3000rpm (1900g), the bottom (butanol) layer was extracted through the upper (water) layer into fresh tubes and a further 4ml of H₂O (*n*-butanol saturated) was added to each tube, and centrifuged. This washing procedure was repeated three times. Finally, 3ml of the remaining butanol layer was added to 10ml Ecoscint and the dpm assessed.

2.2.6 Hepatocyte oxygen consumption

The study of oxygen consumption in intact cells had the advantage of observing mitochondrial function in the intracellular environment. Hepatocyte respiration rates were determined polarographically, using a Clark-type oxygen electrode (Rank Bros., Bottisham, Cambridge, U.K.), which allowed incubation of the hepatocyte suspensions at 37°C. For calibration, the oxygen content of the

medium was assumed to be $0.215\mu\text{mol}/\text{cm}^3$. Freshly isolated cells were incubated, at a density of 3×10^6 cells in 3ml incubation medium, plus 1ml palmitate (0.5mM final concentration in KRB, 2% BSA), in 25ml conical flasks, gassed and placed in a reciprocating water bath for 15min at 37°C . After this pre-incubation, oxygen consumption measurements commenced.

To estimate the contribution of mitochondrial and non-mitochondrial oxygen consumption to total cellular respiration, cells were treated with myxothiazol, which is a strong, irreversible inhibitor of complex III of the respiratory chain, binding to cytochrome *b* with a 1:1 stoichiometry (Taylor *et al.*, 1994). The myxothiazol-resistant oxygen consumption was assumed to be non-mitochondrial. After the pre-incubation stage, 2.5ng/mL myxothiazol was added to appropriate flasks. In preliminary experiments, this concentration had been determined to cause maximal inhibition of oxygen consumption and, therefore, complete inhibition of mitochondrial O_2 consumption (Zamparelli *et al.*, 1999).

2.2.7 Electron microscopy of hepatocytes

Incubations for the electron microscopy were carried out in parallel with the oxygen consumption experiments except that after 30min, cell suspensions were centrifuged in a bench centrifuge for 2 min. Pellets were then fixed in 2.5% glutaraldehyde and 0.1 mol/L cacodylate buffer. The remaining procedures were performed by the histopathology unit. These included:

- (i) secondary fixation with 1% osmium tetroxide and 0.1 mol/L cacodylate buffer;
- (ii) dehydrating samples through graded alcohols, propylene oxide and impregnated with agar 100 epoxy resin;
- (iii) embedding samples in agar resin and polymerised at 60°C for 48h, and
- (iv) preparation of ultrathin sections, double stained using uranyl acetate and Renolds lead citrate and examined using a Jeol 100CX transmission electron microscope (Jeol, Welwyn, Herts, U.K.)

2.2.8 Statistical analysis

Data were analysed using Prism GraphPad software (GraphPad Software Inc, San Diego, CA). Unless otherwise stated, data are expressed as means \pm SEM. Comparisons of the results were performed, unless otherwise stated, using paired or unpaired Student's *t*-test, as appropriate. Results demonstrating probability levels less than 0.05 were considered significant. The computer program Simfit (Bardsley *et al.*, 1997) was used for bottom-up control analysis, details are given in the appropriate chapters.

Chapter 3

Analysing the role of hepatic mitochondrial outer-membrane carnitine palmitoyltransferase in the control of carbon fluxes from palmitate

3.1 Introduction

Historically, intrahepatic control of fatty acid oxidation and ketogenesis has been considered to reside at the level of the entry of acyl groups into the mitochondrion, with mitochondrial outer-membrane carnitine palmitoyltransferase (CPT I) being considered as the 'rate-limiting' or more recently the 'rate-controlling' step of these pathways without consideration of physiological conditions and stages of development.

In this chapter and in chapters 4, 5 and 6, I will investigate the potential of CPT I to control fatty acid oxidation and ketogenesis under a variety of conditions. Metabolic control analysis (MCA, as described in Chapter 1) will be used to make quantitative assessments of control distribution in two complex, dynamic metabolic systems, which are described in detail in Section 3.2.

3.1.1 Historical perspectives in the control of hepatic fatty acid oxidation and ketogenesis

Many experimental studies support the historical view that CPT I is a key control enzyme of fatty acid oxidation and ketogenesis. For example, it has been shown that octanoate, a medium-chain fatty acid, is oxidized to acetyl-CoA at similar rates, irrespective of the metabolic state of the animal (*i.e.* fed, fasted or diabetic), whereas the oxidation rate of long-chain fatty acids is a function of metabolic status (McGarry *et al.*, 1971, 1980). Since octanoate is metabolised independently of the three-step system which includes CPT I, this suggests that a point preceding the intrahepatic oxidative sequence may be a controlling site in the oxidation of long-chain fatty acids. CPT I, with its position at the start of the long-chain fatty oxidation pathway has, therefore, been considered a prime candidate as the site of control by many workers. Additionally, CPT I has a high affinity for its fatty acyl-CoA substrate and a low affinity for the resulting acyl-carnitine product, which gives rise to almost irreversible kinetics. Hence, on the basis of this kinetic argument, many workers have considered CPT I as the 'rate-limiting' step (Guzmán *et al.*, 1993).

Investigations into the changes in ketogenesis and enzyme activity in response to changes in substrate supply, hormones and developmental status have further strengthened and refined the argument for CPT I as the 'rate-limiting' step. For example, in both human and rat fetal liver, the rates of hepatic β -oxidation and ketogenesis are relatively low. However, following birth, these metabolic pathways become more important and an increased capacity for fatty acid oxidation results in a significant increase in the concentrations of blood ketone bodies, from 0.2mM in the rat at birth to 2mM 24 hours later (Ferré *et al.*, 1978). This hyperketonaemia, which is well below the concentration associated with life-threatening ketoacidosis (Yeh *et al.*, 1985), is maintained throughout the suckling period (Girard *et al.*, 1992). Along with gluconeogenesis, it is thought to be a 'safety-mechanism' in periods when blood glucose concentrations may be sub-optimal (Hawdon *et al.*, 1994), since acetoacetate and β -hydroxybutyrate are used as an alternative energy source by peripheral tissues and organs (McGarry, 1995).

These metabolic changes are paralleled in the CPT I system, as the activity, the protein concentration and the level of mRNA encoding CPT I are relatively low in fetal liver, but increase 5-fold during the first day of extrauterine life and the activity and gene expression remain high during the entire suckling period (Thumelin *et al.*, 1994; Asins *et al.*, 1995). A decrease is seen only when rats are weaned on to a high carbohydrate:low fat diet (Decaux *et al.*, 1988; Thumelin *et al.*, 1994). Interestingly, if weaned on to a high fat diet, the activity of CPT I remains as high as in the suckling rat liver. In addition, the sensitivity of CPT I to malonyl-CoA, the first committed intermediate in the lipogenic pathway and a potent physiological reversible inhibitor of CPT I (McGarry *et al.*, 1977; Fraser *et al.*, 1997) decreases in the first 24 hours following birth (Saggerson *et al.*, 1982; Girard *et al.*, 1992). After weaning, however, the sensitivity of CPT I to the inhibitory effect of malonyl-CoA increases nearly 10-fold (Decaux *et al.*, 1988).

Such changes are not observed in CPT II. The activity, protein abundance and mRNA level of CPT II are already high in fetal rat liver, do not change after birth and are not influenced by nutritional and hormonal changes in the postnatal period (Kolodziej *et al.*, 1992; Thumelin *et al.*, 1994; Asins *et al.*, 1995). These observations, therefore, lead many workers to believe that CPT I is a key enzyme in the control of hepatic long-chain fatty acid oxidation.

3.1.2 Control analysis of hepatic fatty acid oxidation and ketogenesis

More recently, the bottom-up approach of metabolic control analysis (BUCA) has been used to investigate quantitatively the role of CPT I in controlling flux over β -oxidation, ketogenesis and tricarboxylic acid cycle activity in adult rats of differing metabolic states (fed, starved, starved/refed, starved/insulin treated) (Drynan *et al.*, 1996). Under all of the conditions examined in this hepatocyte system, the numerical value of the flux control coefficient for CPT I over ketogenesis was high (within the range 0.75 to 0.92) providing quantitative support for the more traditional views discussed previously and suggesting that CPT I could be a primary control site for ketogenesis in adult rats. Similar conclusions can be drawn from the work of Spurway *et al.*, (1997) who also used BUCA. In a defined system consisting of cultured hepatocytes (from adult male rats) and using two independent methods of BUCA to obtain values for flux control coefficients for CPT I over ketogenic flux, these workers also found that the numerical values were high (ranging from 0.67 to 0.79) providing further support for CPT I being the 'rate-limiting' or 'rate-controlling' step of ketogenesis.

Whilst these results indicate that under certain conditions, CPT I may provide a significant contribution to control, traditional approaches have also shown that this enzyme is not the only one involved in hepatic ketogenesis which undergoes changes during the fetal-neonatal transition or the suckling-weaning period. Significant control over ketogenesis may be exerted at another intramitochondrial site, distal to CPT I, for example, 3-hydroxy-3-methylglutaryl-CoA (HMG-CoA) synthase (Quant *et al.*, 1989; Quant *et al.*, 1991; Lascelles *et al.*, 1998; Hegardt, 1999) which catalyses the second step of the HMG-CoA cycle. Like CPT I, the mRNA (Thumelin, *et al.*, 1993) the concentration of the enzyme and its activity (Williamson *et al.*, 1968; Lockwood *et al.*, 1971; Decaux *et al.*, 1988; Quant *et al.*, 1989) show a bell-shaped pattern (i.e. parabola with vertex at the top), which parallels that for ketogenesis. These parameters increase markedly immediately following birth and remain elevated during the suckling period. Again, as with CPT I, levels decrease when rats are weaned on a high carbohydrate diet, but if weaning is to a high fat diet, high levels are maintained (Decaux *et al.*, 1988; Quant *et al.*, 1991). Immediately following birth, there is a plasma glucagon surge, induced by the birth trauma. This increases the activity of HMG-CoA by lowering the concentration of succinyl-CoA and therefore decreasing the extent of succinylation and hence inactivation of HMG-CoA synthase. This in turn results in the stimulation of ketogenesis in neonatal rats and humans (Quant *et al.*, 1989, 1990, 1991;

Lascelles *et al.*, 1998). Glucagon levels and HMG-CoA synthase activity fall with weaning on to a high carbohydrate diet, but remain elevated with weaning on to a high fat diet.

The contribution of the enzymes of the HMG-CoA cycle in the control over ketogenesis has been investigated quantitatively using the top-down approach of control analysis (TDCA) (Quant *et al.*, 1993). Using this approach, it was found that under conditions of non-regulation of CPT I by malonyl-CoA, an absence of NADH and the inhibition of the Krebs cycle by malonate, only approximately 28% of the control over ketogenesis was invested in the group of enzymes responsible for the production of acetyl-CoA (*i.e.* CPT I, the carnitine carrier, CPT II, the enzymes of β -oxidation and the respiratory chain). 72% of the control resided with the enzymes of the HMG-CoA cycle that convert acetyl-CoA to β -hydroxybutyrate plus acetoacetate. Quant and co-workers suggested that within this cycle, control is exerted at the level of HMG-CoA synthase. However, these observations were made under artificial *in vitro* conditions *i.e.* with uncoupled mitochondria.

Further support for a control site beyond CPT I has been provided by inhibitor titrations of some of the enzymes involved in the oxidation of palmitoyl-carnitine, which suggested that control may be exerted at a point after CPT II (Kunz *et al.*, 1991). Although this does not rule out the possibility that CPT I may have significant control over entry of long-chain fatty acids into mitochondria, this work suggested that CPT I was not likely to be the single, 'rate-limiting', step for ketogenesis.

The concept of CPT I being the 'rate-limiting' step of fatty acid oxidation and ketogenesis has been further questioned by the findings of recent experiments where TDCA has been applied in a defined, mitochondrial palmitoyl-CoA-oxidizing system (Krauss *et al.*, 1996). This system enabled these workers to investigate the role of CPT I in control over total carbon flux (although not specifically ketogenesis). It was found that values of group flux control coefficients for CPT I over carbon flux in adult rats was high, ranging from 0.87-1.00. This supported earlier conclusions, that in the adult rat, the control exerted by CPT I over the pathways was high. However, in the same defined system in suckling rats, the calculated group flux control coefficients were lower, in the range 0.73-0.96, indicating that the level of control exerted by CPT I over total carbon flux was lower in this age group. This suggested that at this stage of development, control was shifted away from CPT I. Whilst these values were still relatively high, supporting the idea that CPT I still

exerted a significant level of control in suckling rats and thus could potentially be considered 'rate-controlling', the results suggested that it was unlikely to be a 'rate-limiting' step.

3.1.3 Aims of this section

Despite the central importance of the pathways of fatty acid oxidation and ketogenesis to metabolic adaptation to extrauterine life, control of the onset and development of these pathways in healthy neonates is currently incompletely understood. My primary aim in this chapter was to calculate flux control coefficients for CPT I over carbon fluxes, during the neonatal period. These would provide quantitative assessments of the contribution of this enzyme to control flux in these pathways, at this stage of development.

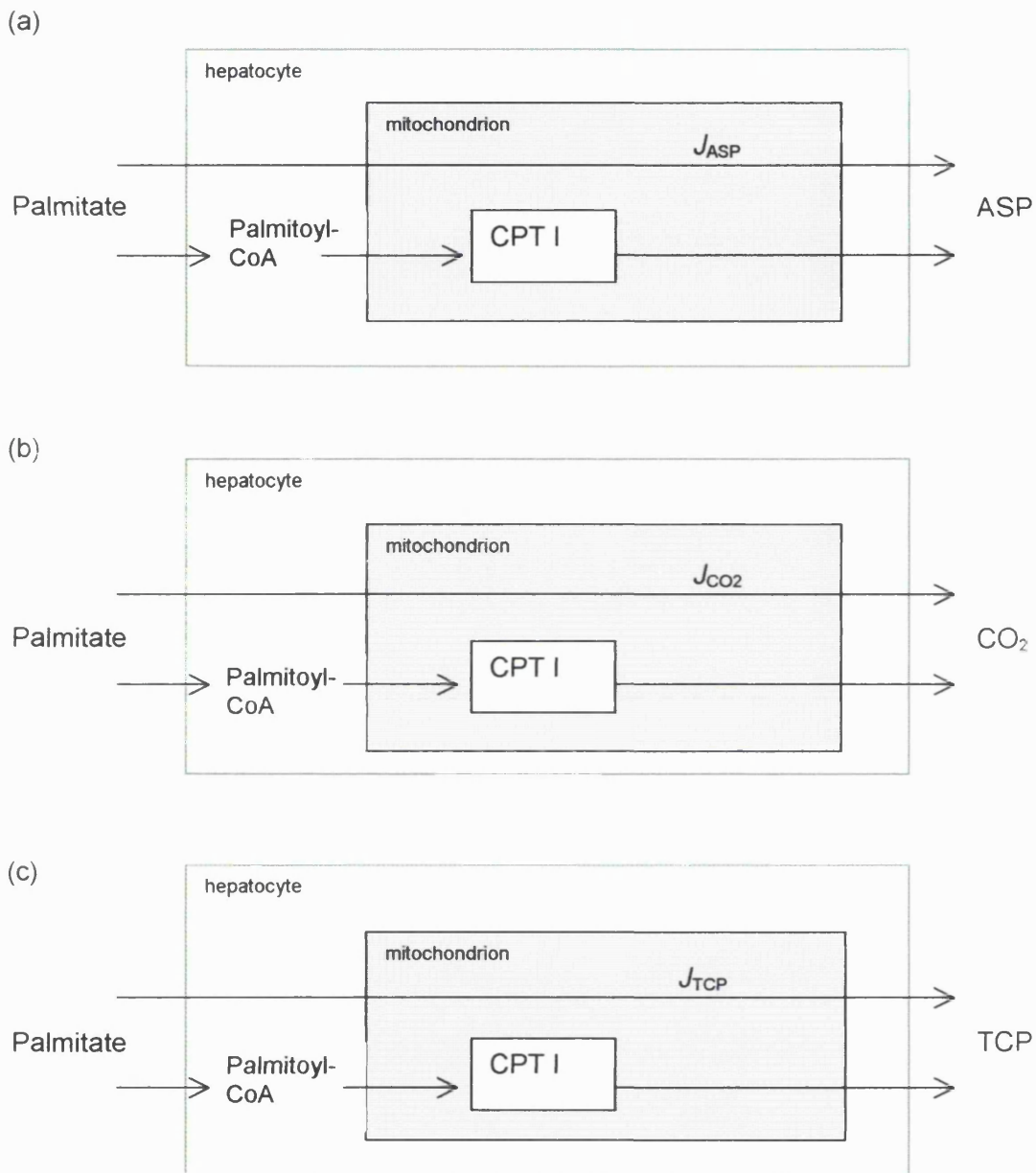
Specifically, the studies in this chapter aimed to use BUCA to calculate and report several flux control coefficients. These coefficients describe the potential of CPT I to control flux to ketone bodies ($C_{CPTI}^{J_{ASP}}$), carbon dioxide ($C_{CPTI}^{J_{CO_2}}$) and total carbon flux ($C_{CPTI}^{J_{TCP}}$) in hepatocytes isolated from suckling rats, respiring on the physiological, long-chain fatty acid, palmitate. Results are compared with those obtained from an equivalent system, which used hepatocytes isolated from rats at a different developmental stage (New *et al.*, 1997,1998(a),1999(b)).

A further aim was to expand on the work performed by Krauss *et al.*, (1996), by performing new analyses on the data from this mitochondrial system, which will enable the individual flux control coefficients, for total carbon and specifically for ketogenesis, to be calculated for the first time (New *et al.*, 1999(b)).

3.2 Theory and approaches

3.2.1 Application of BUCA in hepatocytes isolated from suckling rats

The definition of the 'system' is not a trivial stage in the application of BUCA. The system is an abstraction, which must agree with physiological reality to produce meaningful results (Meléndez-Hevia *et al.*, 1990). This section describes the system used to quantitatively assess the potential of CPT I to control fluxes from palmitate (representing a long-chain fatty acid substrate) to ketone bodies (acid soluble products, ASP) carbon dioxide (CO₂) and total carbon products (TCP) in hepatocytes isolated from suckling rats (Scheme 3.1).



Scheme 3.1 Hepatocyte BUCA system

The hepatocyte BUCA system is represented by the green box. BUCA defines the flux control coefficients as small fractional changes in pathway fluxes brought about by infinitesimal fractional changes in enzyme activity.

- Scheme: (a) represents the system for calculation of flux control coefficients for CPT I with respect to ketogenesis ($C_{CPT I}^{J_{ASP}}$);
 (b) with respect to CO_2 formation ($C_{CPT I}^{J_{\text{CO}_2}}$);
 (c) with respect to total carbon flux ($C_{CPT I}^{J_{\text{TCP}}}$).

In each of the systems described in Scheme 3.1, the extrahepatic control exerted by the supply of non-esterified fatty acids to the liver was excluded by using isolated hepatocytes incubated with a fixed concentration of fatty acids. The activity of CPT I was progressively inhibited with increasing concentrations of etomoxir. This is intracellularly converted to etomoxir-CoA which, over the concentration range used in these studies, is a specific inhibitor of mitochondrial CPT I (Declercq *et al.*, 1987).

Flux control coefficients for CPT I with respect to ketogenesis, CO₂ formation and total carbon flux in this isolated hepatocyte model were calculated using the data in Figures 3.2-3.6, the Simfit package (Bardsley *et al.*, 1997) to calculate initial slopes and the following equations:

Equation 3.1:

$$C_{CPTI}^{J_{ASP}} = \frac{\frac{\delta J_{ASP}}{J_{ASP}}}{\frac{\delta v_{CPTI}}{v_{CPTI}} (i=0)}$$

Equation 3.2:

$$C_{CPTI}^{J_{CO_2}} = \frac{\frac{\delta J_{CO_2}}{J_{CO_2}}}{\frac{\delta v_{CPTI}}{v_{CPTI}} (i=0)}$$

Equation 3.3:

$$C_{CPTI}^{J_{TCP}} = \frac{\frac{\delta J_{TCP}}{J_{TCP}}}{\frac{\delta v_{CPTI}}{v_{CPTI}} (i=0)}$$

Where $C_{CPTI}^{J_{ASP}}$, $C_{CPTI}^{J_{CO_2}}$ or $C_{CPTI}^{J_{TCP}}$ are the flux control coefficients of CPT I over ketogenesis, CO₂ formation and total carbon flux respectively, at zero inhibitor (etomoxir-CoA) concentration ($i = 0$). v_{CPTI} is the activity of CPT I, ASP is acid soluble products and TCP is total carbon products. δ represents infinitesimal changes, where the changes are very small (i.e. tend to zero). J_{ASP} , J_{CO_2} and J_{TCP} , are carbon fluxes to acid soluble products, carbon dioxide and total carbon products respectively.

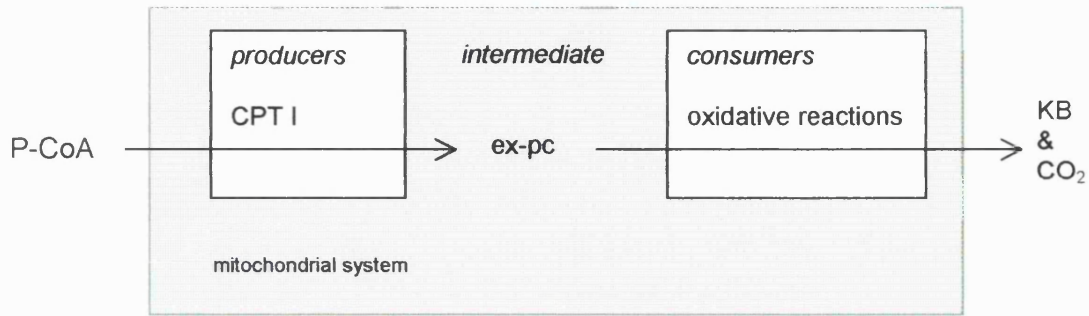
3.2.2 Application of BUCA in mitochondrial systems

This section extends the work of Krauss *et al.*, (1996), by describing the original and re-defined schemes used in the calculation of flux control coefficients for CPT I specifically over ketogenesis, from their original mitochondrial data. The laboratory work for the new analysis described here was performed by Krauss *et al.*, (1996) and the methods used for the isolation and incubation of mitochondria have been described in their original paper. In the original defined mitochondrial system (Scheme 3.2), Krauss *et al.*, applied top down control analysis to their data. In this original system, the substrate, palmitoyl-CoA (P-CoA) is translocated across the inner mitochondrial membrane by CPT I, the acyl-carnitine transferase and CPT II. The pathway is viewed as two blocks of reactions. One block is external to the mitochondrion, comprising only CPT I, and produces the system intermediate, external palmitoylcarnitine (ex-pc). The other block (the consumer block) comprises all the steps involved in the oxidation of ex-pc to ketone bodies (KB) and CO₂ (Krauss *et al.*, 1996).

In this original system, the chosen intermediate, ex-pc, did not fulfil the requirement of being uniquely related to each of the blocks of reactions in a branched system, which defined ketogenesis as an independent flux (Quant, 1993). Therefore, it was only possible to calculate group flux control coefficients for total carbon flux. By re-defining the mitochondrial system (Scheme 3.3), however, it is valid to re-analyse the same data using the bottom-up approach to calculate the individual flux control coefficient for CPT I over flux to ketone bodies.

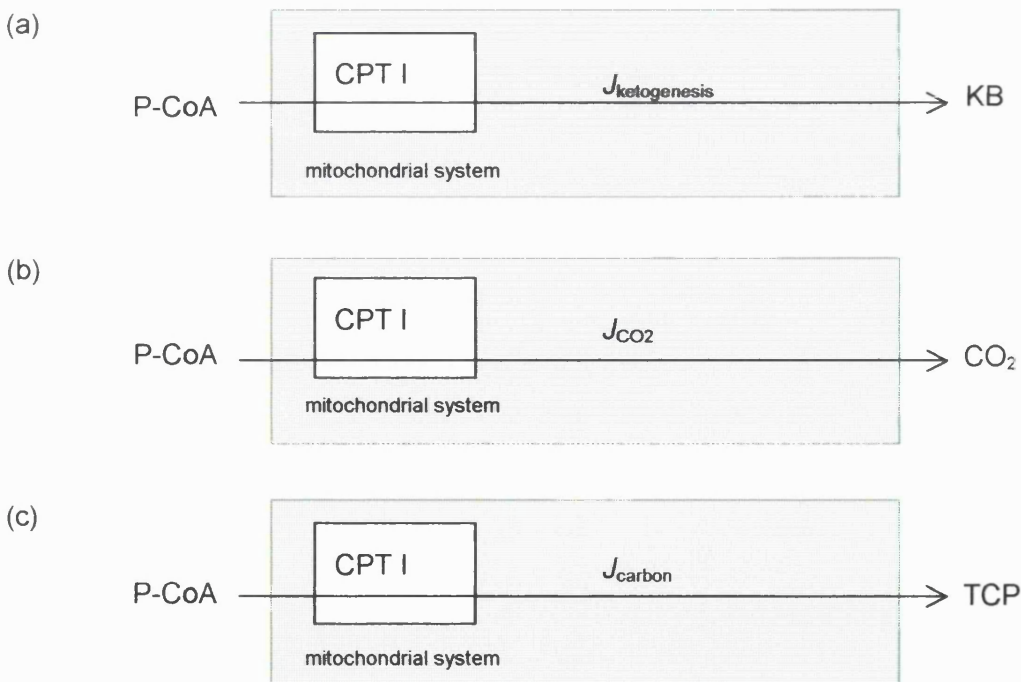
The re-defined mitochondrial systems presented in this thesis (Scheme 3.3), consist of isolated rat liver mitochondria, which oxidize palmitoyl-CoA to ketone bodies and carbon dioxide, where CPT I is the step under study. Scheme 3.3(a) represents flux to ketone bodies, Scheme 3.3(b) represents carbon dioxide formation and Scheme 3.3(c) represents total carbon flux (New *et al.*, 1999(b)). The rates of oxygen consumption and ketone body production were measured directly by Krauss *et al.*, (1996). As in the original published work, all carbon entering the system is assumed to leave it either as carbon dioxide or ketone bodies.

BUCA of this new mitochondrial system defines the flux control coefficients as small fractional changes in pathway fluxes brought about by infinitesimal changes in CPT I activity (induced by a range of malonyl-CoA concentrations) when the system is allowed to relax to a new steady-state.



Scheme 3.2 Original TDCA mitochondrial system

The mitochondrial system is represented by the green box. The pathway is viewed as two blocks of reactions. One block is external to the mitochondrion, comprising only CPT I and produces the system intermediate, external palmitoylcarnitine (ex-pc). The consumer block comprises all the steps involved in the oxidation of ex-pc to ketone bodies (KB) and CO_2 (Krauss *et al.*, 1996). P-CoA represents palmitoyl-CoA. More detail is provided in the main text.



Scheme 3.3 Re-defined BUCA mitochondrial system

The re-defined mitochondrial system is represented by the green box. Scheme (a) represents flux to ketone bodies, Scheme (b) represents carbon dioxide formation and Scheme (c) represents total carbon flux. P-CoA represents palmitoyl-CoA. $J_{\text{ketogenesis}}$, J_{CO_2} and J_{carbon} represent ketogenic, CO_2 and total carbon fluxes respectively. More detail is provided in the main text.

In summary, in both the original mitochondrial system and the re-defined system discussed in this section, palmitoyl-CoA was the substrate and CPT I the step under study. The rates of O₂ consumption and ketone body production were measured directly and used to calculate rates of CO₂ formation and, hence, the rates of total carbon flux and ketone body production (Krauss *et al.*, 1996; New *et al.*, 1999(b)).

These data were used to calculate flux control coefficients directly, as described by Brand *et al.*, (1996) from plots of flux against the intermediate, ex-pc, Figure 3.1 (New *et al.*, 1999(b)). State 3 respiration may be defined as phosphorylating respiration in the presence of ADP, state 3.5 is thought to represent the 'physiological' respiratory state of mitochondria *in situ* in hepatocytes. Respiration that is inhibited by the lack of ADP for phosphorylation is defined as state 4 respiration.

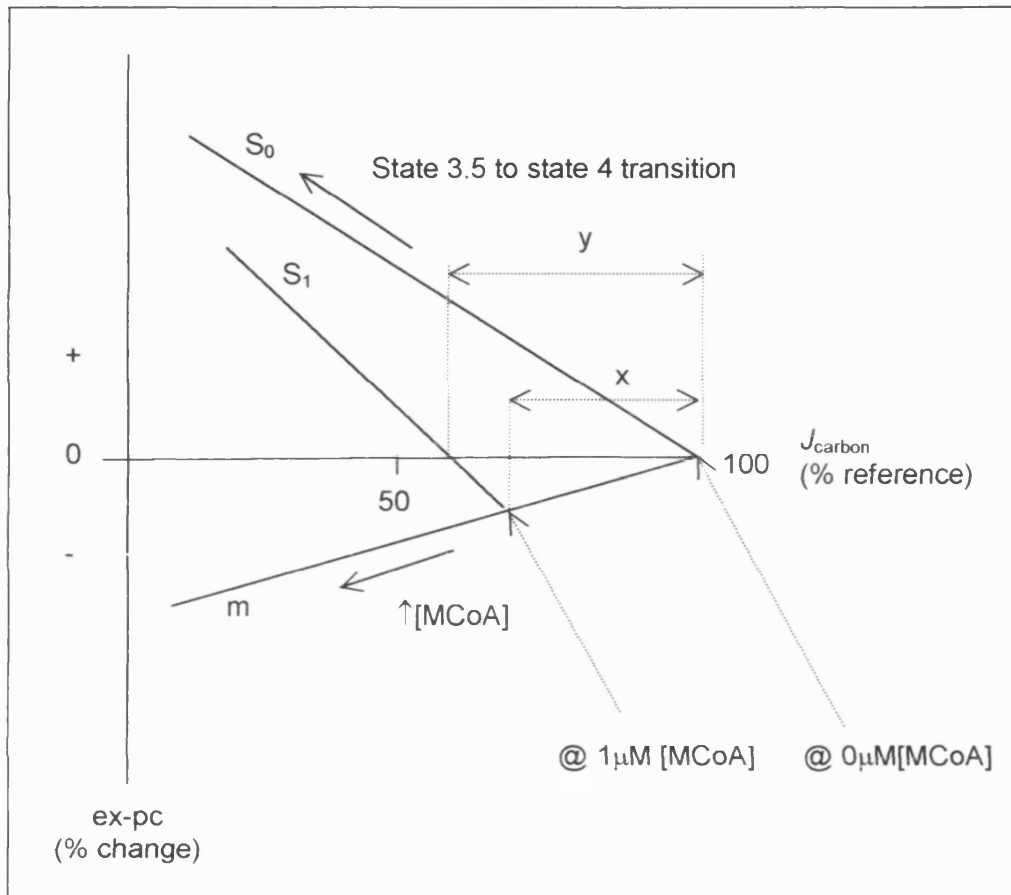


Figure 3.1 Schematic grid for calculation of individual flux control coefficients for CPT I over ketogenesis and total carbon flux in isolated mitochondria

Titration of J_{carbon} (or $J_{\text{ketogenesis}}$) with hexokinase plus ADP, or oligomycin to achieve the state 3.5 to state 4 transition at $0\mu\text{M}$ or $1\mu\text{M}$ malonyl-CoA are represented by lines S_0 and S_1 respectively on Figure 3.1. Further state 3.5 to state 4 transition lines have been omitted from this figure for clarity. Line m represents the titration of the state 3.5 flux with increasing concentrations of malonyl-CoA. Distance x represents the percentage change in pathway flux for the same change in malonyl-CoA concentration ($0\mu\text{M}$ or $1\mu\text{M}$) when the system is allowed to relax to a new steady state flux and ex-pc concentration. The distance y represents the percentage change in CPT I activity brought about by the same change in malonyl-CoA concentration but at a constant ex-pc concentration. The concentration of malonyl-CoA is the only parameter to be changed because substrate (palmitoyl-CoA) and product (ex-pc) are held constant. As malonyl-CoA is a specific inhibitor of CPT I, a fractional change in flux brought about by a fractional change in malonyl-CoA must represent a change in flux through CPT I. In this system, as in the hepatocyte system described in section 3.2.1, the flux control coefficient for CPT I over ketogenesis can be defined as a small fractional change in the pathway flux brought about by infinitesimal fractional changes in CPT I activity. Here, the pathway flux change is due to a range of malonyl-CoA concentrations, when the system is allowed to relax to a steady state, thus x/y represents the numerical value of the relevant individual flux control coefficient for CPT I over carbon fluxes. (Krauss *et al.*, 1996; New *et al.*, 1999(b)).

3.3 Results

3.3.1 BUCA in neonatal hepatocyte systems

Figure 3.2 shows the effect on CPT I activity of using a range of concentrations of etomoxir (0 μ M-100 μ M). As expected for a specific inhibitor, CPT I activity decreases with increasing amounts of etomoxir, and hence, etomoxir-CoA. Since etomoxir-CoA is formed and bound to CPT I during the pre-incubation stage of the assay and free etomoxir is lost during the permeabilisation, the CPT I activity measurements reflect the binding of etomoxir-CoA to CPT I and its inhibition during the pre-incubation stage. Figure 3.2 shows that at 10 μ M etomoxir, CPT I appears to be maximally inhibited and that 100 μ M etomoxir caused \approx 80% inhibition of CPT I activity, therefore the maximal possible contribution of CPT II to the measured activity is \approx 20%. However, as initial slopes are measured to derive flux control coefficients, the contribution of CPT II is negligible.

Figure 3.3 shows the effect of etomoxir on both CPT I activity and ketogenic flux (ASP, acid soluble products) in hepatocytes isolated from suckling rats. These data have been shown on the same graph to enable easier comparison of curves and have been used to calculate the individual flux control coefficient for CPT I over ketogenic flux (Section 3.2.1, Equation 3.1). With increasing etomoxir concentrations, CPT I activity and the flux from palmitate to ASP became increasingly inhibited. As 100 μ M etomoxir causes \approx 80% inhibition of β -oxidation flux, the contribution of peroxisomal β -oxidation to β -oxidation flux is presumed to be low.

Figure 3.4 shows the experimental variation over the data sets used to calculate flux control coefficients for CPT I over ketogenesis. Although standard errors on the mean for these data sets were small, as indicated in Figures 3.2 and 3.3, these figures indicate the difficulties associated with applying a 'best fit curve' to the data.

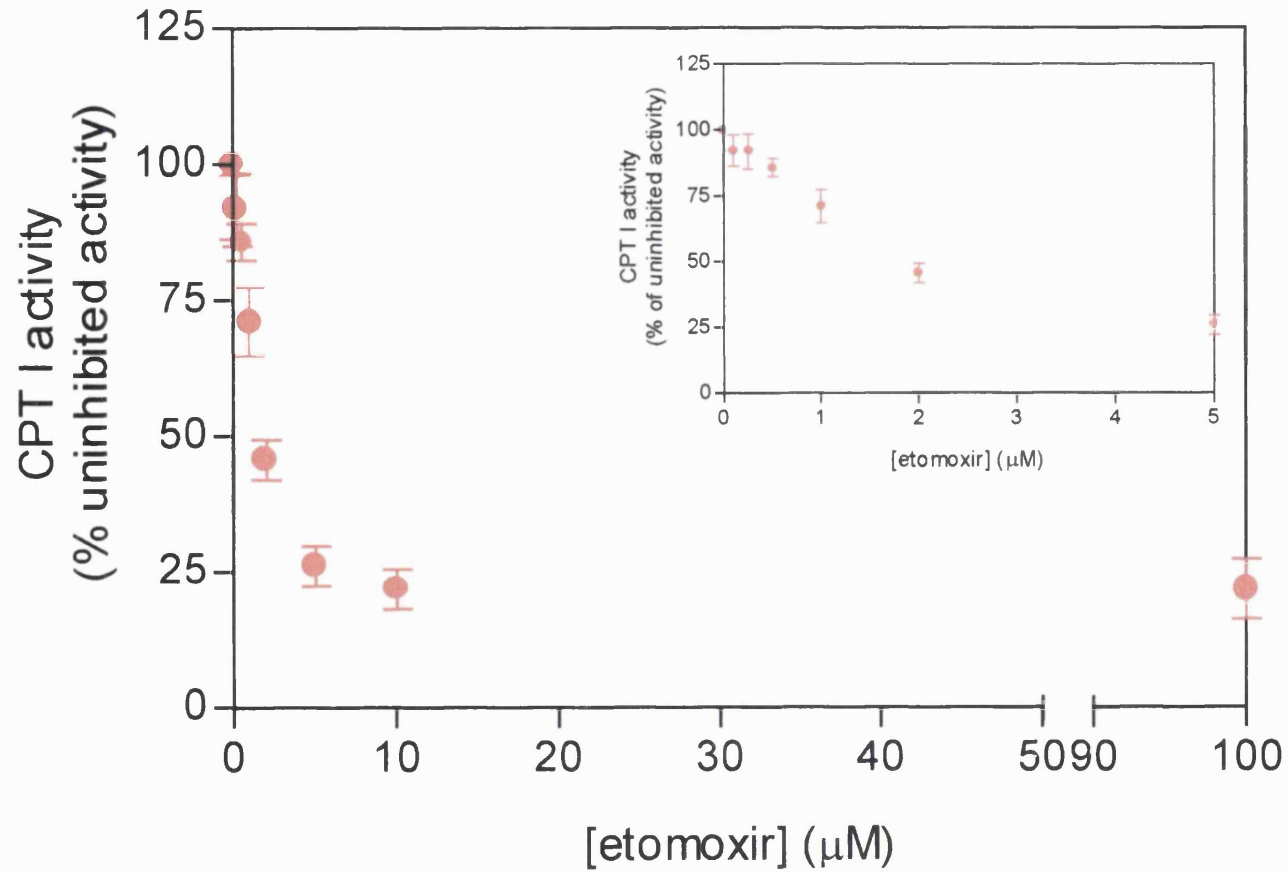


Figure 3.2 Effect of etomoxir on CPT I activity

Neonatal hepatocyte preparations with viability greater than 85% were used for experiments. Hepatocytes were incubated with etomoxir for 10 min, as detailed in Section 2.2.2. CPT I activities were normalised by expressing them as a percentage of those obtained in the absence of etomoxir. Values are means \pm SEM, $n=12$ separate hepatocyte preparations. The activity of CPT I in the absence of etomoxir was 142 ± 18 nmol h^{-1} (10^6 cells) $^{-1}$. (New *et al.*, 1999(b)).

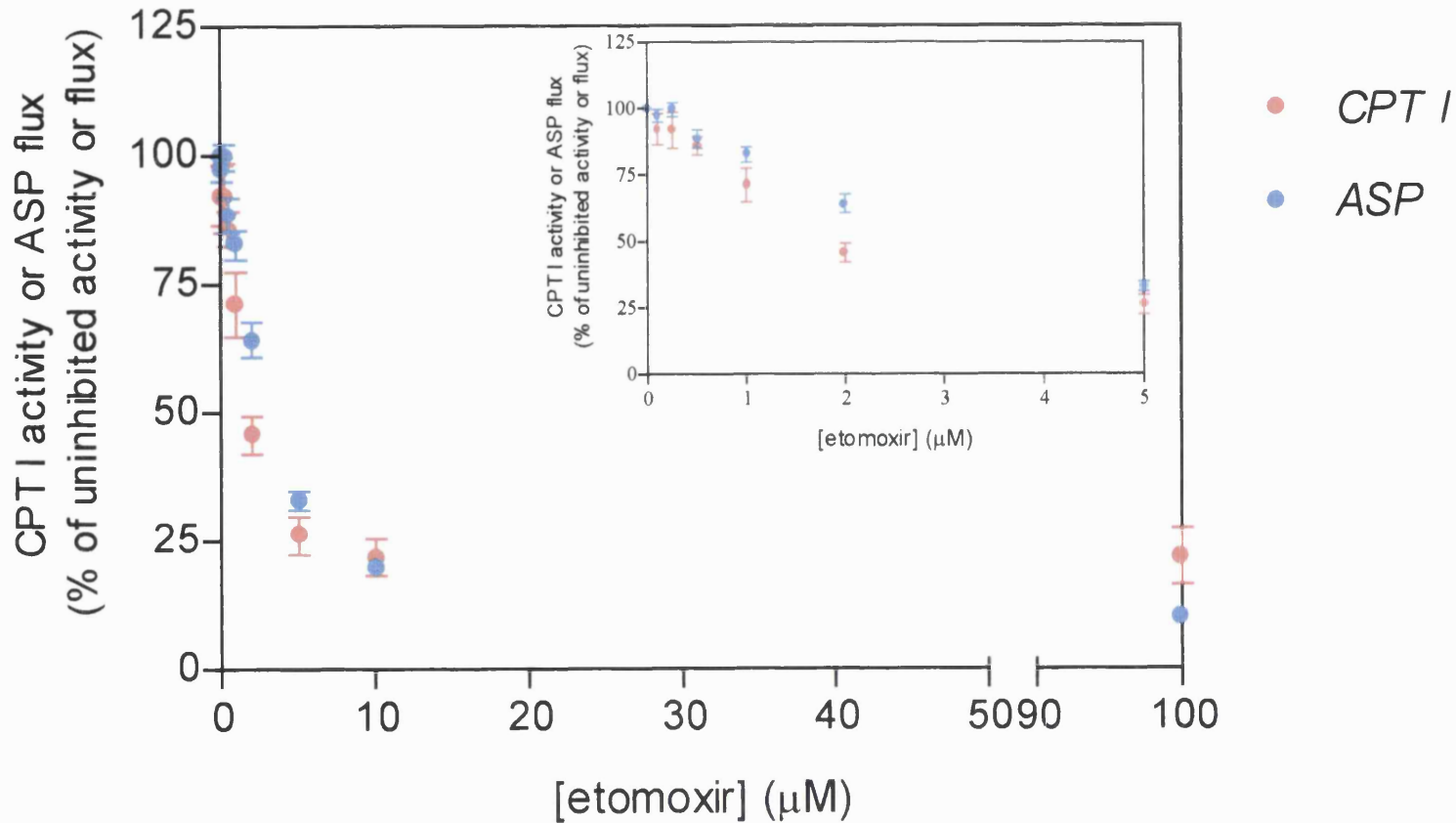
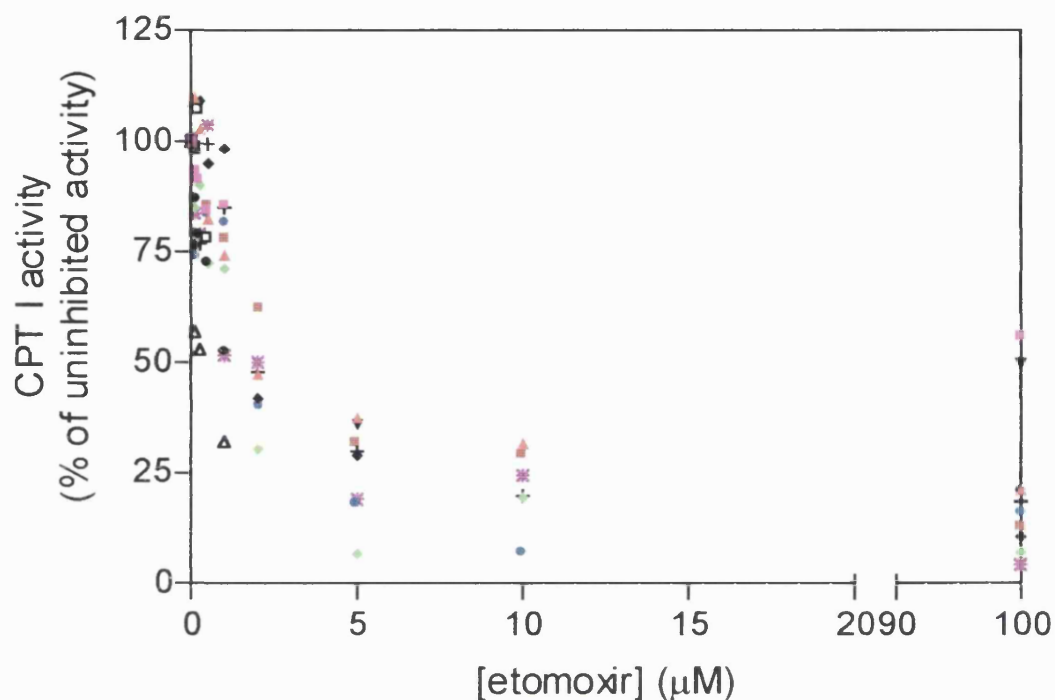


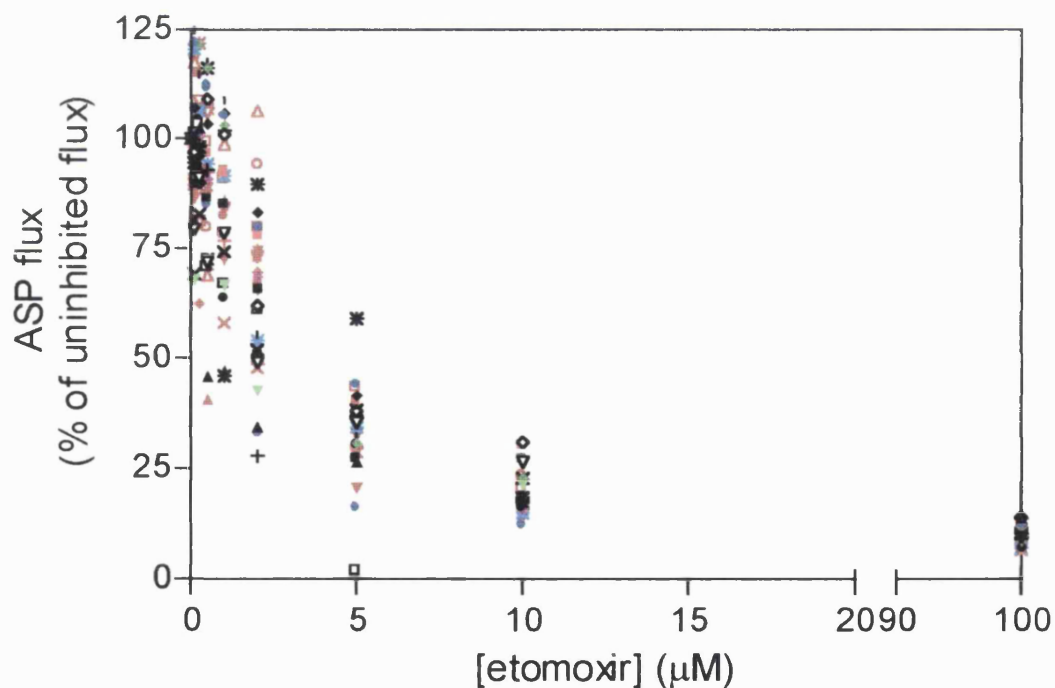
Figure 3.3 Effect of etomoxir on CPT I activity and ketogenic flux

Neonatal hepatocyte preparations with viability greater than 85% were used for experiments. Hepatocytes were incubated with etomoxir for 10 min, as detailed in Section 2.2.2. Following incubation with inhibitor, 1ml [$1\text{-}^{14}\text{C}$]palmitate (0.5mM final concentration, $0.4\mu\text{Ci } \mu\text{mol}^{-1}$, in KRB, 2% BSA) was added to appropriate flasks. Values were normalised by expressing them as a percentage of those obtained in the absence of etomoxir and are means \pm SEM, $n=12$ hepatocyte preparations for CPT I and $n=28$ for ASP. In the absence of etomoxir, the absolute rates of [$1\text{-}^{14}\text{C}$]palmitate consumption and [^{14}C]ASP formation were $39 \pm 7 \text{ nmol h}^{-1} (10^6 \text{ cells})^{-1}$ and $157 \pm 28 \text{ nmol h}^{-1} (10^6 \text{ cells})^{-1}$ respectively. Rates of ketone body formation were linear for at least 60 min. (New *et al.*, 1999(b)).

(a) CPT I activity: experimental variation



(b) Ketogenic flux: experimental variation

**Figure 3.4** Scatter of points from individual data sets

(a) Scatter of individual data sets for CPT I experiments considered in Figure 3.2.

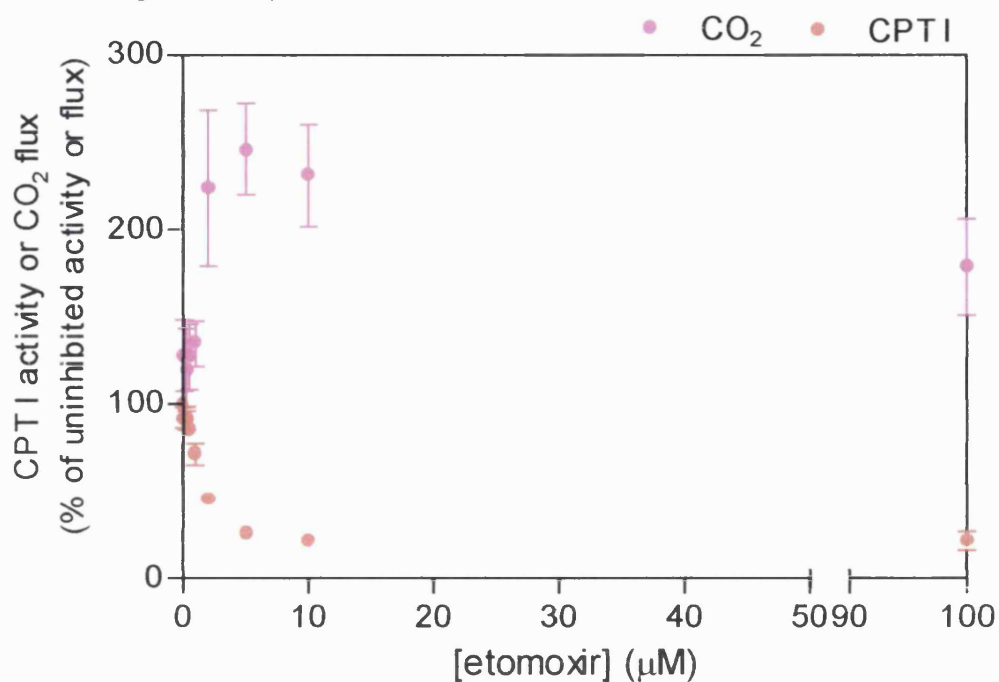
(b) Scatter of individual data sets for ASP experiments considered in Figure 3.3.

These graphs illustrate the range of possible inhibition curves for CPT I activity and ASP flux, and therefore provide an indication of the weighting for the mean curves seen in Figures 3.2 and 3.3.

The effects of etomoxir on CPT I activity and on flux to CO₂ in hepatocytes isolated from suckling rats are illustrated in Figure 3.5. Owing to the shape of the curves, an expansion of the initial points is shown as a separate graph, rather than an insert on a main graph. This enables the details to be more easily determined. As before, these data have been used to calculate the individual flux control coefficient for CPT I over CO₂ (Section 3.2.1, Equation 3.2). With increasing etomoxir concentration, CPT I activity becomes increasingly inhibited. However, with increasing inhibitor, flux to CO₂ increases, until a maximum is reached at approximately 5 μM. After this concentration of etomoxir, flux to CO₂ begins to decrease.

Figure 3.6 shows the effects of etomoxir on CPT I activity and total carbon flux (TCP, total carbon products) in hepatocytes isolated from suckling rats. With increasing etomoxir concentration, CPT I activity and total carbon flux from palmitate is inhibited. BUCA can be applied to this data to calculate the individual flux control coefficient for CPT I over total carbon products (Section 3.2.1, Equation 3.3).

(a) Full range of data points



(b) Expansion of graph over low inhibitor concentration range (0-5 μM etomoxir)

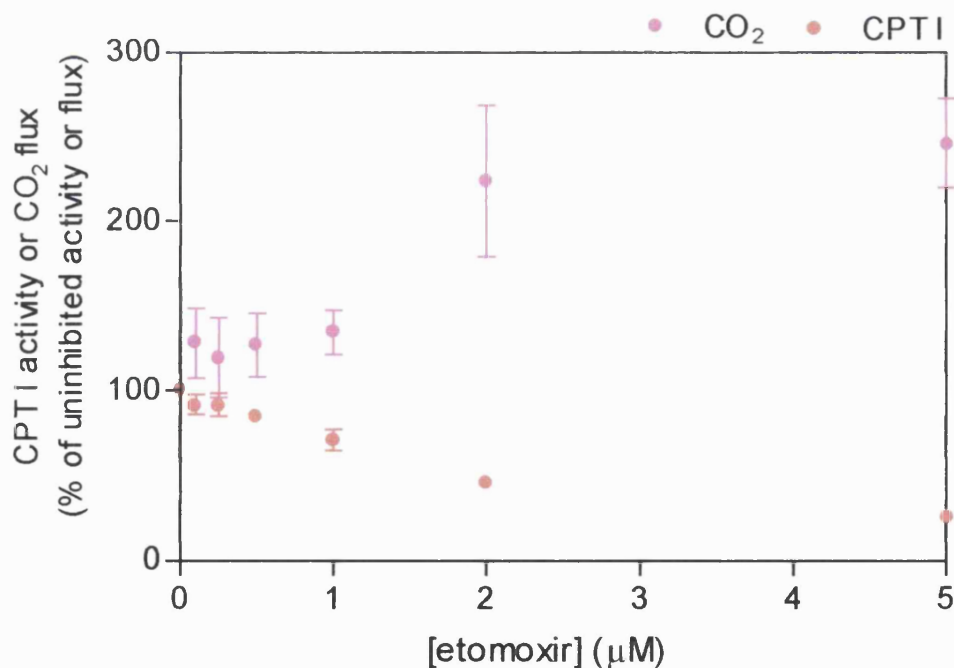


Figure 3.5 Effect of etomoxir on CPT I activity and flux to carbon dioxide

See legend for Figure 3.3 for details. Values are means \pm SEM, $n=12$ hepatocyte preparations. In the absence of etomoxir, the rate of palmitate consumption was 1.2 ± 0.2 nmol [$1\text{-}^{14}\text{C}$]palmitate consumed h^{-1} (10^6 cells) $^{-1}$. In the absence of etomoxir the absolute rate of $^{14}\text{CO}_2$ formation was 19 ± 4 nmol h^{-1} (10^6 cells) $^{-1}$. (New *et al.*, 1999(b)).

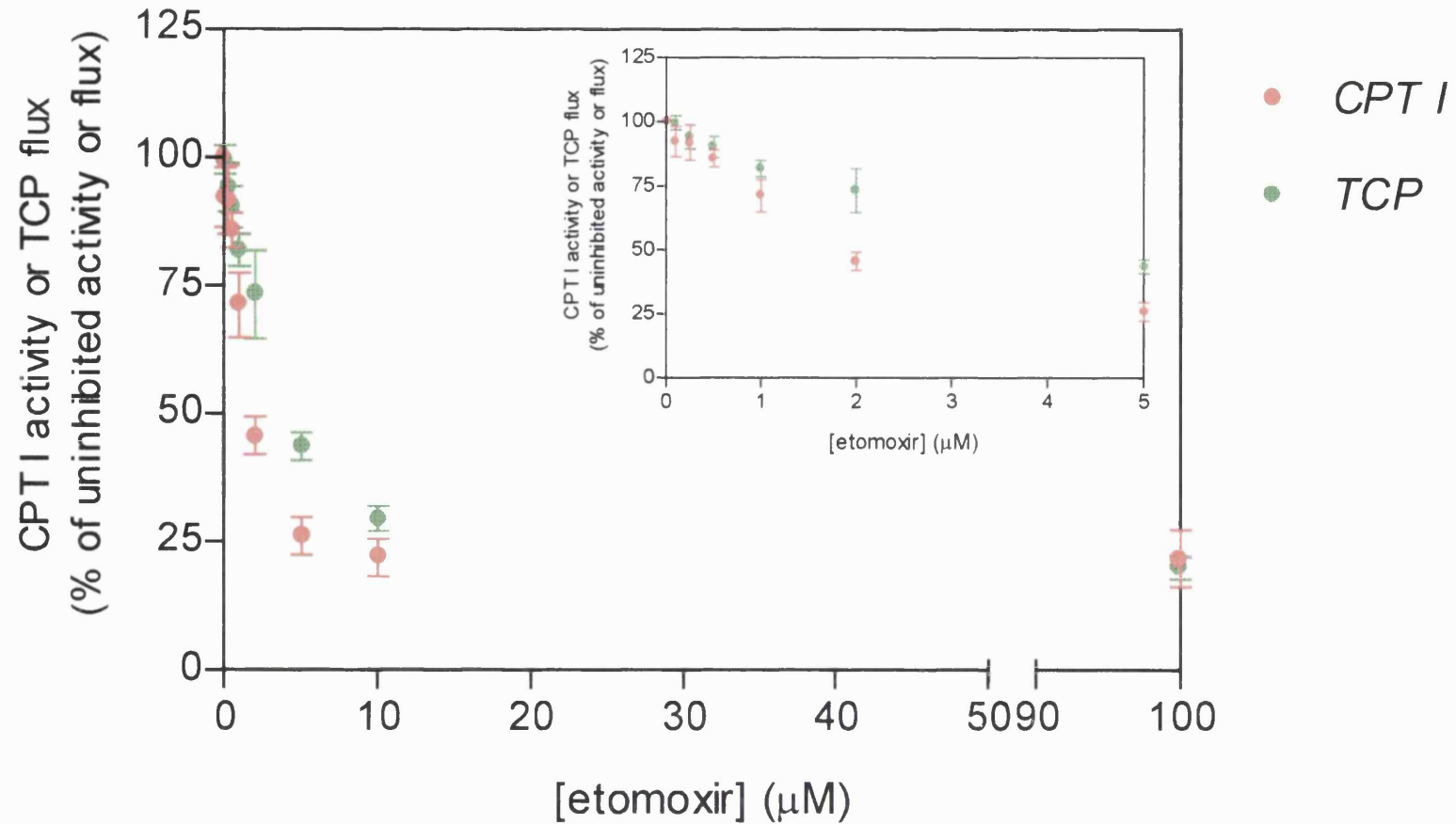


Figure 3.6 Effects of etomoxir on CPT I activity and total carbon flux

See legend for Figure 3.3 for details. TCP have been calculated only where flux data to ASP and CO₂ have been obtained during the same experiment, since they are obtained from the sum of the flux to ASP and CO₂. Values are means ± SEM, n=12 hepatocyte preparations. In the absence of etomoxir, the absolute rate of formation of total ¹⁴C-labelled products was 310 ± 43 nmol h⁻¹ (10⁶ cells)⁻¹. (New *et al.*, 1999 (b)).

Values for the flux control coefficients calculated from the data shown in Figures 3.2-3.6 are summarised in Table 3.1. Values obtained by Drynan *et al.*, (1996), who calculated flux control coefficients for CPT I over ketogenesis, CO₂ and total carbon products in the same system in adult rats, are also shown on this table for comparison. The individual flux control coefficients of the suckling rat system in Table 3.1 are the means \pm SEM, where n = the number of hepatocyte preparations. All the flux control coefficients in the suckling system were significantly different to those obtained in this equivalent adult system, as identified using the Student's *t*-test.

Hepatocyte preparation	$C_{CPTI}^{J_{ASP}}$	$C_{CPTI}^{J_{CO_2}}$	$C_{CPTI}^{J_{TCP}}$
Suckling rats (n=12)	0.51 \pm 0.03*	-1.30 \pm 0.26**	0.45 \pm 0.05*
¹ Fed adult rats (n=5)	0.85 \pm 0.20	0.23 \pm 0.06	1.06 \pm 0.29

Table 3.1 Individual flux control coefficients for CPT I over rates of formation of ketone bodies (ASP), carbon dioxide or total carbon products (TCP) from palmitate in isolated hepatocytes

Individual flux control coefficients were calculated using the data shown in Figures 3.2-3.6, Equations 3.1-3.3 and the Simfit package (Bardsley, 1997) to determine tangents at zero inhibitor. ¹Data from Drynan *et al.*, (1996) are shown for comparison. Values are means \pm SEM where n= the number of independent hepatocyte preparations. **p*<0.01; ***p*<0.001 indicate that values are significantly different from those obtained in the equivalent adult system.

3.3.2 BUCA in mitochondrial systems

(a) Adult rats

Figure 3.7 shows carbon fluxes, expressed as a percentage of the reference flux (state 3, 0 μ M malonyl-CoA) plotted against the percent change in the intermediate, external palmitoyl-carnitine (ex-pc) (from the reference levels) obtained from experiments using adult rats (raw data obtained by Krauss *et al.*, 1996). As indicated in Figure 3.7, the change in intermediate (ex-pc) can be positive or

negative when expressed relative to the steady-state reference intermediate level. The data from this figure were used to calculate the state 3.5 flux control coefficients for CPT I over ketogenic flux and total carbon flux, using the BUCA method, as described in detail in Section 3.2.2, and specifically Figure 3.1.

(b) Suckling rats

Figure 3.8 shows carbon fluxes, expressed as a percentage of the reference flux (state 3, 0 μ M malonyl-CoA) plotted against the percent change in the intermediate, external palmitoyl-carnitine (ex-pc) (from the reference levels) obtained from experiments using suckling rats (raw data obtained by Krauss *et al.*, 1996). As in the adult mitochondrial system, the data from Figure 3.8 were used to calculate the state 3.5 flux control coefficients for CPT I over ketogenesis and total carbon, using the BUCA method (as detailed in Section 3.2.2, Figure 3.1).

The individual flux control coefficients for adult and suckling rats were calculated and are shown in Figure 3.9. The coefficients for CPT I over ketogenesis and total carbon flux were all close to, or slightly greater than 1.0 in mitochondria isolated from adults, with the exception of that for CPT I over total carbon flux at a concentration of 5 μ M malonyl-CoA. In contrast, the flux control coefficients for both ketogenesis and total carbon flux in mitochondria isolated from suckling rats were all less than 1.0. It can be seen that flux control coefficients for CPT I over total carbon and over ketogenesis are greater than 0.75 in both adult and suckling rats.

Since the plots shown in Figures 3.7 and 3.8 were compiled as a composite of partial grids, each rising from one days experiment on one preparation, it is not valid to present the sets of flux control coefficients with error bars in Figure 3.9. This has been described in detail by Krauss *et al.*, (1996), but in summary, in order to show errors, the entire grid would need to be compiled from a single days preparation, which would not have been feasible owing the number of incubations and incubation times.

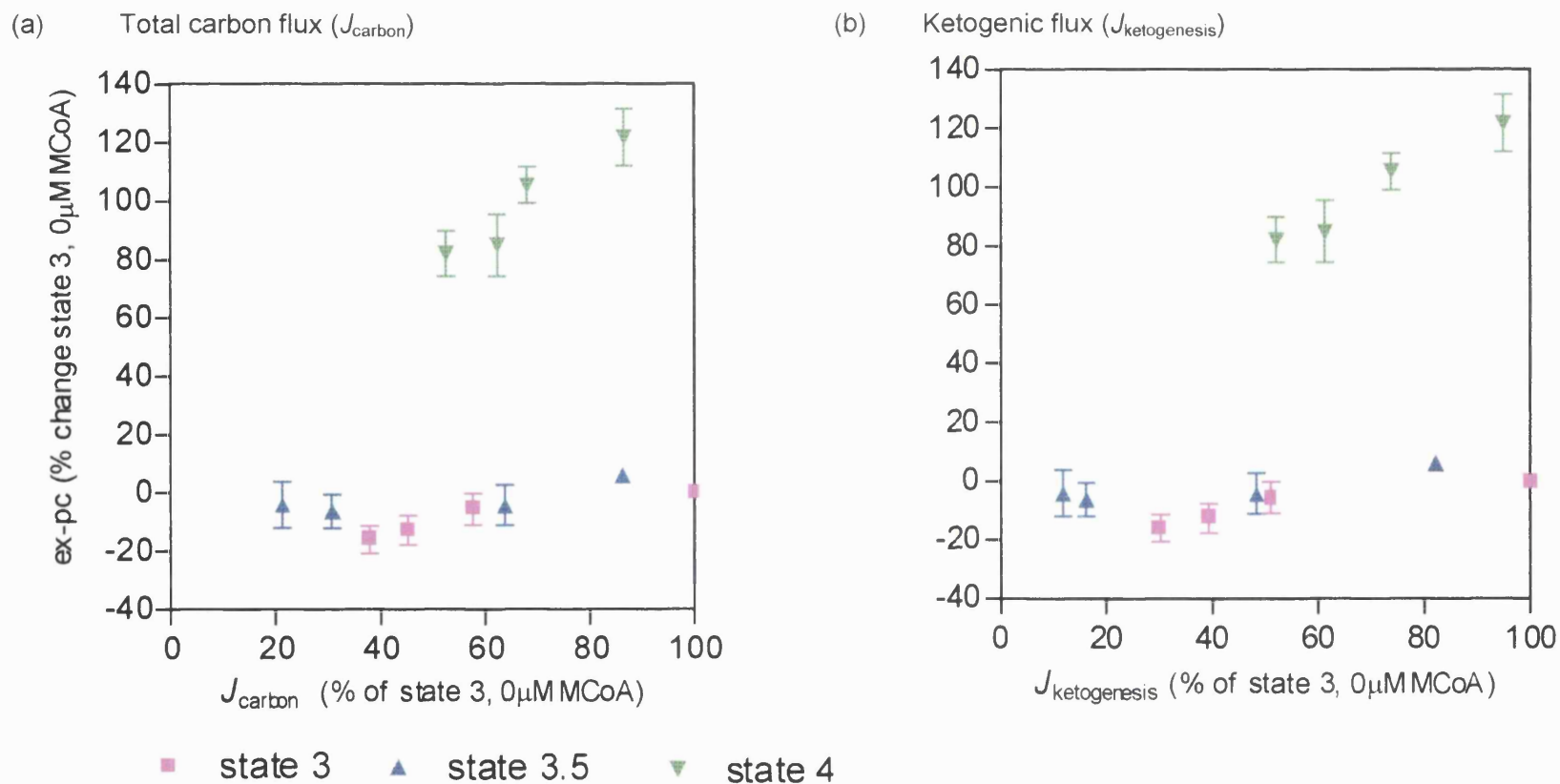


Figure 3.7 Effect of malonyl-CoA concentration and respiratory rate on external palmitoyl-carnitine levels and carbon fluxes from palmitoyl-CoA in mitochondria isolated from adult rats

In these adult mitochondrial systems (a) total carbon flux (J_{carbon}) and (b) ketogenic flux ($J_{\text{ketogenesis}}$) were titrated with increasing [malonyl-CoA] as detailed in Krauss *et al.*, 1996. Values are means \pm SEM where $n=6$ independent mitochondrial preparations. x errors have been omitted for clarity. Each grid (i.e. set of results) consists of a net of twelve points each, through which seven lines can be drawn: four at constant malonyl-CoA and three at constant respiratory state. (New *et al.*, 1999(b)).

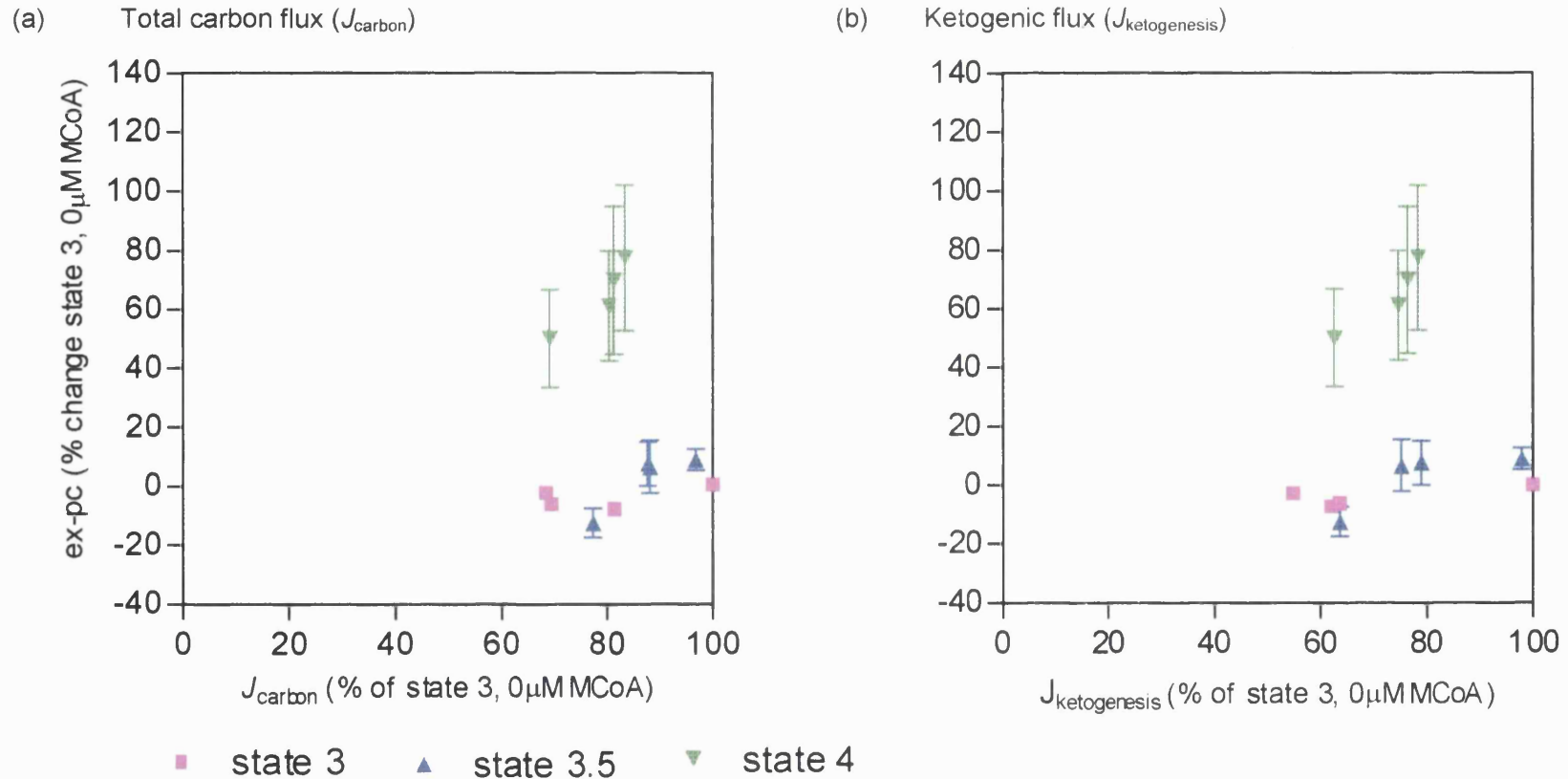
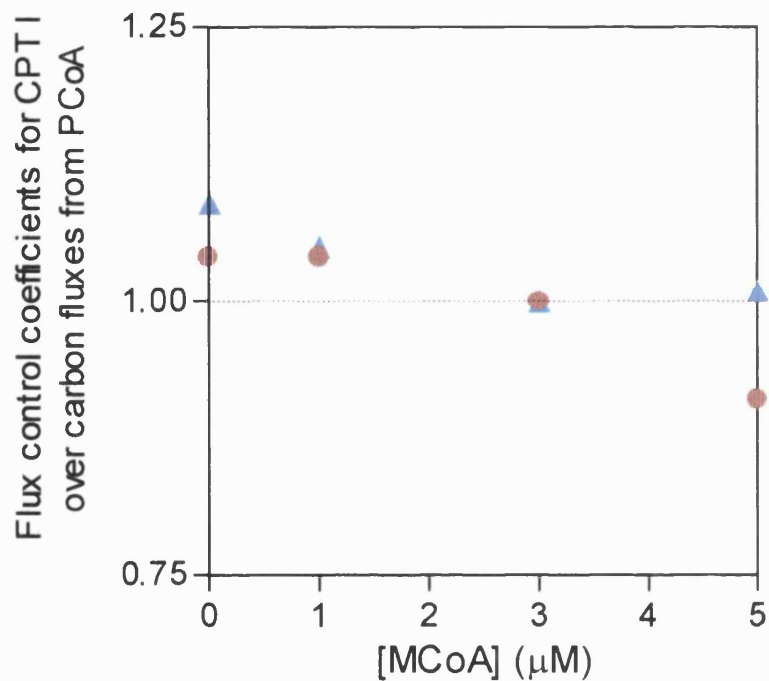


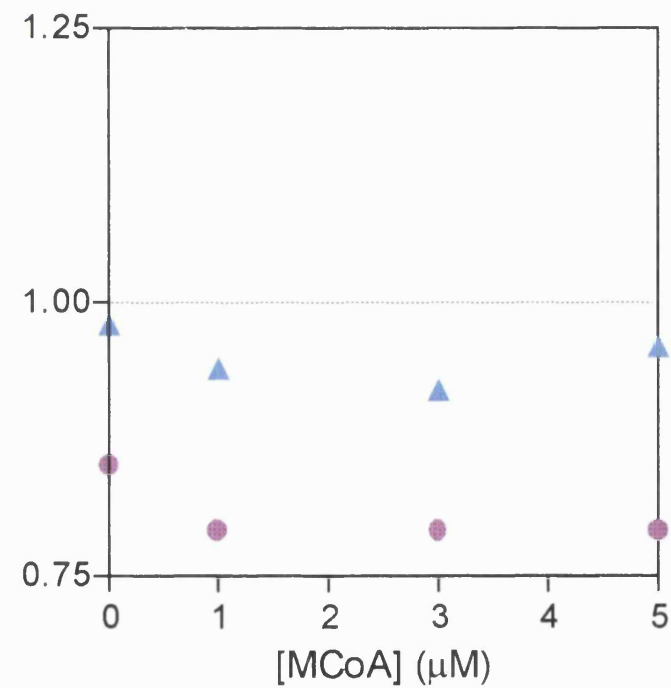
Figure 3.8 Effect of malonyl-CoA concentration and respiratory rate on external palmitoyl-carnitine levels and carbon fluxes from palmitoyl-CoA in mitochondria isolated from suckling rats

See Figure 3.7 for detail. In these suckling mitochondrial systems (a) total carbon flux (J_{carbon}) (b) ketogenic flux ($J_{\text{ketogenesis}}$) were titrated with increasing malonyl-CoA concentrations as detailed in Krauss *et al.*, 1996. Values are means \pm SEM where $n=6$ independent mitochondrial preparations. x errors have been omitted for clarity. (New *et al.*, 1999(b)).

(a) Adult rats



(b) Suckling rats



- Flux control coefficient for CPT I over total carbon flux
- ▲ Flux control coefficient for CPT I over ketogenesis

Figure 3.9 Effect of malonyl-CoA concentration on flux control coefficients for CPT I over carbon fluxes from palmitoyl-CoA in mitochondria isolated from (a) adult or (b) suckling rats

The calculation of flux control coefficients was based on the evaluation of a complete graphical plot representing the different malonyl-CoA titrations and transitions from state 3 to state 4 (Section 3.2.2) as detailed previously. (New *et al.*, 1999(b)).

3.4 Discussion

In this chapter individual flux control coefficients, derived from two different systems, have been presented:

- (i) from hepatocytes isolated from suckling rats, describing the control exerted by CPT I over ketogenesis, flux to carbon dioxide and total carbon products, and
- (ii) from mitochondria isolated from suckling and adult rats, describing the control exerted by CPT I over ketogenesis and flux to total carbon products.

3.4.1 Validation of techniques

The techniques used in the CPT I assay have been extensively validated elsewhere (Guzmán *et al.*, 1988, 1992; Grantham *et al.*, 1988; Zammit *et al.*, 1988). These groups showed that, in permeabilised cells, the carnitine palmitoyltransferase activity measured using palmitoyl-CoA as substrate, represented predominantly mitochondrial CPT I, despite the presence of carnitine acyl-transferase activity in peroxisomes and microsomes. The microsomal enzyme has a much lower affinity for etomoxir-CoA than the mitochondrial and the peroxisomal enzyme is not irreversibly inhibited by this compound (Lilly *et al.*, 1990, 1992). It has also been shown that mitochondria remain intact following the permeabilisation process and that this technique measures CPT I, rather than CPT II (Zammit *et al.*, 1988). These findings are confirmed by the 80% inhibition of flux by etomoxir-CoA in the studies presented here (Figure 3.2).

In this study, approximately 20% of palmitate oxidation was not inhibited by etomoxir (Figure 3.3, and as found by others, for example, Spurway *et al.*, 1997). This may be due to uptake of long-chain fatty acids into the mitochondria by a carnitine-independent mechanism and the subsequent conversion to CoA esters by the medium-chain acyl-CoA synthase, or peroxisomal β -oxidation, chain shortening and subsequent mitochondrial CPT I-independent β -oxidation.

It has been shown elsewhere that [^{14}C]acid soluble products represent primarily ketone bodies (Garland *et al.*, 1968).

3.4.2 Tangents to inhibitor curves (where inhibitor tends to zero)

The graphs in Figure 3.4 show the scatter of data obtained from individual experiments, for both CPT I activity and ASP flux. They illustrate one of the inherent difficulties with the application of this approach of BUCA: the need to determine the initial slope, and the problem of 'the best fit curve'. In order to reduce subjectivity relating to calculations, the computer package Simfit (Bardsley *et al.*, 1997) was used. This series of programs assesses all data, draws the best fit curve through the points, draws a tangent to the curve (where inhibitor tends to 0) and then calculates the gradient of the tangent. Others have approached this problem by using the techniques of linear regression on the initial points of the inhibition curves (Spurway *et al.*, 1997). This latter approach, however, is not strictly valid, since the curves are *not* linear. It is likely that flux control coefficients calculated using this approach, rather than the one used in this work, are over estimations.

3.4.3 Application of BUCA in hepatocytes isolated from suckling rats

Figure 3.3 shows that the inhibition curves for CPT I activity and [¹⁴C]ASP formation which were used for the calculation of the flux control coefficient for CPT I over ketogenesis, were similar in this system. The ratio of the initial slopes of these curves gave a value for the flux control coefficient of $C_{CPTI}^{J_{ASP}} = 0.51 \pm 0.03$. As this value falls mid-way in the scale of the normal range of values for flux control coefficients, where 0 would signify low levels of control and 1 would suggest very high levels of control, this result supports the view that CPT I has an important contribution to control over flux from palmitate to ketone bodies. However, Fell and Thomas (1995) have suggested that unless a flux control coefficient has a value greater than 0.6, the effects on the pathway flux by changing the amount of a single enzyme may be limited. This result, therefore, suggests that whilst CPT I may be considered 'rate-controlling', it may no longer be appropriate to consider CPT I to be a 'rate-limiting' step over ketogenesis, since the flux control coefficient has a value below 0.6.

As shown in Table 3.1, the flux control coefficient for CPT I over ketogenesis is significantly lower in suckling rats than in fed adult rats. This suggests that the contribution of CPT I to control ketogenic flux is different in the two developmental stages. Figure 3.10 provides a comparison of the control distribution in suckling rats and an equivalent adult system (Drynan *et al.*, 1996).

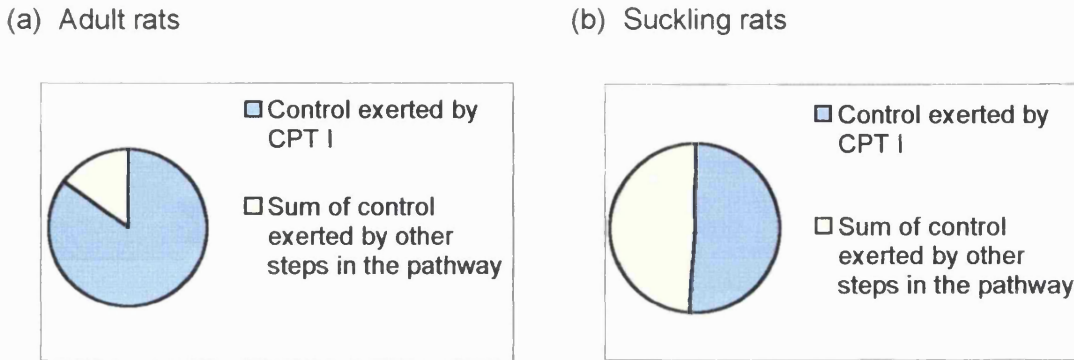


Figure 3.10 Comparison of the distribution of control over ketogenic flux observed in (a) adult rats and (b) suckling rats

As shown in Figure 3.10, the proportion of control exerted by CPT I over ketogenesis from palmitate, relative to that exerted by all the other steps in the pathway, is lower in suckling rats than in equivalent adult rats. This suggests that CPT I has a reduced capacity to control flux from palmitate to ketone bodies in suckling rats. The other steps in the pathways of fatty acid oxidation and ketogenesis (which would include, for example, all the steps of β -oxidation and the HMG-CoA cycle) share only approximately 15% of the control over ketogenic flux in adult rats. In the suckling rat, however, these other steps of the pathway have an increased contribution (approximately 49%) to control flux. These results, therefore, support the concept of multi-site control (Section 1.4.3; Fell *et al.*, 1995).

From the present study, it is not possible to say which particular step or steps within the pathways of fatty acid oxidation and ketogenesis have increased their flux control. Repeated application of BUCA, centred around different steps in these pathways would provide such information. This approach, however, is currently not possible because there is no means of independently manipulating the HMG-CoA cycle. In the following chapter, however, TDCA will be applied to a system of isolated suckling rat hepatocytes, with the aim to further characterise control distribution at this stage of development, since such analysis enables the control exerted by 'blocks of reactions' to be assessed. In this way, for example, the control exerted by the 'HMG-CoA block of reactions' can be quantitatively examined and compared to that exerted by other blocks, such as the block which includes CPT I.

Through their work using TDCA in mitochondria isolated from adult rats, Quant *et al.*, (1993) have suggested that the enzymes of the HMG-CoA cycle may have a significant contribution to control ketogenic flux.

In the suckling rat hepatocyte system used in this study, progressive inhibition of CPT I (and flux to ketone bodies) was accompanied by an increase in the incorporation of label into CO₂ (Figure 3.5). Thus the ratio of the initial slopes of these curves resulted in a large and negative flux control coefficient, $C_{CPTI}^{J_{CO_2}} = -1.30 \pm 0.26$. This value was significantly different to the small positive flux control coefficient obtained from an equivalent adult system, as illustrated in Figure 3.11. It can be seen, therefore, that the control exerted by CPT I over flux from palmitate to CO₂ in hepatocytes isolated from adult and suckling rats is not the same.

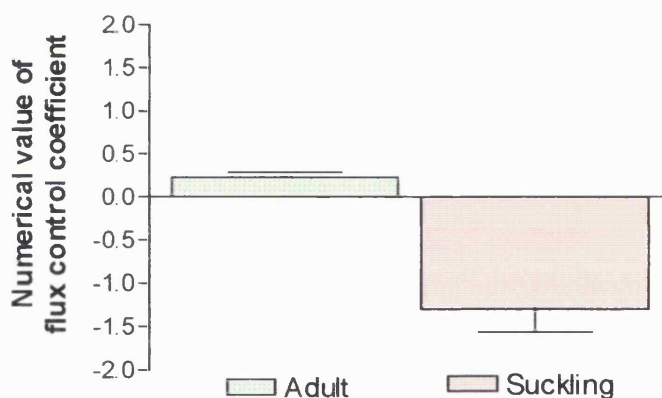


Figure 3.11 Comparison of the flux control exerted by CPT I over flux to CO₂ in adult and suckling rats

Whilst this pattern was not seen in the equivalent adult system, it was observed in starved/re-fed adult rats and in groups which had been starved/insulin treated (Drynan *et al.*, 1996), thus the value of the flux control coefficient for CPT I over flux to CO₂ in this suckling system is numerically similar to that found in these treated adult rats. This large and negative value suggests that an increase in flux through CPT I results in a decrease in flux to CO₂. Since the numerical value of the coefficient for CPT I over flux to CO₂ for suckling rats is not significantly different from that in 24 h-starved/insulin treated adult rats (-0.75 ± 0.70 , $n=3$, Drynan *et al.*, 1996) and the hormonal and nutritional profiles of suckling rats are more similar to

those of 24 h-starved/insulin treated rats (Girard *et al.*, 1992; Prip-Buus *et al.*, 1995), mechanisms similar to those described by Drynan *et al.*, (1996) may be operating to effect this change in control distribution in these suckling rats. Briefly, these would involve sequential reduction in maximal β -oxidation flux, brought about by etomoxir-CoA inhibition of CPT I, resulting in a change in redox state. Changes in the intramitochondrial concentration of oxaloacetate arising from a low NADH/NAD⁺ ratio would shift the equilibrium position of the reaction catalysed by malate dehydrogenase towards oxaloacetate. This in turn would lead to a diversion of acetyl-CoA towards citrate synthesis and an increased rate of formation of ¹⁴CO₂.

The results presented in this chapter indicate that the proportion of overall palmitate oxidation utilized for CO₂ formation represents a small fraction of the carbon product of palmitate oxidation. This is in agreement with a number of groups who have shown that ¹⁴CO₂ production accounts for less than 5% of palmitate oxidation (Cook *et al.*, 1980; Veerkamp *et al.*, 1986; Sherratt *et al.*, 1994; Drynan *et al.*, 1996).

The inhibition curves for CPT I activity and [¹⁴C]TCP shown in Figure 3.6 were similar and it is therefore not surprising that the resulting flux control coefficient is similar in value to that found for ASP, $C_{CPT I}^{J_{TCP}} = 0.45 \pm 0.05$. As before, this lower value for the flux control coefficient in suckling rats compared to adults (Figure 3.12) suggests that the contribution of CPT I to control total carbon flux is lower at this stage of development. Furthermore, it suggests changes in control distribution over the pathways, in suckling rats compared to adults. In adults, significant control over pathway flux is situated at a single step, whereas in the suckling rats, the proportion of control exerted by other steps is greater.

(a) Adult rats

(b) Suckling rats

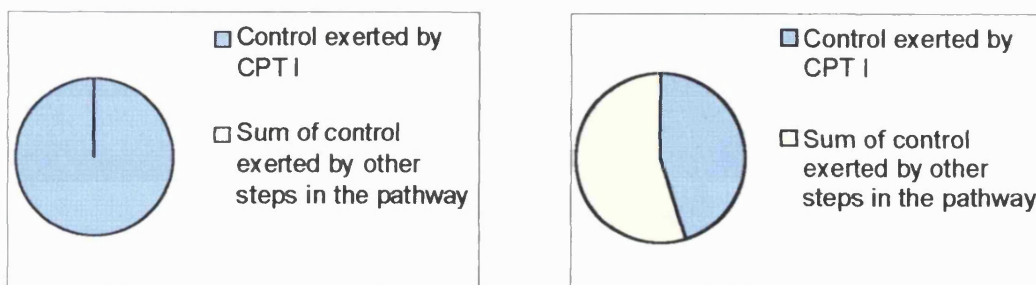


Figure 3.12 Comparison of the distribution of control over total carbon flux observed in (a) adult and (b) suckling rats

3.4.4 Application of BUCA in mitochondria

Due to constraints in their original mitochondrial system, detailed in Section 3.2.2, Krauss *et al.*, (1996) were unable to use TDCA to assess the control exerted by CPT I over flux to ketone bodies. However, it is possible to apply BUCA in the re-defined system (Scheme 3.3), and a range of individual flux control coefficients have been calculated for CPT I over total carbon flux and over ketogenesis.

Flux control coefficients were calculated for a range of malonyl-CoA concentrations added to the state 3.5 mitochondrial systems (which is thought to represent the 'physiological' respiratory state of mitochondria *in situ* in hepatocytes) because the concentration of malonyl-CoA *in situ* in hepatocytes, is uncertain. Top-down regulation analyses, which can be used to derive response coefficients that quantify the response of a system to an effector, have been performed in rat liver mitochondria (Makins *et al.*, 1995). The results from their analyses suggest that CPT I responds most acutely to malonyl-CoA concentrations within the range 0 to 5 μM , which are the ranges used in these studies. Additionally, the physiological range of malonyl-CoA concentration is 1 to 5 μM (Zammit, 1981) and Decaux *et al.*, (1988) have obtained average values of 16 and 6.1 nmol (g wet mass)⁻¹ of malonyl-CoA from hepatocytes isolated from suckling and weaned rats respectively.

It can be seen in Figures 3.9(a) and (b), however, that there is only a slight variation in the numerical value of the flux control coefficient, with changing malonyl-CoA concentration. Figure 3.9(a) shows that with the exception of 5 μM malonyl-CoA, all of the individual flux control coefficients for CPT I over total carbon flux in adult mitochondria (i.e. for each concentration of malonyl-CoA) are close to 1.0. These values contrast with those in Figure 3.9(b), which shows the equivalent sets of coefficients in suckling mitochondria, and which are consistently lower. Such trends are also observed when considering the individual flux control coefficients for CPT I over ketogenesis. In adults, Figure 3.9(a), the values are all at or greater than 1.0. In contrast, in the suckling system, all are less than 1.0 (Figure 3.9(b)). In all cases the BUCA flux control coefficients for CPT I over ketogenesis are greater than those for total carbon flux suggesting that the flux control coefficients over Krebs cycle flux are small and/or negative, which was observed in the suckling hepatocyte systems discussed previously.

Since all of the values for flux control coefficients reported in Figures 3.9(a) and (b)

are above 0.75, they are higher than is usually seen for most allosterically regulated enzymes, which typically have values below 0.6 (Fell, 1995; Mazat *et al.*, 1996). These results suggest that the level of control exerted by other steps in the pathways of palmitoyl-CoA oxidation is likely to be low. In support of this conclusion, CPT II has been found to have only a small contribution to control flux (Bonfont *et al.*, 1996) with low values for flux control coefficients reported (Kunz *et al.*, 1991).

This new bottom-up analysis performed on the data reinforces the conclusions drawn from the original top down analysis in these systems, i.e. that the distribution of control over carbon fluxes in mitochondria differed in the two different developmental stages, with control shifting away from CPT I in the suckling stage. These results also support the conclusions drawn from the BUCA in hepatocytes isolated from suckling rats, as discussed in Section 3.4.3. Since it is difficult to prepare hepatocytes from adult rats using the same method used for suckling rats, this mitochondrial analysis provides confirmation of the change in the flux control coefficient of CPT I between the two developmental stages, with the lower value observed in the suckling rats.

3.4.5 Interpretation of BUCA results

It is important to realise that because the two different systems considered here (cells *versus* mitochondria) have different pathways and therefore different numbers of components, it should not necessarily be expected that the numerical value for the flux control coefficients will be the same. Another consequence of the differences between these systems is that it is not strictly valid to make comparisons of flux control coefficients obtained in each system – although such comparisons are frequently made in the literature. Similarly, it is not strictly valid to compare an individual flux control coefficient obtained through BUCA with a group flux control coefficient obtained by application of TDCA unless the top-down system has been defined so that there is only one component in the block.

It is also important to remember that CPT I is a transmembrane protein, which interacts with cytosolic effectors within the cell and which is sensitive to allosteric inhibition by malonyl-CoA. Using hepatocytes, which contain these effectors, as a model system eliminates the need to add effectors back into the system, which would involve assumptions regarding their cellular concentrations. A possible

criticism of the use of hepatocytes is that flux and CPT I measurements may not be from the same 'starting point', since intact hepatocytes will contain malonyl-CoA. However, since all hepatocytes used during these experiments were obtained from animals from standardized litters, with animals of the same nutritional state and age range, and from several pups per preparation, this potential problem has been minimized.

In the mitochondrial investigations, the cellular environment is replaced with an artificial one. Thus the results obtained from the mitochondrial analysis considered here may not necessarily reflect the control exerted in the intact cell and may, therefore, be of less physiological relevance than those from hepatocytes.

3.4.6 Factors effecting the values for flux control coefficients for CPT I over carbon fluxes

The lower capacity of CPT I to control catabolic carbon fluxes in the suckling period, compared to adult systems could be a function of several factors. For example, not only are the inhibitory effects of malonyl-CoA altered under certain (patho)physiological conditions, such as starvation (Kolodziej *et al.*, 1990) and diabetes (Kashfi *et al.*, 1988), but CPT I also shows reduced sensitivity to malonyl-CoA during suckling (Herbin *et al.*, 1987) and is exposed to lower concentrations of this effector.

Changes in the fluidity of the outer mitochondrial membranes (reviewed in Zammit, 1994) may effect the interaction between the N- and C-terminal domains of CPT I (Fraser *et al.*, 1997). This, along with changes in the number and nature of contact sites, may influence the kinetic properties of CPT I through changes in its environment (Fraser *et al.*, 1998). The functional capacity of CPT I may also be modified by changes in hepatocyte cell volume (Guzmán *et al.*, 1994) and recent evidence indicates that CPT I activity is also controlled by interactions between mitochondria and cytoskeletal components (Velasco *et al.*, 1996; Guzmán *et al.*, 2000). Although a 'physiological' pH was maintained during the experiments reported in this thesis, it should be noted that the effects of pH on CPT I may be of physiological relevance (Moir *et al.*, 1995). Whilst a broad pH optimum has been reported for CPT I, the work of Stephens *et al.*, (1983) suggests the sensitivity of CPT I to malonyl-CoA inhibition changes with intracellular pH and may provide a physiological mechanism for attenuating the production of ketone bodies during

periods of acidosis. Such mechanisms may change the potential of CPT I to control oxidative carbon fluxes to ketone bodies and CO₂.

It is also important to note that the summation theorem of MCA states that all of the steps in a metabolic pathway contribute to control over pathway flux and that the flux control coefficients in a pathway sum to 1 (Kacser and Burns, 1979; Section 1.4.3). Therefore, differences in flux control coefficients for CPT I will arise if there are different values for other enzymes (for example, trifunctional protein or HMG-CoA synthase) although these have not been quantitatively assessed in the pathway.

3.4.7 Conclusions

The studies presented and discussed in this chapter have shown that MCA supports the historical view that CPT I does have a significant contribution to control over ketogenic flux in adult rats. However, these studies also demonstrate that control distribution changes with developmental stage. In contrast to the pattern of control distribution observed in adult rats, where a high level of control is exerted at a single step, in suckling rats control is distributed throughout the pathways of fatty acid oxidation and ketogenesis. These results therefore support the concept of multi-site control (Fell *et al.*, 1995). Furthermore, these results suggest that the control exerted by CPT I over the pathways of ketogenesis is lower in the suckling stage than in the adult. The results presented here, therefore, suggest that in suckling rats, the historical assumption that CPT I is necessarily the 'rate-limiting' step of fatty acid oxidation and ketogenesis is no longer appropriate (New *et al.*, 1999(b)).

The results presented in this chapter prompted further investigations into the distribution of control over the pathways of fatty acid oxidation and ketogenesis. These further experiments, presented in the following chapter, use the top-down control analysis approach to quantify and compare the control exerted by different sections of the pathway over carbon fluxes. Additionally, in Chapter 5, the studies presented here are further expanded, by consideration of the distribution of control in response to different physiological substrates. This is highly relevant, since neonatal diet differs to that found during adulthood and thus the potential of CPT I to control carbon fluxes may not necessarily be the same.

Chapter 4

Application of top-down control analysis in hepatocytes to investigate the distribution of control over carbon fluxes in the pathways of fatty acid oxidation, ketogenesis and the Krebs cycle

4.1 Introduction and aims

In the preceding chapter, the role of CPT I in controlling carbon fluxes from palmitate (C_{CPTI}^{JASP} ; C_{CPTI}^{JCO2} ; C_{CPTI}^{JTCP}) in suckling rats was examined and compared to an equivalent adult system. The work presented in this chapter expands on these studies by exploring how control over carbon fluxes is distributed over the whole pathway, rather than considering a single step. To perform this investigation, top-down control analysis (TDCA) is applied to the pathways, which enables the control exerted by groups of reactions, over pathway flux to be described.

As discussed previously, a large body of evidence suggests that a significant proportion of control over ketogenesis during the suckling period may be situated at sites other than CPT I, for example, at the level of the HMG-CoA cycle. In the work presented in this chapter, therefore, I aim to provide a quantitative assessment of the control exerted by 'blocks' of the pathways of fatty acid oxidation and ketogenesis, over flux through those 'blocks'. Each of the blocks of reactions is defined in detail in the following section.

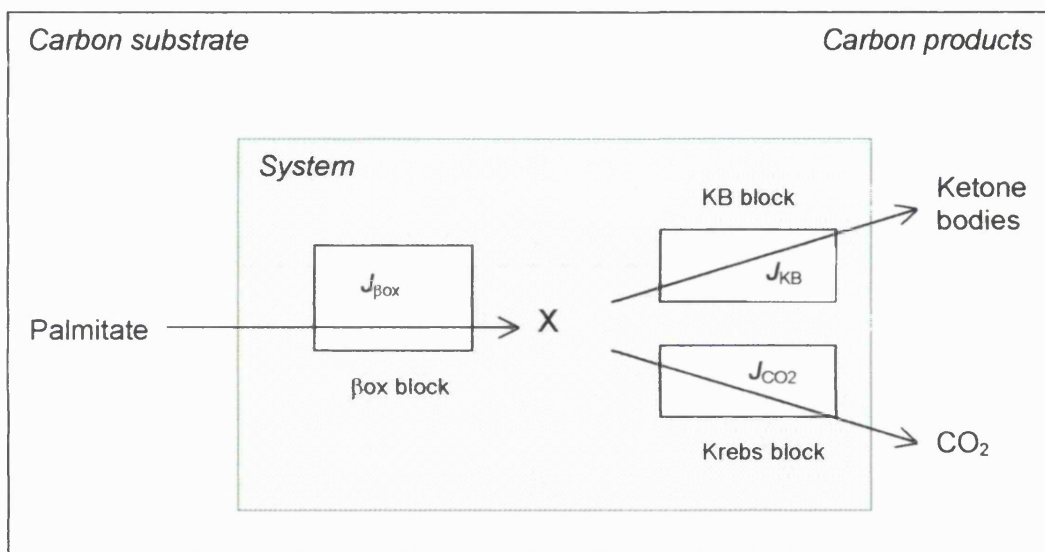
4.2 Theory and approaches

4.2.1 Application of TDCA in hepatocytes

As discussed in Section 3.2.1, control over fluxes is system specific and, therefore, the definition of the system is an important stage in the application of MCA. This section describes the system used to apply TDCA in hepatocytes isolated from suckling rats.

To apply TDCA it is necessary to conceptually divide the system into a small number of 'blocks' that may contain many reactions. These blocks are connected through a common intermediate, as described in more general terms in Section 1.4.7 and as illustrated in this specific system, in Scheme 4.1. The single producer block in this specific system produces the intermediate, X (a complex and unidentified carbon entity). This block comprises all the steps involved in the entry

of fatty acid into the cell and mitochondria, fatty acid activation and β -oxidation, and the reactions of the respiratory chain. There are two blocks that consume the intermediate in this system, one involves the reactions of the HMG-CoA cycle and the other involves the reactions of the Krebs cycle, resulting in the formation of ketone bodies and CO_2 respectively. Through relatively simple experimental and theoretical techniques, TDCA provides an overview of control in complex metabolic systems such as this, which is not easily accessible using other approaches (Brown *et al.*, 1990; Quant, 1993; Brand, 1996).



Scheme 4.1 Conceptually simplified system used for TDCA in hepatocytes

Using the same convention as detailed earlier in this thesis, the system is represented by a green box. This system consisted of hepatocytes isolated from suckling rats, oxidizing palmitate to ketone bodies and CO_2 . $J_{\beta\text{ox}}$, J_{KB} , J_{CO_2} represent carbon fluxes through β -oxidation, to ketone bodies and carbon dioxide, respectively. β ox block represents all the steps involved in the entry of fatty acid into the cell and mitochondria, fatty acid activation and β -oxidation, and the reactions of the respiratory chain. Krebs block involves the reactions of the Krebs cycle, resulting in the formation of CO_2 and the KB block involves the reactions of the HMG-CoA cycle resulting in the formation of ketone bodies. X represents the system intermediate, as discussed in the main text.

TDCA of the branched system described in Scheme 4.1 will describe the potential of each of the blocks of reactions (the single producer block and the two consumer blocks) to control system fluxes. This is achieved through the calculation of flux

control coefficients. Since these flux control coefficients refer to whole blocks, or sections, of the pathway under consideration, they are termed *group* flux control coefficients (as opposed to the *individual* flux control coefficients determined *via* bottom-up control analysis, BUCA). To distinguish it from an individual flux control coefficient derived from BUCA, a group flux control coefficient derived from TDCA is designated by a superscript star before the coefficient (for example, $*C_{block}^J$).

The number of possible group flux control coefficients depends on the number of branches in the defined system: TDCA states that where there are n branches in a system, there are n^2 flux control coefficients. Thus, in a three branched system, there are nine group flux control coefficients, for example:

- (i) the group flux control coefficients for each block over the flux through the producer block of reactions;
- (ii) the group flux control coefficients for each block over the flux through the first consumer block of reactions; and
- (iii) the group flux control coefficients for each block over the flux through the other consumer block of reactions,

The complete series of group flux control coefficients specific to this system is set out in Table 4.1 below.

Series 1	$*C_{KB}^{J_{KB}}$	$*C_{\beta OX}^{J_{KB}}$	$*C_{CO_2}^{J_{KB}}$	Flux control coefficient for each block over flux through J_{KB} block of reactions
Series 2	$*C_{KB}^{J_{\beta OX}}$	$*C_{\beta OX}^{J_{\beta OX}}$	$*C_{CO_2}^{J_{\beta OX}}$	Flux control coefficient for each block over flux through $J_{\beta OX}$ block of reactions
Series 3	$*C_{KB}^{J_{CO_2}}$	$*C_{\beta OX}^{J_{CO_2}}$	$*C_{CO_2}^{J_{CO_2}}$	Flux control coefficient for each block over flux through J_{CO_2} block of reactions

Table 4.1 Full series of flux control coefficients in hepatocyte TDCA system described in Section 4.1

The number of independent experimental manipulations which need to be made in order to obtain the full series of group flux control coefficients also depends on the

number of branches in the system: TDCA states that where there are n branches in a system, $n - 1$ manipulations are required. In this three-branched system, therefore, two independent experimental manipulations were made to obtain the full series of flux control coefficients detailed in Table 4.1. Prior to manipulation, steady state fluxes were measured in the absence of any inhibitor. As in BUCA in the hepatocyte systems described in Chapter 3, flux from palmitate through to ketone bodies and carbon dioxide was measured by the accumulation of radiolabelled products, ($[^{14}\text{C}]\text{ASP}$ and $^{14}\text{CO}_2$) and flux through the β -oxidation block (β ox block) was calculated as the sum of the fluxes through the other two branches. A series of concentrations of etomoxir (which is converted to etomoxir-CoA intracellularly and which specifically inhibits CPT I within this block) was used to manipulate the β ox block and the system was allowed to relax to a new steady state and system fluxes measured/calculated. The second manipulation, on the Krebs cycle block of reactions producing CO_2 (Krebs block), involved a series of concentrations of malonate, specifically inhibiting succinate dehydrogenase in the Krebs cycle. Again, the system was allowed to relax to a new steady state and the system fluxes measured/calculated.

Thus TDCA overcomes the restrictions which apply to BUCA: at present specific independent manipulation of any of the enzymes of the KB block is not possible and therefore BUCA cannot be performed on these particular steps of the pathway. By using TDCA, however, and considering the pathways of fatty acid oxidation, Krebs cycle and the HMG-CoA cycle as separate blocks of reactions, it is possible to obtain a quantitative assessment of the relative proportion of control each block exerts over the other blocks. In this way, for example, the contribution of the HMG-CoA block (although not of mHMG-CoA synthase specifically) to control ketogenesis can be calculated.

The TDCA described in Chapter 3, performed by Krauss *et al.*, (1996), required measurement of the system intermediate. In the system described here, however, the intermediate is necessarily complex and direct measurement would be difficult and prone to large errors, making it unreasonable to measure accurately. To overcome this complication, in this TDCA, group flux control coefficients are calculated from flux data alone, using the equations set out in the following sections (derived in Appendix I and restated in their final form in Table A1.2) without the need to measure (or even define) the system intermediate.

4.3 Results

4.3.1 Effects of manipulation of the Krebs block

In order to establish the appropriate concentration of inhibitor to bring about a small but significant change in the Krebs block of reactions, a range of concentrations of malonate (0-15mM) have been used to manipulate this block. As shown in Figure 4.1 flux to $^{14}\text{CO}_2$ was inhibited at concentrations $>2.5\text{mM}$ malonate.

Figure 4.2 shows the effect of this same range of malonate concentrations on flux through the KB block and the β ox block (where β ox flux is calculated as the sum of fluxes to ^{14}C ASP and $^{14}\text{CO}_2$). Since no significant variations in these fluxes are observed over this range of malonate concentrations (0-15mM) these results validate the use of this particular inhibitor, which is manipulating only a single block of reactions in the system (the Krebs block). Fluorimetric assays (Section 2.2.5) confirmed that ^{14}C ASP primarily represent ketone bodies in these hepatocytes, both in the absence and presence of the range of malonate concentrations used in these experiments.

The results presented in Figures 4.1 and 4.2 indicate that flux data obtained at the manipulation point 5mM malonate would be appropriate for calculation of the group flux control coefficients, since this concentration of inhibitor resulted in small but significant changes in system fluxes.

4.3.2 Effects of manipulation of the β -oxidation block

Figure 4.3 shows the effect of manipulation of the β ox block of reactions with etomoxir. As shown in the Figure 4.3(b), β ox flux was inhibited at concentrations $>2\mu\text{M}$ etomoxir.

Figures 4.4 (a) and (b) show the effect of the same range of etomoxir concentrations on flux to $^{14}\text{CO}_2$ and ^{14}C ASP. As seen in Figures 3.3 and 3.5, manipulation of CPT I within this block of reactions using a range of concentrations of etomoxir (0-100 μM) decreased flux to ^{14}C ASP, whilst initially, flux to $^{14}\text{CO}_2$ was increased (New *et al.*, 1999). The results presented in Figure 4.4(b) suggest that a concentration of 2 μM etomoxir results in small but significant changes to that block, but results in non-significant changes in flux through the other blocks of reactions. It would be appropriate, therefore, to substitute flux data obtained at this data point into the equations for the calculation of the group flux control coefficients.

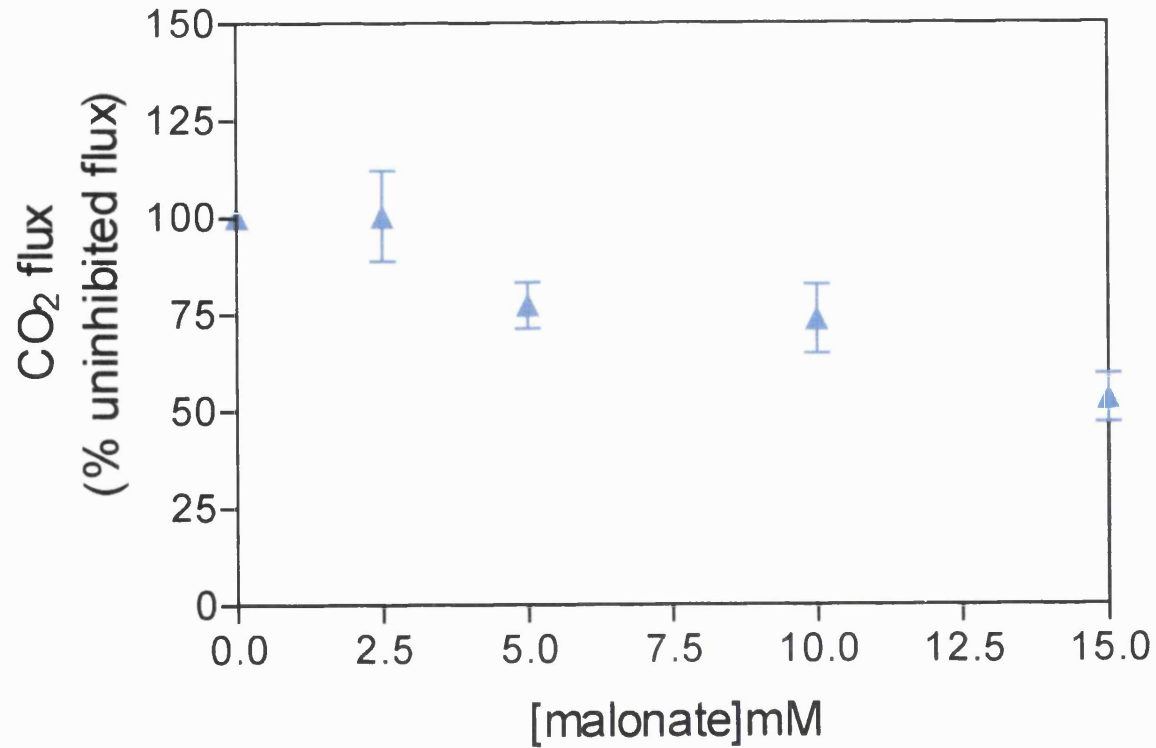
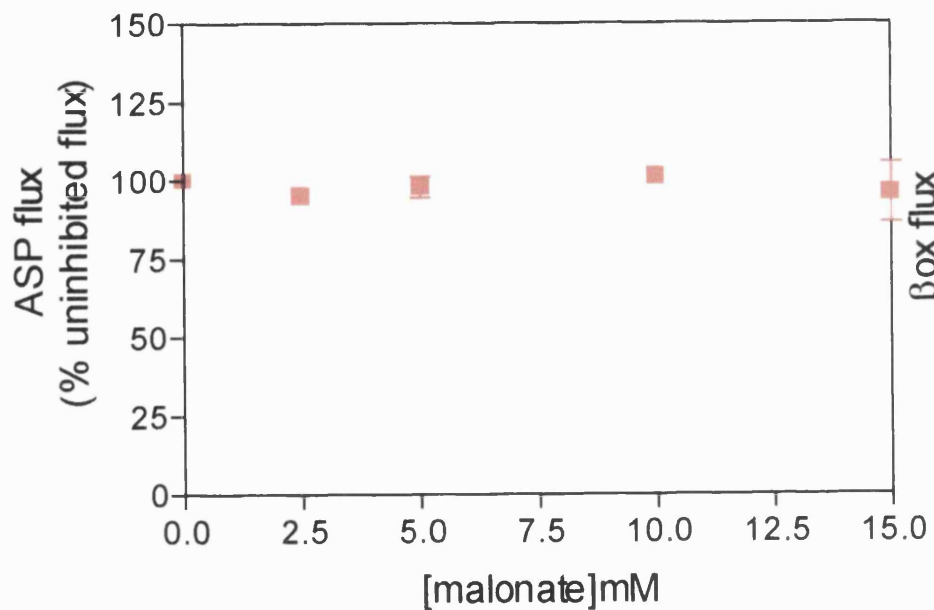


Figure 4.1 Effect of malonate on flux through the Krebs cycle block of reactions

Hepatocyte preparations with viability greater than 85% were used for experiments, and hepatocytes were incubated with malonate for 10 min, as detailed in Chapter 2, Section 2.2.2. Following incubation with inhibitor, 1ml [14 C]palmitate (0.5mM final concentration, $0.4\mu\text{Ci}\mu\text{mol}^{-1}$, in KRB, 2% BSA) was added to flasks. Flux data were normalised by expressing them as a percentage of those obtained in the absence of malonate. Values are means \pm SEM, $n=17$ separate hepatocyte preparations.

(a) Flux through ketogenic block (KB block) of reactions



(b) Flux through β -oxidation block (β ox block) of reactions

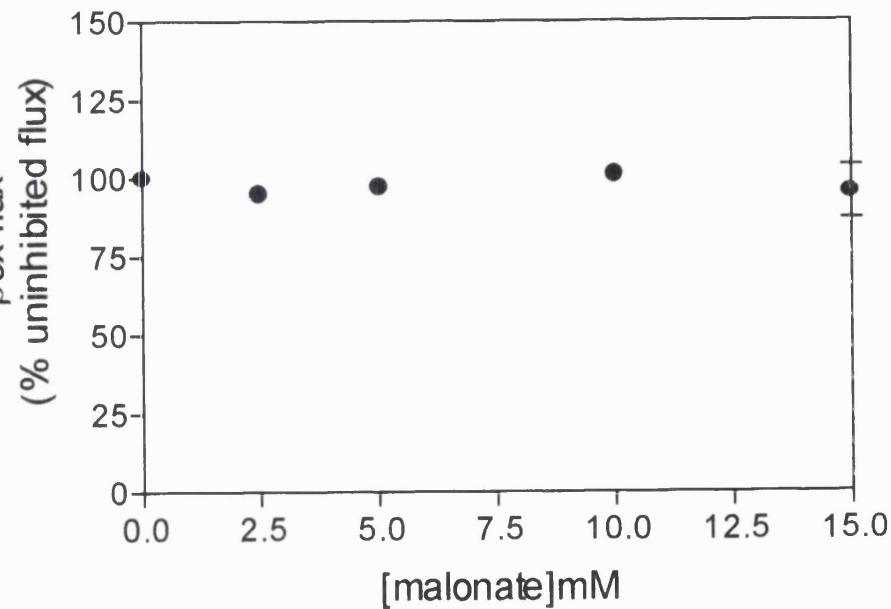
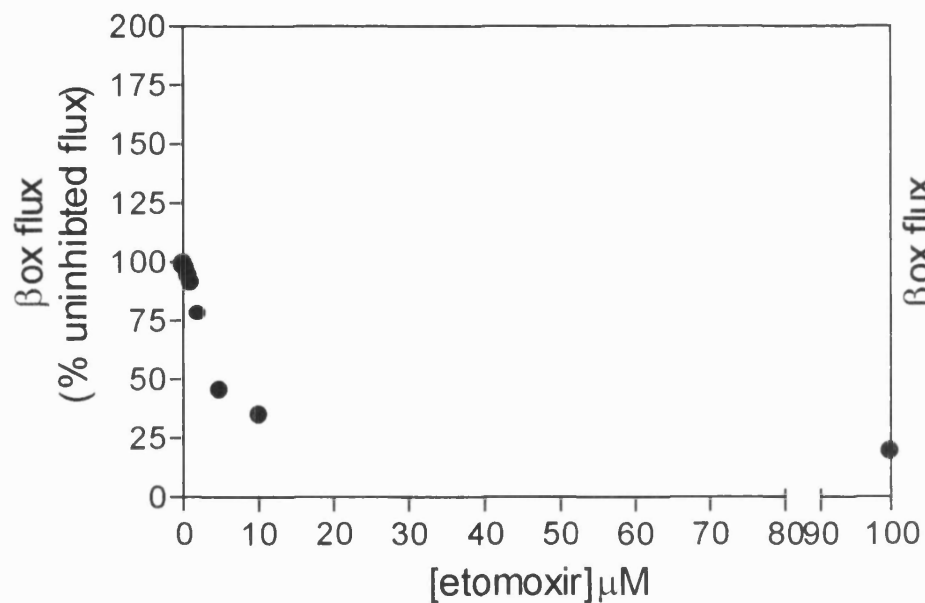


Figure 4.2 Effect of malonate on flux through the KB and β ox blocks of reactions

See Figure 4.1 for detail. Hepatocyte preparations with viability greater than 85% were used for experiments and hepatocytes were incubated with malonate for 10 min, as detailed in Chapter 2, Section 2.2.2. Flux data were normalised by expressing them as a percentage of those obtained in the absence of malonate. Values are means \pm SEM, n=17 separate hepatocyte preparations.

(a) Full range of data points



(b) Expansion of graph over low inhibitor concentration range

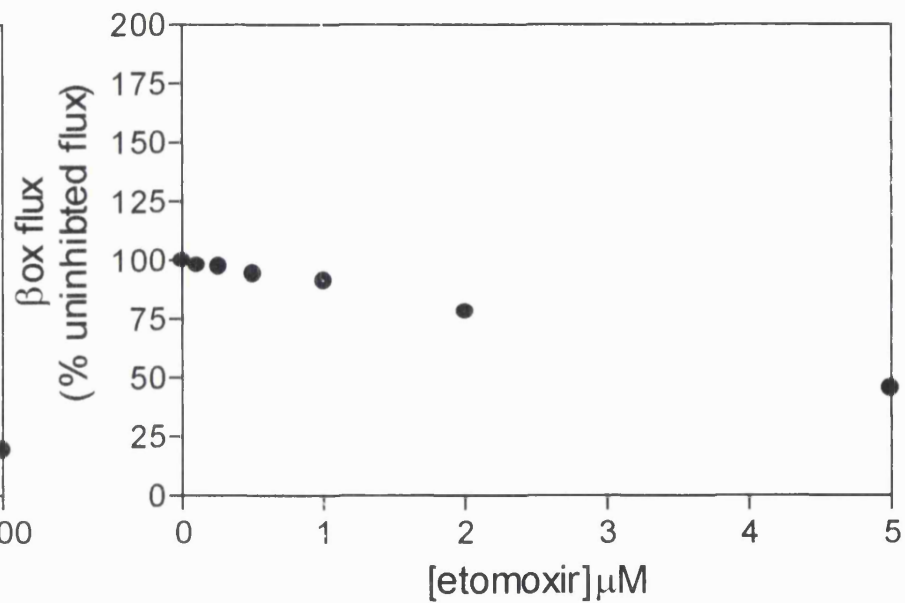
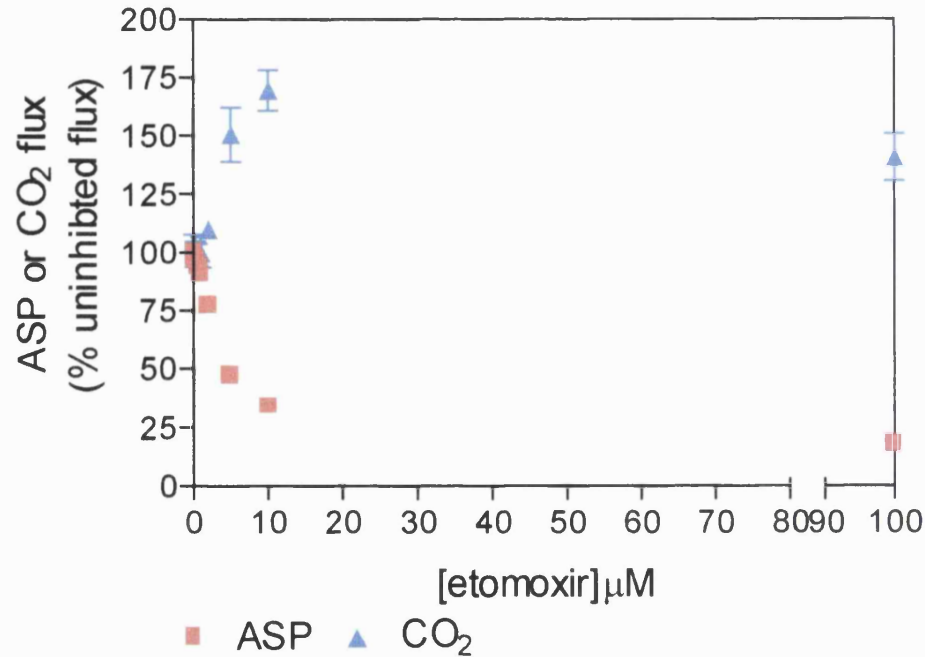


Figure 4.3 Effect of etomoxir on the β ox block of reactions

See Figure 4.1 for detail. Hepatocyte preparations with viability greater than 85% were used for experiments and hepatocytes were incubated with etomoxir for 10 min, as detailed in Chapter 2, Section 2.2.2. Flux data were normalised by expressing them as a percentage of those obtained in the absence of etomoxir. Values are means \pm SEM, $n=20$ separate hepatocyte preparations.

(a) Full range of data points



(b) Expansion of graph over low inhibitor concentration range

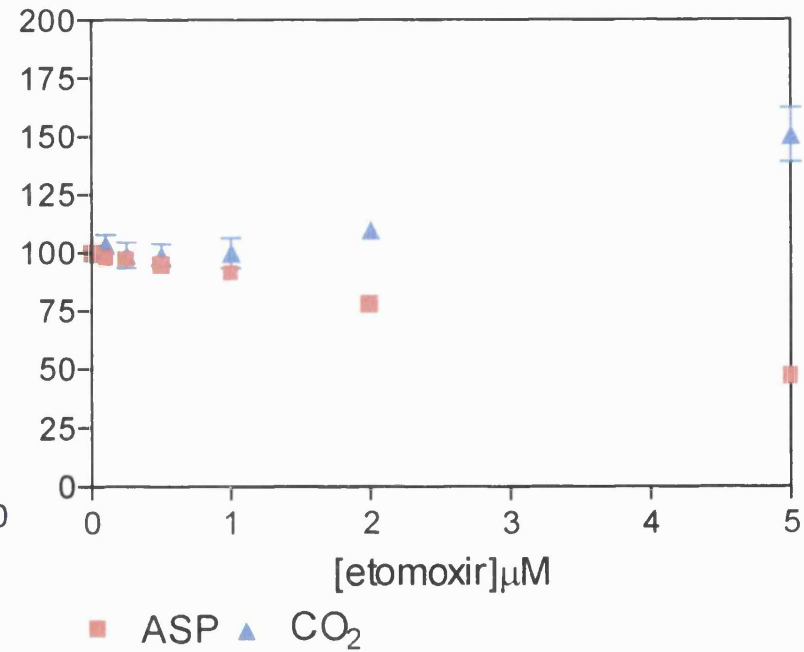


Figure 4.4 Effect of etomoxir on flux through the KB and Krebs cycle blocks of reactions

See Figure 4.1 for detail. Hepatocyte preparations with viability greater than 85% were used for experiments, and hepatocytes were incubated with etomoxir for 10 min, as detailed in Chapter 2, Section 2.2.3. Flux data were normalised by expressing them as a percentage of those obtained in the absence of etomoxir. Values are means \pm SEM, $n=20$ separate hepatocyte preparations.

4.3.3 Flux data from two independent manipulation experiments

To apply TDCA, fluxes should be expressed in the same units, typically in terms of production and consumption of the system intermediate. Since the intermediate is not defined in this system, to ensure the data is considered in the same units here, fluxes are expressed as percentages (Table 4.2).

Manipulation	ASP	CO ₂	β-oxidation
[Malonate] mM			
0	100.00	100.00	100.00
2.5	94.95	100.40	94.96
5.0	97.71	77.30	97.52
10.0	101.39	73.60	101.12
15.0	95.85	53.10	95.43
[Etomoxir] μM			
0	100.00	100.00	100.00
0.10	97.88	103.77	97.91
0.25	97.19	99.24	97.25
0.50	94.18	99.10	94.27
1.00	90.89	100.09	91.11
2.00	77.89	109.94	78.17
5.00	47.16	150.59	45.61
10.00	34.24	169.64	35.32
100.00	17.88	140.59	19.04

Table 4.2 Data from each experimental manipulation expressed in terms of percent change in flux

Values for malonate titrations were calculated from the means of 17 independent hepatocyte preparations. Values for etomoxir titrations were calculated from the means of 20 independent hepatocyte preparations.

Comparison of the effects of each manipulation on flux to ASP, CO₂ and βox (Figures 4.1 to 4.4) indicated that flux data obtained using the 5mM malonate and 2μM etomoxir should be substituted into the appropriate equations (as discussed in Sections 4.3.1 and 4.3.2).

4.3.4 Calculation of group flux control coefficients

The calculation of the first group flux control coefficient for series 1 (Table 4.1), uses specific equation 1 (summarised in Table A1.2 and repeated here for information):

$$*C_{\beta OX}^{J_{KB}} = \frac{-J_{\beta OX} / J_{KB}}{1 + \left(\frac{\delta J_{\beta OX}^{(CO_2)}}{\delta J_{KB}^{(CO_2)}} \right) + \left(\frac{\delta J_{CO_2}^{(\beta OX)}}{\delta J_{KB}^{(\beta OX)}} \right)}$$

Substitution of appropriate flux data into specific Equation 1, using the sign convention detailed in Section A1.2:

$$*C_{\beta OX}^{J_{KB}} = \frac{-(-100) / +100}{1 + \left(\frac{(-97.52) - (-100)}{(97.71) - (100)} \right) + \left(\frac{(-109.94) - (-100)}{(77.89) - (100)} \right)} \quad *C_{\beta OX}^{J_{KB}} = 0.39$$

The calculation of the second flux control coefficient in this first series uses specific equation 2, (summarised in Table A1.2 and repeated here for information):

$$*C_{KB}^{J_{KB}} = \frac{\left(\frac{\delta J_{\beta OX}^{(CO_2)}}{\delta J_{KB}^{(CO_2)}} \right) + \left(\frac{\delta J_{CO_2}^{(\beta OX)}}{\delta J_{KB}^{(\beta OX)}} \right)}{1 + \left(\frac{\delta J_{\beta OX}^{(CO_2)}}{\delta J_{KB}^{(CO_2)}} \right) + \left(\frac{\delta J_{CO_2}^{(\beta OX)}}{\delta J_{KB}^{(\beta OX)}} \right)}$$

Substitution of appropriate flux data into specific Equation 2:

$$*C_{KB}^{J_{KB}} = \frac{\left(\frac{(-97.52) - (-100)}{(97.71) - (100)} \right) + \left(\frac{(-109.94) - (-100)}{(77.89) - (100)} \right)}{1 + \left(\frac{(-97.52) - (-100)}{(97.71) - (100)} \right) + \left(\frac{(-109.94) - (-100)}{(77.89) - (100)} \right)} \quad *C_{KB}^{J_{KB}} = -1.70$$

The calculation of the final flux control coefficient in this first series uses specific equation 3, repeated on the left here for information, and with the final value following substitution of flux control coefficients calculated above, on the right:

$$*C_{CO_2}^{J_{KB}} = 1 - (*C_{KB}^{J_{KB}} + *C_{\beta OX}^{J_{KB}}) \quad *C_{CO_2}^{J_{KB}} = 2.31$$

Whilst the value for the flux control coefficient for the β -oxidation block over ketogenic flux is not an unreasonable numerical value, the other two coefficients are unusually large. Subsequent recalculation over the whole range of data points gave similarly unusual results (data not presented). Since the remaining group flux control coefficients are obtained using this data, these have not been calculated.

4.4 Discussion and conclusions

Substitution of flux data into specific TDCA equations, as described in Section 4.3, resulted in values outside the typical range for flux control coefficients. There may be several reasons for this result as discussed below.

The results presented here, and in Chapter 3, indicate that the proportion of overall [1- 14 C]palmitate oxidation utilized for 14 CO₂ formation represents a very small fraction of the total oxidative rate (<5%), which is consistent with the results of Sherratt *et al.*, (1994), Cook *et al.*, (1980) Veerkamp *et al.*, (1986), and Drynan *et al.*, (1996). Here, for example, even with 17 independent hepatocyte preparations, the errors on this small value are large (or as large as the mean value). Thus the small changes necessary for TDCA are lost within these errors and realistic group flux control coefficients cannot be calculated.

Additionally, $J_{\beta\text{ox}}$ is a calculated value in this system, which has compounded errors in the calculations, since rather than presenting the primary effects of the experimental manipulation, the calculation would actually be presenting a secondary effect of manipulation of βox , derived from the primary effect on the other two fluxes. On reflection, a more appropriate method for assessment of βox flux in this system, for this type of analysis, would have been *via* measurement of oxygen consumption from palmitate – since this would have provided a direct measurement, rather than a value calculated from the sum of the other two fluxes.

In summary, although it has not been possible to obtain an overview of the control structure of the pathways of fatty acid oxidation and ketogenesis, a fuller appreciation of the pathway fluxes and the limitations of the assays used in the experiments has been gained.

Chapter 5

Analysing the role of CPT I in control of carbon flux from medium-chain fatty acids and mixtures of long- and medium-chain fatty acids

5.1 Introduction

In Chapter 3, BUCA was used to examine the role of CPT I in controlling fatty acid oxidation and ketogenesis in suckling rats (compared with an equivalent system in adult rats). In this chapter, I will apply BUCA to assess the role of CPT I in controlling the rate of fatty acid oxidation and ketogenesis from medium-chain and long/medium-chain fatty acid mixtures in suckling rats.

During the suckling period, the activities of CPT I and HMG-CoA synthase are high, as is the concentration of the respective mRNA (Thumelin *et al.*, 1993). These decrease on weaning to low fat diets (Williamson *et al.*, 1968; Lockwood *et al.*, 1971; Decaux *et al.*, 1988; Quant *et al.*, 1989), but remain high if rats are weaned on high fat diets (Decaux *et al.*, 1988; Quant *et al.*, 1991). This suggests that these changes are dependent upon hormonal and/or nutritional factors rather than the precise stage of development (Prip-Buus *et al.*, 1995). Thus, when considering the control of fatty acid oxidation and ketogenesis in the neonatal period, it is vital to consider the diet to which the animal is exposed. A recent overview of pre- and post partum nutrition and metabolism can found in the Biochemical Society Transactions, Volume 26, 1998 and is briefly considered in the following sections.

5.1.1 *In utero* nutrition

The fetal environment is characterised by continuous, transplacental, intravenous delivery of substrates into the bloodstream, essential for growth and oxidative metabolism, from the mother to the fetus and also dissipation of the by-products of fetal metabolism (including carbon dioxide, urea and heat) back to the mother for excretion (Battaglia *et al.*, 1978, 1986). At this stage of development, glucose is the principle energy substrate (Aldoretta *et al.*, 1994), since, for example:

- (i) free fatty acids may not cross the placenta (Koren *et al.*, 1964; Girard *et al.*, 1982);
- (ii) in species where fatty acid transfer exists (for example, humans, rabbits or guinea pigs, although the transport mechanisms are still incompletely understood) there is poor fatty acid oxidation by fetal tissues (Drahota *et al.*,

1964; Augenfeld *et al.*, 1970, Girard *et al.*, 1985). During the third trimester, lipids account largely for fat accretion (Aldoretta *et al.*, 1994); and (iii) although ketone bodies can freely cross the placenta (Williamson, 1992) maternally derived ketone bodies meet only a small proportion of fetal energy requirements, since the mother's plasma ketone body concentration is typically low, except when fasting.

5.1.2 Immediate *post-partum* nutrition

Following birth, nutritional support changes dramatically. The neonate experiences a transient period of starvation after the cord has been severed and until milk feeding becomes established. During this time it is entirely dependent upon its own reserves to maintain adequate circulating concentrations of glucose or alternative fuels to supply its needs (Girard *et al.*, 1973; Medina *et al.*, 1996). Thus the mobilization of glycogen and fat stores are vital for survival. The amount of fat laid down during the fetal period and available for utilization as fuel varies among different species (Widdowson, 1950; Girard *et al.*, 1982). Full-term human infants have some adipose tissue (approximately 16% of body weight) providing reserves from which non-esterified fatty acids can be mobilised in the absence of milk (Widdowson, 1981; Kuzawa, 1998). However, in most mammals, the body fat content of the newborn is very low, for example, less than 1% in the rat, and they have no adipose tissue (Hahn *et al.*, 1975; McCance *et al.*, 1977). The liver glycogen stores accumulated during the fetal period are rapidly mobilised and are exhausted within 12 hours of birth (Shelley, 1961; Ballard *et al.*, 1963; Dawkins, 1963). After these stores have been utilized, suckling newborns from most species, including humans, are dependent on glucose supplied by gluconeogenesis from galactose (Kliegman *et al.*, 1985) through maternal milk, which supplies between 20-50% of the glucose requirements of the newborn (Girard *et al.*, 1982; Hay, 1984). Thus newborn rats are entirely dependent on exogenous fat supplies and need to perform active gluconeogenesis to maintain normoglycaemia (Ferré, 1977). Furthermore, active fatty acid oxidation is also essential in the suckling period to sustain a high gluconeogenic flux (Pégorier *et al.*, 1977). Despite these mechanisms, the newborn rat develops profound hypoglycaemia in the first postnatal hour (Girard *et al.*, 1973; Di Marco *et al.*, 1976) and transient hypoglycaemia is almost universal in all newborn mammals (Hawdon *et al.*, 1994).

Since fat reserves are only developed in the last trimester of pregnancy (Aldoretta *et al.*, 1994, Hamosh, 1995) the fat stores of small-for-gestational-age infants and pre-

term infants are frequently limited, and these infants are particularly vulnerable to hypoglycaemia (Lubchenco *et al.*, 1971; Hawdon, 1993). Neurological dysfunction has been associated with hypoglycaemia in newborn infants (Beard *et al.*, 1971; Hawdon, 1999). It has been demonstrated in pre-term rats that prolonged postnatal hypoglycaemia is associated with lower rates of glucose production through glycogenolysis and gluconeogenesis, and there is a delayed induction of phosphoenolpyruvate carboxykinase activity, resulting in lower rates of gluconeogenesis (Fernandez *et al.*, 1983).

5.1.3 Neonatal nutrition

In contrast to the fetal stage, neonatal feeding is characterised by intermittent enteral milk feeds and periods of fasting. In addition, the previous high-carbohydrate diet experienced *in utero* is replaced by the high-fat, low-carbohydrate diet of milk (Luckey *et al.*, 1954). In maternal rat milk, for example, triglycerides contribute 60-70% of the ingested calories (Edmond *et al.*, 1985) and in human milk, whilst the concentration of lactose is higher, fat still accounts for 55-60% of the caloric content (Jenness, 1974; Edmond *et al.*, 1985). The nutrient profile in this neonatal period not only contrasts with that experienced *in utero*, but also with that found in the adult diet which is, in most species, rich in carbohydrates (60% of energy) and low in fats (15% energy) (Prip-Buus *et al.*, 1995). The large amount of fatty acid in maternal milk acts as a positive effector of gluconeogenesis, and provides substrates for lipid biosynthesis and ketogenesis (Frost *et al.*, 1981).

In a variety of studies in suckling rats, where, for example, liver homogenates (Lockwood *et al.*, 1970, 1971; Lee *et al.*, 1971; Chalk *et al.*, 1983), liver slices (Drahota *et al.*, 1964) and isolated hepatocytes (Sly *et al.*, 1978), have been used, it has been shown that ketone body production increases substantially immediately following birth. Furthermore, in many mammalian species, including the rat and the human, the production of ketone bodies remains high throughout the suckling period (Bailey *et al.*, 1973; Girard *et al.*, 1982; Williamson, 1982). During the suckling period, acetoacetate and β -hydroxybutyrate act as alternative energy sources, minimizing the breakdown of muscle protein for the purposes of gluconeogenesis and acting to spare carbohydrate (Section 1.3). During weaning to the high-carbohydrate diet of adult rats, concentrations of ketone bodies progressively decrease (Drahota *et al.*, 1964; Lockwood *et al.*, 1971; Robles-Valdes *et al.*, 1976)

5.1.4 Metabolic fate of the fatty acid components of milk

The composition of milk shows marked inter-species variation. In humans, for example, approximately 5-15% of fatty acids in triglycerides are of medium-chain length (Bitman *et al.*, 1983), whilst rat milk contains approximately 40% (Smith *et al.*, 1968). An even higher proportion of medium-chain fatty acids is found in rabbit milk, where they represent between 60-70% of the fatty acids in triglycerides (Demarne *et al.*, 1978). However, even within species, there may be large variations between individuals, since the nutrient content of milk varies with the stage of lactation (Gibson *et al.*, 1981), time of day (Harzer *et al.*, 1983), within feeds and with maternal diet (Genzel-Boroviczeny *et al.*, 1997). Furthermore, the lipid composition of breast milk also differs between mothers of term or pre-term infants. Whilst medium-chain fatty acids amount to approximately 10% of the total fatty acids in the mature milk of mothers of term infants, they contribute approximately 17% of total fatty acids in the milk produced by mothers of pre-term infants (Bitman *et al.*, 1983; Hamosh, 1991).

Fatty acids have different metabolic fates depending on chain length: long-chain fatty acids are re-esterified in the gut, packaged to form chylomicrons, transported to the circulation via the lymphatic system and delivered first to the heart and lungs and then to peripheral tissues (Mattson *et al.*, 1964). In contrast, medium-chain fatty acids are transported from the gut in the portal venous system and, therefore, reach the liver directly (Playhous *et al.*, 1964; Senior, 1968; Hamosh, 1979; Aw *et al.*, 1980). Furthermore, analysis of the stomach contents of suckling rats indicates preferential release of medium-chain fatty acids during digestion (Helander *et al.*, 1970; Fernando-Warnakulasurya *et al.*, 1981). During lipolysis in both the suckling rat and neonatal human, there is rapid uptake of medium-chain fatty acids from the gut, which reflects the absorption of medium-chain fatty acids by the portal system (Aw *et al.*, 1980; Hamosh *et al.*, 1989).

In contrast to the long-chain fatty acids, which require the CPT I system to enter mitochondria, fatty acids with chain lengths 10 carbons or less (*i.e.* medium- and short-chain fatty acids) can cross the mitochondrial membranes independently of this system (Smith *et al.*, 1968; McGarry *et al.*, 1980). They are activated to their corresponding acyl-CoA entities by medium- or short-chain acyl-CoA synthases located in the mitochondrial matrix (Killenberg *et al.*, 1971; McGarry, 1974), whereupon they undergo β -oxidation. This may have implications for the control structure of the pathways of fatty acid oxidation and ketogenesis, at this stage of

development, where medium-chain fatty acids form an important part of the diet. Since medium-chain fatty acids, such as octanoate, can be metabolised independently of the three-step system including CPT I this suggests that sites other than CPT I may be involved in control over ketogenic flux, particularly during this stage of development.

There is evidence that in suckling rats, medium-chain fatty acids are preferentially oxidized over long-chain fatty acids and are not used directly for triglyceride synthesis (Frost *et al.*, 1981). Such a mechanism may act to spare long-chain fatty acids from oxidation, thus allowing them to be incorporated into complex lipids, which are required for growth. In addition, studies have shown that feeding medium-chain triglycerides to suckling rats leads to a greater elevation of blood ketone bodies than when fed long-chain fatty acids, even though the increase in plasma non-esterified fatty acids was lower when medium-chain triglyceride were fed. It has also been shown using liver cells from newborn rats, that medium-chain fatty acids are more ketogenic than long chain fatty acids (Ferré, 1981; Frost *et al.*, 1981).

Thus, to summarise, medium-chain fatty acids in rat milk are potentially important for body fuel homeostasis, providing a readily available energy source for the newborn:

- (i) the rate of oxidation of medium-chain triglycerides is higher than that of long-chain fatty acids (Sauer *et al.*, 1994);
- (ii) medium-chain fatty acid oxidation in the liver allows a higher rate of ketone body production than from long-chain fatty acids and thus more ketone bodies are available for the oxidative needs of peripheral tissue (Frost *et al.*, 1981; Ferré, 1981);
- (iii) medium-chain fatty acids are as efficient as long-chain fatty acids in providing the necessary cofactors to sustain high rates of gluconeogenesis (Ferré, 1981); and
- (iv) the preferential metabolism of medium-chain fatty acids may allow the preferential delivery of long-chain fatty acids to adipose issue (Frost *et al.*, 1981) which in some species, including the rat, begin to become deposited with lipid as soon as 6hr after birth (Péquignot-Planche *et al.*, 1977; Cryer *et al.*, 1978).

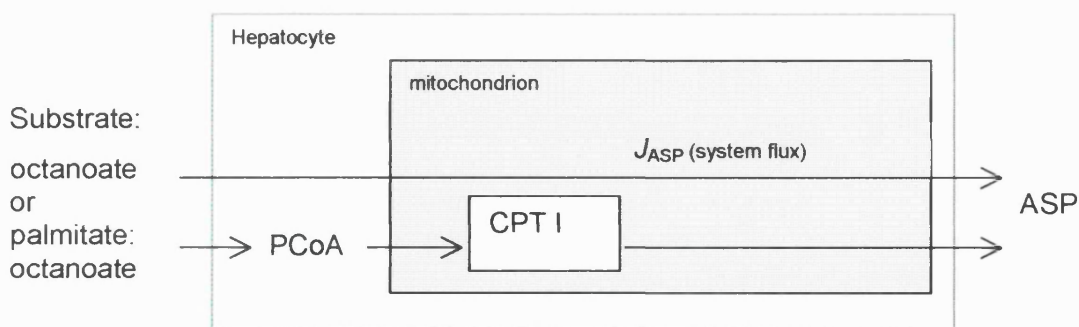
5.1.5 Aims of this section

As indicated in previous chapters, despite the importance of the pathways of fatty acid oxidation and ketogenesis, their regulation and control are still not fully understood. In this chapter, I aim to extend studies described in Chapter 3, investigating control over ketogenesis in the suckling rat, but using substrates that are more likely to be representative of those found in neonatal rats during the suckling period. In this chapter, BUCA was used to calculate the flux control coefficients that describe the potential of CPT I to control flux from different substrates (octanoate, representing a medium-chain fatty acid and octanoate:palmitate mixtures, representing a more 'physiological situation') to ketone bodies, in hepatocytes isolated from suckling rats (New *et al.*, 1998(b),1999(a)).

5.2 Theory and approaches

5.2.1 Application of BUCA in hepatocytes

In this section I describe the system used (Scheme 5.1) to assess quantitatively the potential of CPT I to control fluxes from octanoate or a mixture of palmitate:octanoate, to ketone bodies (ASP) in hepatocytes isolated from suckling rats.



Scheme 5.1 Hepatocyte BUCA system

The system is represented by the green box. BUCA defines the flux control coefficients as small fractional changes in pathway fluxes brought about by infinitesimal fractional changes in enzyme activity. The above scheme represents the system for calculation of the flux control coefficient of CPT I with respect to ketogenesis from either octanoate or palmitate:octanoate mixtures.

In order to calculate ketogenic flux in response to different physiological substrates, and particularly to fully understand system flux in response to mixed fats, it was

necessary to do the following series of experiments, where ketogenic flux was assessed:

- (a) in single substrate experiments, i.e from [1-¹⁴C]palmitate (0.5mM, Chapter 3) or from [1-¹⁴C]octanoate (2mM, Pégrier *et al.*, 1989);
- (b) in mixed fat experiments, where a labelled substrate was in the presence of unlabelled substrate, i.e. flux from [1-¹⁴C]palmitate (0.5mM) in the presence of unlabelled octanoate (0.33mM) or [1-¹⁴C]octanoate (0.33mM) in the presence of unlabelled palmitate (0.5mM); and
- (c) in experiments where both fatty acid substrates present in the mixture were labelled ([1-¹⁴C]palmitate (0.5mM) : [1-¹⁴C]octanoate(0.33mM)).

Thus the experiments in (b) provide a suitable control for the final experiment (c), since the sum of ketogenic flux for the two singly labelled mixed fat experiments detailed in (b) should be the same as the ketogenic flux obtained where both the fatty acid substrates present in the incubations were labelled.

As in the hepatocyte systems described in Chapter 3 and 4, the extrahepatic control exerted by non-esterified fatty acid supply to the liver has been bypassed by using isolated hepatocytes incubated with a fixed concentration of fatty acids. As before, the activity of CPT I was progressively inhibited with increasing concentrations of etomoxir, which generates the specific, irreversible inhibitor etomoxir-CoA *in situ*, and the system allowed to relax to a new steady state, whereupon ketogenesis was assessed as described in Section 2.2.2. Flux control coefficients for CPT I with respect to ketogenesis in this isolated hepatocyte model were calculated using the data in Figures 5.1-5.4, the Simfit package (Bardsley *et al.*, 1997) to calculate initial slopes and the following equation:

Equation 5.1:

$$C_{CPTI}^{J_{ASP}} = \frac{\delta J_{ASP}}{J_{ASP}} \bigg/ \frac{\delta v_{CPTI}}{v_{CPTI}} \bigg|_{(i=0)}$$

where $C_{CPTI}^{J_{ASP}}$ is the flux control coefficient of CPT I over ketogenesis at zero inhibitor concentration ($i = 0$) and v_{CPTI} is the activity of CPT I. δ represents infinitesimal changes, where the changes are very small (i.e. tend to zero). J_{ASP} represents carbon flux to acid soluble products.

5.3 Results

5.3.1 BUCA in hepatocytes (octanoate as substrate)

Figure 5.1 shows the effects of etomoxir on both CPT I activity and ketogenic flux (called ASP for simplicity, although strictly representing ^{14}C -non-heptane extractable products) in hepatocytes isolated from suckling rats using $[1-^{14}\text{C}]$ octanoate (2mM) as substrate. CPT I activity decreases with increasing amounts of etomoxir and at $100\mu\text{M}$ the inhibition was greater than 80%. However, $100\mu\text{M}$ etomoxir caused only $\approx 20\%$ inhibition of ketogenic flux from octanoate. The activity of CPT I in the absence of etomoxir was $108 \pm 31\text{nmol h}^{-1} (10^6 \text{ cells})^{-1}$. In the absence of etomoxir, the absolute rate of $[1-^{14}\text{C}]$ octanoate consumption was $152 \pm 24\text{nmol h}^{-1} (10^6 \text{ cells})^{-1}$, and $303 \pm 47\text{nmol (ketone bodies produced) h}^{-1} (10^6 \text{ cells})^{-1}$. Rates of ketone body formation were linear over the course of the experiment. The data shown in Figure 5.1 have been used to calculate the flux control coefficient for CPT I over ketogenic flux (Section 5.2.1, Equation 5.1), which has a value of $C_{CPTI}^{J_{ASP}} = 0.11 \pm 0.01$.

5.3.2 BUCA in hepatocytes: ($[1-^{14}\text{C}]$ octanoate:unlabelled palmitate as substrate)

Figure 5.2 shows the effects of etomoxir on both CPT I activity and ketogenic flux in hepatocytes isolated from suckling rats using $[1-^{14}\text{C}]$ octanoate and unlabelled palmitate as substrate. Once more, CPT I activity decreases with increasing amounts of etomoxir (and hence, etomoxir-CoA). Inhibition of CPT I activity at $100\mu\text{M}$ was $\approx 75\%$. However, incubation with increasing concentrations of etomoxir resulted in an apparent increase in ketogenic flux from this fatty acid mixture, with $100\mu\text{M}$ etomoxir resulting in a ketogenic flux of $\approx 150\%$ compared to that in the absence of etomoxir. The activity of CPT I in the absence of etomoxir was $105 \pm 4\text{nmol h}^{-1} (10^6 \text{ cells})^{-1}$. In the absence of etomoxir, the absolute rate of $[1-^{14}\text{C}]$ octanoate consumption was $55 \pm 5\text{nmol octanoate consumed h}^{-1} (10^6 \text{ cells})^{-1}$. In the absence of etomoxir the absolute rate of $[^{14}\text{C}]$ ASP formation was $110 \pm 10\text{nmol (ketone bodies from octanoate) h}^{-1} (10^6 \text{ cells})^{-1}$. The rates of ketone body formation were linear over the course of the experiment. BUCA was applied to these data to calculate the 'apparent' flux control coefficients of CPT I over ketogenic flux (Section 5.2.1, Equation 5.1), which has a value of $C_{CPTI}^{J_{ASP}} = -0.52 \pm 0.02$.

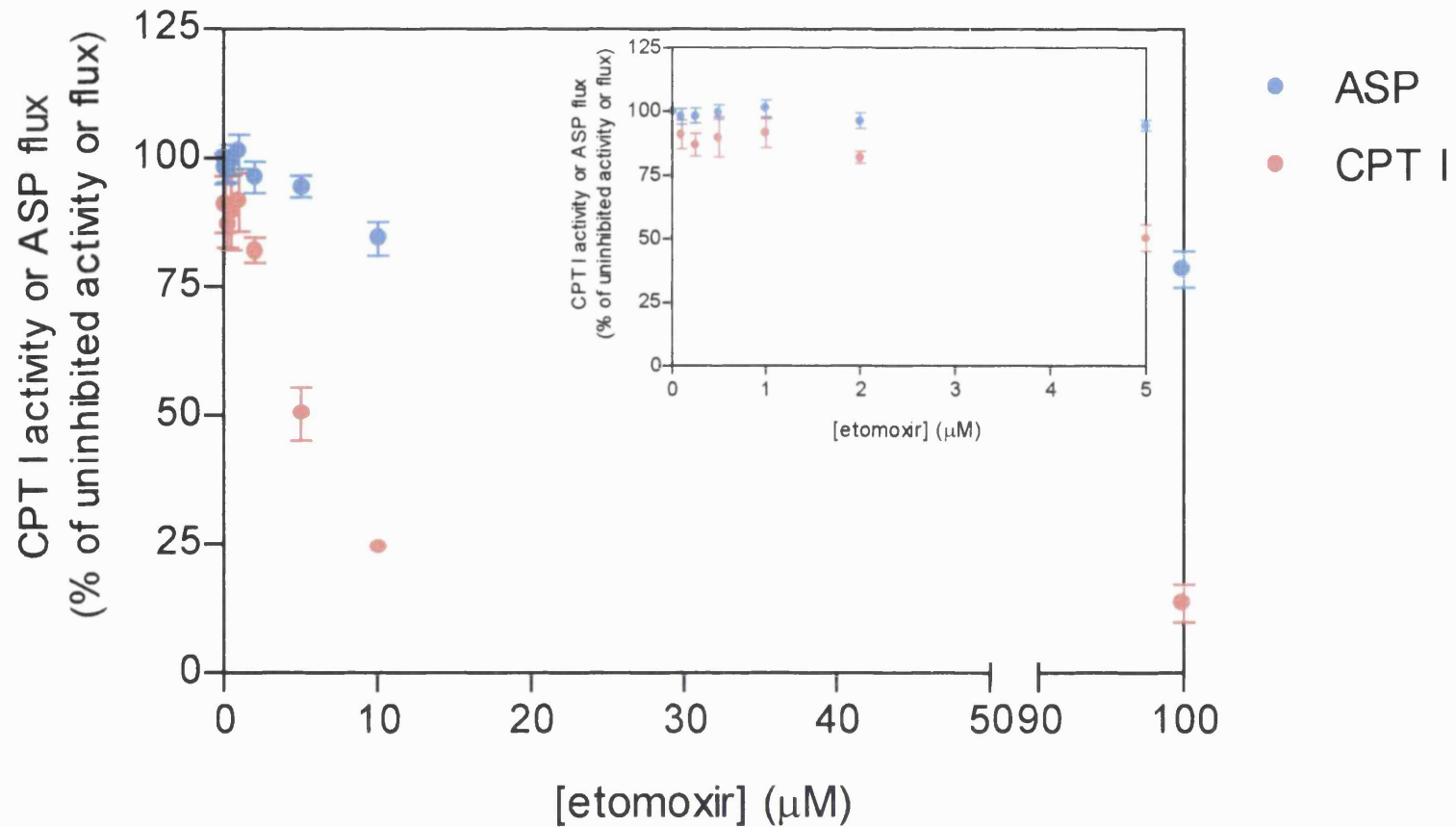


Figure 5.1 Effect of etomoxir on CPT I activity and ketogenic flux in the presence of octanoate as substrate

Hepatocyte preparations with viability greater than 85% were incubated with etomoxir for 10 min. Substrate: $[1-^{14}\text{C}]$ octanoate (2mM final concentration, $0.8\mu\text{Ci } \mu\text{mol}^{-1}$, in KRB, 2% BSA). Values were normalised by expressing them as a percentage of those obtained in the absence of etomoxir. Values are means \pm SEM, $n=5$ separate hepatocyte preparations for CPT I and $n=12$ for ASP.

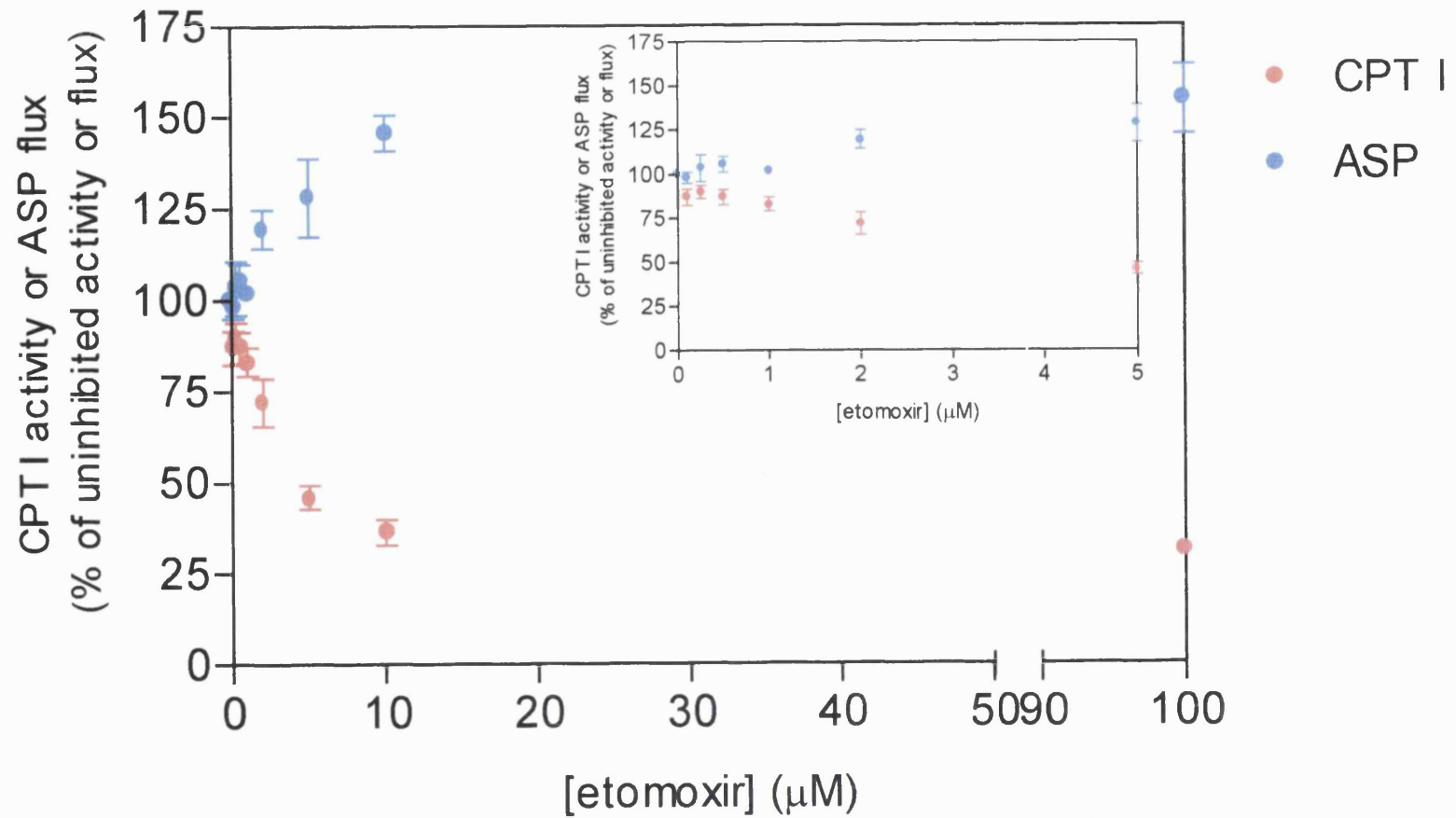


Figure 5.2 Effect of etomoxir on CPT I activity and ketogenic flux in the presence of $[1-^{14}\text{C}]$ octanoate:unlabelled palmitate

Hepatocyte preparations with viability greater than 85% were incubated with etomoxir. Substrate: $[1-^{14}\text{C}]$ octanoate (0.33mM final concentration, $0.8\mu\text{Ci } \mu\text{mol}^{-1}$, in KRB, 2% BSA) in the presence of 0.5mM unlabelled palmitate were added to incubations. Values were normalised by expressing them as a percentage of those obtained in the absence of etomoxir. Values are means \pm SEM, $n=7$ separate hepatocyte preparations for CPT I and $n=4$ for ASP.

5.3.3 BUCA in hepatocytes: ([1-¹⁴C]palmitate:unlabelled octanoate as substrate)

Figure 5.3 shows the effects of etomoxir on both CPT I activity and ketogenic flux (ASP, acid soluble products) in hepatocytes isolated from suckling rats, using labelled palmitate and unlabelled octanoate as substrate. CPT I activity decreases with increasing amounts of etomoxir (and hence, etomoxir-CoA). Inhibition of CPT I activity at 100 μ M was \approx 75%. At low concentrations of etomoxir (<2 μ M), β -oxidation flux showed an increase. However, at >2 μ M etomoxir, the ketogenic flux decreased and 100 μ M, etomoxir caused an \approx 85% inhibition of ketogenic flux from this fatty acid mixture.

These data have been used to calculate 'apparent' flux control coefficients of CPT I over ketogenic flux (Section 5.2.1, Equation 5.1), which has a value of $C_{CPTI}^{J_{ASP}} = 0.03 \pm 0.02$. In the absence of etomoxir, the absolute rate of [1-¹⁴C]palmitate consumption was 24 ± 4 nmol palmitate consumed h^{-1} (10^6 cells)⁻¹. In the absence of etomoxir the absolute rate of [¹⁴C]ASP formation was 95 ± 18 nmol (ketone bodies from palmitate) h^{-1} (10^6 cells)⁻¹. Rates of ketone body formation were linear over the course of the experiment.

5.3.4 BUCA in hepatocytes: ([1-¹⁴C]palmitate:[1-¹⁴C]octanoate as substrate)

Figure 5.4 shows the effects of etomoxir on both CPT I activity and ketogenic flux (acid soluble products) in hepatocytes isolated from suckling rats, where labelled palmitate and labelled octanoate were used as substrate. Inhibition of CPT I activity at 100 μ M was \approx 75%. Over the range of concentrations of etomoxir used in these experiments, ketogenic flux was seen to decrease and 100 μ M etomoxir caused \approx 35% inhibition of ketogenic flux from this fatty acid mixture.

These data have been used to calculate BUCA flux control coefficient of CPT I over ketogenic flux (Section 5.2.1, Equation 5.1), which has a value of $C_{CPTI}^{J_{ASP}} = 0.11 \pm 0.01$. In the absence of etomoxir, 170 ± 14 nmol (ketone bodies) h^{-1} (10^6 cells)⁻¹. The rates of ketone body formation were linear over the course of the experiment.

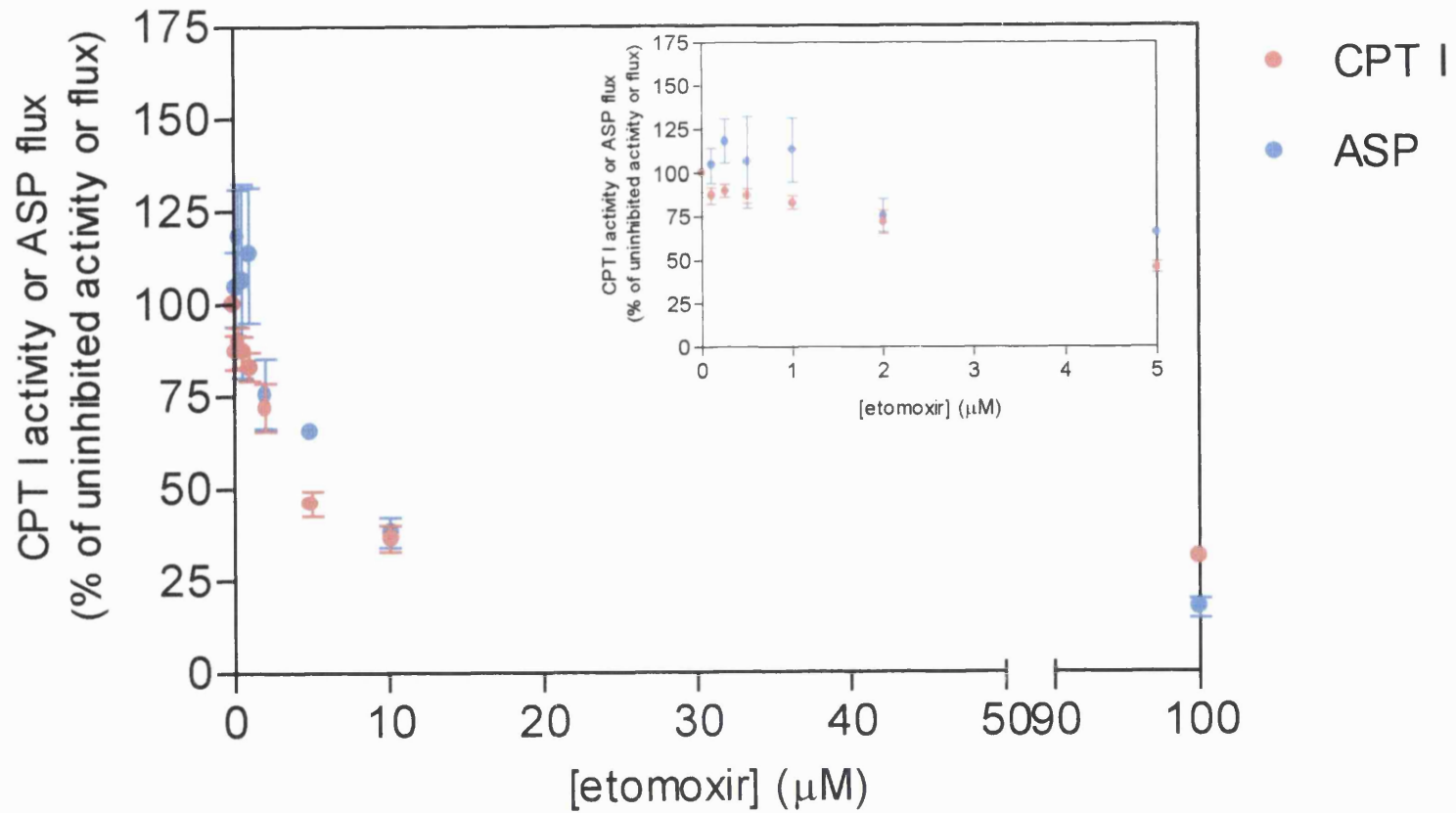


Figure 5.3 Effect of etomoxir on CPT I activity and ketogenic flux in the presence of [1-¹⁴C]palmitate:unlabelled octanoate

Hepatocyte preparations with viability greater than 85% were incubated with etomoxir. Substrate: [1-¹⁴C]palmitate (0.5mM final concentration, 0.4μCi μmol⁻¹, in KRB, 2% BSA) in the presence of 0.33mM unlabelled octanoate were added to incubations. Values were normalised by expressing them as a percentage of those obtained in the absence of etomoxir. Values are means ± SEM, n=7 separate hepatocyte preparations for CPT I and n=4 for ASP.

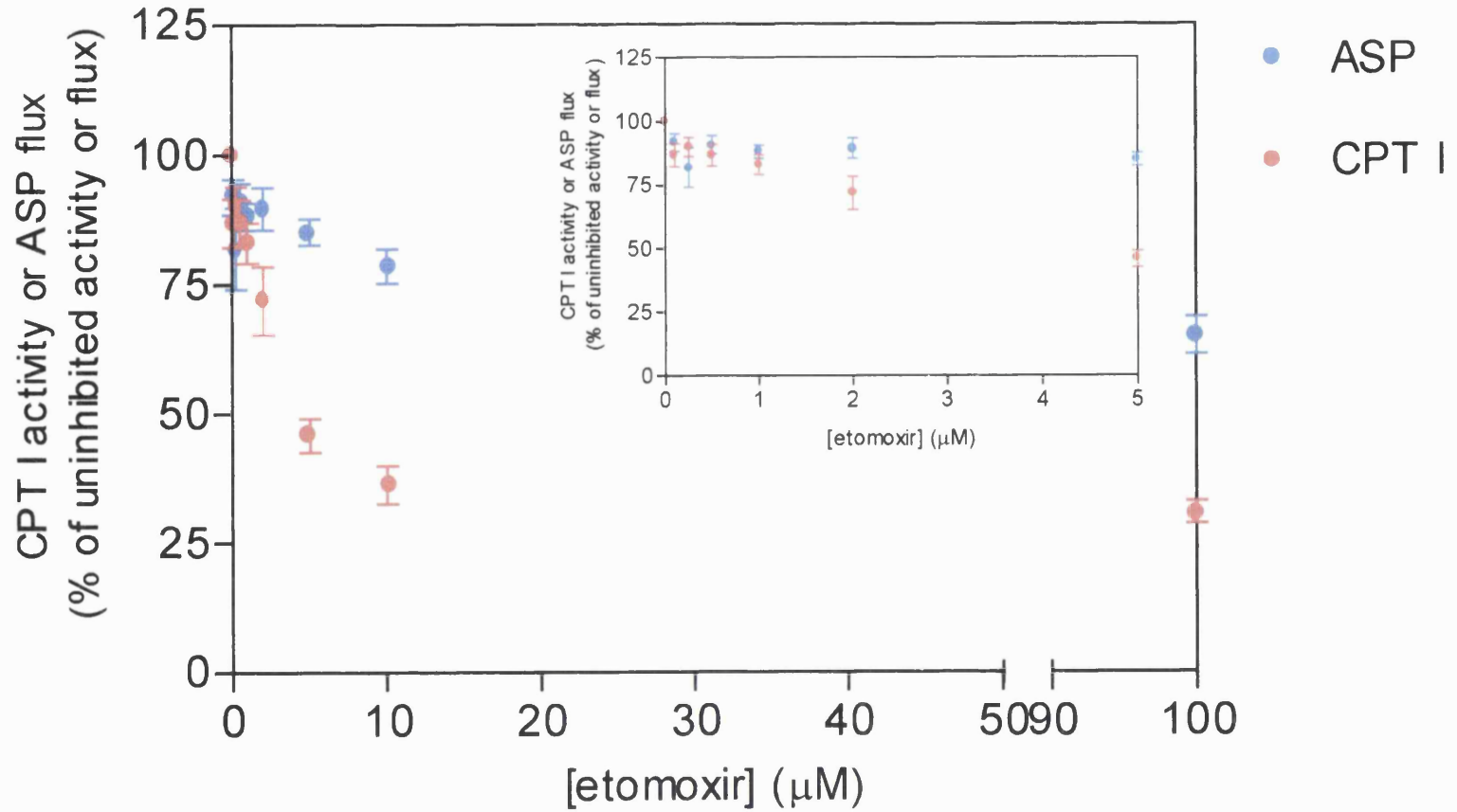


Figure 5.4 Effect of etomoxir on CPT I activity and ketogenic flux in the presence of ($[1-^{14}\text{C}]$ palmitate: $[1-^{14}\text{C}]$ octanoate)

Hepatocyte preparations with viability greater than 85% were incubated with etomoxir. 1ml 'mixed fat solution' ($[1-^{14}\text{C}]$ palmitate, 0.5mM final concentration, $0.8\mu\text{Ci } \mu\text{mol}^{-1}$ and $[1-^{14}\text{C}]$ octanoate, 0.33mM final concentration, $0.4\mu\text{Ci } \mu\text{mol}^{-1}$ in KRB, 2% BSA) was added to flasks (ie final volume 4ml). Values were normalised by expressing them as a percentage of those obtained in the absence of etomoxir. Values are means \pm SEM, $n=7$ separate hepatocyte preparations for CPT I and $n=8$ for ASP.

Figure 5.5 demonstrates the sigmoid inhibition shape of the ketogenic flux inhibition curve. For the initial points on the curve, where there is low etomoxir concentration, little variation in ketogenic flux is observed. This is indicative of a low flux control coefficient (Mazat *et al.*, 1994). Beyond 80% CPT I inhibition, however, ketogenic flux sharply decreases to reach zero level.

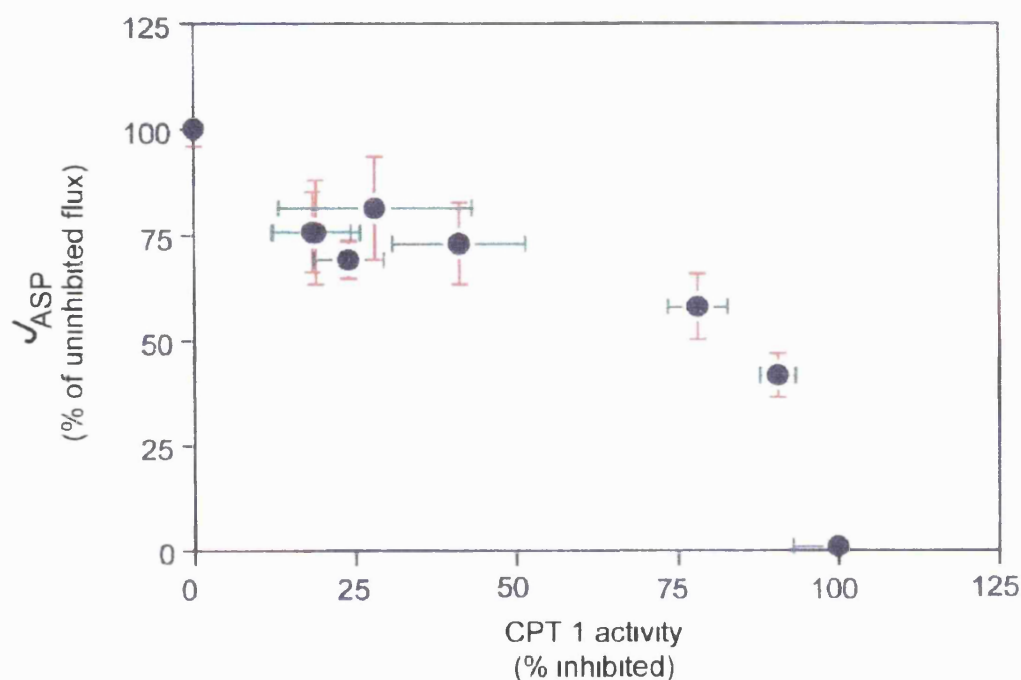


Figure 5.5 Ketogenic flux as a function of CPT I inhibition

Redrawn from the information presented in Figure 5.4, where the substrate supplied to isolated hepatocytes represented the 'physiological mixture' of long-chain:medium-chain fatty acids.

5.4 Discussion

5.4.1 Control exerted by CPT I over flux from octanoate to ketone bodies

Almost twice the amount of ketone bodies were formed in the absence of inhibitor, when the medium-chain fatty acid octanoate was used as substrate (Figure 5.1) compared to the use of the long-chain fatty acid palmitate (Figure 3.3). This is in agreement with the results of others, including Frost *et al.*, (1981) and Ferré (1981) who, as discussed in the introduction, observed a higher rate of ketone body production from medium-chain than from long-chain fatty acid oxidation. Incubation

with the inhibitor etomoxir resulted in only a 20% decrease in flux from octanoate to ASP in this system (Figure 5.1), which is consistent with the observations of Pégrier *et al.*, (1989) who assessed the rate of octanoate oxidation in fetal and newborn rabbits. These workers found that following inhibition of CPT I with tetradecylglycidic acid, a specific inhibitor of CPT I, ketogenic flux was only inhibited by 20%. These results suggest that the majority of the octanoate oxidized in hepatocytes isolated from suckling rats is activated intra-mitochondrially, by-passing the three-part transport system into the mitochondria, which involves CPT I. Interestingly, however, the results presented in this thesis suggest that some octanoate does appear to be oxidized *via* the CPT I system. This is consistent with the work of Labadaridis *et al.*, (2000), who have provided clinical evidence for the involvement of carnitine in medium-chain triglyceride metabolism.

CPT I, however, was inhibited to a similar degree (approximately 80% inhibition) in these experiments with octanoate as when palmitate was present in the pre-incubation medium (Figure 3.2). These results, therefore, produced different shapes of inhibition curves for CPT I activity and [¹⁴C]ASP formation (Figure 5.1). Since flux control coefficients using the bottom up method of control analysis are calculated by the ratio of slopes applied to the initial points of the curve (i.e. at low inhibitor levels), this has resulted in a value for the flux control coefficient of $C_{CPTI}^{J_{ASP}} = 0.11 \pm 0.01$. As flux control coefficients typically have values between 0 and 1, it can be seen that this is a low value, indicating that CPT I has a low contribution to control ketogenic flux from octanoate.

Although the numerical value of the flux control coefficient for CPT I over flux from octanoate is low and thus the potential of CPT I to control ketogenesis is also low, the value of the coefficient is not zero. These results, therefore, provide quantitative support for the observations that medium-chain fatty acids may be oxidized *via* the CPT I system.

Figure 5.6 compares the numerical value of the flux control coefficients for CPT I over ketogenesis calculated from data presented in this chapter with those presented and discussed in Chapter 3, and illustrates the changes in control exerted by CPT I, in response to developmental age and substrate supplied. As discussed in Chapter 3, the value of this coefficient is lower during suckling, than in an equivalent adult system. The work presented in this chapter indicates that when a

medium-chain fatty acid is used as substrate during suckling, the contribution of CPT I to control over ketogenesis is even lower, such that it may no longer be appropriate to consider CPT I to be 'rate-controlling' over this pathway. These results are physiologically relevant, since during the neonatal period, rat milk (the primary source of food) contains a high proportion of medium-chain fatty acids, whereas their presence is low in adult diets. These results may also be of clinical significance, since a high proportion of medium-chain triglycerides is found in the breast milk of mothers of pre-term infants (Bitman *et al.*, 1983). Furthermore, human infant milk formulas, and particularly those produced specifically for premature infants, contain a high percentage of medium-chain triacylglycerides (Heim, 1985).

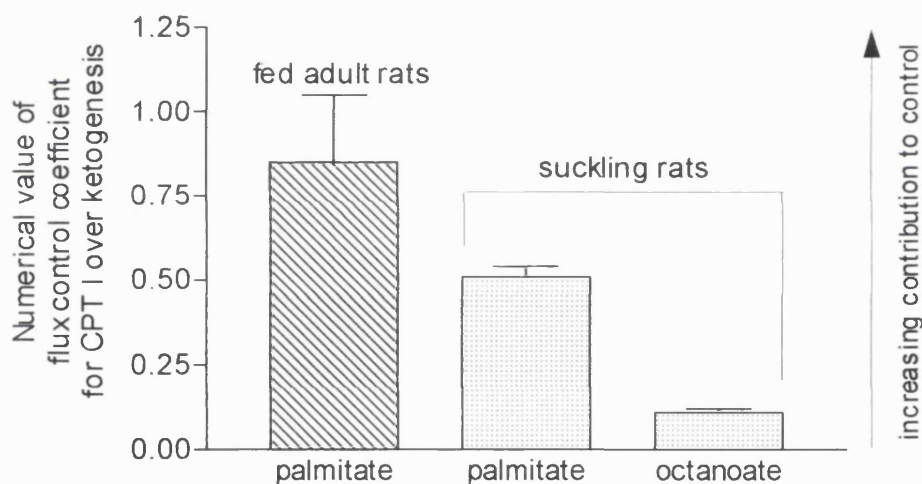


Figure 5.6 Comparison of flux control coefficients from adult rats and from suckling rats

The flux control coefficients were calculated as described in Chapter 3 and in Section 5.2 of this Chapter. Each of the above bars is significantly different to the other ($p < 0.05$). Adult data from Drynan *et al.*, (1996).

One of the basic tenets of MCA is that control tends to be distributed throughout all the steps in a pathway, rather than situated at a single step, and it is interesting to note that some workers (reviewed in Girard, 1992) have suggested, on the basis of observations made in hepatocytes isolated from newborn rabbits, that the

mitochondrial branch point of acetyl-CoA metabolism may have an important role in controlling ketogenesis, in addition to the control which has traditionally been considered to reside at CPT I.

5.4.2 Control exerted by CPT I over flux from singly labelled mixed fats to ketone bodies

It is important to note that the final concentration of octanoate in the incubation medium is much lower in the mixed fatty acid experiments, than in the experiment with octanoate alone (0.33mM *versus* 2mM). This was to ensure that the two fatty acid substrates were present in a similar proportion to that found in maternal rat milk, where approximately 40% of the triglycerides present are of medium-chain length (Smith *et al.*, 1968). It is also important to note that this lower concentration does not become limiting in these experiments, since less than 13% was used over the 60 min time-period of these experiments.

Although the data in Figures 5.2 and 5.3 were used to calculate flux control coefficients (summarised in Figure 5.7), it is worth emphasising that the coefficients from this stage are only 'apparent' flux control coefficients and are unlikely to be physiologically relevant. This is because ketone body production is not accurately reflected where labelled fatty acid is used in the presence of unlabelled fatty acid. This arises due to an uneven dilution of label, particularly at higher inhibitor concentrations, which would result in incorrect assessments of ketone body production. In the case of labelled octanoate in the presence of unlabelled palmitate, for example, ketone body production would be underestimated and the resulting 'apparent' flux control coefficient will be large and negative. However, it is still valid to present 'apparent' coefficients, since these are calculated from initial data points on the curve, where inhibitor tends to zero. The data used for the calculation of these 'apparent' flux control coefficients was an essential control for the procedure in the calculation of the 'actual' flux control coefficients, which are calculated from data obtained where both fatty acids are labelled, as discussed in Section 5.2.1.

5.4.3 Control exerted by CPT I over flux to ketone bodies, where both substrates have been labelled

Inhibition curves for CPT I activity and [¹⁴C]ASP flux from the 'mixed fat'

experiments, where both palmitate and octanoate were labelled (Figure 5.4) were more similar in shape than those seen with labelled octanoate in the presence of unlabelled palmitate (Figure 5.2). Thus the slopes of the tangents applied to the initial points of the curves are more similar. This has the effect of increasing the value of the flux control coefficient: $C_{CPTI}^{JASP} = 0.11 \pm 0.01$ compared with $C_{CPTI}^{JASP} = -0.52 \pm 0.02$ where labelled octanoate was used in the presence of unlabelled palmitate (Figure 5.7).

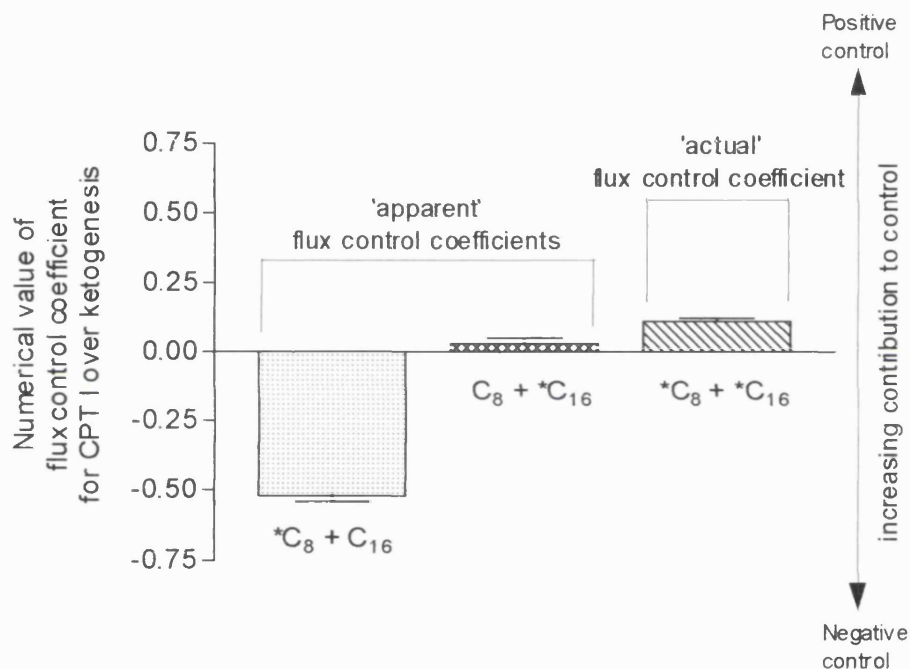


Figure 5.7 Comparison of flux control coefficients calculated from suckling rats in mixed fatty acid experiments

Asterisk indicates labelled substrate. The concept of 'positive' and 'negative' control is discussed in Section 1.4.3.

The flux control coefficient for CPT I over ketogenesis, where both substrates have been labelled, provides a quantitative assessment of the contribution of CPT I to control flux over this pathway in response to the more 'physiologically relevant' substrate. This low value, which is almost identical to that obtained where only octanoate is used as substrate (Figure 5.6), suggests that CPT I has a low capacity

to control flux from this 'physiological mix'. This may indicate that the control exerted by CPT I over hepatic ketogenesis *in vivo*, in neonatal rats may be trivial. Furthermore, the results from these experiments have potential implications in the clinical environment, since, for example, treatments relating to disorders of ketone body metabolism in neonates, which focus only at the level of CPT I, may be unlikely to achieve the desired therapeutic result. The values of the flux control coefficients presented in this chapter, therefore, supports the general conclusions of Kascier *et al.*, (1993) and Fell (1998) who have shown that it is often necessary to alter more than one step to achieve changes in flux or product.

5.4.4 Potential implications for inborn errors of metabolism

Figure 5.5 demonstrates a threshold in ketogenic flux when it is plotted against CPT I inhibition: until approximately 80% inhibition of CPT I, ketogenic flux decreases slowly, beyond this point, however, ketogenic flux sharply decreases. This result suggests that if only approximately 20% CPT I activity is present, for example, due to low levels of expression, or defects in the enzyme itself, ketogenic flux may be compromised, with resulting physiological implications for the individual. However, below this threshold, the effects of a defect may not be observed. These results are in broad agreement with those of Mazat *et al.*, (1994, 1998), who have used MCA, and in particular flux control coefficients, to investigate and explain some of the consequences of inborn errors of metabolism, and found that thresholds can be high. For example, using specific inhibitors to mimic a deficiency of a respiratory complex, these workers found that 80% of inhibition of Complex I activity was required in order to achieve substantial inhibition of respiration. Letellier *et al.*, (1998), have shown that a 70% deficit of cytochrome *c* oxidase decreases the oxidative flux by just 10%. Additionally, Kuznetsov *et al.*, (1994) have shown, for example, that there was no difference in maximal rates of respiration between controls and brindled mice (which demonstrate severe copper deficiency and are frequently used to model Menkes syndrome) even if the activity of cytochrome *c* oxidase was 50% that found in normals, although the flux control coefficient for cytochrome *c* oxidase was higher in the model compared to controls.

Mazat *et al.*, (1998) suggested that metabolism may be very tolerant towards enzyme deficiencies, due to the buffering power of metabolite intermediates. Such behaviour is a consequence of the summation theorem, which states that the sum of control coefficients is equal to 1, so that most of the control coefficients are low,

suggesting that control of a pathway can be shared among various steps in the pathway, rather than a single rate-limiting step (Kacser and Burns, 1979). Mazat *et al.*, (1998) also suggested that thresholds may provide an explanation for cases in which the pathological state is only revealed under certain circumstances. Defects in the pathways of fatty acid oxidation, for example, may not become apparent until the individual experiences additional stress, such as fasting.

The work I have presented in these current studies has only considered CPT I in neonatal liver, since the liver has such a central role in ketone body metabolism. However, an investigation into the role of CPT I in control over carbon fluxes in other tissues/organs would be of academic and clinical significance, particularly since intestine and kidney, for example, can contribute to ketone body production at this stage of development (Asins *et al.*, 1995; Thumelin *et al.*, 1993). Neither control coefficients nor thresholds would necessarily be the same in different tissues.

5.4.5 Diet-related changes in the ability of CPT I to control carbon fluxes

Although probably not applicable over the time-scale of the experiments in this study, it is interesting to note that the changes in the ability of CPT I to control ketogenic flux in response to different substrates may result from changes in the fluidity of the membrane in which CPT I resides. This will, in part, be determined by the nature of the fatty acids present in the phospholipids. The major component of the phospholipids of the outer mitochondrial membrane are phosphatidylcholine (44-59%) and phosphatidylethanolamine (20-35%), with low levels of cardiolipin (3-10%). However, the phospholipid fatty acid composition can be altered by changing the fat load and the fatty acid composition of the diet, for example, linoleic, and arachadonic acids are replaced with *n*-3 polyunsaturated fatty acids, following fish oil diets (Power *et al.*, 1994). This would effect CPT I activity and its sensitivity to inhibition by malonyl-CoA (Clouet *et al.*, 1995; Power *et al.*, 1997). Furthermore, investigations into the desensitisation of CPT I to malonyl-CoA, using fluorescent-probe techniques, indicate that CPT I is also sensitive to changes in the membrane core (rather than peripheral lipid order). Zammit *et al.*, (1998) have shown that the kinetic characteristics of CPT I are sensitive to changes in lipid composition that are localised to specific membrane microdomains which may be related to changes in the number of contact sites.

CPT I also displays a marked difference in its kinetic behaviour towards various acyl-CoAs and the pattern of substrate preference differs between species where diets are qualitatively different. This has been suggested as providing further support for the idea that modification to the kinetic properties of CPT I may be modulated through the fatty acid composition of the diet (Power *et al.*, 1997).

As discussed in Chapter 8, the investigations into the potential of CPT I to control carbon fluxes, presented in this chapter, should be further expanded to consider the effect of other nutrients usually present in the neonatal diet, for example, by the addition of other factors to the experimental substrate mixture, such as amino acids. In this way, it would be possible to provide a description of the control exerted by CPT I over the pathways of fatty acid oxidation and ketogenesis, which is likely to be of even more physiological significance.

5.4.6 Conclusions

The results from my work discussed in this chapter support the conclusions in Chapter 3, namely, that during the suckling period, the control exerted by CPT I over hepatic ketogenesis is low and that the overall control structure of the pathways must be different in suckling compared to adult rats. My work suggests that it may not be appropriate to consider CPT I as a 'rate-limiting' step over the pathways of ketogenesis, at this stage of development. Furthermore, the very low values for the flux control coefficients suggest that it may not be appropriate to consider CPT I as 'rate-controlling' and that the level of control exerted by CPT I over hepatic ketogenesis *in vivo*, in neonatal rats may be very small.

These results also illustrate the threshold effect, which can explain some of the clinical presentations of some inborn errors of metabolism, where an enzyme deficiency may have little or no observable effect on flux through a metabolic pathway, until a threshold is reached and, furthermore, may not become apparent until the individual experiences additional 'stress'. As discussed in the Section 1.2.4, CPT I deficiencies are frequently characterised by recurrent episodes of Reye's-like Syndrome, which may be associated with infection/endotoxin stimulation i.e. an additional stress on the system (Section 7.1.5).

Chapter 6

Analysing the role of CPT I in control of ketogenic flux in *in vitro* models of neonatal sepsis

6.1 Introduction

There are many different experimental models of sepsis, both *in vitro* and *in vivo*, but there are few studies of sepsis in the neonate. The purposes of the research reported in this chapter were two-fold: firstly, to establish *in vitro* models suitable for investigation of neonatal sepsis and secondly, to examine the role of CPT I in the control of ketogenic flux in such models. Direct observations of hepatic function at the biochemical level during sepsis are difficult to achieve due to the relative inaccessibility of the liver. Within the Department of Paediatric Surgery, Institute of Child Health, we have been modelling neonatal sepsis in freshly isolated liver cells using a variety of approaches: for example, exposing isolated hepatocytes *in vitro* to a range of doses of hydrogen peroxide (Patil *et al.*, 1998; Romeo *et al.*, 1999) or nitric oxide (Romeo *et al.*, 2000) or studying hepatocytes which have been isolated from neonatal rats following intraperitoneal injection of lipopolysaccharide (LPS) (Markley *et al.*, 2000). Each of these models mimics the later stages of sepsis. In the work I describe in this chapter, I aim to develop models that mimic the early metabolic changes in sepsis and then use them to explore the role of CPT I at this earlier stage. To achieve this, various agents involved in the 'septic response' were added to hepatocytes during the isolation procedures (Section 6.2.1).

6.1.1 Sepsis

Sepsis is part of a broad-ranging clinical syndrome (systemic inflammatory response syndrome, SIRS) which may progress from bacteraemia (where viable bacteria are detected in the blood) to multiple-organ failure and death. The term "sepsis" itself is used specifically when SIRS is derived from a proven infectious cause and evidence of a systemic response to infection, such as tachycardia and hyperthermia, are present (reviewed in Anderson *et al.*, 1997). The symptoms of septic shock, such as fever and metabolic derangements, arise as a result of the response of the immune system of the host to infection, rather than the invading organism directly injuring the host by secretion of toxins (Nanbo *et al.*, 1999). The agents involved in such a response are considered in Section 6.1.3.

Despite medical advances, such as potent, broad-spectrum antibiotics, improvements in perioperative care and resuscitation methods and considerable scientific research, sepsis remains a major clinical problem with a high mortality rate (Rackow *et al.*, 1991; Thiermermann, 1995). In the United States, for example, the incidence of septic shock (sepsis with hypotension) has been quoted to be as high as 200,000 per annum, with 40% of these cases caused by gram-negative bacteria (reviewed in Samra *et al.*, 1996) which include *Escherichia Coli* and enterbacteriaceae. Once septic shock has become established mortality rate has been quoted as being between 50-75% (Maclaren, 1997). Investigations into the regional/systemic metabolic alterations associated with sepsis, and in particular the biochemical effects of the agents involved in the septic response, are of particular relevance in neonates, who are at increased risk of sepsis because of their reduced immune function (Lewis, 1998). In the neonate, sepsis and septic shock represent a significant source of mortality and morbidity (Carcillo *et al.*, 1997).

6.1.2 Common causes of sepsis

Positioned between the portal and systemic circulation, the liver is the first organ to be exposed to substances absorbed and translocated from the gut, which is a major source of gram-negative bacteria. For example, *E. Coli* colonizes the infant bowel soon after birth and represents a small fraction of total intestinal flora throughout life (reviewed in Maclaren, 1997). Although the intestinal mucosal layer provides some protection from intestinal flora, newborns and young infants are known to have an immature mucosal barrier (Urao *et al.*, 1999). Furthermore, damage to this layer, arising for example, through inflammatory bowel disease, haemorrhagic shock, trauma or reperfusion injury (reviewed in Samra *et al.*, 1996) facilitates translocation of intraluminal bacteria and toxins across the gut mucosa and allows them to enter the portal circulation with subsequent contact with liver cells (O'Neil *et al.*, 1997). Given its position, and that it has a central homeostatic role, it should not be surprising that the liver is one of the first organs to show metabolic alterations in sepsis.

Gram-negative infection may arise for a number of other reasons. Sepsis is particularly common in premature infants, infants with abnormal gastrointestinal flora and/or those receiving total parenteral nutrition (TPN) (Pierro, 1996, 1998; Lewis, 1998). TPN is a method of nutritional support for patients for whom enteral feeding may not be appropriate, for example, for infants with congenital gastrointestinal

abnormalities or very low birthweight newborns. However, despite its widespread use for over 30 years, sepsis remains the most frequent serious complication of TPN, with incidences as high as 20-30% (Yeung *et al.*, 1998). Sepsis may arise for a number of reasons, for example, as a result of infection at the entry site of the catheter; contamination of the catheter and connections and/or contamination of the TPN fluid during preparation/entry into the system (Yeung *et al.*, 1998). In addition, long-term TPN may increase the likelihood of bacterial translocation from the gut mucosa (McAndrew *et al.*, 1999).

Furthermore, individuals may be predisposed to sepsis, following impairment of their host defence mechanisms, for example, following burn injuries, diabetes and treatment with immunosuppressive and/or chemotherapeutic agents (Rackow *et al.*, 1991).

6.1.3 Agents involved in the sepsis response

This chapter is concerned with sepsis arising from infection with gram-negative bacteria, which are considered to be the initial agents involved in the septic response. Gram-negative bacteria contain an outer membrane consisting of polysaccharide, lipid and protein and it is essential at this stage to clarify the terminology used to describe these components. The terms endotoxin and lipopolysaccharide (LPS) are frequently, although incorrectly, used interchangeably (Fink *et al.*, 1990). In this thesis, LPS refers specifically to a purified, non-protein fraction of the outer membrane of gram-negative bacteria, whilst the term endotoxin refers to unpurified samples containing small amounts of cell wall proteins, lipids, lipoproteins and polysaccharides in addition to LPS. The LPS used in the studies presented here and the following chapter, was derived from *E. Coli*.

LPS is amphiphilic and comprises two main regions.

- (i) The lipid region (known as lipid A) is the biologically active region of the LPS molecule (Galanos *et al.*, 1972). This hydrophobic region is embedded in the outer leaflet of the membrane and is the most highly conserved part of the LPS molecule, with little variation between species (Hull, 1997).
- (ii) The polysaccharide region renders the lipid water soluble and can itself be divided into two key parts: the highly conserved core oligosaccharide region,

and the o-polysaccharide region, which shows considerable variation, even within the same species (Hull, 1997).

Observations following the incorporation of ^{14}C -labelled LPS into the membranes of adult rat hepatocytes suggested that rather than binding to specific LPS-receptors, LPS binds to components of the membrane bilayer and that this interaction induces destabilisation of the membrane (Pagani *et al.*, 1981). More recently, however, using ^{123}I -labelled LPS, Parent (1990) found that hepatocytes have high affinity receptors for LPS. It has been found that LPS also binds to a specific glycoprotein, LPS-binding protein, which is synthesized in the liver and that this binding is a prerequisite for LPS-induced cell activation (Schumann *et al.*, 1990). However, the relationship between these receptors and the LPS-binding protein described by Schumann *et al.*, (1990) is unknown.

Exposure to LPS induces an acute response in the liver. This response consists of:

- (a) a local reaction at the site of injury, characterised by a number of processes such as aggregation of platelets, clot formation and the production of various soluble, hormone-like agents, known as cytokines, and
- (b) a systemic reaction, characterised by fever, changes in lipid metabolism and changes in the concentration of various plasma proteins, known as acute phase proteins (APPs) (Heinrich *et al.*, 1990). These are involved in restoring homeostasis following infection, tissue injury or immunological disorders (Miller, 1951). APPs can be divided into two broad groups, type I and type II, although their precise roles and interactions are still unclear. Following infection, the liver is almost exclusively responsible for the synthesis of both types of APP.

There is a well-defined temporal cascade following exposure to LPS, which involves various cytokines. Cytokines can be broadly defined as a family of cell signalling peptides produced by a wide variety of cells following stimulation. Hepatocytes, for example, are capable of both producing and responding to a number of different cytokines (Simpson *et al.*, 1997). Generally, cytokines are not produced constitutively, but are generated in response to various stimuli, such as the presence of products of bacterial origin in the bloodstream. Two of the most

prominent cytokines linked to sepsis are tumour necrosis factor-alpha ($\text{TNF}\alpha$) and interleukin-6 (IL6). The temporal appearance in plasma of a number of cytokines following a challenge with LPS is shown in Figure 6.1. Similar patterns have been found in a range of animal models and clinical investigations (Sullivan *et al.*, 1992).

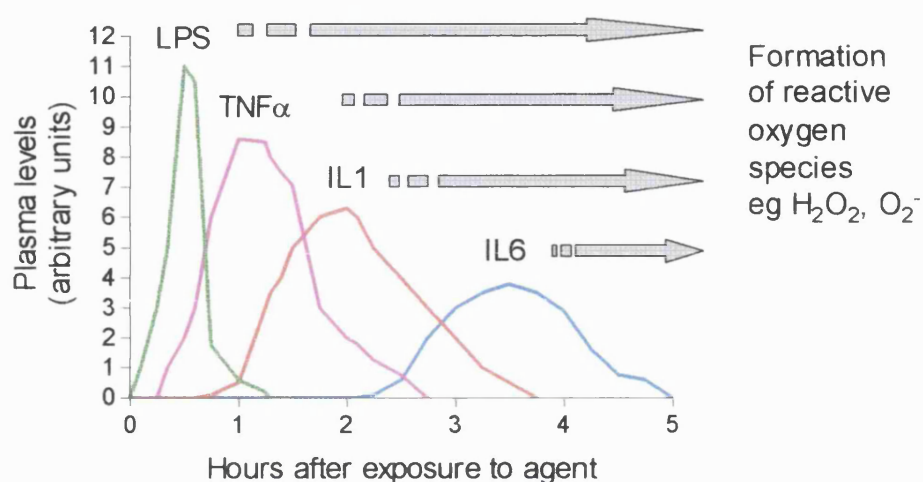


Figure 6.1 Schematic representation detailing the time course of cytokine appearance in plasma

Adapted from Anderson *et al.*, 1997.

The first agent to appear following endotoxin/LPS challenge is $\text{TNF}\alpha$. It belongs to a family of molecules, which display similar biological activity but have varying degrees of structural relationships (Old, 1985). $\text{TNF}\alpha$ is produced by a variety of different cells, including monocytes and adipocytes, but predominantly macrophages. Although macrophages are present in several organs, the largest population of tissue macrophages is the Kupffer cells in the liver, which is likely, therefore, to play a substantial role in the production of $\text{TNF}\alpha$. LPS of gram-negative bacteria are the most potent stimulators of $\text{TNF}\alpha$ production, although viral, fungal and parasitic agents can also stimulate synthesis. There are two types of hepatocyte receptors for $\text{TNF}\alpha$ (Moshage, 1997). $\text{TNF}\alpha$ binding may induce a wide variety of intracellular second messenger mechanisms including: stress-activated protein kinase, tyrosine kinases and reactive oxygen species (Simpson *et al.*, 1997).

TNF α has a broad spectrum of biological activity (Grunfeld *et al.*, 1990, 1991). It may act *via* mediation through hormones, by direct action and/or through interaction with other cytokines. Depending on its concentration and site of secretion it can have different functions. For example, at low concentrations, TNF α has been associated with tissue repair, at slightly higher concentrations it can lead to tumour necrosis and may also damage normal tissues, whilst at higher concentrations, it can lead to lethal toxic shock syndrome (Stadler *et al.*, 1991; Bazzoni *et al.*, 1996). In the liver, TNF α can induce type I APPs (Mosage, 1997) and may induce necrosis and/or apoptosis in hepatocytes *via* a direct mechanism and indirectly, *via* induction of NO synthase (reviewed in Simpson *et al.*, 1997; Ayala *et al.*, 1998). TNF α is also capable of stimulating the production of other cytokines, including IL1 and IL6 (McIntosh *et al.*, 1989).

Like TNF α , IL1 is capable of inducing type I APPs, however, it may inhibit the induction of type II APPs (Mosage, 1997). Additionally, IL1 induces other cytokines, including IL6, in a wide variety of cell types. IL6 is believed to be involved in the pleiotrophic effects of IL1 and appears in the plasma after TNF α and IL1 (Figure 6.1). It is synthesised by many different cell types but endothelial cells, fibroblasts and monocytes/macrophages are believed to be the major sources during systemic infection. This cytokine has a strong pyrogenic activity (Helle *et al.*, 1988). There is much uncertainty about hepatic IL6 receptors. Some research suggests the presence of low numbers of receptor sites (approximately 1500 IL6 receptors/hepatocyte) (Hipp, unpublished work discussed in Heinrich *et al.*, 1990), and since IL6 results in significantly raised APP synthesis, this suggests an efficient amplification system (Heinrich *et al.*, 1990). Castell and co-workers (1989) have proposed that in rodent hepatocytes or hepatoma cell lines, TNF α is an important mediator of APP synthesis, whereas in adult human hepatocytes, IL6 is the major APP inducer.

From this brief introduction to some of the agents involved in the septic response, it can be seen that the liver is capable of a wide range of responses to infection. However, the precise biochemical effects are not fully understood. It is important to recognise that not only do these agents have varied individual effects, which depend on many factors, but also their effects may be altered and different when they are

present in combination. These interactions have been reviewed by Vilcek (1998), but in summary:

- cytokines tend to have multiple target cells and multiple actions;
- different cytokines may have similar actions;
- exposure of cells to two or more cytokines at the same time may lead to qualitatively different responses;
- a cytokine may increase or decrease the production of another cytokine;
- a cytokine may increase or decrease the expression of receptors for another cytokine or growth factor;
- a cytokine may increase or decrease signalling by receptors for another cytokine or growth factor.

It has been suggested that circulatory levels of TNF α and IL6 correlate with mortality rates, which may indicate their importance in the pathogenesis of sepsis (Damas *et al.*, 1991; Sullivan *et al.*, 1992; Roumen *et al.*, 1993), although such relationships are controversial (Pinsky *et al.*, 1993) and standardised assay techniques need to be established (Kossodo *et al.*, 1995).

LPS and various cytokines have been implicated in the generation of reactive oxygen species (ROS) (Figure 6.1) such as superoxide, hydrogen peroxide, hydroxyl radicals and nitric oxide. These highly reactive, but short-lived chemical species are produced during a number of normal physiological processes, including mitochondrial metabolism (considered further in Chapter 7) and by neutrophils and macrophages during the 'respiratory burst'. Intracellular components are protected from the adverse effects of ROS by a number of endogenous ROS scavenging enzymes, such as superoxide dismutase. Such scavengers interact with free radicals but do not in turn produce self-propagating chain reactions. However, oxidative stress may occur where there is an imbalance between ROS production and antioxidant activity. Enhanced generation of ROS has been proposed as an explanation of cellular injury in sepsis (Portolés *et al.*, 1993; Taylor *et al.*, 1995).

6.1.4 Fatty acid oxidation and ketogenesis during sepsis

Although there has been considerable scientific and clinical research, there is still much uncertainty with regards to fatty acid oxidation and ketogenesis during sepsis.

In this section, I will briefly consider some recent literature (in which sepsis is modelled in a variety of systems) which are relevant to these pathways.

Some studies have suggested that several organs may demonstrate altered fuel preferences during sepsis. Romanosky *et al.*, (1980) found that following LPS treatment, the uptake and oxidation of long-chain fatty acids was decreased in skeletal muscle. Other groups, however, have shown that during sepsis, fat is the preferred fuel for oxidation (Stoner *et al.*, 1983; Nanni *et al.*, 1984).

The rate of fat oxidation is in part determined by the plasma concentration of non-esterified fatty acids (NEFA) (Groop *et al.*, 1991; Ebeling *et al.*, 1994), therefore it is important to consider how the concentration of NEFA is effected by sepsis. There is, however, some conflict in the literature regarding the effect of sepsis on NEFA concentration. Some studies have reported raised plasma NEFA concentrations in patients with sepsis (Lefevre *et al.*, 1988) whilst normal and depressed levels have also been observed (Neufeld *et al.*, 1976; Kuzin *et al.*, 1984). During sepsis, fat mobilization has been reported to be greater than fat oxidation (Nordenström *et al.*, 1983), which may imply a degree of cycling (Wolfe *et al.*, 1987, 1991). In such a 'triglyceride-fatty acid cycle' fatty acids are released at a rate in excess of their oxidation. A 'recycling process' occurs, whereby non-oxidized fatty acids are re-esterified back into triglyceride. These newly formed triglycerides are transported from the liver *via* very low density lipoproteins to peripheral adipose tissue for storage (Wolfe, 1991). Under some 'stress' conditions, it has been found that the percentage of fatty acids released by lipolysis, which are then re-esterified increases from 'normal' levels of approximately 50% to greater than 65% (Wolfe *et al.*, 1987).

Memon *et al.*, (1998) have used endotoxin and cytokines to investigate the effects of sepsis on the expression of fatty acid transport protein (FATP) and fatty acid translocase (FAT), which are involved in the transport of fatty acids across biological membranes. These workers found that LPS or cytokine administration decreased FATP mRNA levels in the liver by approximately 80%, but increased FAT mRNA expression fivefold. These workers suggested that FATP may be involved in the transport of fatty acids towards mitochondria for oxidation, which has been reported as decreased during sepsis, whilst FAT may be involved in the transport of fatty acids to the cytosol for re-esterification.

Recently, Memon *et al.*, (1999) have investigated the *in vivo* effects of LPS and

cytokines on FABPs in liver. As discussed in Chapter 1, these proteins facilitate the diffusion of fatty acids through the aqueous medium of the cytosol to membrane-bound enzymes. Administration of LPS and cytokines lead to a substantial decrease in FABP mRNA levels and protein content, which these workers suggest was likely to contribute to the decrease in fatty acid oxidation frequently observed during sepsis. Additionally, LPS and cytokines have been found to alter acyl-CoA synthase (ACS) mRNA levels and activity (Memon *et al.*, 1998). As previously discussed, ACS are involved in the activation of fatty acids to acyl-CoA esters. Following exposure to LPS and cytokines, Memon *et al.*, (1998) found a decrease in mitochondrial ACS mRNA levels and activity, which would be in accordance with the reduced fatty acid oxidation reported during sepsis. These workers also found that microsomal ACS activity was enhanced, which they suggest supports the reesterification of fatty acids for triglyceride synthesis which is frequently reported during sepsis.

Neufeld, (1976) reported that anorexia is a characteristic of mammals subjected to infectious diseases. As discussed in the preceding chapters, in the absence of an adequate food intake, alternative substrates are oxidized to produce energy by compensatory mechanisms. In non-septic animals, during prolonged and/or acute starvation, part of this compensatory mechanism involves a lowered malonyl-CoA concentration. This results in a decreased inhibition of CPT I and permits the diversion of long-chain fatty acids into the mitochondria for oxidation (McGarry *et al.*, 1989). This in turn leads to increased levels of ketogenesis and the resulting acetoacetate and β -hydroxybutyrate are transported from the liver, to be used as an alternative energy source by peripheral tissues and organs, including the brain (Nehlig *et al.*, 1993; Nehlig, 1996). This mechanism reduces the need for energy derived from glucose, which in turn spares body protein by decreasing the rate of amino acid usage for gluconeogenesis (Wannemacher *et al.*, 1979). However, in experimental and human sepsis, there is a failure to mount this compensatory response, and ketogenesis does not increase, despite raised glucagon, cortisol and catecholamine concentrations (Neufeld *et al.*, 1976; Kaminski *et al.*, 1979; Neufeld *et al.*, 1980; Vasconcelos *et al.*, 1987). Under such conditions, skeletal muscle proteolysis is accelerated, supplying amino acids for the synthesis of APPs and gluconeogenesis (Pailla *et al.*, 1998) and critically ill patients with sepsis frequently demonstrate a progressive loss of body cell mass and develop malnutrition (Chioléro *et al.*, 1997).

In addition to reduced ketogenesis, the hypoketonaemia frequently observed during sepsis could result from an increased use of ketone bodies. There is still some controversy regarding this matter, since although there are several studies which shown that this unlikely:

- the rate of ketone body clearance is unaffected in sepsis or surgical stress, despite marked hypoketonaemia (Schofield *et al.*, 1987);
- whilst the liver is the primary site of ketogenesis it is unable to metabolise ketone bodies at an appreciable rate (McGarry *et al.*, 1980); and
- studies using labelled acetoacetate and β -hydroxybutyrate have not found an increased useage by peripheral tissues, in septic rats compared to controls (Wannemacher *et al.*, 1979).

However, Lanza-Jacob *et al.*, (1990), have recently reported that in fed and fasted rats treated with *E. coli*, the observed reduction in ketogenesis could be attributed to both impaired ketogenic capacity and increased peripheral utilization.

6.1.5 Control of ketogenesis during sepsis: the role of CPT I

Given the traditional view of its role as a control point for fatty acid oxidation and ketogenesis, as discussed in the introduction to Chapter 3, much research has focused on the effects of sepsis on CPT I. In rats, the activity of CPT I has been found to be decreased after LPS administration (Takeyama *et al.*, 1989). Furthermore, in mitochondria isolated from rats that had received an intraperitoneal injection of LPS, it was found that octanoate oxidation, which can be considered as largely CPT I independent (although see Section 5.4.1) was unaffected, whereas the oxidation of palmitoyl-CoA (CPT I dependent) was significantly reduced (Takeyama *et al.*, 1990). These workers suggested, therefore, that the enzymes of β -oxidation, CPT II and intramitochondrial acyl-CoA synthase were not affected by LPS administration, that they may have little contribution to the failure of the ketogenic response during the fasting associated with endotoxemia and that the contribution of CPT I to control ketogenesis may be increased under certain conditions.

The hypothesis that control of fatty acid oxidation and ketogenesis is exerted at the level of CPT I during sepsis is further supported by Wannemacher *et al.*, (1979). They found that in a sepsis model where adult rats were injected subcutaneously with *S. pneumoniae*, a 29% decrease in ketogenesis was observed when the long-

chain fatty acid, oleic acid was used as substrate. However, when the medium-chain fatty acid, octanoate was used, *S. pnem.* infection had little effect on the rate of ketogenesis in treated groups compared to controls. Additionally, in another experimental model of sepsis (caecal ligation and puncture) studies comparing the short-chain fatty acid, butyrate, to the long-chain fatty acid, oleate, have also shown that hepatic ketogenesis was not decreased with the short-chain fatty acid, whilst it was depressed when the long-chain fatty acid was used as substrate (Vasconcelos *et al.*, 1987). These workers, therefore, suggested that the site of inhibition of ketogenesis in the septic liver may be the entry of long-chain fatty acids into the mitochondria, i.e. at the level of CPT I and that modulation of CPT I activity during sepsis may be through changes in the concentration of malonyl-CoA.

Interestingly, glucagon levels have been shown to be raised during bacterial infection (Neufeld *et al.*, 1982). Typically, this would be expected to lead to increased ketogenesis, since under such conditions acetyl-CoA carboxylase is phosphorylated to its inactive form, leading to a decrease in malonyl-CoA concentration and subsequently decreasing CPT I inhibition. Additionally, raised glucagon would be expected to increase the activity of mHMG-CoA synthase due to decreased succinylation of this enzyme, which would also increase ketogenesis (Quant *et al.*, 1989). However, it has been suggested that during sepsis, the stimulatory effects of glucagon on ketogenesis and gluconeogenesis may be antagonized by raised plasma insulin levels (Vasconcelos *et al.*, 1987). Elevated insulin would stimulate acetyl-CoA carboxylase by dephosphorylation (Witters *et al.*, 1988), which in turn would increase malonyl-CoA levels, thus depressing ketogenesis. In support of this, several studies have reported hyperinsulinemia in sepsis (Zensor *et al.*, 1974; Neufeld *et al.*, 1980; Hargrove *et al.*, 1983). However, Spitzer *et al.*, (1988) have reported unchanged plasma insulin levels during sepsis and others workers have been unable to find a relationship between insulin levels and the degree of impairment of ketogenesis (Beylot *et al.*, 1989). However, Beylot and co-workers suggested that the persistent insulin secretion by subjects in their study may have been sufficient to restrain ketogenesis.

When considering the effect of sepsis on malonyl-CoA specifically, the literature again presents a conflicting picture. In a sepsis model where adult rats were injected with *S. pnem*, no difference in the hepatic concentrations of malonyl-CoA was found in the infected rats compared to controls (Wannemacher *et al.*, 1979). However, in studies where adult rats received an injection of TNF α an approximate

three-fold increase in hepatic malonyl-CoA concentration was found (Memon *et al.*, 1992). In other studies, where adult rats received TNF α via intraperitoneal injection, increases in the concentration of malonyl-CoA were also observed (Beylot *et al.*, 1992) and these workers suggested the increase was due to TNF α increasing levels of hepatic citrate. From studies using an *in vitro* adult rat hepatocyte model, where cytokines were added to isolated hepatocytes, Nachiappan *et al.*, (1994) proposed three mechanisms to account for the accumulation of citrate during sepsis. Firstly, it could result from a redirection of alanine carbon away from gluconeogenesis into the TCA cycle. Secondly, citrate could accumulate due to the inhibition of aconitase in the TCA cycle. Alternatively, they suggest that citrate could accumulate due to increased acetyl-CoA input into the TCA cycle. Regardless of the mechanism of increase, as an allosteric activator for acetyl-CoA carboxylase, increased levels of citrate would lead to increased malonyl-CoA levels and subsequently decreased CPT I activity. This would divert hepatic fatty acid metabolism away from oxidation and ketogenesis and towards re-esterification (Nachiappan *et al.*, 1994). Additionally, Takeyama *et al.*, (1990) have reported that CPT I becomes 5-fold more sensitive to malonyl-CoA inhibition in endotoxic rats.

Other workers, however, have questioned the importance of CPT I in controlling ketogenesis during sepsis. In a sepsis model where hepatocytes were isolated from adult rats, cultured and exposed to TNF α and/or IL6, a decrease in ketogenesis was observed when octanoic acid was used as substrate (Pailla *et al.*, 1998). Although as seen in Section 5.4.1, it is apparent that some octanoate enters mitochondria *via* the three-step transport system which includes CPT I, the majority of octanoate is oxidized independently of these steps, and this result therefore questions the role of CPT I in controlling flux under these experimental conditions. Furthermore, in an experimental system where TNF α was added to hepatocytes isolated from starved rats, there were no changes in ketogenesis and palmitate metabolism (Rofe *et al.*, 1987). It has, however, been suggested by others that this failure to see an effect in isolated hepatocytes is because TNF α does not necessarily work in isolation and an intraperitoneal injection of TNF α into adult rats decreased ketone body concentrations relative to controls, which was related to decreased ketone body production, and unchanged ketone body clearance (Beylot *et al.*, 1992).

A further factor to be considered is that TNF α on its own produces alterations in hepatic fatty acid oxidation within a narrow concentration range. Outside of its bell-

shaped concentration dependency curve, the inhibitory effects of $\text{TNF}\alpha$ on fatty acid oxidation are diminished (Nachiappan *et al.*, 1994). These workers also found that in hepatocytes isolated from adult rats which were subsequently exposed to IL6, this cytokine also had a direct effect on fatty acid oxidation and when used in combination, $\text{TNF}\alpha$ +IL6 produced significantly increased inhibition of ketone body production (31%) as compared with either $\text{TNF}\alpha$ or IL6 on its own. In addition, the cytokine-induced inhibition observed during these studies was specific for long-chain fatty acids (Nachiappan *et al.*, 1994), supporting the earlier conclusions from work using LPS.

Although CPT I gene expression is significantly increased following starvation under 'normal' conditions, in a rat model of peritoneal sepsis superimposed on starvation, hepatic CPT I gene expression is inhibited, partly due to increased expression of the leucine-zipper DNA transcription factor *c-fos* (Barke *et al.*, 1991, 1996). These workers suggest that this down-regulation, which is observed 12 hours after the initial insult, may be responsible, at least in part, for decreased ketogenesis following sepsis.

In summary, therefore, there appears to be a variety of abnormalities in hepatic lipid metabolism during sepsis. Whilst the precise mechanisms of these alterations are unclear, several lines of evidence have suggested that sepsis may have an effect on the entry of long-chain fatty acids into the mitochondria, i.e. at the step catalysed by CPT I. To date, there has been no quantitative assessment of the potential of CPT I to control flux during sepsis.

6.1.6 Aims of this section

In this Chapter, I aim to develop *in vitro* models of neonatal sepsis which may be used to assess quantitatively the role of CPT I in control of ketogenic flux during sepsis. To achieve these aims, I will investigate the effects on cell yield and viability of the addition of various agents known to be involved in the septic response, specifically, LPS, $\text{TNF}\alpha$ and LPS plus $\text{TNF}\alpha$ (LPS+ $\text{TNF}\alpha$) and LPS plus $\text{TNF}\alpha$ plus IL6 (LPS+ $\text{TNF}\alpha$ +IL6) during the hepatocyte isolation procedure. To assess the potential of CPT I in the control of ketogenic flux during sepsis BUCA will be applied to *in vitro* models (New *et al.*, 2000).

6.2 Theory and approaches

6.2.1 Isolation of hepatocytes in the presence of lipopolysaccharide (LPS) and/or tumour necrosis factor α (TNF α), interleukin 6 (IL6)

Suckling rat pups, of the same age range as described in Section 2.1.2 were used in the experiments detailed in this chapter. For each experiment, the hepatocyte isolation procedures were carried out in parallel for the control and treated groups, each using 5 pups from the same litter per preparation. The procedures for liver removal/cell isolation were as described previously (Section 2.2.1), with modifications as set out below.

To mimic an initial bacterial insult, hepatocytes were exposed to LPS and/or TNF α and/or IL6, agents that are known to induce the septic response (Table 6.1). In this manner, the agents were added in measured and controlled doses, which ensured reproducibility of the septic challenge.

Agent	Details	Dosage
Lipopolysaccharide (LPS)	<ul style="list-style-type: none"> • <i>E Coli</i> serotype 055:B55 • 6mg in 600μl KRP 	<ul style="list-style-type: none"> • Full dose: 3 additions of 200μl • Half dose: 3 additions of 100μl
Tumour necrosis factor (TNF α)	<ul style="list-style-type: none"> • Human recombinant • Endotoxin <10 EU/ml • 4μl in total 200μl KRP 	<ul style="list-style-type: none"> • Full dose: 3 additions of 50μl • Half dose: 3 additions of 25μl
Interleukin 6 (IL6)	<ul style="list-style-type: none"> • Human natural • Endotoxin <10 EU/ml 	<ul style="list-style-type: none"> • Full dose: 3 additions of 30μl • Half dose: 3 additions of 15μl

Table 6.1 *In vitro* model of neonatal sepsis: agents used during cell preparation

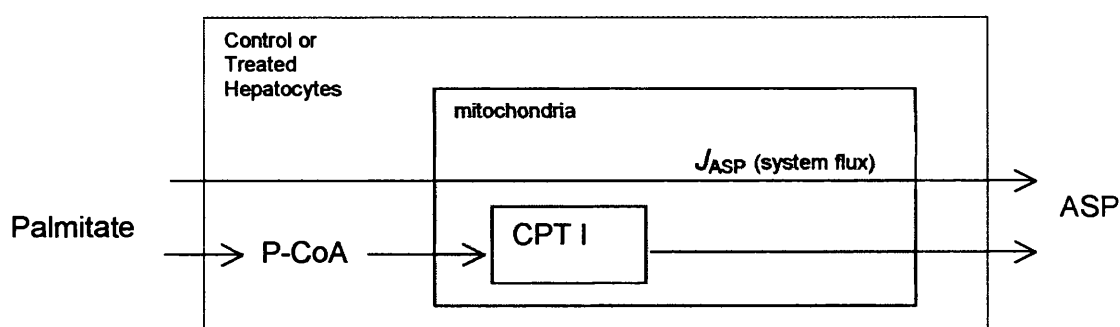
All agents purchased from Sigma, Poole, Dorset, U.K.

In treated groups, the appropriate agent(s) were added at the start of the pre-incubation stage of the isolation procedure described in Section 2.2.1 (i.e. at the start of stage (a)) and again at the beginning of the 40min incubation stage (i.e. during stage (c)) when the original medium was replaced. The third and final addition of agent(s) was at the end of the cell isolation procedure, when cells had been isolated and had been resuspended in "incubation medium", prior to

experimentation. In control groups appropriate volumes of KRP were added to the incubations at the same key stages. Where agents were used in combination, the same 'dosage' was used as when the agents were added individually (Table 6.1). LPS was stored at 4°C and solutions prepared daily. TNF α and IL6 were aliquoted into single dose samples on purchase, which were stored at -40°C and thawed prior to use.

6.2.2 Application of BUCA in control and treated hepatocytes

This section describes the system used to quantitatively assess the potential of CPT I to control flux from palmitate to ketone bodies (acid soluble products, ASP) in control hepatocytes isolated from suckling rats and in hepatocytes exposed to LPS+TNF α or LPS+TNF α +IL6 during the cell isolation procedure. The system for BUCA is essentially the same as that used in Chapter 3 and is detailed in Scheme 6.1.



Scheme 6.1 Hepatocyte BUCA system

The scheme is represented by a green box and represents the system for calculation of the flux control coefficients for CPT I with respect to ketogenesis ($C_{CPTI}^{J_{ASP}}$), in control or treated hepatocytes. P-CoA represents palmitoyl-CoA, ASP, acid soluble products and J_{ASP} , ketogenic flux.

As before, in Chapters 3, 4 and 5, the extrahepatic control exerted by non-esterified fatty acid supply to the liver has been excluded by using isolated hepatocytes incubated with a fixed concentration of fatty acid. The activity of CPT I was progressively inhibited with increasing concentrations of etomoxir. The system was allowed to relax to a new steady state and ketone body production assessed (Sections 2.2.4). The flux control coefficients for CPT I with respect to ketogenesis

were calculated using the data in Figures 6.7-6.8 and Figures 6.11-6.12, the Simfit package (Bardsley *et al.*, 1997) to calculate initial slopes and the following equation:

Equation 6.1:

$$C_{CPTI}^{J_{ASP}} = \frac{\frac{\delta J_{ASP}}{J_{ASP}}}{\frac{\delta v_{CPTI}}{v_{CPTI} (i=0)}}$$

where $C_{CPTI}^{J_{ASP}}$, is the flux control coefficients of CPT I over ketogenesis at zero inhibitor (etomoxir-CoA) concentration ($i = 0$). v_{CPTI} represents the activity of CPT I, ASP represents acid soluble products. δ represents infinitesimal changes (i.e. tend to zero).

6.3 Results

6.3.1 Effect on cell yield and viability of addition of LPS, TNF α and/or IL6 during the hepatocyte isolation procedure

With the exception of the experiments investigating the effect of ½ dose LPS+TNF α +IL6, where there was a small sample size and a large scatter of values in the control group, the addition of these agents, either singly or in combination during the hepatocyte isolation procedure, resulted in a significant decrease in cell yield in the treated groups compared to appropriate paired controls (Table 6.2).

The cell viability of resulting preparations was not significantly different in treated groups and controls, with the exception of the LPS exposed group, where there was a significant decrease in viability of isolated cells compared to controls (Table 6.2). It is not clear why LPS on its own would lead to a significant decrease in cell viability, whereas in combination, it showed no effect. It must be emphasised, however, that cell preparations with viability less than 85% were not used for any experiments.

Absolute values for total cell yield, in terms of (10^6 cells) (g wet mass liver) $^{-1}$ and yield after correcting for viability are provided in Table 6.3.

Agent(s) added during hepatocyte isolation	Number of hepatocyte preparations	Cell yield ((10 ⁶ cells) (g wet mass liver) ⁻¹)		Cell yield ((10 ⁶ viable cells) (g wet mass liver) ⁻¹)	
		Control	Treated cells	Control	Treated cells
LPS	13	37.3 ± 3.0	29.7 ± 2.9	32.8 ± 2.6	25.7 ± 2.3
TNF α	7	42.8 ± 4.4	31.5 ± 4.7	36.8 ± 3.7	27.0 ± 4.0
LPS+TNF α	40	35.1 ± 1.5	29.8 ± 1.6	31.2 ± 1.3	26.4 ± 1.4
½ LPS+TNF α	3	36.9 ± 2.0	26.2 ± 2.8	32.0 ± 1.8	22.7 ± 2.6
LPS+TNF α +IL6	31	30.9 ± 1.1	27.5 ± 1.2	27.4 ± 1.0	24.4 ± 1.1
½ LPS+TNF α +IL6	4	31.9 ± 5.6	24.6 ± 2.0	28.0 ± 4.7	21.4 ± 1.6

Table 6.2 Absolute cell yields following addition of LPS and/or cytokines during hepatocyte isolation procedure

See Table 6.2 for details. The cell isolation procedures for the control or treated cells were performed in parallel. Cell number and viability were assessed by trypan blue exclusion (Section 2.2.1). Cell preparations with viability less than 85% were not used for experiments.

Agent(s) added during hepatocyte isolation	Number of hepatocyte preparations	Mean difference in cell yield ((10 ⁶ cells) (g wet mass liver) ⁻¹)	<i>P</i>	Mean difference in cell viability (%)	<i>p</i>
LPS	13	-7.6 ± 3.2	<i>p</i> <0.05	-1.8 ± 0.8	<i>p</i> <0.05
TNF α	7	-11.2 ± 3.0	<i>p</i> <0.05	-0.3 ± 0.3	NS
LPS+TNF α	40	-5.3 ± 1.7	<i>p</i> <0.05	-0.4 ± 0.4	NS
½ LPS+TNF α	3	-10.7 ± 1.2	<i>p</i> <0.05	-0.3 ± 1.2	NS
LPS+TNF α +IL6	31	-3.4 ± 1.2	<i>p</i> <0.05	-0.03 ± 0.5	NS
½ LPS+TNF α +IL6	4	-7.3 ± 4.3	NS	-2.0 ± 2.0	NS

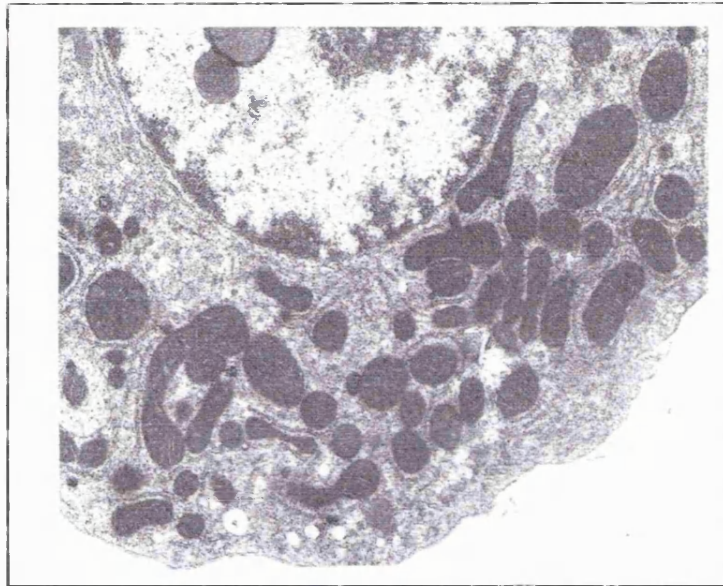
Table 6.3 Effect of addition of LPS and/or cytokines during hepatocyte isolation procedure on hepatocyte yield and viability

The cell isolation procedures for the control or treated cells were performed in parallel. Values are mean differences ± SEM, where mean difference has been calculated as the difference in cell yield between treated cells and paired control. Results were analysed using the paired Student's *t* test (since two sets of five livers from the same litter are compared). NS = not significant. Cell number and viability were assessed by trypan blue exclusion (Section 2.2.1). Cell preparations with viability less than 85% were not used for experiments.

6.3.2 Effect of addition of LPS+TNF α on hepatocyte gross morphology

Electron microscopy was used to investigate the effect of LPS+TNF α on cell ultrastructure (Figure 6.2). No gross morphological differences were observed between LPS+TNF α treated and control hepatocytes: in both cases the cell membranes appeared intact, smooth endoplasmic reticulum was abundant and mitochondria appeared intact with well-formed cristae.

(a) Control hepatocytes



(b) Treated hepatocytes

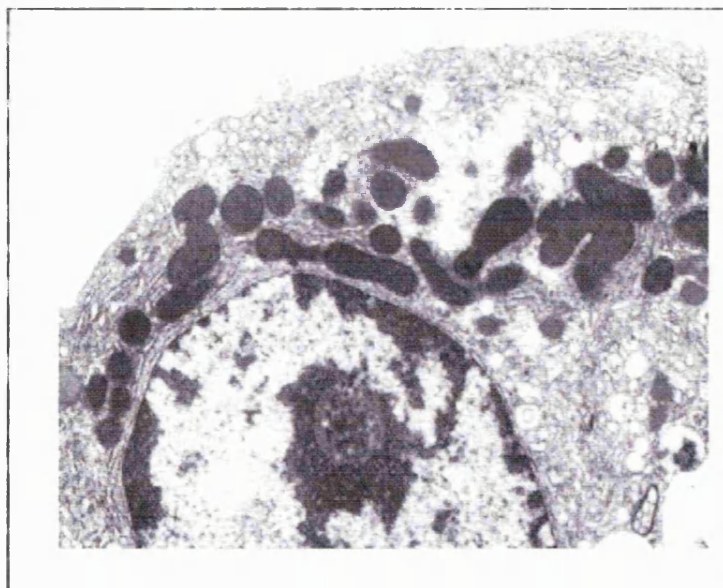


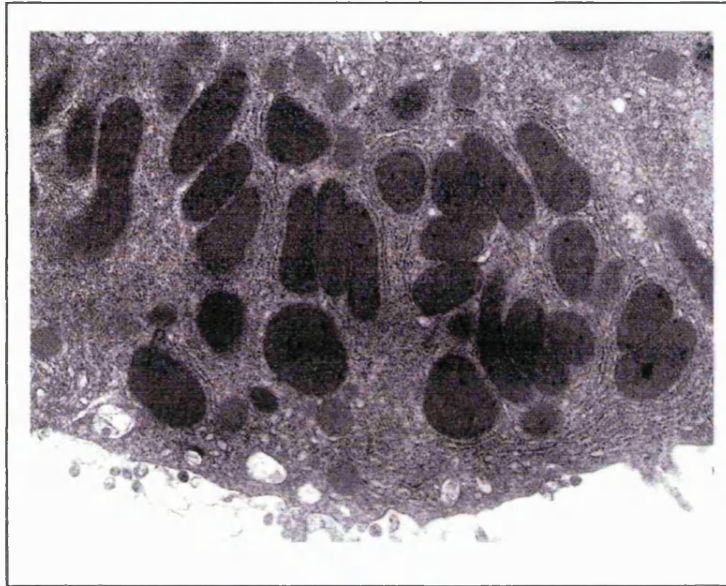
Figure 6.2 Effect of addition of LPS+TNF α during hepatocyte isolation on the ultrastructure of isolated hepatocytes

incubations were carried out in parallel with the oxygen consumption experiments reported in Chapter 7, except that after a 30min incubation, cell suspensions were centrifuged and the resulting pellets were fixed in 2.5% glutaraldehyde and 0.1 mol/L cacodylate buffer.

6.3.3 Effect of addition of LPS+TNF α +IL6 on hepatocyte gross morphology

Electron microscopy was used to investigate the effects of this combination of agents on cell ultrastructure (Figure 6.3). As in the previous combination model, no gross morphological differences were observed between LPS+TNF α +IL6 treated and untreated control cells. However, in both control and treated cells, whilst the cell membrane appears intact, slight blebbing was visible.

(a) Control hepatocytes



(b) Treated hepatocytes

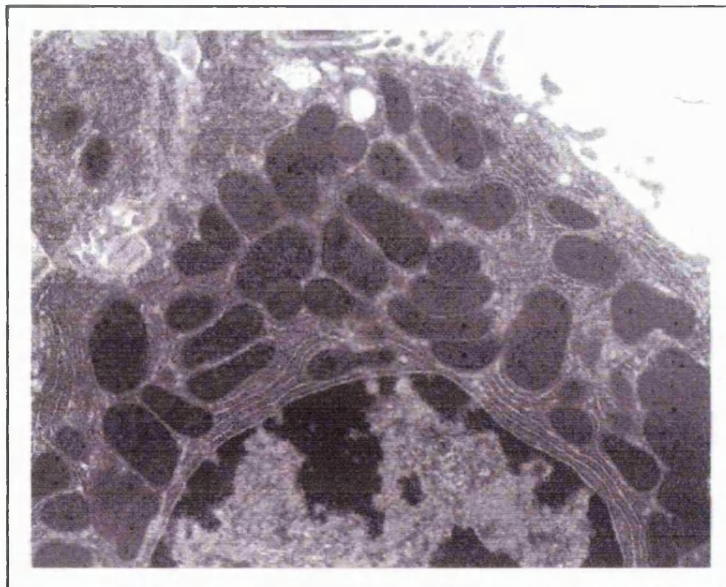


Figure 6.3 Effect of addition of LPS+TNF α +IL6 during hepatocyte isolation on the ultrastructure of isolated hepatocytes

Incubations were carried out in parallel with the oxygen consumption experiments reported in Chapter 7, except that after a 30min incubation, cell suspensions were centrifuged and the resulting pellets were fixed in 2.5% glutaraldehyde and 0.1 mol/L cacodylate buffer.

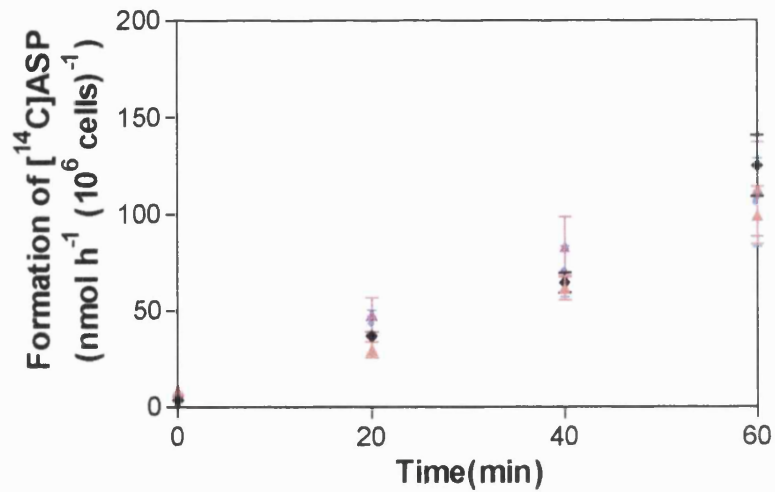
6.3.4 Effect of LPS, TNF α and/or IL6 on ketone body production

The formation of labelled acid soluble products ([¹⁴C]ASP), as a measure of ketone body production over time was assessed for the following groups:

- i. untreated controls paired with the appropriate treated groups;
- ii. hepatocytes exposed to LPS alone;
- iii. hepatocytes exposed to TNF α alone;
- iv. hepatocytes exposed to LPS+TNF α ; and
- v. hepatocytes exposed to LPS+TNF α +IL6.

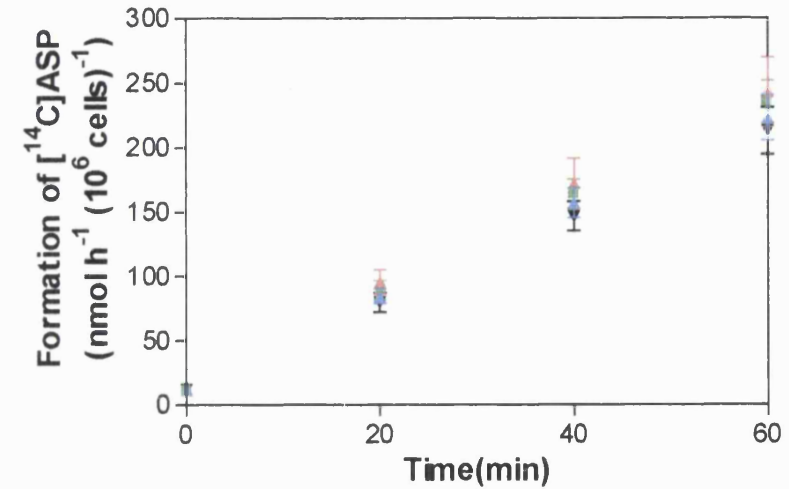
In all cases, production of [¹⁴C]ASP was linear over time and was unchanged between control and treated groups over the 60min period. For clarity, results where agents were used singly, with appropriate paired controls, are shown in Figure 6.4(a) whilst those for experiments where agents were used in combination (i.e. LPS+TNF and LPS+TNF+IL6, with appropriate paired control groups) are shown in Figure 6.4(b).

(a) Experiments where agents were used singly



▲ Control (LPS) ○ LPS
 ▼ Control (TNF α) ◆ TNF α

(b) Experiments where agents have been used in combination



▲ Control (LPS+TNF α +IL6) ○ LPS+TNF α +IL6
 ▼ Control (LPS+TNF α) ◆ LPS+TNF α

Figure 6.4 Formation of [^{14}C]ASP over time

Control and appropriate treated preparations were performed in parallel. Substrate: [$1\text{-}^{14}\text{C}$]palmitate, 0.5mM final concentration, $0.4\mu\text{Ci } \mu\text{mol}^{-1}$, in KRB, 2% BSA). Values are means \pm SEM, $n=5$ parallel hepatocyte preparations for control and LPS models, $n=5$ for control and TNF α models, $n=8$ for control and LPS+TNF α models, and $n=5$ for control and LPS+TNF α +IL6 models. Hepatocyte preparations with viability greater than 85% were used for experiments.

6.3.5 Effect of combinations of LPS, TNF α and/or IL6 on the role of CPT I in control of carbon flux from palmitate

(a) CPT I activity in control and LPS+TNF α treated groups

Figure 6.5 shows the effect of manipulations of CPT I activity, using a range of concentrations of etomoxir (0 μ M-100 μ M). In control and LPS+TNF α -treated groups approximately 75% inhibition of CPT I activity was observed at 100 μ M. As in Chapter 3, this suggested that the possible contribution of CPT II to the measured activity is relatively low. In control and LPS+TNF α -treated groups the activities of CPT I in the absence of etomoxir were 194 ± 56 and 120 ± 7 nmol h $^{-1}$ (10 6 cells) $^{-1}$ respectively. No significant differences in CPT I activity were observed between LPS+TNF α -treated and control groups.

(b) ASP formation in control and LPS+TNF α treated groups

Figure 6.6 shows the effect of a range of concentrations of etomoxir (0 μ M-100 μ M) on ketogenic flux, as assessed by formation of acid soluble products in control and LPS+TNF α -treated groups. 100 μ M etomoxir caused approximately 90% inhibition of β -oxidation flux, suggesting that the contribution of peroxisomal β -oxidation in these models is low. No significant difference in ketone body production was observed between control and LPS+TNF α -treated groups. In the absence of etomoxir, the absolute rates of [14 C]palmitate consumption were 35 ± 2 and 37 ± 2 nmol h $^{-1}$ (10 6 cells) $^{-1}$ in control and LPS+TNF α -treated groups respectively, whilst rates of formation of [14 C]ASP were 139 ± 6 and 149 ± 6 nmol h $^{-1}$ (10 6 cells) $^{-1}$ in control and LPS+TNF α -treated groups.

(c) Application of BUCA in control and LPS+TNF α treated groups

Figure 6.7 and 6.8 show the data from Figures 6.5 and 6.6 combined on to single graphs, one each for control and treated groups. This enables easier comparison of the curves used in the calculation of the individual flux control coefficients for CPT I over ketogenic flux, which are summarised in Table 6.4.

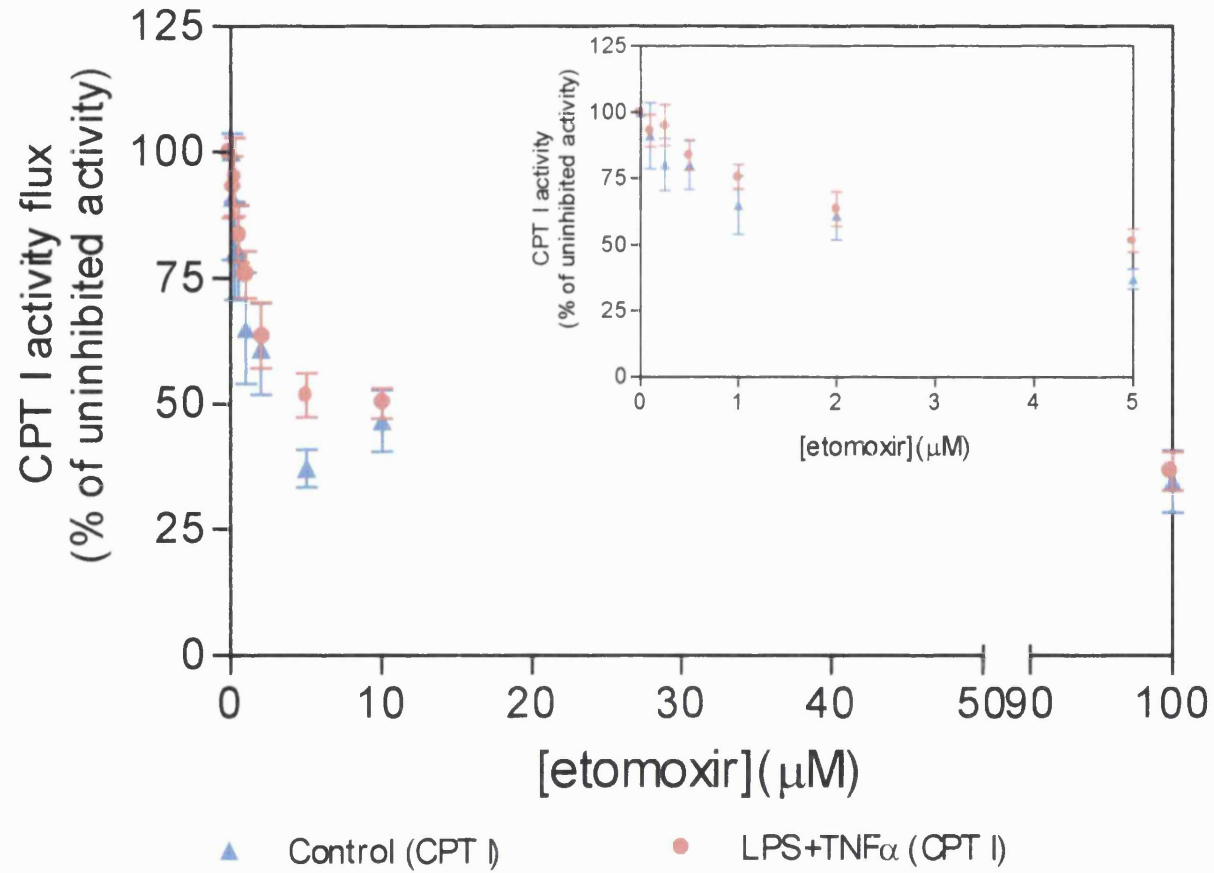


Figure 6.5 Effect of etomoxir on CPT I activity in control and LPS+TNF α treated groups

Hepatocyte preparations with viability greater than 85% were used for experiments. Control and LPS+TNF α -treated preparations were performed in parallel and were incubated with etomoxir for 10 min. Values were normalised by expressing them as a percentage of those obtained in the absence of etomoxir. Values are means \pm SEM, n = 7 parallel hepatocyte preparations.

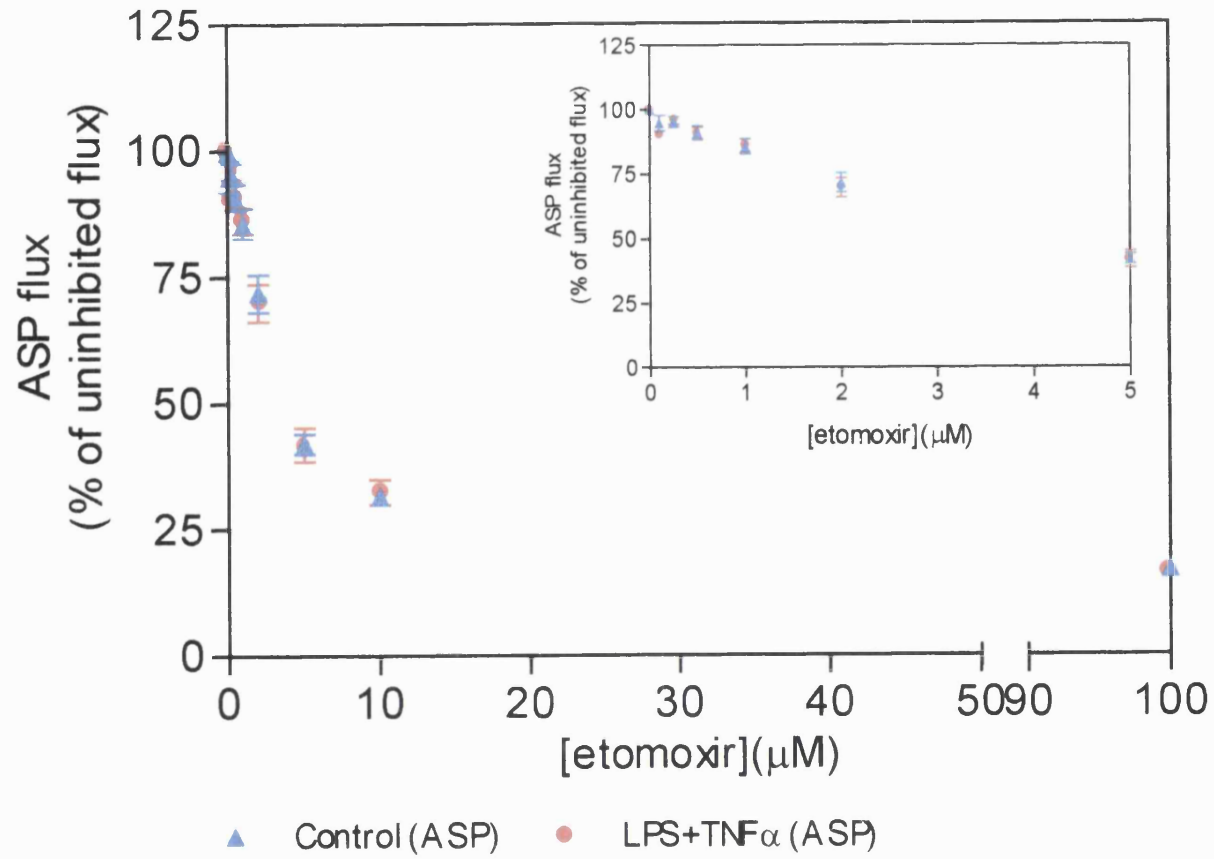


Figure 6.6 Effect of etomoxir on ketogenic flux in control and LPS+TNF α treated groups

Hepatocyte preparations with viability greater than 85% were used for experiments. Control and LPS+TNF α -treated preparations were performed in parallel and were incubated with etomoxir for 10 min. Substrate: [1- 14 C]palmitate, 0.5mM final concentration, 0.4 μ Ci μ mol $^{-1}$, in KRB, 2% BSA). Values were normalised by expressing them as a percentage of those obtained in the absence of etomoxir. Values are means \pm SEM, n = 10 parallel hepatocyte preparations.

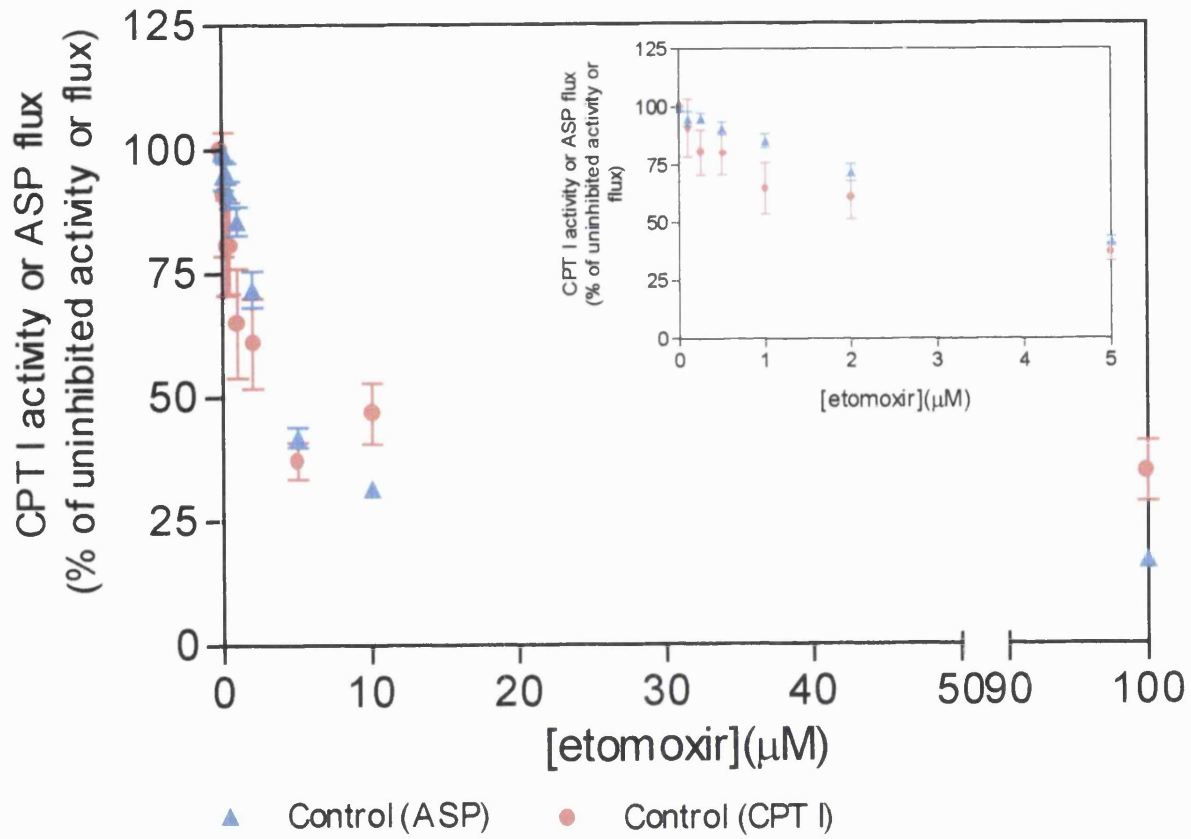


Figure 6.7 Data used for the calculation of individual flux control coefficients for CPT I over ketogenic flux in control groups

Data from control groups have been extracted from Figures 6.5 and 6.6 and combined on a single graph to enable easier comparison of curves for calculation of flux control coefficients. See legend for Figures 6.5 and 6.6 for more detail.

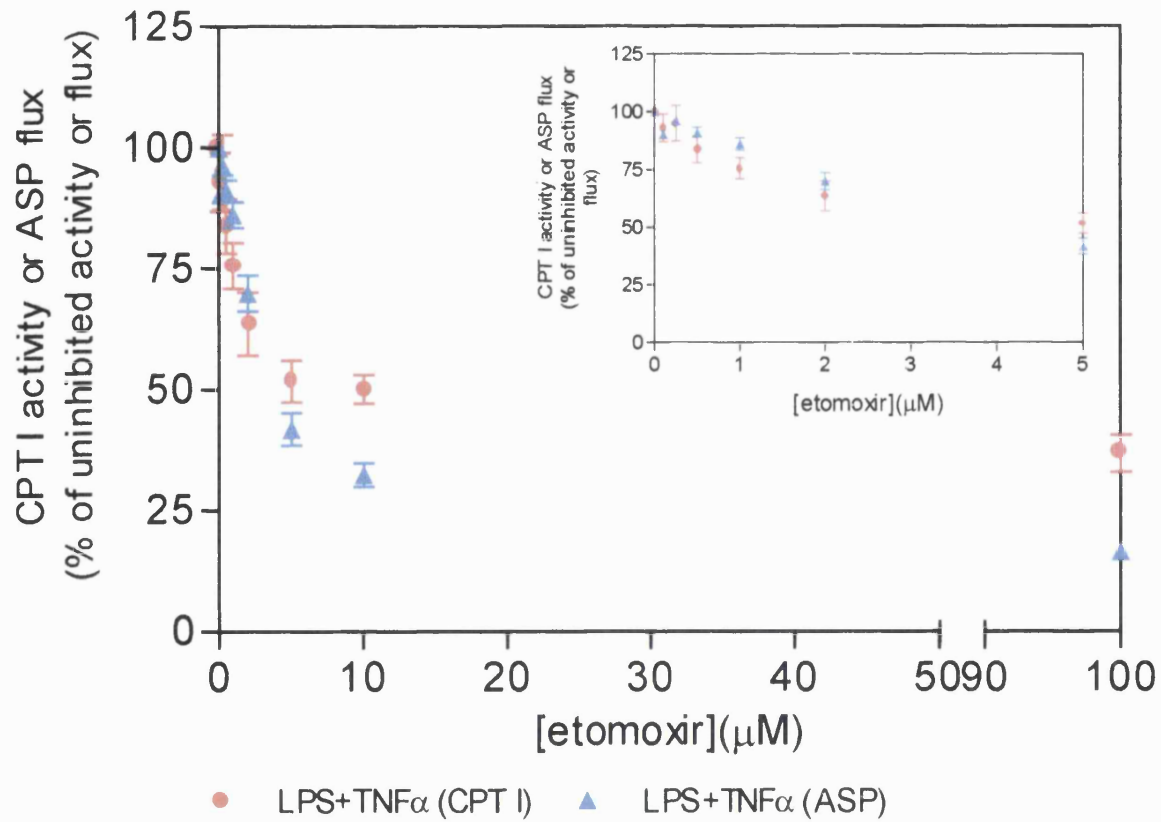


Figure 6.8 Data used for the calculation of individual flux control coefficients for CPT I over ketogenic flux in LPS+TNF α treated groups

Data from treated groups have been extracted from Figures 6.5 and 6.6 and combined on a single graph to enable easier comparison of curves for calculation of flux control coefficients. See legend for Figures 6.5 and 6.6 for more detail.

(d) CPT I activity in control and LPS+TNF α +IL6 treated groups

Figure 6.9 shows the effect of manipulations of CPT I activity, using a range of concentrations of etomoxir (0 μ M-100 μ M) in control and LPS+TNF α +IL6 treated groups. As seen in Figure 6.5, approximately 70% inhibition of CPT I was observed in the control group whereas only approximately 60% inhibition was observed in the LPS+TNF α +IL6 treated group. In control and LPS+TNF α +IL6-treated groups the activities of CPT I in the absence of etomoxir were 168 ± 13 and 145 ± 16 nmol h⁻¹ (10⁶ cells)⁻¹ respectively. There was no significant difference in CPT I activity between LPS+TNF α +IL6-treated and control groups in the absence of etomoxir. In the presence of maximal etomoxir, however, CPT I activity in the controls was $31.1 \pm 2.1\%$, which was significantly lower than in the LPS+TNF α +IL6-treated group, $43.9 \pm 3.1\%$ ($p < 0.05$).

(e) ASP formation in control and LPS+TNF α +IL6 treated groups

Figure 6.10 shows the effect of a range of concentrations of etomoxir (0 μ M-100 μ M) on ketogenic flux, as assessed by formation of acid soluble products in control and LPS+TNF α +IL6 treated groups. In both control and LPS+TNF α +IL6 treated groups, the maximum concentration of etomoxir used in these experiments caused approximately 90% inhibition of β -oxidation flux. Therefore the contribution of peroxisomal β -oxidation in these models appears to be low. No significant difference in ketone body production was observed between control and LPS+TNF α +IL6-treated groups. The absolute rates of [1-¹⁴C]palmitate consumption were 42 ± 4 and 45 ± 3 nmol h⁻¹ (10⁶ cells)⁻¹ in control and LPS+TNF α +IL6-treated groups respectively, whilst rates of formation of [¹⁴C]ASP were 168 ± 17 and 180 ± 9 nmol h⁻¹ (10⁶ cells)⁻¹ in control and LPS+TNF α +IL6-treated groups.

(f) Application of BUCA in control and LPS+TNF α +IL6 treated groups

Individual flux control coefficients for CPT I over ketogenic flux in control or LPS+TNF α +IL6 treated groups (Section 6.2, Equation 6.1) were calculated from the data presented in Figures 6.11 and 6.12 for the control and treated cells respectively. This enables easier comparison of the curves, which have been used in the calculation of the individual flux control coefficients for CPT I over ketogenic flux, summarised in Table 6.4.

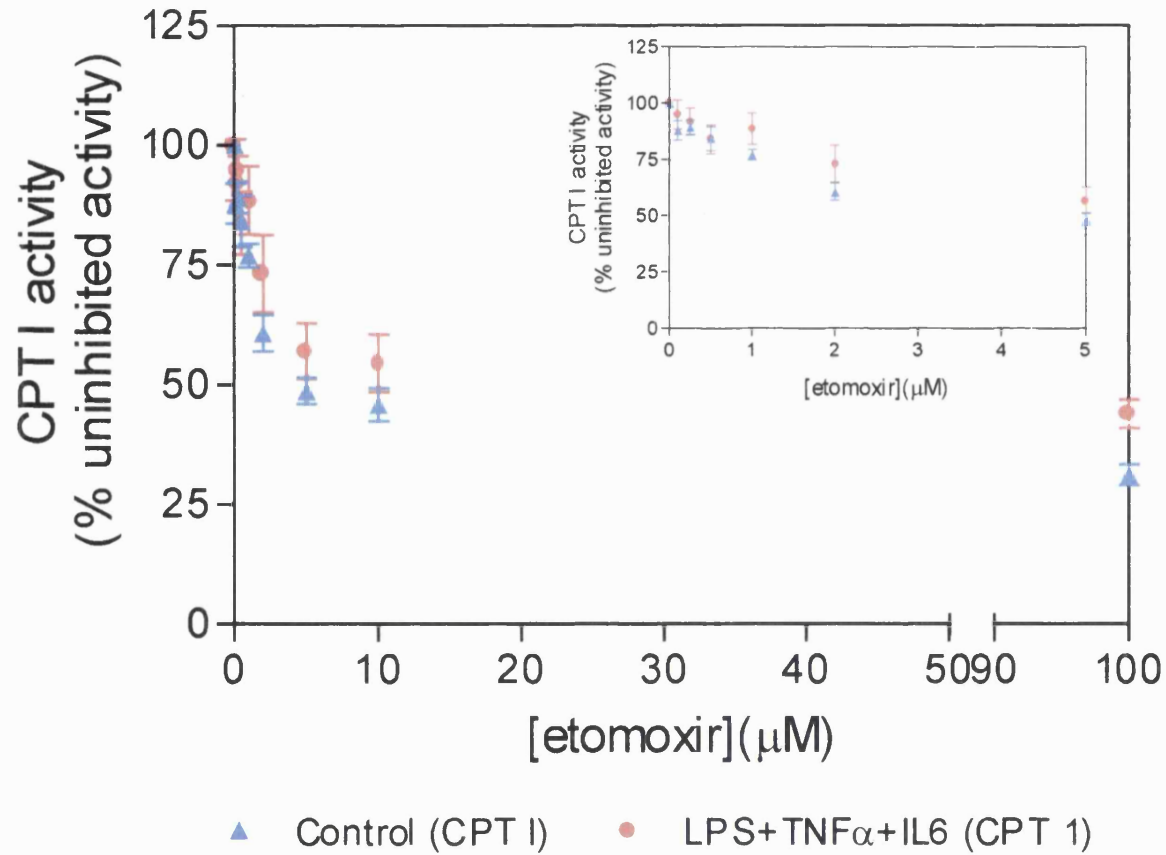


Figure 6.9 Effect of etomoxir on CPT I activity in control and LPS+TNF α +IL6 treated groups

Hepatocyte preparations with viability greater than 85% were used for experiments. Control and LPS+TNF α +IL6-treated preparations were performed in parallel and were incubated with etomoxir for 10 min. Values were normalised by expressing them as a percentage of those obtained in the absence of etomoxir. Values are means \pm SEM, n=7 parallel hepatocyte preparations.

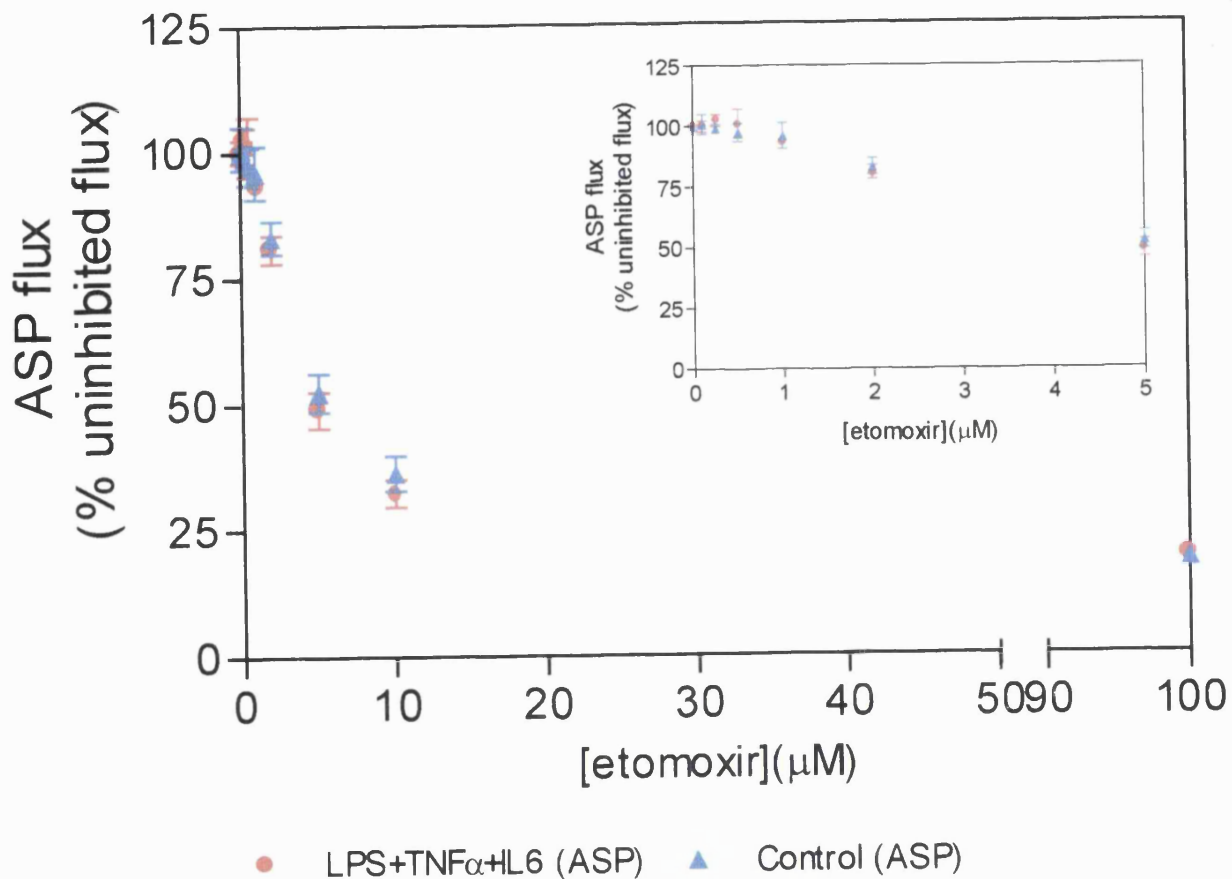


Figure 6.10 Effect of etomoxir on ketogenic flux in control and LPS+TNF α +IL6 treated groups

Hepatocyte preparations with viability greater than 85% were used for experiments, control and treated preparations performed in parallel and were incubated with etomoxir for 10 min. Substrate: [1- 14 C]palmitate, 0.5mM final concentration, 0.4 μ Ci μ mol $^{-1}$, in KRB, 2% BSA). Values were normalised by expressing them as a percentage of those obtained in the absence of etomoxir. Values are means \pm SEM, n=10 parallel hepatocyte preparations.

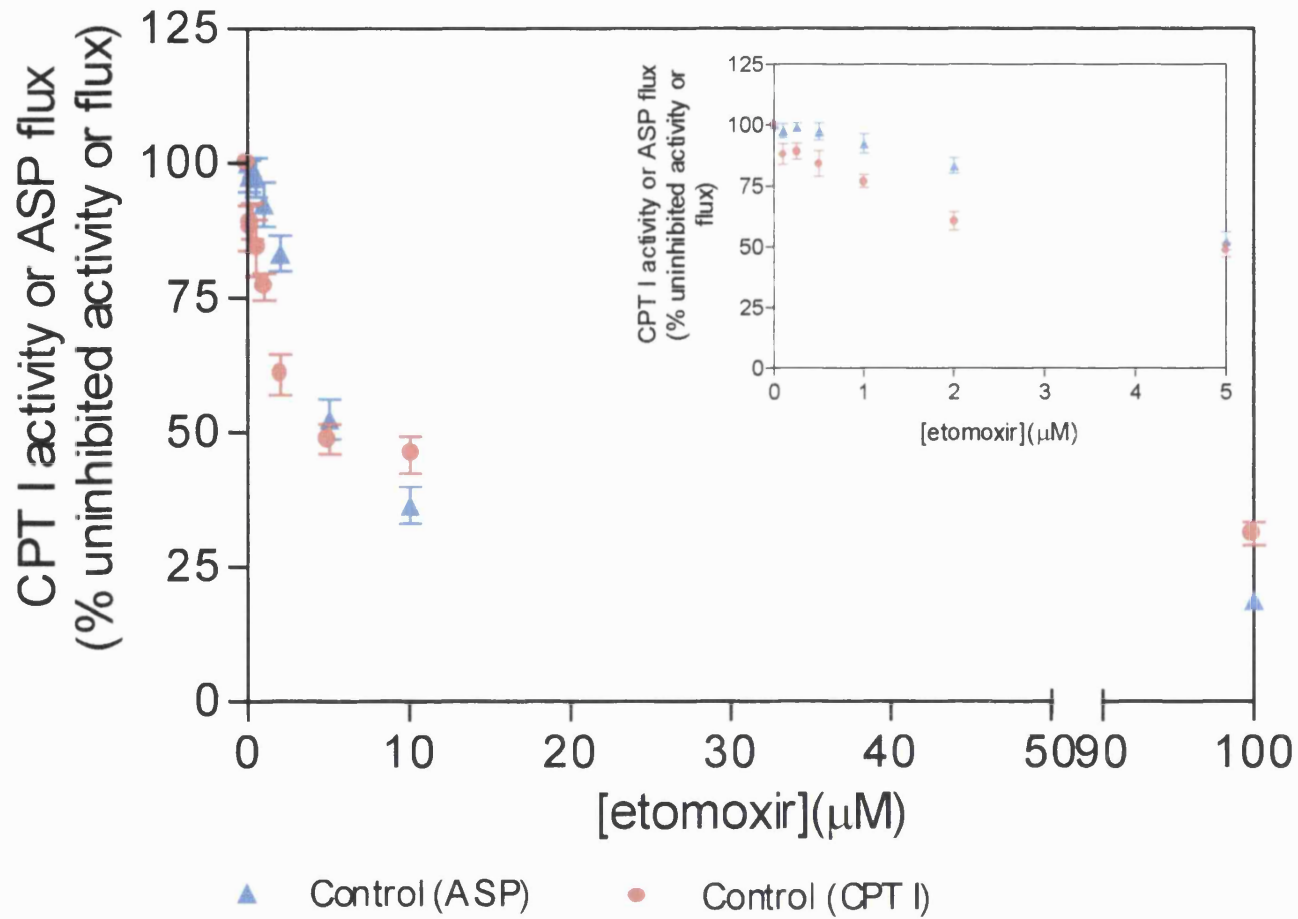


Figure 6.11 Data used for the calculation of individual flux control coefficients for CPT I over ketogenic flux in control groups

Data from control groups have been extracted from Figures 6.9 and 6.10 and combined on a single graph to enable easier comparison of curves for calculation of flux control coefficients. See legend for Figures 6.9 and 6.10 for more detail.

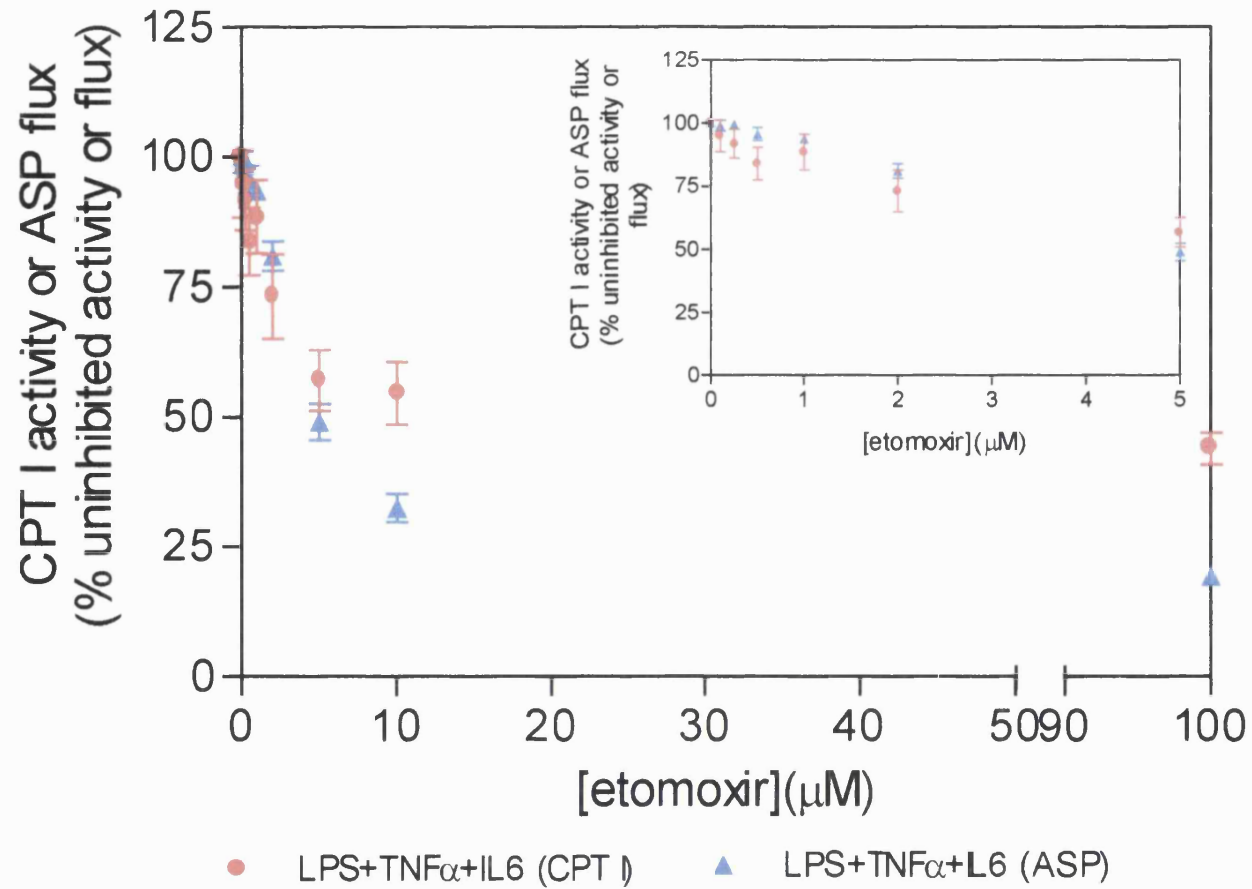


Figure 6.12 Data used for the calculation of individual flux control coefficients for CPT I over ketogenic flux in LPS+TNF α +IL6 treated groups

Data from treated groups have been extracted from Figures 6.9 and 6.10 and combined on a single graph to enable easier comparison of curves for calculation of flux control coefficients. See legend for Figures 6.9 and 6.10 for more detail.

Values for the individual flux control coefficients for CPT I over ketogenic flux, calculated for control and treated hepatocytes, are summarised in Table 6.4. Only the flux control coefficient for the full combination model, where LPS+TNF α +IL6 were added during the hepatocyte preparation procedure, was different to that for untreated control hepatocytes.

$Untreated C_{CPTI}^{JASP}$	$LPS+TNF\alpha C_{CPTI}^{JASP}$	$LPS+TNF\alpha+IL6 C_{CPTI}^{JASP}$
0.53 ± 0.11 (n=3)	0.54 ± 0.04	0.99 ± 0.07

Table 6.4 Individual flux control coefficients for CPT I over rates of formation of ketone bodies (ASP) from palmitate in untreated control and treated hepatocytes

The individual flux control coefficient for untreated hepatocytes ($Untreated C_{CPTI}^{JASP}$) represents the mean of 3 flux control coefficients obtained from untreated hepatocyte preparations. Individual flux control coefficients for each treatment, ($LPS+TNF\alpha C_{CPTI}^{JASP}$ and $LPS+TNF\alpha+IL6 C_{CPTI}^{JASP}$) were calculated as appropriate, from the data shown in Figures 6.7-6.8 and 6.11-6.12, Equation 6.1 and the Simfit package (Bardsley, 1997) to determine tangents at zero inhibitor.

6.4 Discussion

6.4.1 The addition of agents during the cell isolation procedure

The first aim of the studies outlined in this chapter was to investigate the effect on hepatocyte yield and viability, of addition of LPS, TNF α and IL6, either singly or in combination during the isolation procedure. Although a full dose-response curve was not performed in the current investigation, the effect of ½ dose combination models was also investigated.

The significant decrease in cell yield seen with these agents, either singly or in combination (with the exception of ½ dose LPS+TNF+IL6 model) (Tables 6.2 and 6.3) suggested that they may have caused damage to a number of hepatocytes

during the cell preparation, such that they lost integrity and were lost during the isolation procedures. Kantrow *et al.*, (1997) found that following isolation of mitochondria in control and 'septic' groups, a mixed population of both injured and hyperfunctional mitochondria were found during sepsis (Kantrow *et al.*, 1997). However, from the current investigations it is unclear whether this procedure has resulted in the recovery of different populations of hepatocytes from control and treated groups.

Although other groups have found morphological differences between mitochondria/hepatocytes isolated from control or septic animals, including for example, enlargement of mitochondria with loss of matrix and cristae structure (Kantrow *et al.*, 1997; Patil *et al.*, 1998, Romeo *et al.*, 1999; Markley *et al.*, 2000), no changes in gross morphological features were found in the present study. This may indicate that the various models used in the current study, may reflect early biochemical changes, rather than the less subtle changes observed in other sepsis models, where changes in cell architecture become apparent. Additionally, studies by Young *et al.*, (1986) using hepatocytes isolated from neonatal rats, which had received an intraperitoneal injection of *E. Coli*, demonstrated that there was a marked variability in the degree of morphological alteration between adjacent hepatocytes. Currently, the timescale and sequence of such morphological changes is not fully understood. Changes may have occurred within the models discussed in this thesis, which were not detectable by the protocol used for the electron microscopy. However, it is possible that hepatocytes that were grossly morphologically different were lost during the isolation procedure, thus contributing to the decrease in cell yield. Thus any severely damaged hepatocytes were lost prior to experimentation and the differences between the control and treated groups, with respect to ketone body formation and/or CPT I activity, were minimized.

It is possible that the protocol used to isolate the hepatocytes may have affected the receptors for the cytokines and, therefore, may have altered the response of the hepatocytes to the cytokine challenge. Rofe *et al.*, (1987) have found, however, that hepatocytes isolated in this way are still responsive to adrenaline, which suggests that this is unlikely. As in the current study, these workers found no difference in cell viability, as assessed by trypan blue exclusion, between controls and TNF α treated groups.

Since under natural conditions a cell will rarely encounter single cytokines, the two

full dose combination models, LPS+TNF α and LPS+TNF α +IL6, were used to investigate the control exerted by CPT I over ketogenic flux in response to neonatal sepsis. These models attempted to mimic, in a controlled manner, the environment of the stressed hepatocyte, where the biological response reflects the various synergistic and antagonistic interactions of all the agents present. However, as is clear from Figure 6.1, there is a temporal difference in the appearance of LPS, TNF α and IL6 which would have been difficult to reproduce using this technique.

6.4.2 Ketone body production in hepatocytes exposed to LPS and/or cytokines during isolation

In the preliminary experiments assessing formation of [¹⁴C]ASP over time it was found that, in all cases (i.e. control and various treated groups), ketone body production was linear over time (Figure 6.4). [¹⁴C]ASP formation was, however, lower in the series of experiments where agents were used singly than in the series of experiments where agents were used in combination. Since these lower values were also obtained in the appropriate paired control groups, it is unlikely that it reflects an affect of the agents used. It is not clear why these values were low during these series of experiments. There was no significant difference between appropriate controls and any of the singly or combination treated groups over the 60min period. This is not in agreement with the results of Wannemacher *et al.*, (1979) where decreased concentrations of ketone bodies were found in response to sepsis. As discussed further in Chapter 7, the models developed in the present experiments mimic the biochemical changes which occur in the early stages of neonatal sepsis and some metabolic responses to sepsis, for example, changes in ketone body production may occur at later stages. However, I am unaware of any other studies in an equivalent neonatal rat model, which may support or refute this hypothesis.

It is clear, however, that there is much controversy in the literature regarding aspects of fatty acid metabolism in response to sepsis. In order to resolve some of the apparent discrepancies in these findings it is important to consider the following factors:

- at present, there is no single reliable marker for the severity of the septic response (Rosser *et al.*, 1998);
- the dose response in the whole animal is non-linear (Rosser *et al.*, 1998);

- the dose response pattern varies within the same model (Rosser *et al.*, 1996);
- there is considerable interspecies variation in response to endotoxin and variation in response to endotoxins from different bacteria in the same species (Horan *et al.*, 1989);
- the nutritional and hormonal status of the host and stage of infection may effect the results obtained (Vasconcelos *et al.*, 1987);
- the age of the host at onset of infection;
- individual cytokines, and different combination of cytokines, may have a wide variety of effects when added in isolation or combination (Vilcek, 1998). Physiologically, it is the sum of these interactive effects which determines the final consequences on hepatic metabolic regulation (Nachiappan *et al.*, 1994);
- the time period over which sepsis is reviewed and the time period of exposure to agents (Rosser *et al.*, 1998); and
- the effects observed are likely to be model dependent (Dahn *et al.*, 1995). Isolated organelles may not accurately reflect the conditions in the intact cell, due to loss of cytosolic factors, whilst cellular models may not reflect regional or systemic responses.

These points do not necessarily dismiss any particular experimental model as an inappropriate tool for modelling aspects of sepsis, rather they emphasize the caution which needs to be taken when interpreting/comparing the results from different model systems.

It is worth commenting on the choice of substrate (long-chain fatty acid, palmitate) used in the studies reported here, since previous chapters have discussed the importance of diet in the neonatal period (during which time diet is low in carbohydrate, high in fat) where a significant proportion of fatty acids present are of medium-chain length. Palmitate was used in these studies to provide a simple comparison with the studies presented in Chapter 3 and those published in the literature. As discussed in Chapter 8, it is anticipated that the studies presented here will be repeated in the presence of a more physiological mix of fatty acids, similar to that used in the studies reported and discussed in Chapter 5.

6.4.3 BUCA in LPS+TNF α or LPS+TNF α +IL6 treated hepatocytes isolated from suckling rats

Since the values for the flux control coefficients calculated in this chapter depend on CPT I activity and ketogenic flux (Equation 6.1) it is interesting to compare these aspects in each combination model investigated. Considering CPT I activity first: Figure 6.5 demonstrated the similarity between the inhibition curves for CPT I activity in the control and LPS+TNF α treated groups. CPT I activity in the absence of etomoxir was not significantly different between control and LPS+TNF α -treated groups. The inhibition curves for CPT I activity in control and LPS+TNF α +IL6 treated groups (Figure 6.9) demonstrates that here, as in the previous combination model, the inhibition curves for CPT I activity in control and LPS+TNF α +IL6 treated groups were similar in shape and no significant difference was found in CPT I activity between the two groups in the absence of etomoxir. However, the activity of CPT I in LPS+TNF α +IL6-treated groups is significantly less inhibited by maximal etomoxir than control groups.

The inhibition curves for [14 C]ASP formation in the control and LPS+TNF α -treated groups (Figure 6.6) were almost superimposable. This was to be expected from the time-series experiments, which indicated no significant differences in flux to ketone bodies between control and LPS+TNF α -treated groups and since ketogenic flux was linear for control and LPS+TNF α -treated groups over the course of the experiment (Figure 6.4). Figure 6.10 shows the inhibition curves for [14 C]ASP formation in control and LPS+TNF α +IL6-treated groups, which, as with the previous combination model, were almost superimposable in the two groups. Again, this was as expected, since a series of time course experiments also indicated no significant differences between flux to ketone bodies in control and LPS+TNF α +IL6 treated groups and flux was linear in both control and treated groups over the course of the experiment (Figure 6.4).

The mean flux control coefficient for CPT I over ketogenic flux in untreated hepatocytes isolated from suckling rats ($C_{CPTI}^{JASP, Untreated}$) was 0.53 ± 0.11 (Table 6.4). This value was lower than that obtained in an equivalent adult system ($C_{CPTI}^{JASP} = 0.85 \pm 0.20$, Drynan *et al.*, 1996). This supports the conclusions drawn from the study presented in Chapter 3, where the low values for the flux control coefficients in suckling rats suggested that the level of control exerted by CPT I over ketogenic flux

in suckling rats, was lower than that found in the equivalent adult system (Drynan *et al.*, 1996) (Figure 6.13).

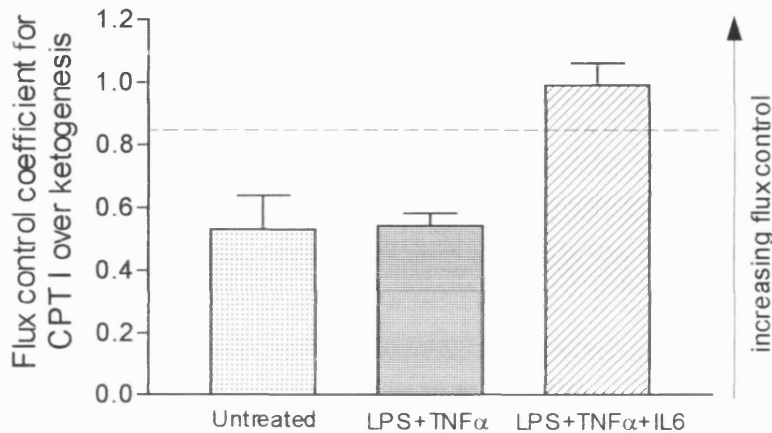


Figure 6.13 Comparison of flux control coefficients for CPT I over ketogenesis in untreated control, LPS+TNF α - or LPS+TNF α +IL6-treated hepatocytes isolated from suckling rats

The three bars represent the individual flux control coefficients for CPT I over ketogenesis in hepatocytes isolated from suckling rats. The dashed line indicates the value of the flux control coefficient obtained in an equivalent (untreated) adult system (Drynan *et al.*, 1996).

The value of the flux control coefficient for CPT I over ketogenesis in the LPS+TNF α treated group was calculated to be ${}^{LPS+TNF\alpha}C_{CPTI}^{JASP} = 0.54 \pm 0.04$. Again, this is lower than that obtained in the equivalent coefficient found in the adult (untreated) group (Table 6.4, Figure 6.13) and comparison of this coefficient with that obtained from the untreated controls, suggests that exposure to this combination of agents did not effect the potential of CPT I to control ketogenic flux in suckling rats. However, the value of the flux control coefficient for CPT I over ketogenesis in the LPS+TNF α +IL6 treated group was calculated to be ${}^{LPS+TNF\alpha+IL6}C_{CPTI}^{JASP} = 0.99 \pm 0.07$. As illustrated in Figure 6.13, this value is greater than that found in the untreated control group, the previous combination *in vitro* model and that found in the adult (untreated) system. These results suggest that the potential of CPT I to control ketogenesis changes when hepatocytes have been exposed to certain combinations of agents involved in

the septic response. In the 'full combination' model, which is likely to be more representative of the complex situation which occurs *in vivo* during sepsis, the contribution of CPT I to control ketogenic flux is increased, such that almost all of the control over ketogenic flux is situated at the level of CPT I (New *et al.*, 2000). Whilst it is possible to state that under these conditions CPT I is 'rate-controlling' for ketogenesis, it is still inappropriate to describe it as 'rate-limiting', since a full control analysis on all the steps of the pathway has not been performed and there may be the potential for other steps to exert negative control. The results presented here provide a quantitative assessment of the control exerted by CPT I over ketogenesis, and support the conclusions drawn by Wannemacker *et al.*, (1979), which suggested the importance of CPT I in controlling ketogenesis in sepsis.

6.4.4 Factors affecting the capacity of CPT I to control flux in response to cytokines and LPS

As discussed in Chapter 3, a variety of factors may be responsible for the changes in the values for the flux control coefficient for CPT I over ketogenesis and these may also apply in the treated and untreated groups considered in this chapter. In particular, sepsis and endotoxin/LPS have been implicated in changes in liver mass (Pedersen *et al.*, 1989; Jepson *et al.*, 1986) and hepatocyte volume (Brosnan *et al.*, 1994). Guzmán and co-workers (1994) have found that CPT I activity in hepatocytes isolated from adult rats is affected by changes in hepatocyte volume.

Although no changes in the gross morphology of the treated hepatocytes compared with untreated controls were found in either the LPS+TNF α or the LPS+TNF α +IL6 models considered in this chapter (Section 6.4.1), others, using proliferating rat liver cells have found that LPS exposure caused changes in cell morphology resulting in loss of cell architecture, with enlargements and distortion of mitochondria (Vergani *et al.*, 1999). Such changes in cell morphology in cultured liver cells, following exposure to LPS (Vergani *et al.*, 1999), may be reflected by changes at the cell surface, for example, with large-scale blebbing or ruffles, which may also indicate damage to the cytoskeleton (Pagani *et al.*, 1981, 1987, 1993). This would effect the microenvironment of CPT I, since it has been shown that CPT I may interact with cytoskeleton components (Velasco *et al.*, 1996). Whilst the precise nature of these interactions is currently incompletely understood, Velasco and co-workers have suggested that CPT I activity may be dependent on mitochondrial shape, and therefore, interactions reflect a physical phenomenon. Alternatively, they suggest

that CPT I activity may be modulated by specific interactions between CPT I and regulatory cytoskeleton components. Whatever their precise nature, it is likely that the kinetics of CPT I and its contribution to control pathway flux would be altered.

Furthermore, it is possible that the various agents added during hepatocyte isolation may interact directly with CPT I to alter its membrane environment, and may also modify the concentration of effectors within the cell. This would then modify the functional capacity of CPT I as discussed previously in this and other chapters. The work of Memon *et al.*, (1992) and other groups, suggested that cytokines raise hepatic malonyl-CoA levels. An intramuscular injection of LPS, for example, was found to increase malonyl-CoA from the control concentration of 2.31 ± 0.23 to 5.67 ± 0.88 nmol (g liver)⁻¹ in the injected rats. This would result in increased inhibition of CPT I and would divert long-chain fatty acids towards esterification (McGarry *et al.*, 1980). This would be predicted to have the effect of increasing the flux control coefficient for CPT I over flux from long-chain fatty acids to ketone bodies. In the present studies, malonyl-CoA concentrations were not assessed in either treated or control groups and so it is not possible to comment further on this effector.

Since the Summation Theory of MCA (Kacser and Burns, 1979) states the sum of all of the flux control coefficients in a pathway is 1, any change in the value of the flux control coefficient for CPT I under these conditions, must also lead to changes in the values of flux control coefficients for other enzymes in the pathway, such as mHMG-CoA synthase. Since the calculated value for the flux control coefficient for CPT I over ketogenic flux was increased in the LPS+TNF α +IL6 treated model, this suggests that the control exerted by other steps in the pathway has decreased, although without a more detailed control analysis, some caution needs to be applied to such interpretations.

6.4.5 Conclusions

Data obtained from models of adult sepsis cannot be extrapolated to model the neonatal condition, since the multiple metabolic derangements observed in adult septic models may not reflect the response of the neonate or infant with severe infection. This may result from differences in the way neonates mount an appropriate immunological response and to the presence of different intestinal

microbial flora in infants compared to adults. The development, therefore, of models appropriate for this age-group is important. The models used in this thesis may be suitable tools for further investigation of the morphological and biochemical changes in neonates, in response to cytokine treatment, over time and in response to dose.

Whilst it is important to keep in mind the complex interactions between cytokines and the type of experimental system used before extrapolating to the human situation, it is clear from these results that 'control' over pathway flux is not a static property. The work presented in this chapter demonstrates that the distribution of control in a pathway may change: in this instance, the control structure changes when hepatocytes are challenged with a variety of agents involved in the septic response and under these conditions, the potential of CPT I to control ketogenic flux is increased such that CPT I may be described as 'rate-controlling'. Furthermore, the work presented in this chapter also provides further support for one of the basic concepts of MCA, that of multi-step control (Fell *et al.*, 1995), as discussed in Section 1.4.3

The *in vitro* models of neonatal sepsis presented in this chapter are further characterised in the following chapter, which investigates oxygen consumption hepatocytes in response to LPS and/or cytokine challenge.

Chapter 7

Effects of lipopolysaccharide and/or cytokines on neonatal oxidative liver metabolism

7.1 Introduction

In the previous chapter, the effects of LPS, TNF α , or combinations of agents, LPS+TNF α , LPS+TNF α +IL6 on the results of the hepatocyte isolation procedure and the effects of the 'combination models' on the potential of CPT I to control ketogenic flux were discussed. In this chapter, I will focus on the effect of these agents on hepatocyte respiration to further characterise these *in vitro* models of neonatal sepsis.

Many investigations into the effects of sepsis concentrate on adults and extrapolate the resulting conclusions to neonates. This is not necessarily appropriate: the work in previous chapters has demonstrated that control of hepatocyte metabolism changes during development. It has also been shown that, in a perfused liver system, rates of oxygen consumption do not remain constant throughout development (Mollica *et al.*, 1998). These workers suggest that in rats, basal oxygen consumption gradually decreases with age, which could be a reflection of:

- (i) lower energy requirements;
- (ii) a decreased supply of substrate to the electron transport chain and/or
- (iii) age-dependent decrease in respiratory chain activity.

The efficiency of mitochondrial respiration in the liver has also been found to change with age. Lionetti *et al.*, (1998) found that during the transition from weaning to adulthood in the rat, there was no increase in phosphorylation, although the substrate oxidation pathway was stimulated and there was an increased cytochrome content. Furthermore, as discussed in the literature review in Chapter 1, there are also modifications of the hepatic mitochondrial compartment immediately following birth, such as decreased mitochondrial volume and an increased number of mitochondria per hepatocyte (Rohr *et al.*, 1971; Herzfeld *et al.*, 1973; Valcarce *et al.*, 1988). Thus, even without the complications caused by illness or infection, oxidative liver metabolism is different in neonates compared to adults.

Considering the situation in response to sepsis, Townsend *et al.*, (1986) used an animal model of peritonitis where rats underwent caecal ligation and puncture

(CLP). They found that mitochondrial function in immature rats was less tolerant to severe intra-abdominal infection than adults. Furthermore, Powis *et al.*, (1997) and Turi *et al.*, (unpublished data) have recently shown that human neonates have a different metabolic response to sepsis and/or trauma than adults.

7.1.1 Mitochondrial oxygen consumption

H₂O and CO₂ are products of respiration and, as discussed in Chapter 1, the Krebs cycle can account for the formation of CO₂. Within mitochondria the reduction of O₂ to H₂O accounts for the 'consumption' of oxygen. This occurs via the reactions of the respiratory chain.

The respiratory chain is a complicated multi-part structure, composed of a number of assemblies containing strongly interacting proteins and centres capable of undergoing cyclic reduction and oxygenation. These assemblies (complexes) are situated in the inner mitochondrial membrane, which is composed of approximately 30% lipid and 70% protein. A significant proportion of the protein fraction of the inner membrane is concerned with the reactions of the respiratory chain. For example, in bovine heart mitochondria, the enzyme systems that catalyse oxidative phosphorylation comprise approximately 50% of the inner membrane protein and the remaining protein fraction includes various transport proteins and enzymes with functions that relate to electron transfer as part of the respiratory chain (reviewed in Hatefi, 1985).

Many workers have contributed to the understanding of these components, which are shown schematically in Figure 7.1. The composition and function of each of the enzyme complexes of the mitochondrial oxidative phosphorylation system is summarised in this section.

Complex I (NADH:ubiquinone oxidoreductase, E.C. 1.6.5.3) contains approximately 42 polypeptides (Skehel *et al.*, 1998) which can be divided into three groups: (i) a water-soluble iron-sulfur protein fraction; (ii) a water-soluble iron-sulfur flavoprotein fraction; and (iii) an insoluble hydrophobic fraction which surrounds the other two groups (reviewed in Hatefi, 1985).

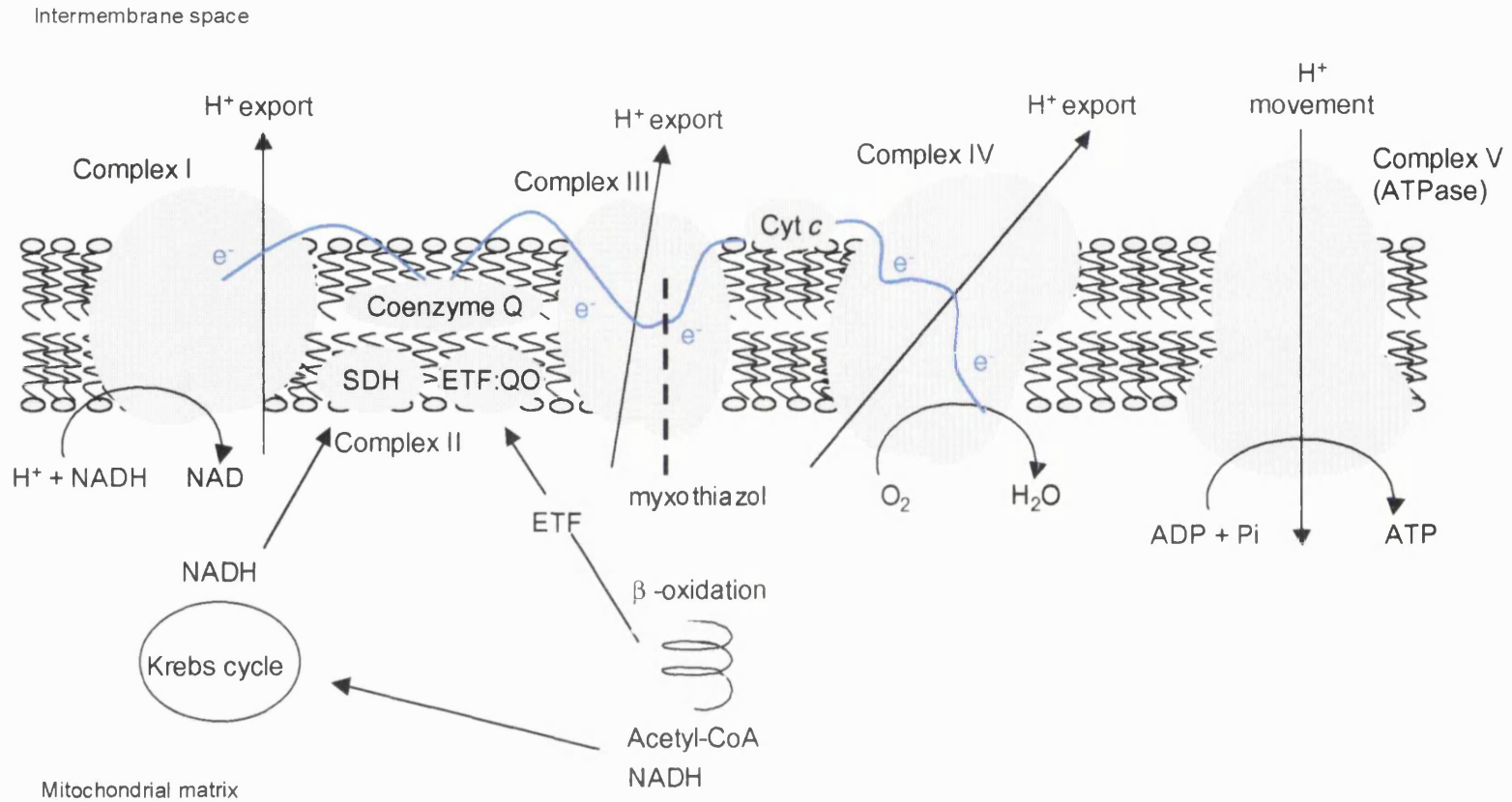


Figure 7.1 Schematic arrangement of the ATPase, the complexes of the respiratory chain and association of proton pumping

The complexes of the respiratory chain are closely associated with the mitochondrial inner membrane. At three stages along the respiratory chain, complexes I, III and IV, oxidative energy is conserved *via* proton translocation and creation of an inner membrane electrochemical potential. Oxygen is the ultimate electron acceptor. Myxothiazol blocks electron transport within Complex III of the respiratory chain (Thierbach *et al.*, 1981).

The non-protein components of this complex include phospholipids, flavin mononucleotide (FMN), which acts as the initial electron-accepting group, several iron-sulfur clusters, which are also involved in electron carrying and co-enzyme Q (also known as ubiquinone). Ubiquinone accepts reducing equivalents from Complex I. The reduction of ubiquinone is coupled to outward, transmembrane proton translocation (Figure 7.1).

Ubiquinone also acts as a 'collecting point' for reducing equivalents derived from succinate, and the transfer of electrons from succinate to ubiquinone is catalysed by Complex II. The major component of complex II is succinate dehydrogenase (succinate:ubiquinone oxidoreductase, E.C. 1.3.5.1, SDH Figure 7.1), which is present in all aerobic organisms as a membrane bound enzyme of the Krebs cycle. Complex II is composed of four polypeptides and is associated with iron-sulfur clusters and FAD, which act as electron carriers (reviewed in Hatefi 1985).

The transfer of electrons from reduced ubiquinone (ubiquinol) to cytochrome *c* is catalysed by complex III (ubiquinol-cytochrome *c* reductase, E.C. 1.10.2.2), and this reaction is coupled to outward transmembrane proton translocation (Figure 7.1). This translocation of protons is linked to electron transfer *via* the protonmotive Q-cycle, originally proposed by Mitchell (1976). Complex III comprises 9-10 proteins, three of which are associated with redox centres: cytochromes *b* and *c*, as well as an iron-sulfur protein (reviewed in Hatefi 1985).

Myxothiazol, an antibiotic produced by the myxobacterium *Myxococcus fulvus*, binds stoichiometrically to cytochrome *b*, thereby blocking ubiquinol reoxidation and the entire respiratory chain (Figure 7.1) (Becker *et al.*, 1981). Since it blocks the respiratory chain, myxothiazol provides an experimental tool to investigate the relative contributions of mitochondrial and non-mitochondrial oxygen consumption, to total cellular oxygen consumption. From investigations using mitochondria and submitochondrial particles, Thierbach and co-workers (1981) found that although myxothiazol shares some features with the inhibitor antimycin, for example, the same number of binding sites, these binding sites are not identical.

The terminal unit of the mitochondrial electron transport chain is complex IV. Within this unit, the transfer of electrons to molecular oxygen is catalysed by cytochrome *c* oxidase (E.C. 1.9.3.1). The final step of electron transfer from cytochrome a_3 to oxygen may be regarded as the only reaction of the respiratory chain that is not

reversible, since the K_m for oxygen is very low, and as a result the equilibrium of the system is displaced towards electron transport (and thus in the direction of ATP synthesis). Outward transmembrane proton translocation also occurs at this complex (Figure 7.1).

It can be seen, therefore, that as electrons are transferred along the respiratory chain, hydrogen ions are exported from the mitochondrial matrix across the inner membrane into the intermembrane space. This generates both a proton concentration gradient across the membrane (ΔpH) and a charge separation ($\Delta\phi$), which together constitute the protonmotive force (PMF). Mitchell *et al.*, (1966) developed the chemiosmotic theory, which indicated that respiration and proton translocation are obligatory within respiratory chain systems. They stated that the free energy stored within the electrochemical gradient is harnessed by the H^+ -transporting ATP-synthase (E.C. 3.6.1.34), which allows protons back into the mitochondrial matrix and utilizes their energy for the formation of ATP from ADP and phosphate. Thus the highly active ATPase, which is a component of Complex V, generates ATP from ADP and inorganic phosphate at the expense of protonic energy derived from the respiratory complexes I, III and IV (Figure 7.1). This catalytic region of Complex V is also known as the F_1 segment, which is linked by a 'stalk region' to F_0 , the membrane segment, which is concerned with inward transmembrane proton translocation.

The PMF also provides the energy for the translocation of ions and other metabolites across the inner mitochondrial membrane. Additionally, some of the PMF can dissipate without protons passing through the H^+ -transporting ATP-synthase. Thus mitochondrial oxidative phosphorylation can be uncoupled from ATP formation, leading to increased oxygen consumption. This proton-cycle or 'leak' reaction can be stimulated by uncouplers such as dinitrophenol or carbonyl cyanide p-trifluoromethoxyphenylhydrazone (FCCP), which act to increase the permeability of the mitochondrial membrane to protons and by physiologically regulated uncoupling proteins, such as uncoupling proteins 1-3. The mitochondrial proton leak may be an important component of the reactions making up the standard metabolic rate and it has been suggested that differences in proton leak may partly explain the differences in standard metabolic rate between mammals of different body mass (Porter *et al.*, 1993). In isolated rat liver cells, it has been shown that (non-phosphorylating) proton-cycling processes make a significant contribution to cellular respiration and its control (Brown *et al.*, 1990) and in the

absence of ATP synthesis, the proton leak is a major determinant of respiration rate, with a large flux control coefficient of 0.7 (Brand *et al.*, 1988). When ATP synthesis occurs, proton flux through the leak decreases and the flux control coefficient also decreases (Groen *et al.*, 1982, Hafner *et al.*, 1990). In isolated hepatocytes 20-40% of the respiration rate may be involved in driving the proton leak and direct heat production, rather than ATP synthesis (Nobes *et al.*, 1990). More recently, Rolfe *et al.*, (1999) have calculated that the proton cycle accounts for 15% of the metabolic rate in the liver, which although lower than previous figures derived from work in hepatocytes, supports the hypothesis that the cycle has a significant contribution to the metabolic rate.

Incomplete reduction of oxygen may occur at multiple sites in the inner mitochondrial membrane. As a result mitochondria are a source of reactive oxygen species (ROS) such as hydrogen peroxide H_2O_2 , hydroxyl radicals $OH\bullet$, and superoxide radicals O_2^- . For example, ROS can be generated from complex III of the mitochondrial ETC, where ubisemiquinone formed by ubiquinone oxidation can react directly with molecular oxygen to form O_2^- (Dawson *et al.*, 1993). Intracellular components are protected from the adverse effects of ROS by a number of endogenous ROS scavenging enzymes, however, as discussed in the previous chapter, oxidative stress may occur where there is an imbalance between ROS production and antioxidant activity. ROS are capable of producing tissue injury during endotoxic shock by initiating lipid peroxidation, and damage to protein components of the mitochondria and DNA, which may affect the oxidative capacity and production of ATP (Portolés *et al.*, 1993; Taylor *et al.*, 1995).

7.1.2 Non-mitochondrial oxygen consumption

It has been estimated that 90% of the oxygen consumed by aerobic organisms participates in the di-oxygen chemistry of cytochrome *c* oxidase and becomes reduced to water in the terminal step of respiration, within mitochondria (Chan *et al.*, 1990). However, extra-mitochondrial pathways may also be involved in the consumption of oxygen including, for example, the reactions of the cytochrome P_{450} family of enzymes. These mixed-function oxidases are found within the endoplasmic reticulum of many animal and plant tissues and are so termed due to the ability of their reduced forms to strongly absorb light at 450nm. Cytochrome P_{450} enzymes have been implicated in the oxidative detoxification of a huge variety of both endogenous and xenobiotic compounds (Figure 7.2).

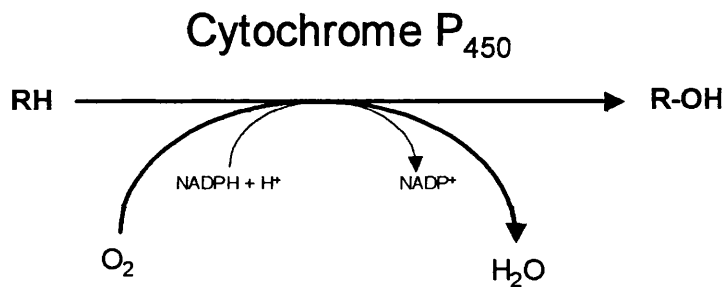


Figure 7.2 Hydroxylation by cytochrome P₄₅₀

Generalised hydroxylation reaction catalysed by cytochrome P₄₅₀. The product R-OH has greater solubility in water and may, therefore, be more readily excreted. This family of enzymes therefore have important roles in cellular detoxification.

This family of enzymes catalyse the hydroxylation reactions in which an organic substrate RH is hydroxylated to R-OH, at the expense of one molecule of O₂ (Figure 7.2) whilst the other is reduced by reducing equivalents formed by NADH or NADPH. This hydroxylation process renders compounds more soluble, therefore forming a vital step in their detoxification and excretion. Whilst many tissues, for example, kidney, lung and intestine contain members of the cytochrome P₄₅₀ family, the mammalian liver is the major site of cytochrome P₄₅₀ mediated metabolism of endogenous and exogenous compounds. Multiple forms of cytochrome P₄₅₀ have been purified from rat liver (Lu, 1980) and in the human liver, there are at least 12 distinct P₄₅₀ enzymes (Nebert *et al.*, 1991). Different forms have different substrate specificities and closely related P₄₅₀ enzymes may participate in the same reaction.

Oxygen consumption may also occur within peroxisomes, which have important functions in cellular metabolism. One function of peroxisomal respiration is to dispose of excess reducing equivalents, which is done without the conservation of energy as ATP and is therefore thermogenic. Additionally, peroxisomes protect cells against the toxic effects of hydrogen peroxide, by compartmentalising its decomposition by catalase (Lazarow, 1987). These reactions are summarised in Figure 7.3.

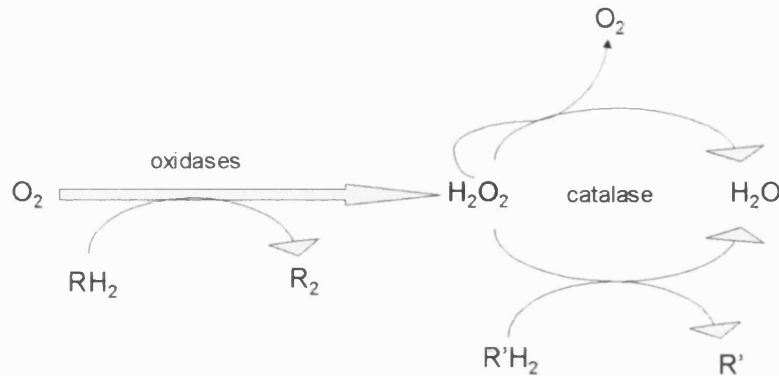


Figure 7.3 Schematic representation of peroxisomal respiration

Adapted from de Duve and Baudhuin (1966). The pathway is based on the formation of hydrogen peroxide by a collection of oxidases and the decomposition of the hydrogen peroxide by catalase (catalytic action, top part of figure, peroxidatically, lower part of figure).

From Figure 7.3 it can be seen that hydrogen peroxide is a key intermediate in peroxisomal oxidative metabolism, being produced *via* reactions of the general type $RH_2 + O_2 \rightarrow R + H_2O_2$, which are catalysed by a variety of type II oxidases. The resulting hydrogen peroxide may be removed a peroxidative mode, where it is reduced to water using electrons derived from an organic donor. Alternatively, *via* a catalytic method, one molecule of hydrogen peroxide may be oxidized whilst a second is reduced: $H_2O_2 + H_2O_2 \rightarrow O_2 + 2H_2O$. This second reaction has the net result of removal of hydrogen peroxide and the evolution of oxygen.

7.1.3 Total cellular oxygen consumption

From the brief account considered in the previous sections, it can be seen that total cellular oxygen consumption can be considered to have two components:

- (i) a mitochondrial component, where O_2 is consumed for the production of either ATP (phosphorylation) or heat (proton leak); and
- (ii) non-mitochondrial processes, which are mainly concerned with detoxification (Figure 7.4)

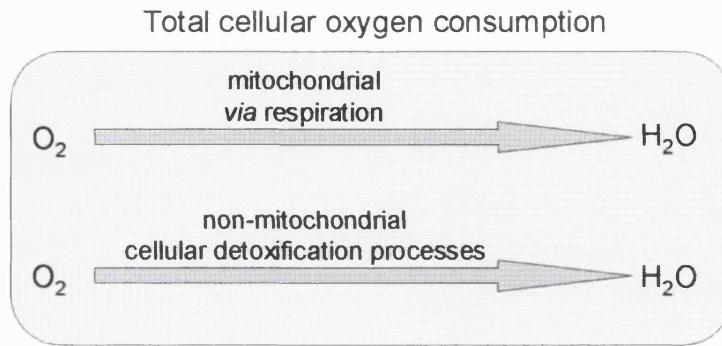


Figure 7.4 Summary of total oxygen consumption

Both of these pathways consume oxygen and ultimately yield water. Any investigation into cellular oxygen consumption should, therefore, investigate the relative contributions of each of these fractions. The careful use of inhibitors such as myxothiazol, provide a means of distinguishing between these different components.

7.1.4 Oxygen consumption during sepsis

There are conflicting reports on the effects of sepsis on cellular respiration. For example, mitochondrial respiration has been reported to be unchanged, inhibited or stimulated in response to sepsis (reviewed in Singer *et al.*, 1999). The differences in reported observations may be due to the reasons discussed in Sections 6.1.3 and 6.4.2. It is clear, however, that there are abnormalities in cellular respiration during sepsis and the mechanisms by which the changes occur have been the subject of numerous investigations. For example, in an adult rat model of sepsis, Kantrow *et al.*, (1997) found that liver mitochondria isolated from a rat caecal ligation and puncture (CLP) model of sepsis included uncoupled mitochondria with abnormal structure and defective ETC. In addition, they found cellular respiration was decreased in hepatocytes in cells isolated during sepsis, with apparent dysfunction of complex II (succinate dehydrogenase). This supported the earlier work of Taylor *et al.*, (1995) who, in a similar adult rat model, had found that OH^- and H_2O_2 production were greater in mitochondria isolated from the livers of septic rats compared to the sham-operated controls. Since these effects of 'sepsis' were enhanced by FAD-linked but not NAD-linked substrates, this implicated Complex II

of the ETC. Kantrow and co-workers (1997) suggested that it was possible that these reactive species may cause damage to mitochondrial constituents and other cellular structures. Furthermore, increased ROS may result in increased mitochondrial permeability and account for the mitochondrial swelling which has been observed by some groups during sepsis. From work using mouse fibrosarcoma cells, Schulze-Osthoff and co-workers (1992) found that TNF α activated ROS production in mitochondria at the ubisemiquinone site in addition to causing changes in the mitochondrial ultrastructure, which included clumping of mitochondrial cristae.

From investigations in rats, where sepsis was established by CLP, Astiz *et al.*, (1988) suggested that despite the maintenance of systemic blood flow and tissue oxygenation, cellular energy metabolism was affected early in the course of severe sepsis. Rosser *et al.*, (1998) found that an initial rise in oxygen consumption rate was observed in cultured hepatocytes exposed to endotoxin compared to untreated controls. Within 24 hours, however, there was a significant decrease in oxygen consumption in the sepsis group.

This is consistent with other studies, which have suggested that there are two main states of sepsis. These are discussed in Mela-Riker *et al.*, (1992) and can be summarised as follows:

- (i) the initial state, State A, is characterised by increased heart rate, cardiac index, improved myocardial contractility and increased whole body oxygen consumption. It is typical of a "normal" stress response seen in compensated sepsis and/or after trauma or major surgery;
- (ii) state B represents a more advanced stage, which, although hypermetabolic, with increased cardiac index and heart rate, has decreased systemic vascular resistance and decreased whole body oxygen consumption.

However, there is some uncertainty as to whether the hypermetabolic response to sepsis observed in adults (Plank *et al.*, 1998) also occurs in infants and children (Turi *et al.*, in press). There are few investigations into neonatal sepsis in the literature which investigate the temporal changes occurring in sepsis, or which specifically investigate the changes occurring during State A, the early stage of sepsis.

7.1.5 Reye's Syndrome

Reye's Syndrome (RS) is a rare but serious disorder, typically affecting children and adolescents. It may lead to coma, convulsions and death. Although the precise aetiopathogenesis is unknown, it is apparent that infection/endotoxin stimulation, together with aspirin consumption, are risk factors for initiating the cascade of events that culminates in RS (Green *et al.*, 1992). TNF α has also been implicated in this syndrome, and endotoxin, viral infection or ingestion of aspirin stimulate TNF α production (Cooperstock *et al.*, 1975; Larrick *et al.*, 1986).

At present the only specific diagnostic marker of RS is electron microscopy of liver biopsy tissue, which shows gross ultrastructural changes, including proliferation of smooth endoplasmic reticulum, loss of glycogen, proliferation of peroxisomes, decrease in number of the mitochondria and mitochondrial damage including enlarged, irregularly shaped mitochondria, which are less electron-dense. Tonsgard (1989) mimicked these morphological changes by exposing isolated mitochondria to serum from RS patients and found that the serum demonstrated similar effects to dinitrophenol, an uncoupler of oxidative phosphorylation. Both RS and aspirin poisoning (salicylate intoxication) lead to increased oxygen consumption and it has been found that at low concentrations and physiological pH, salicylic acid functions as a proton carrier (Gutknecht, 1992) supporting the earlier reports of the uncoupling effects.

Although the incidence of RS has greatly declined in recent years, which is believed to be due to public and professional warnings about aspirin (and aspirin containing products), the withdrawal of paediatric aspirin formulations (Green *et al.*, 1992) and increased diagnostic awareness of inherited disorders of metabolism, which frequently have similar clinical presentations (Rowe *et al.*, 1988), the serious nature of RS warrants continued investigation. This disease principally occurs in childhood, however, animal models in the literature are frequently based on adult animals and the resulting conclusions extrapolated to neonates.

7.1.6 Aims of this section

From the introduction to this chapter, it can be seen that the multiple metabolic derangements observed in adults both *in vivo* and in some *in vitro* septic models, may not reflect the response of neonates or infants and, therefore, it is not possible to extrapolate conclusions drawn from adults to the paediatric population. It is

important, therefore, to investigate changes in oxidative metabolism during sepsis in neonates. In the studies in this chapter, therefore, I aimed to explore the effect of LPS, TNF α , or a combination of agents, (LPS+TNF α ; LPS+TNF α +IL6) on total respiration and on the relative contributions of mitochondrial and non-mitochondrial respiration, as assessed by myxothiazol-resistant oxygen consumption, in hepatocytes isolated from suckling rats. In this manner, I aimed to characterise further the *in vitro* models of sepsis introduced in the previous chapter. An additional aim of the studies in this chapter was to investigate the effects of salicylic acid in an *in vitro* model of neonatal sepsis.

7.2 Results

In the literature, data is presented either in terms of cell number or dry mass. For ease of reference, both types of analysis are provided here. Table 7.1 summarises the effect of LPS and/or various cytokines on the absolute rates of oxygen consumption, expressed in terms of nmol O₂ min⁻¹ (10⁶ viable cells)⁻¹ whilst Table 7.2 summarises the effect of LPS and/or various cytokines on the absolute rates of oxygen consumption, expressed in terms of nmol O₂ min⁻¹(mg dry mass)⁻¹.

7.2.1 Effect of LPS on hepatocyte respiration

As shown in Tables 7.1 and 7.2, there were no significant differences in oxygen consumption between controls and LPS treated cells, with and without myxothiazol and whether the data is expressed per cell number or dry mass.

7.2.2 Effect of TNF α on hepatocyte respiration

As shown in Tables 7.1 and 7.2, there were no significant differences in total oxygen consumption between controls and TNF α treated cells whether the results were expressed per cell number or dry mass. However, when non-mitochondrial oxygen consumption was expressed in terms of number of cells, there was a significant increase in the treated group, compared to controls (p<0.05).

Agent added during hepatocyte isolation	Total oxygen consumption (nmol O ₂ min ⁻¹ (10 ⁶ viable cells) ⁻¹)			Non-mitochondrial oxygen consumption (nmol O ₂ min ⁻¹ (10 ⁶ viable cells) ⁻¹)		
	Control	Treated	<i>p</i>	Control	Treated	<i>p</i>
LPS (n=3)	2.18±0.27	2.70±0.61	NS	1.21±0.03	1.01±0.20	NS
TNF α (n=3)	2.66±0.24	3.02±0.38	NS	1.05±0.23	1.35±0.21	<i>p</i> <0.05
LPS+TNF α (n=6)	2.04±0.16	2.95±0.39	<i>p</i> <0.05	0.81±0.05	1.61±0.40	NS
½ LPS+TNF α (n=3)	2.24±0.50	2.14±0.44	NS	0.73±0.17	0.96±0.17	<i>p</i> <0.05
LPS+TNF α +IL6 (n=6)	2.44±0.21	2.80±0.32	<i>p</i> <0.05	0.93±0.09	1.64±0.26	<i>p</i> <0.05
½ LPS+TNF α +IL6 (n=4)	2.00±0.15	1.99±0.10	NS	0.83±0.11	0.79±0.11	<i>p</i> <0.05

Table 7.1 Effect of LPS and/or various cytokines on hepatocyte respiration expressed in terms of cell number

Control and treated oxygen consumption experiments were carried out in parallel. Values are presented as means \pm SEM, where n = number of preparations (e.g. n=4 indicates data from 4 parallel hepatocyte preparations). Results were analysed using the Student's paired *t*-test.

Agent added during hepatocyte isolation	Total oxygen consumption (nmol O ₂ min ⁻¹ (mg dry mass) ⁻¹)			Non-mitochondrial oxygen consumption (nmol O ₂ min ⁻¹ (mg dry mass) ⁻¹)		
	Control	Treated	<i>p</i>	Control	Treated	<i>p</i>
LPS (n=3)	2.46±0.41	2.66±0.60	NS	1.37±0.52	1.16±0.26	NS
TNF α (n=3)	2.54±0.23	1.90±0.41	NS	0.97±0.12	0.97±0.15	NS
LPS+TNF α (n=6)	1.83±0.20	2.30±0.27	NS	0.74±0.20	1.26±0.30	NS
½ LPS+TNF α (n=3)	2.14±0.42	2.05±0.57	NS	0.75±0.17	0.91±0.22	NS
LPS+TNF α +IL6 (n=6)	1.60±0.14	2.22±0.29	<i>p</i> <0.05	0.64±0.06	1.25±0.17	<i>p</i> <0.05
½ LPS+TNF α +IL6 (n=4)	2.17±0.17	1.97±0.21	<i>p</i> <0.05	0.94±0.16	0.77±0.10	NS

Table 7.2 Effect of LPS and/or various cytokines on hepatocyte respiration expressed in terms of dry mass

Control and treated oxygen consumption experiments were carried out in parallel. Values are presented as means \pm SEM, where n = number of preparations (e.g. n=4 indicates data from 4 parallel hepatocyte preparations). Results were analysed using the Student's paired *t*-test.

7.2.3 Effect of LPS+TNF α on hepatocyte respiration

The total oxygen consumption in cells treated with LPS+TNF α expressed per cell number was significantly greater than controls ($p < 0.05$) although where data is expressed per dry mass, the increase is not significant. As shown in Tables 7.1 and 7.2, there was no significant difference in non-mitochondrial oxygen consumption. The absolute rates of mitochondrial respiration in control and LPS+TNF α treated hepatocytes have been calculated from the mean of total oxygen consumption for a given experimental day minus the mean of oxygen consumption in presence of myxothiazol for a given experimental day. There was no significant difference in mitochondrial respiration between control and LPS+TNF α treated hepatocytes. Absolute values of intramitochondrial oxygen consumption was 1.22 ± 0.16 nmol O₂ min⁻¹(10⁶ viable cells)⁻¹ for controls and 1.34 ± 0.36 nmol O₂ min⁻¹(10⁶ viable cells)⁻¹ for treated cells. Analysis by dry weights results in absolute values of control intramitochondrial oxygen consumption was 1.08 ± 0.19 nmol O₂ min⁻¹(mg dry mass)⁻¹ and treated group intramitochondrial oxygen consumption was 1.03 ± 0.27 nmol O₂ min⁻¹(mg dry mass)⁻¹

It should be noted that the errors stated in the above section may not necessarily reflect the true errors, since intramitochondrial oxygen consumption is a derived figure, as stated above. An alternative approach would be to calculate the combined errors on the means, using the following equations:

$$\text{Equation 7.1} \quad se(diff) = S \sqrt{\frac{1}{n_1} + \frac{1}{n_2}}$$

$$\text{Equation 7.2} \quad S = \sqrt{\frac{S_1^2(n_1 - 1) + S_2^2(n_2 - 1)}{n_1 + n_2 - 2}}$$

Whilst the above equations should strictly be used where there at least 20 observations in each group, this method enables the combined errors to be calculated. Since the sample sizes are smaller than 20, it is likely that the resulting errors may still not reflect the true errors, but are likely to provide reasonable estimates. Using this alternative approach to calculate errors, the results for

intramitochondrial oxygen consumption can be restated as: 1.22 ± 0.17 (control) compared with 1.34 ± 0.56 (treated) $\text{nmol O}_2 \text{ min}^{-1} (10^6 \text{ viable cells})^{-1}$, and 1.08 ± 0.21 (control), compared with 1.03 ± 0.30 (treated) $\text{nmol O}_2 \text{ min}^{-1} (\text{mg dry mass})^{-1}$. The conclusions remain unchanged: i.e. there is no significant difference in intramitochondrial oxygen consumption between control and LPS+TNF α -treated hepatocytes.

7.2.4 Effect of half dose LPS+TNF α on hepatocyte respiration

As shown in Tables 7.1 and 7.2, there were no significant differences in total oxygen consumption between controls and half dose LPS+TNF α treated cells whether the results were expressed per cell number or dry mass. However, when non-mitochondrial oxygen consumption was expressed in terms of number of cells, there was a significant increase in the treated group, compared to controls ($p < 0.05$).

7.2.5 Effect of LPS+TNF α +IL6 on hepatocyte respiration

Tables 7.1 and 7.2 and Figures 7.5(a) and (b) demonstrate that total oxygen consumption in cells treated with LPS+TNF α +IL6, whether expressed per cell number or per dry mass, was significantly greater than controls ($p < 0.05$). Although in the study presented here, I am interested in the effect of sepsis on 'populations' of hepatocytes (i.e. untreated *versus* sepsis) it is interesting to note the effects of this combination of agents in each paired hepatocyte preparation and for further information, total oxygen consumption in each paired hepatocyte preparation is shown in Figures 7.5 (c) and (d). Figures 7.5(a) and (b) also demonstrate that non-mitochondrial oxygen was also significantly greater in the treated group compared to controls using either method for expressing the results ($p < 0.05$).

The mitochondrial fraction of total oxygen consumption, calculated as described previously and reported in Figure 7.5(e) and (f), was not significantly different between controls and cells exposed to LPS+TNF α +IL6. Control intramitochondrial oxygen consumption was $1.52 \pm 0.25 \text{ nmol O}_2 \text{ min}^{-1} (10^6 \text{ viable cells})^{-1}$ Treated group intramitochondrial oxygen consumption was $1.15 \pm 0.24 \text{ nmol O}_2 \text{ min}^{-1} (10^6 \text{ viable cells})^{-1}$. Control intramitochondrial oxygen consumption was $0.96 \pm 0.10 \text{ nmol O}_2 \text{ min}^{-1} (\text{mg dry mass})^{-1}$ Treated group intramitochondrial oxygen consumption was $0.97 \pm 0.25 \text{ nmol O}_2 \text{ min}^{-1} (\text{mg dry mass})^{-1}$.

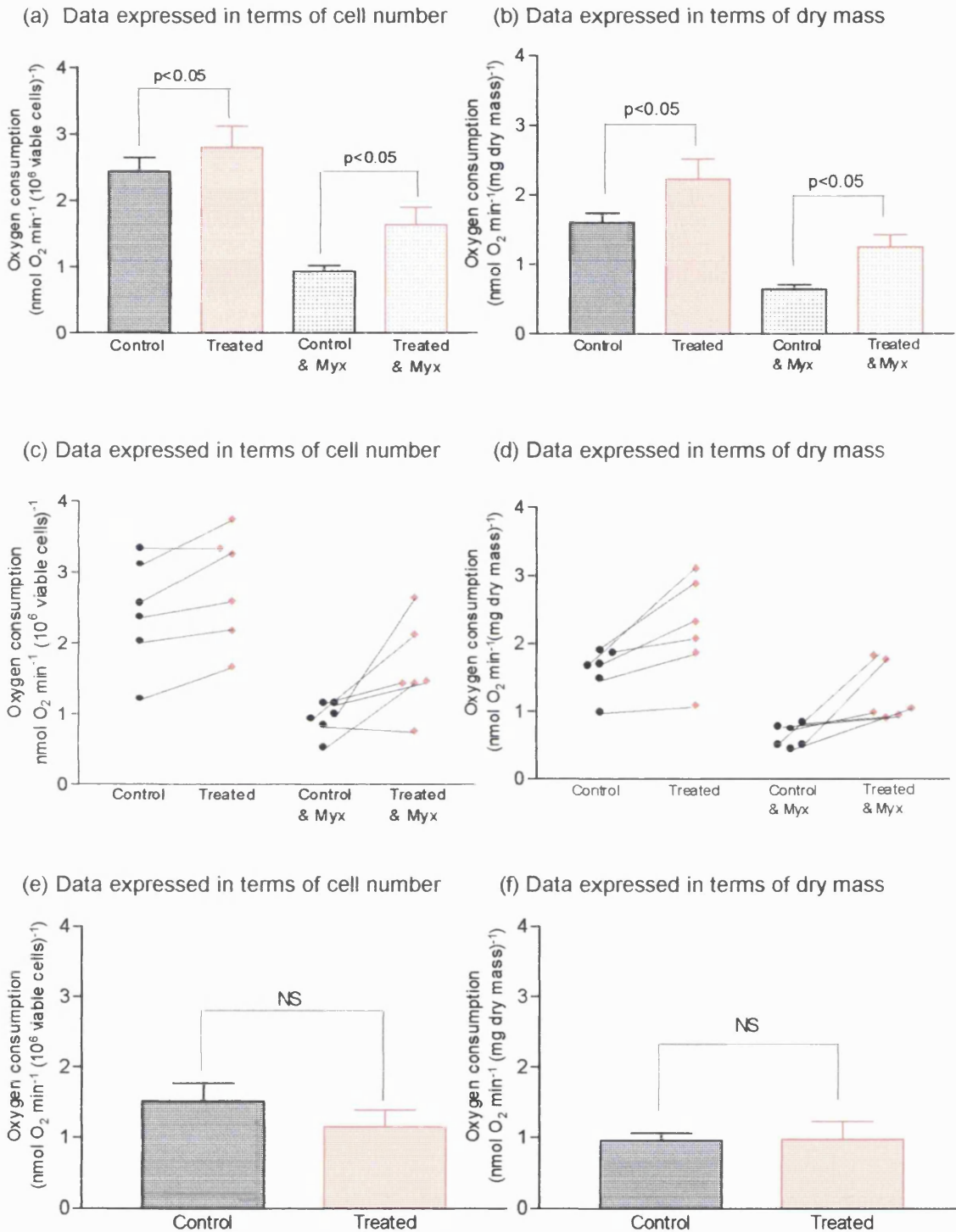


Figure 7.5 Total endogenous, non-mitochondrial and/or mitochondrial respiration of isolated hepatocytes from control and LPS+TNF α +IL6 treated groups

Control and treated oxygen consumption experiments carried out in parallel. In Figures (a), (b), (e) and (f) all individual data points from a particular experiment have been averaged, with these figures showing the mean of these averaged values \pm SEM, $n=6$ (ie from 6 parallel hepatocyte preparations). Figures (c) and (d) show the paired data sets for (a) and (b). Results were analysed using paired Student's t test. Note: 'treated' indicates LPS+TNF α +IL6 treated groups.

As before, errors on the derived intramitochondrial data can be re-calculated using equations 7.1 and 7.2. The restated figures are as follows: 1.52 ± 0.31 (control) compared with 1.15 ± 0.42 (treated) $\text{nmol O}_2 \text{ min}^{-1} (10^6 \text{ viable cells})^{-1}$ and 0.96 ± 0.15 (control) compared with 0.97 ± 0.35 (treated) $\text{nmol O}_2 \text{ min}^{-1} (\text{mg dry mass})^{-1}$. The conclusions remain unchanged: i.e. there was no significant difference in the control intramitochondrial oxygen consumption, compared with LPS+TNF α +IL6-treated cells.

7.2.6 Effect of half dose LPS+TNF α +IL6 on hepatocyte respiration

The effect of this combination of agents, at this lower dose, on total cellular and non-mitochondrial oxygen consumption was examined and has been reported in Tables 7.1 and 7.2. There was no significant difference in either total oxygen consumption or non mitochondrial oxygen consumption between controls and half dose LPS+TNF α +IL6 treated cells where the results were expressed per cell number. However, there was a significant decrease in total oxygen consumption in the treated group, compared to the control, where the results were expressed per dry mass.

7.2.7 Effect of salicylic acid on total endogenous hepatocyte respiration in control and in LPS+TNF α +IL6 exposed hepatocytes

Absolute rates of total oxygen consumption in the absence or presence of 1 or 2mM sodium salicylate are shown in Table 7.3. Figure 7.6, considered in detail below, compares the effect of salicylic acid on total endogenous hepatocyte respiration in control and in LPS+TNF α +IL6-exposed hepatocytes. For ease of interpretation in this figure, hepatocytes not exposed to agents during the cell preparation technique have been labelled as 'control' groups and hepatocytes exposed to LPS+TNF α +IL6 during the isolation procedure have been labelled as 'sepsis' groups.

When control hepatocytes were exposed to 1mM sodium salicylate there was an increase in total oxygen consumption, although this was not significantly increased compared to control hepatocytes in the absence of salicylate (Figures 7.6(a) and (b)) unless the data was analysed in terms of dry mass. When the cells were

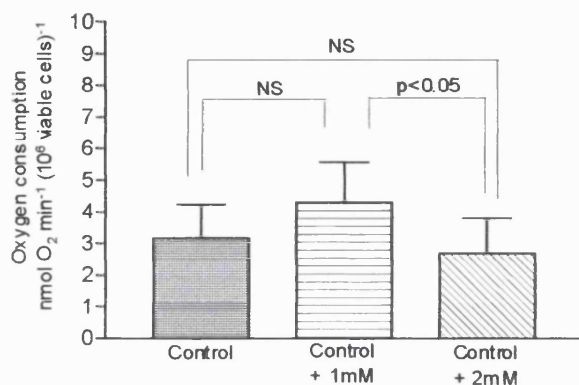
Treatment following isolation	Total oxygen consumption (nmol O ₂ min ⁻¹ (10 ⁶ viable cells) ⁻¹)		Total oxygen consumption (nmol O ₂ min ⁻¹ (mg dry mass) ⁻¹)	
	Control	LPS+TNF+IL6	Control	LPS+TNF+IL6
Absence of sodium salicylate	3.17 ± 1.06	3.66 ± 1.02	2.00 ± 0.56	3.17 ± 1.27
1mM sodium salicylate	4.28 ± 1.30	5.07 ± 1.40	2.76 ± 0.63	4.56 ± 1.88
2mM sodium salicylate	2.68 ± 1.11	3.78 ± 0.96	1.73 ± 0.59	3.24 ± 1.17

Table 7.3 Absolute rates of total oxygen consumption in the absence or presence of sodium salicylate

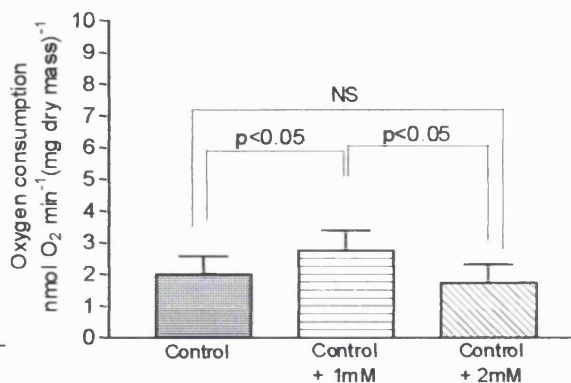
Control and treated oxygen consumption experiments were carried out in parallel. Values are presented as means ± SEM, n=4 parallel hepatocyte preparation. Results were analysed using the Student's paired *t* test.

Control cells plus/minus salicylic acid:

(a) Data expressed in terms of cell number

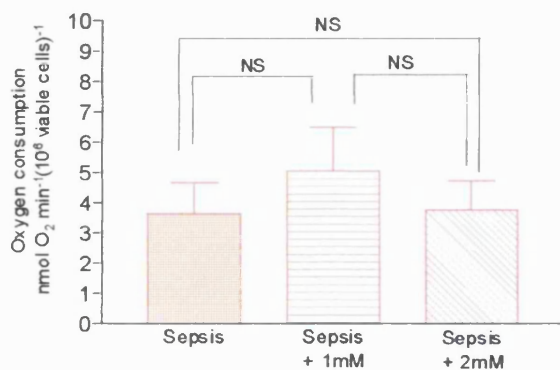


(b) Data expressed in terms of dry mass

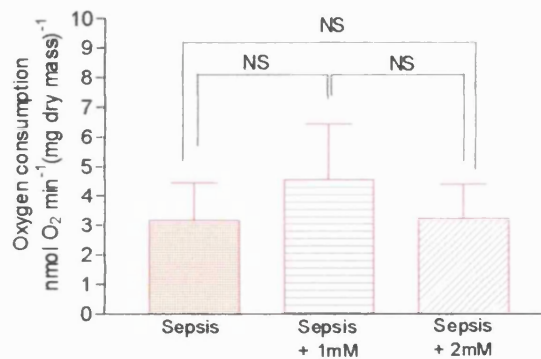


Sepsis cells plus/minus salicylic acid:

(c) Data expressed in terms of cell number

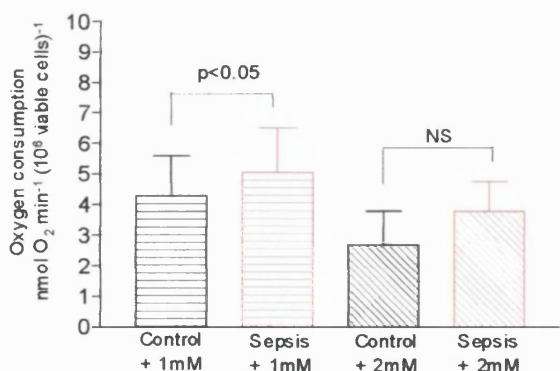


(d) Data expressed in terms of dry mass



Control and sepsis cells compared:

(e) Data expressed in terms of cell number



(f) Data expressed in terms of dry mass

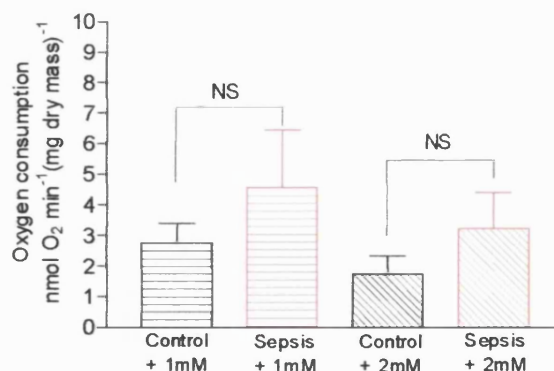


Figure 7.6 Total oxygen consumption: Control or LPS+TNF α +IL6-exposed cells in absence or presence of salicylic acid

All individual data points from a particular experiment have been meaned, these figures show the mean of these averaged values \pm SEM, $n=4$. Results analysed using paired Student's t test. Note: 'sepsis' indicates LPS+TNF α +IL6 model.

exposed to 2mM dose sodium salicylate, total oxygen consumption was similar to that found in control hepatocytes in the absence of salicylate. When the data were analysed in terms of dry mass or cell number the total oxygen consumption was significantly lower with 2mM than 1mM sodium salicylate (Figure 7.6 (a) and (b)).

There were no significant differences in total oxygen consumption in LPS+TNF α +IL6-treated hepatocytes exposed to 1mM and 2mM sodium salicylate following cell preparation compared to LPS+TNF α +IL6-treated hepatocytes in the absence of salicylate, whether the data were analysed in terms of number of cells or dry weights (Figure 7.6(c) and (d)). However, the same trends were seen in these LPS+TNF α +IL6 groups, as in the controls \pm salicylic acid reported above, i.e. increased total oxygen consumption following 1mM sodium salicylate, whilst oxygen consumption in the group exposed to the 2mM dose was similar to that seen in the absence of sodium salicylate.

Figure 7.6(e) and (f) shows a comparison of the control and LPS+TNF α +IL6-treated hepatocytes, exposed to 1mM and 2mM sodium salicylate. The LPS+TNF α +IL6-treated group have significantly higher levels of total oxygen consumption compared to untreated hepatocytes in the presence of 1mM sodium salicylate, when the data were analysed by number of cells. There was no significant difference between untreated and LPS+TNF α +IL6-treated groups when both groups were treated with 2mM sodium salicylate. There were no significant differences when the data were analysed per dry mass.

7.3 Discussion

7.3.1 The effect of LPS or individual cytokines on hepatocyte respiration

Although LPS has been found to result in changes to oxygen consumption in some models of sepsis, the results from the current study found that there was no statistically significant difference in total cellular oxygen consumption between control cells and cells exposed to LPS during the cell isolation procedure whether the data were expressed in terms of number of viable cells or by dry mass. The myxothiazol-resistant (i.e. non-mitochondrial) fraction of cellular oxygen consumption was also unchanged in the two groups, whether the data were expressed by number of cells or by dry mass. These results, using isolated

hepatocytes, support the work of Stadler *et al.*, (1991) who found that addition of LPS to rat hepatocyte cultures had no effect on mitochondrial respiration.

Similarly, the addition of TNF α during the cell isolation procedure did not lead to a significant difference in total cellular oxygen consumption between controls and the TNF α exposed group, whether the data was expressed in terms of number of cells or by dry mass. Non-mitochondrial respiration was unchanged between the controls and the TNF α exposed group when the data were analysed by dry mass, but was significantly increased where the data was analysed in terms of number of viable cells (Tables 7.1 and 7.2). It is likely that these apparently conflicting trends have arisen due to the relatively small sample size rather than due to the effects of the treatment itself, since no difference was found in the ratio of number of cells:mg dry mass between treated and untreated groups. When comparing the different ways of expressing the results, it is also important to note that dry mass includes non-viable cells and that the oxygen consumption of such cells is not known.

7.3.2 The effect of combinations of LPS and cytokines on hepatocyte respiration

As discussed in the previous section, when added during the cell isolation procedure singly neither LPS nor TNF α had a significant effect on total hepatocyte respiration. However, when added to the cell preparation in combination (LPS+TNF α), a statistically significant increase in total cellular oxygen consumption was observed when the data were analysed in terms of number of viable cells. The same trend was also seen when analysed by dry mass, although with this alternative way of expressing the data, the difference between the two groups was not significant. These results may suggest that in combination, these agents affect oxidative metabolism. It is important, however, not to over-interpret the results from this model since there is an apparent discrepancy between the alternative methods for expressing the results. As with the previous models, incubations in the presence of myxothiazol were performed to characterise the site of action of the agents on hepatocyte oxygen consumption and no significant difference in extra-mitochondrial oxygen consumption was observed with either method for expressing the data.

To investigate further the possible effects of this combination of agents, a half-dose model of the LPS+TNF α combination was also examined. With this lower dose,

non-mitochondrial oxygen consumption was significantly increased in the treated group compared to controls where the results are expressed by number of cells, whilst total cellular oxygen consumption was unchanged. When using the alternative method for expressing the data, no significant differences were observed. It is, therefore, difficult to draw firm conclusions from these results. However, it is possible that at this half-dose, total oxygen consumption is unchanged since any increase in extra-mitochondrial respiration is offset by decreased mitochondrial oxygen consumption.

Since the addition of LPS and TNF α in combination to the hepatocyte isolation technique resulted in an apparent trend towards increased total hepatocyte respiration, which was significantly greater in terms of number of cells, the effect of the addition of a further cytokine, IL6, to this combination model was examined (Figures 7.5(a)-(f)). This more complex combination of agents resulted in a significant increase in total cellular respiration in the treated group, compared to the controls and in significant increases in non-mitochondrial respiration in the treated group, regardless of the method of analysis applied to the data.

The results from the LPS+TNF α +IL6 model presented here, support the work of Moss *et al.*, (1969), where liver homogenates from rats after *E. coli* endotoxin injection were observed to consume more oxygen than controls. Furthermore, whilst a decrease in oxygen consumption is observed in the later stages of sepsis, in the early stages of sepsis there is an initial rise in oxygen consumption (Mela-Riker *et al.*, 1992; Rosser *et al.*, 1998). The results presented here are also similar to those found by Wang *et al.*, (1993) who implicated TNF α , either alone or in combination with IL6, as the mediator(s) responsible for producing the hepatocellular dysfunction observed in the early hypermetabolic stage of sepsis. It is possible that injury in sepsis, mediated through TNF α and/or additional cytokines could result in mitochondrial generation of ROS, which could lead to organelle damage. The results reported here, together with those presented in the previous chapter, where the potential of CPT I to control ketogenic flux was examined in *in vitro* models of neonatal sepsis, suggest, therefore, that the addition of LPS+TNF α +IL6 during the hepatocyte isolation procedure may mimic the early hypermetabolic stages of sepsis, before major structural damage has occurred to organelles and/or components of the respiratory chain, which would ultimately lead to decreased total oxygen consumption.

The observed increase in total oxygen consumption could be due to several factors, as summarised in Table 7.4:

Increase in total oxygen consumption	
Mitochondrial fraction	Extra-mitochondrial fraction
Increased	Increased
Increased	Unchanged
Unchanged	Increased
Decreased	Increased
Increased	Decreased

Table 7.4 Possible combinations resulting in increased total oxygen consumption

Since non-mitochondrial oxygen consumption was significantly increased in this LPS+TNF α +IL6 model and no significant difference was observed between treated and untreated controls with respect to mitochondrial oxygen consumption, these results suggest that the observed increase in total oxygen consumption in this combination model was predominately extramitochondrial in origin. These results contrast with those of Kantrow *et al.*, (1997) where no difference was observed in non-mitochondrial oxygen consumption between sepsis or control cells. However, these workers used cyanide to inhibit mitochondrial respiration, which they suggest may have also inhibited some cytosolic oxygen consuming enzymes. Furthermore, their model used adult rather than neonatal rats. The increased non-mitochondrial oxygen consumption seen in this model has also been observed in an *ex vivo* model of neonatal sepsis where neonatal rats have received intraperitoneal injection of LPS (Markley *et al.*, 2000). In subsequently isolated hepatocytes, these workers found a decrease in intramitochondrial oxygen consumption and an increase in extramitochondrial oxygen consumption. It is interesting to note that mitochondrial respiration in the LPS+TNF α +IL6 model presented here shows an apparent decrease in mitochondrial oxygen consumption, although this difference is not significant. The increase in extramitochondrial oxygen consumption may be due to the action of, for example, the cytochrome P₄₅₀ family of enzymes. The cytochromes in this system utilize oxygen for the oxidation of a wide range of substrates, and the increase may therefore result from an increased oxygen requirement for cytosolic detoxification and repair purposes. The present study did not, however, assess the activities of individual oxygen-dependent enzymes.

In the control groups for the various models of neonatal sepsis presented here, under conditions of saturating myxothiazol, 60% of the hepatocyte oxygen consumption was inhibited, suggesting that the largest contributor to total oxygen consumption was mitochondrial in origin (Figure 7.7(a)). In these controls, approximately 40% of total cellular oxygen consumption arose from non-mitochondrial processes. These results support the general conclusions of Romeo *et al.*, (1999), although these workers found that 78% of total oxygen consumption derived from mitochondrial sources, with 22% non-mitochondrial in origin. The apparent discrepancy between the figures presented here and the figures presented by these workers, may have arisen due to the age range of the rat-pups used in the studies by Romeo *et al.*, which was wider than that used in the studies discussed here: 11-15d, compared with 11-13d. From experience gained during the studies discussed in this thesis, rats older than 13d may have opened their eyes and may no longer feed exclusively on maternal rat milk (Henning, 1981). The results presented by these authors, therefore, may not be a true reflection of the distribution of oxygen consumption in neonatal (suckling) rats. Furthermore, the work of Lionetti *et al.*, (1998) has highlighted that important changes occur in hepatic respiratory function with aging.

(a) control hepatocytes

(b) treated hepatocytes

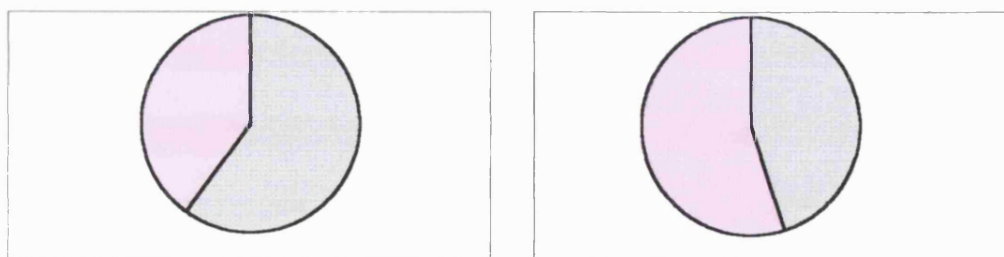


Figure 7.7 Comparison of the distribution of oxygen consumption in isolated hepatocytes from (a) control and (b) LPS+TNF α +IL6 treated groups

○ Mitochondrial respiration ● Non-mitochondrial respiration

Comparing the distribution of oxygen consumption in control cells, as discussed above, to that observed in the LPS+TNF α +IL6 treated cells, it can be seen that the relative contributions of the two fractions to total oxygen consumption had changed (Figure 7.7(b)). In this neonatal model of sepsis, 55% of total cellular oxygen

consumption was myxothiazol resistant, i.e. non-mitochondrial in origin. This suggested that the contribution of the non-mitochondrial processes to total cellular oxygen consumption was greater in the LPS+TNF α +IL6 treated groups.

As with the previous combination model, the effect of a 'half dose' of the LPS+TNF α +IL6 cocktail on oxygen consumption was examined. This 'half dose' cocktail had no significant effect on either total oxygen consumption or on non-mitochondrial oxygen consumption, compared to controls when the data was analysed by number of cells. However, a significant decrease in total oxygen consumption was found where the data was analysed by dry weights. This apparent discrepancy may be due to the small sample size used for this model.

7.3.3 Comparison of the effects of the different models of neonatal sepsis on oxygen consumption

In summary, Figure 7.8 compares the percentage change in total oxygen consumption in each of the models of neonatal sepsis presented in this chapter. Each full dose model shows a rise in oxygen consumption compared to control, which becomes significant (as indicated by the asterisk in Figure 7.8) in the models where agents have been used in combination.

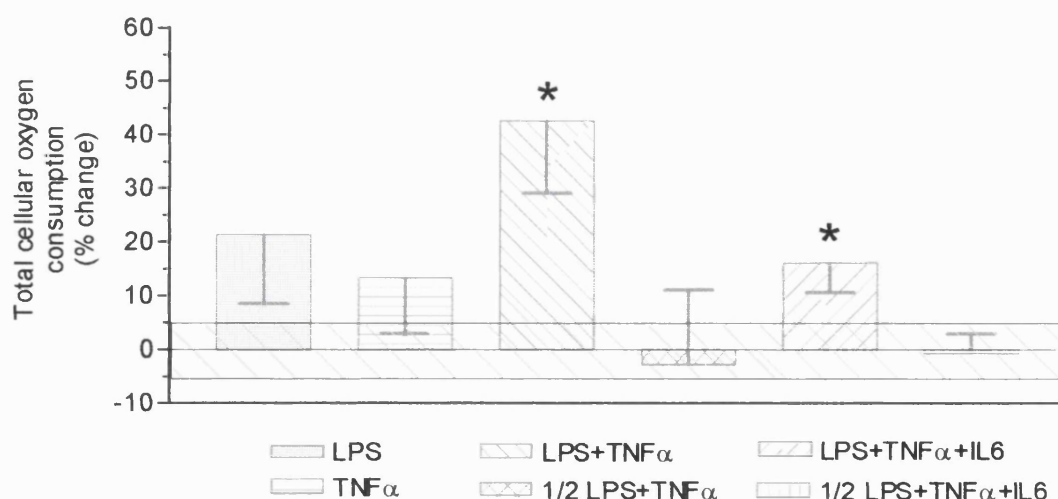


Figure 7.8 Percentage change in total endogenous respiration in hepatocytes

Values have been calculated as the percentage change in oxygen consumption, compared to appropriate control values. The range of control values is indicated by the shaded band and the mean absolute rate for untreated controls was 2.25 ± 0.11 nmol O $_2$ min $^{-1}$ (10^6 viable cells) $^{-1}$ n=25.

As discussed above, it is not sufficient to consider only changes in total oxygen consumption. Any changes observed could be due to changes in the distribution of oxygen consumption, i.e. changes in the mitochondrial and/or non-mitochondrial contribution to total oxygen consumption. By using myxothiazol, the changes in the distribution of oxygen consumption were investigated. Figure 7.9(a) and 7.9(b) summarise the results for each of the models considered in this thesis.

Figure 7.9(a) demonstrates that little variation is seen in the relative contribution of the extramitochondrial fraction to total oxygen consumption across the various control groups, which is to be expected, since they represent equivalent groups. Based on the mean of all the control groups, approximately 40% of oxygen consumption was non-mitochondrial in origin, i.e. a greater proportion of total oxygen consumption, 60%, was due to mitochondrial processes (as shown in Figure 7.7).

In contrast, Figure 7.9(b) demonstrates the changes in the relative contributions of the non-mitochondrial fraction in response to the different treatments. The proportion of non-mitochondrial oxygen consumption shows apparent increases, with increasing complexity of model used. Using the information here, and from Tables 7.1 and 7.2 and Figures 7.5-7.9, this suggests that the trend towards increased total oxygen consumption seen in each of the models, which was significantly increased in the two full-dose, combination models, may have different origins, although some caution needs to be applied, since not all of the trends were significantly different. $\text{TNF}\alpha$ used in isolation appears to increase oxygen consumption in the extra-mitochondrial fraction more than the addition of LPS alone. When used together, these agents further increase the contribution of the non-mitochondrial proportion to total oxygen consumption, whilst the mitochondrial fraction is apparently unchanged. In the most complex model considered here, LPS+ $\text{TNF}\alpha$ +IL6, whilst the mitochondrial contribution is lowered the non-mitochondrial fraction has increased such that overall, there is still a net increase in total oxygen consumption. This may indicate damage to the electron transport chain complexes.

(a) Appropriate control groups

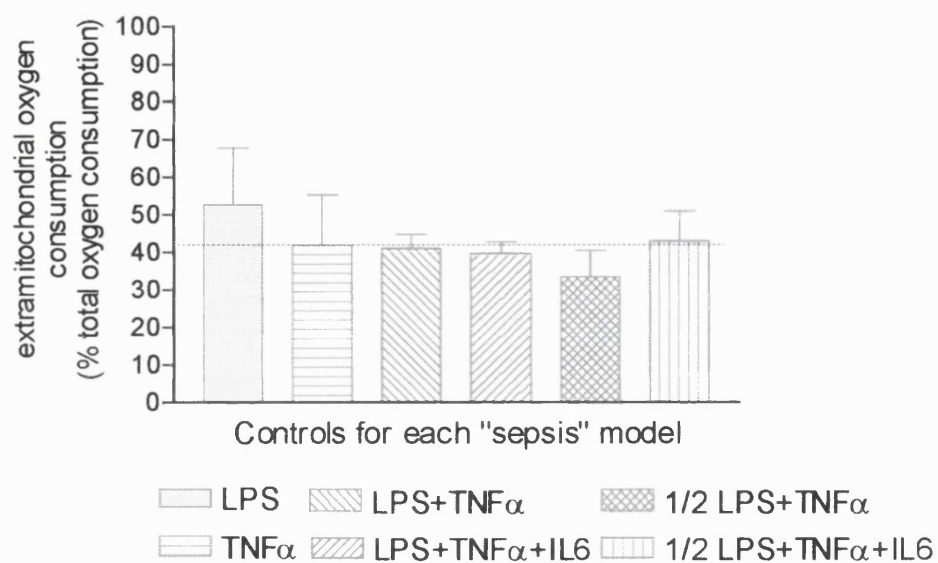
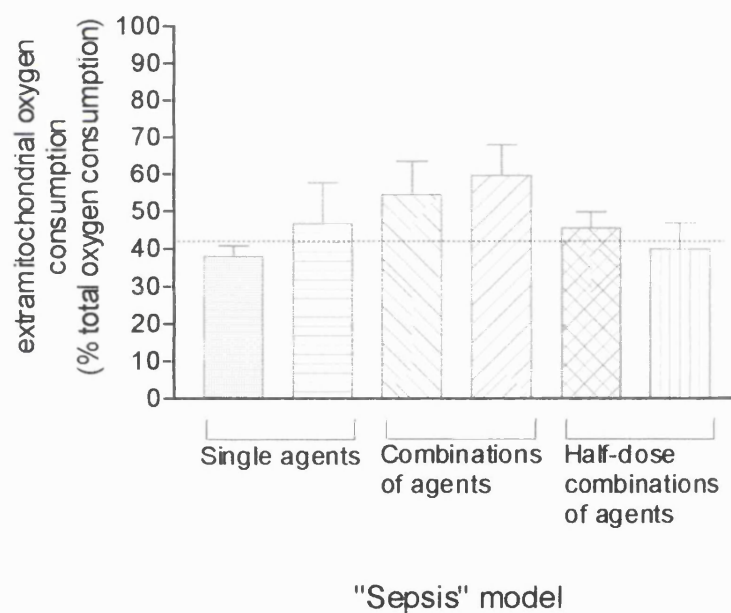
(b) *in vitro* models of neonatal sepsis

Figure 7.9 Changes in the contribution of the non-mitochondrial fraction to total oxygen consumption

Both (a) and (b) show the myxothiazol-resistant oxygen consumption expressed as a percentage of total oxygen consumption.

(a) each bar represents the appropriate control group for each model of sepsis, and as expected, there is little variation across the control groups.

(b) each bar represents a treated group for each model of sepsis.

The dashed line indicates the mean value for all control groups.

7.3.4 Investigating the effects of salicylic acid on hepatocyte respiration in the LPS+TNF α +IL6 *in vitro* model of neonatal sepsis

Kilpatrick *et al.*, (1989) have administered sub-lethal doses of endotoxin and aspirin (acetylsalicylic acid, which is hydrolysed *in situ* to produce salicylic acid), to adult rats to produce metabolic and histopathic alterations similar to those that have been reported in Reye's Syndrome. The experiments presented in this Chapter provide a preliminary investigation into the effects of salicylic acid on control and a model of neonatal sepsis, with the aim to develop a model which mimics the effects seen during Reye's Syndrome in the neonate. The LPS+TNF α +IL6 model was chosen since it showed significantly increased oxygen consumption compared to untreated controls, regardless of the method used to express the data. Figure 7.10 below summarises the changes in total oxygen consumption presented in Section 7.2.7.

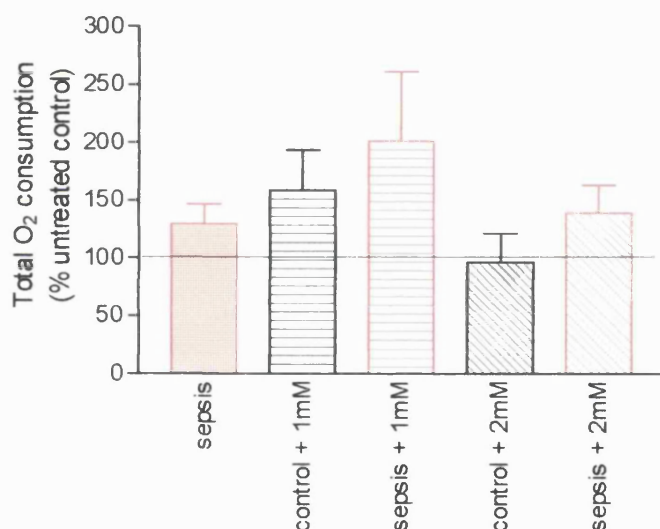


Figure 7.10 Comparison of total oxygen consumption in control and LPS+TNF α +IL6 exposed hepatocytes in response to two different doses of salicylic acid

Total oxygen consumption was increased in control and LPS+TNF α +IL6 exposed hepatocytes when 1mM sodium salicylate was added to the incubation medium. However, when 2mM sodium salicylate was added, respiration in the control group was the same as in control cells not exposed to salicylic acid. Oxygen consumption in LPS+TNF α +IL6 cells was also lower than in response to the half salicylic acid dose.

The work presented in this chapter is in broad agreement with other published work, i.e. there is a tendency for hepatocytes exposed to 1mM sodium salicylate to demonstrate increased oxygen consumption compared to appropriate controls, although this is only significantly increased where the data is expressed in terms of

dry weight. These results may indicate that salicylic acid causes the hydrogen ion gradient across the inner mitochondrial membrane to be dissipated, by allowing hydrogen ions to pass through without the production of ATP, effectively uncoupling oxidative phosphorylation from ATP formation, removing negative feedback and increasing oxygen consumption, as has been shown in studies using planar phospholipid bilayer membranes (Gutknecht, 1992), although from the current preliminary investigation, this has not been confirmed. Curiously, addition of salicylic acid at the higher dose resulted in decreased total cellular oxygen consumption compared to the 1mM dose, although this decrease was only significant in the control groups. Rates of total cellular oxygen consumption with 2mM salicylic acid were similar to that found in groups in the absence of salicylic acid (summarised in Figure 7.10). This may indicate an additional process acting to depress the oxygen consumption rate, for example, damage to the components of the respiratory chain.

Further investigations of oxygen consumption using different doses of salicylic acid would be advantageous in explaining the events observed here. In addition, it would be of interest to carry out electron microscopy studies on the gross morphological features in response to various doses of salicylic acid, and to use myxothiazol to dissect out the relative contributions of mitochondrial and non-mitochondrial oxygen consumption to total cellular oxygen consumption.

7.3.5 Conclusions

The data presented in this chapter, together with the electron micrographs from Chapter 6, where no gross morphological differences were observed between treated and untreated controls, suggest that these results may reflect changes occurring at the biochemical rather than the gross morphological level within these models. The results presented in this study also demonstrate that addition of combinations of agents resulted in abnormal neonatal hepatic oxidative metabolism, which may mimic that seen in the early stages of sepsis. Furthermore, these results indicate that the transient hypermetabolism observed in the early stages of neonatal sepsis may be due to an increase in extramitochondrial metabolism.

The preliminary results of the effects of salicylic acid on hepatocytes suggest that this model may warrant further investigation into its suitability as an *in vitro* model of Reye's Syndrome in the neonate.

Chapter 8

Conclusions and future research

8.1 The effects of development and substrate on the potential of CPT I to control carbon fluxes

As discussed in the main introduction and other relevant chapters of this thesis, the distribution of control over the pathways of fatty acid oxidation and ketogenesis are incompletely understood. In this thesis, I have sought to begin to address this issue, with the primary aim to report and discuss the control exerted by CPT I over carbon fluxes through the pathways of fatty acid oxidation, ketogenesis and Krebs cycle, in hepatocytes isolated from suckling rats and the effect of different substrates or clinical status on control distribution over these pathways. Through the application of MCA in neonatal rat models, the work I have presented in this thesis has provided answers to some fundamental questions, which are considered below.

- “How much control does CPT I exert over carbon fluxes from palmitate to ketone bodies, carbon dioxide and total carbon products, in suckling rats?”

The results presented in this study have suggested that the distribution of control over ketogenic flux, flux to carbon dioxide and total carbon products, is different in suckling rats compared to an equivalent adult group (Drynan *et al.*, 1996, Chapter 3). Although the numerical value of the flux control coefficient for CPT I over ketogenic flux was high in adult rats, which suggested its contribution to control was high; the value of the coefficient was significantly lower in suckling rats. This indicated that the control exerted by CPT I over ketogenic flux during this stage of development was low and that the sum of other steps of the pathway have a larger contribution to control. The results presented in this thesis suggested, therefore, that in this suckling system, the traditional assumption that CPT I is necessarily the ‘rate-limiting’ step of fatty acid oxidation and ketogenesis may not be appropriate. These results also supported the concept of multi-site control (Fell *et al.*, 1995).

These conclusions, drawn from the work using hepatocytes systems, were supported by those obtained from work using mitochondrial systems. Through the application of BUCA on data obtained from the original system used for TDCA by Krauss *et al.*, (1996) individual flux control coefficients for CPT I over ketogenesis and over total carbon flux were calculated and reported for the first time (Chapter 3). Through comparisons of equivalent sets of coefficients from suckling and adult

mitochondria, it was demonstrated that coefficients were consistently lower in the suckling system than in the adults. These results suggested, therefore, that the potential of CPT I to control hepatic β -oxidation flux was low during suckling and that the contribution of other steps to control flux was greater at this stage.

- “What control do sections of the pathway, for example, the Krebs cycle block of reactions, or the HMG-CoA cycle block, exert over pathway carbon fluxes?”

This question remains outstanding. The application of TDCA in this suckling rat system was investigated and reported in this thesis in Chapter 4 and Appendix I. It appears, however, there are complications arising due to the very low carbon dioxide flux, which lead to large errors when flux data is substituted into the appropriate equations.

- “How much control does CPT I exert over carbon flux to ketone bodies in a system using different substrates?”

Quantitative assessment of the potential of CPT I to control ketogenic flux in response to different physiological substrates suggested that the pattern of control distribution changed with the different substrates used (Chapter 5). The numerical value of the flux control coefficients for CPT I over ketogenesis were lower in experiments using medium-chain, or mixtures of medium-/long-chain fatty acids, compared to those using the long-chain fatty acid as substrate, which indicated that the potential of CPT I to control ketogenesis was also low under these conditions. The results presented in this thesis suggested that it may no longer be appropriate to consider CPT I as a ‘rate-controlling’ step over the pathways of ketogenesis and that the level of control exerted by CPT I *in vivo*, in neonatal rats, may be very small. These results also demonstrate a threshold: if only approximately 20% CPT I activity is present, for example, due to low levels of expression, or defects in the enzyme itself, ketogenic flux may be compromised, with resulting physiological implications for the individual. However, prior to this threshold (i.e. up to approximately 80% enzyme inactivity), the effects of a defect may not be observed.

Since the results presented in this thesis indicate that ‘control’ is not a static process and that the distribution of control may vary with nutrition or age, further investigation into the distribution of control over the pathways of ketogenesis in response to age/nutritional factors would be beneficial. For example, the distribution

of control is likely to be different in fetal, premature and immediately post-weaning rats, which has implications for the clinical environment. In addition, the distribution of control over carbon fluxes is likely to differ, for example, in formula fed infants, those receiving TPN and in babies receiving breast milk, for several reasons including differences in the composition of these diets. It would, therefore, be interesting, and of some clinical relevance, to develop neonatal rat models where newborns received differing diets, for example, mimicking the differences between maternally fed rats and those receiving an alternative, for example, infant formula mixture. Additionally, an investigation into the role of CPT I in tissues other than liver would be of interest, since other tissues, such as the intestine and kidney, have a role in ketogenesis during the neonatal period.

8.2 Development and use of *in vitro* neonatal model of sepsis

A further aim was to investigate and report on the development of an *in vitro* neonatal hepatocyte model to study the onset and progression of neonatal sepsis (Chapters 6 and 7). This was achieved through the addition of LPS, TNF α and IL6, either alone or in combination, during the cell isolation procedure.

In Chapter 6, the effect of these various agents on hepatocyte yield and viability was reported and discussed. In summary, the addition of these agents, either singly or in combination, resulted in a significant decrease in cell yield in the treated groups, compared to untreated controls, whilst cell viability, was unchanged between treated and untreated controls. Additionally, no difference in gross cell morphology was observed, with both treated and untreated groups having an intact cell membrane, dense mitochondria with intact cristae and no vacuolisation of the cytoplasm or nucleus.

Also in Chapter 6, the two combination models (LPS+TNF α and LPS+TNF α +IL6) were used to answer the following question:

- “How much control does CPT I exert over pathway carbon fluxes in response to clinical conditions, for example, sepsis?”

The work presented in this chapter demonstrated that the control structure for the ketogenic pathways changed when hepatocytes were challenged to the more complex combination of agents known to be involved in the septic response

(LPS+TNF α +IL6), compared to controls. The numerical value of the flux control coefficient was significantly higher in the group exposed to this combination of agents compared to untreated controls and the more simple combination model. These results suggested that the potential of CPT I to control ketogenic flux was greater under the treated conditions. It is, of course, important to keep in mind the complex interactions between cytokines and type of experimental system used before extrapolating to human situation however, once again, these results indicated that 'control' over pathway flux is not a static property.

The work presented in Chapter 7 further characterised the models developed and used in Chapter 6, through investigation of the effect of the addition of LPS and/or various cytokines on neonatal hepatic oxidative metabolism. In both combination models (LPS+TNF α and LPS+TNF α +IL6), an increase in total cellular oxygen consumption compared to appropriate controls was observed, which was predominantly extra-mitochondrial in origin (although these differences between control and model were only significant, for either method of data expression, in the LPS+TNF α +IL6 model). In conclusion, the results presented in this thesis suggested that the addition of LPS and/or various cytokines may be suitable models for the early stages of sepsis.

The results from the preliminary investigation into the effects of salicylic acid on oxygen consumption in the combination sepsis models compared to appropriate paired controls were presented and reported in Chapter 7 and suggested that salicylic acid may act as an uncoupler. Whilst these results supported conclusions from other workers, as discussed in Chapter 7, the effect of the dose of salicylic acid and the exposure time needs to be investigated before any conclusions can be made on this aspect of the study.

The models of neonatal sepsis reported and discussed in Chapters 6 and 7 could be further investigated in a variety of ways. For example, future research could focus on:

- Assessment of leakage of enzymes and/or determination of intracellular concentrations of, for example, glutathione, Ca²⁺, K⁺, ATP and/or H₂O₂ production.

- Dose/time-response profiles, and addition of other cytokines to develop a more complex *in vitro* model, which more closely represents that found *in vivo*.
- Use of regulation analysis with MCA to assess 'effectiveness' of agents on hepatocytes.
- Addition of cytokine mixtures to attempt to mimic later stages in the progression of sepsis, with appropriate investigations into oxygen consumption / application of control analysis.
- Application of control analysis in hepatocytes which have been exposed to H₂O₂ to provide a comparison with results found in models where addition of cytokines are used to mimic the septic response.
- Investigation into the control exerted by CPT I over pathway carbon fluxes in response to clinical conditions, for example, sepsis, using different substrates.
- Dose/time-response profiles for the addition of salicylic acid to further characterise a Reye's Syndrome Model.

By using the models reported and discussed in this thesis, I aimed to investigate the early metabolic changes in response to sepsis with a long-term aim to investigate factors that may pre-empt/reverse the changes seen. It would be interesting to investigate whether the changes in the potential of CPT I to control carbon flux and the changes in oxidative metabolism, in response to 'sepsis', are reversible. In particular, glutamine has been implicated in the reversal of some of the responses to sepsis (Markley *et al.*, unpublished work) and an investigation into its effect on these models would be interesting, for both academic and clinical reasons.

Appendix I

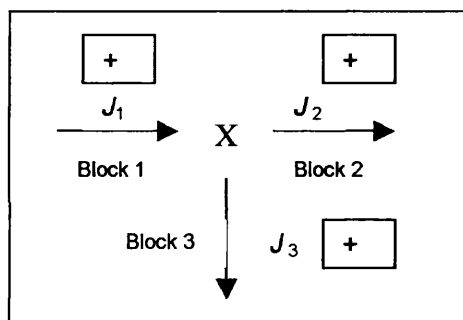
Derivation of generalised and specific forms of the equations used in the TDCA in Chapter 4

A1.1 Introduction

This appendix outlines the derivation of the general and the specific equations for the calculation of group flux control coefficients, in a three branched system, from flux data alone. The convention used for naming equations in this appendix is as follows: equations named a, b, etc., relate to the *intermediate equations* used in the derivation of the equations of Brown *et al*, (1990), Quant (1993) and Brand (1996) modified from the *original equations* set out by Kacser and Burns (1973). These *modified equations*, which are named A, B, C, etc., form the starting point for the derivation of the *key equations* for this particular system. *Key equations*, which are used in the top down control analysis described in Chapter 4, are named 1,2,3 etc.,. Equations named A₁, A₂, B₁, B₂, C₁, C₂ etc., are *intermediate equations*, used in the derivation of the *key equations* from the *modified equations*.

A1.2 Consideration of sign convention

Until recently, it has been assumed that in a three branched system, such as that shown in Scheme A1.1, fluxes towards and away from the intermediate should be considered as 'positive'.



Thus:

$$J_1 = J_2 + J_3 \quad \text{and, therefore,}$$

$$J_1 - J_2 - J_3 = 0$$

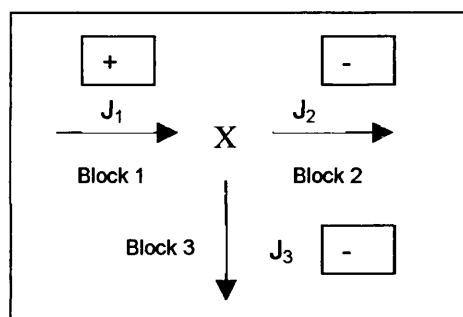
Scheme A1.1

Whilst this sign convention enables the three flux control coefficients relating to J_1 to be calculated (i.e. $*C_{Block1}^{J_1}$; $*C_{Block2}^{J_1}$; $*C_{Block3}^{J_1}$) due to limitations imposed by the branching theory, which relates flux control coefficients to fluxes as follows:

$$\frac{C_{Block2}^{J_1}}{C_{Block3}^{J_1}} = \frac{J_2}{J_3}, \text{ the flux control coefficients for the other blocks, for example, } *C_{Block1}^{J_2}$$

could not be obtained.

However, the sign convention formalised by Brand (1996), provides more flexibility and enables the sign to be an arbitrary designation (note, this is a mathematical device, it does not reflect chemical behaviour). For example, in the scheme considered previously, fluxes towards the intermediate may be considered as 'positive' and those away from the intermediate may be considered as 'negative', as shown in Scheme A1.2:



Thus:

$$J_1 = -J_2 - J_3 \quad \text{and, therefore,}$$

$$J_1 + J_2 + J_3 = 0$$

Scheme A1.2

Using this new sign convention it is possible to describe the control exerted (expressed as group flux control coefficients, $*C^J$) by each block of reactions (Block 1; Block 2; Block 3) over the flux (J_1 ; J_2 ; J_3) through its own block of reactions ($*C_{Block1}^{J_1}$; $*C_{Block2}^{J_2}$; $*C_{Block3}^{J_3}$) respectively, and over the fluxes through the other two blocks. The complete set of nine flux control coefficients for a three branched system is set out in general terms in Table A1.1, whilst Table 4.1 provides the complete series specific to the system described in Chapter 4.

Series 1	$*C_{Block1}^{J_1}$	$*C_{Block2}^{J_1}$	$*C_{Block3}^{J_1}$	Flux control coefficient for each block over flux through J_1 block of reactions
Series 2	$*C_{Block1}^{J_2}$	$*C_{Block2}^{J_2}$	$*C_{Block3}^{J_2}$	Flux control coefficient for each block over flux through J_2 block of reactions
Series 3	$*C_{Block1}^{J_3}$	$*C_{Block2}^{J_3}$	$*C_{Block3}^{J_3}$	Flux control coefficient for each block over flux through J_3 block of reactions

Table A1.1 Full series of generalised flux control coefficients in hepatocyte TDCA system

A1.3 Derivation of generalised equations using sign convention set out by Brand (1996)

The connectivity theorem (Section 1.4.5) states that the sum of each flux control coefficient on a particular flux, J , multiplied by its elasticity with respect to X , equals zero, thus:

$$(*C_{Block1}^{J1} \cdot * \mathcal{E}_{*x}^{Block1}) + (*C_{Block2}^{J1} \cdot * \mathcal{E}_x^{Block2}) + (*C_{Block3}^{J1} \cdot * \mathcal{E}_x^{Block3}) = 0 \quad \text{Equation a}$$

Note: as with flux control coefficients, a superscript * indicates a *group* elasticity rather than an *individual* elasticity.

Rearrangement of Equation a provides:

$$C_{Block1}^{J1} = \frac{(-(* \mathcal{E}_x^{Block2} \cdot * C_{Block2}^{J1}) - (* \mathcal{E}_x^{Block3} \cdot * C_{Block3}^{J1}))}{* \mathcal{E}_x^{Block1}} \quad \text{Equation b}$$

Since Summation (Section 1.4.3) can be stated as:

$$*C_{Block1}^{J1} = 1 - (*C_{Block2}^{J1} + *C_{Block3}^{J1}) \quad \text{Equation c}$$

Substitution of Equation c into Equation b provides:

$$1 - (*C_{Block2}^{J1} + *C_{Block3}^{J1}) = \frac{(-(* \mathcal{E}_x^{Block2} \cdot * C_{Block2}^{J1}) - (* \mathcal{E}_x^{Block3} \cdot * C_{Block3}^{J1}))}{* \mathcal{E}_x^{Block1}} \quad \text{Equation d}$$

Multiply through Equation d with $* \mathcal{E}_x^{Block1}$ to give Equation e:

$$* \mathcal{E}_x^{Block1} - (*C_{Block2}^{J1} \cdot * \mathcal{E}_x^{Block1}) - (*C_{Block3}^{J1} \cdot * \mathcal{E}_x^{Block1}) = -(* \mathcal{E}_x^{Block2} \cdot * C_{Block2}^{J1}) - (* \mathcal{E}_x^{Block3} \cdot * C_{Block3}^{J1})$$

Divide all terms in Equation e by $*C_{Block2}^{J1}$ and rearrange to = 0, gives Equation f:

$$\frac{* \mathcal{E}_x^{Block1}}{*C_{Block2}^{J1}} - * \mathcal{E}_x^{Block1} - \frac{*C_{Block3}^{J1}}{*C_{Block2}^{J1}} \cdot * \mathcal{E}_x^{Block1} + * \mathcal{E}_x^{Block2} + \frac{*C_{Block3}^{J1}}{*C_{Block2}^{J1}} \cdot * \mathcal{E}_x^{Block3} = 0$$

Since Branching theorem states that: $\frac{*C_{Block3}^{J1}}{*C_{Block2}^{J1}} = \frac{J_3}{J_2}$ Equation f can be restated as:

$$\frac{* \mathcal{E}_x^{Block1}}{* C_{Block2}^{J_1}} - * \mathcal{E}_x^{Block1} - \frac{J_3}{J_2} * \mathcal{E}_x^{Block1} + * \mathcal{E}_x^{Block2} + \frac{J_3}{J_2} * \mathcal{E}_x^{Block3} = 0 \quad \text{Equation g}$$

Multiplication of this with $* C_{Block2}^{J_1} J_2$ gives Equation h

$$J_2 * \mathcal{E}_x^{Block1} - * C_{Block2}^{J_1} J_2 * \mathcal{E}_x^{Block1} - * C_{Block2}^{J_1} J_3 * \mathcal{E}_x^{Block1} + * C_{Block2}^{J_1} J_2 * \mathcal{E}_x^{Block2} + * C_{Block2}^{J_1} J_3 * \mathcal{E}_x^{Block3} = 0$$

Rearrangement of Equation h gives Equation i:

$$* C_{Block2}^{J_1} (-J_2 * \mathcal{E}_x^{Block1} - J_3 * \mathcal{E}_x^{Block1} + J_2 * \mathcal{E}_x^{Block2} + J_3 * \mathcal{E}_x^{Block3}) = -J_2 * \mathcal{E}_x^{Block1} \quad \text{Equation i}$$

Since the sign convention formalised by Brand (1996) states that: $J_1 = -J_2 - J_3$

Equation i can be rearranged to provide Equation j:

$$* C_{Block2}^{J_1} = \frac{-J_2 * \mathcal{E}_x^{Block1}}{* \mathcal{E}_x^{Block1} (-J_2 - J_3) + (J_2 * \mathcal{E}_x^{Block2}) + (J_3 * \mathcal{E}_x^{Block3})} \quad \text{Equation j}$$

Finally, this can be stated as Equation A

$$* C_{Block2}^{J_1} = \frac{-J_2 * \mathcal{E}_x^{Block1}}{(J_1 * \mathcal{E}_x^{Block1}) + (J_2 * \mathcal{E}_x^{Block2}) + (J_3 * \mathcal{E}_x^{Block3})} \quad \text{Equation A}$$

Similarly, Equation B can be derived, using the same sign convention:

$$* C_{Block1}^{J_1} = \frac{(J_2 * \mathcal{E}_x^{Block2}) + (J_3 * \mathcal{E}_x^{Block3})}{(J_1 * \mathcal{E}_x^{Block1}) + (J_2 * \mathcal{E}_x^{Block2}) + (J_3 * \mathcal{E}_x^{Block3})} \quad \text{Equation B}$$

Equations A and B enable the flux control coefficients for the first series in Table A1.1 to be calculated. However, in their present form, these equations require information on fluxes and elasticities. The next section will discuss the derivation of equations to calculate flux control coefficients using flux data alone.

A1.4 Derivation of generalized equations for the calculation of group flux control coefficients as a function of fluxes alone

Equations A and B derived in Section A1.3 can be used as detailed below, to obtain the generalised equations for the calculation of group flux control coefficients as a function of fluxes alone.

In Equation A, all group elasticities may be expressed as a function of fluxes and all terms divided by the expanded form of (ε_x^{Block} , Section 1.4.4) as shown below in

Equation A₁:

$$*C_{Block2}^{J_1} = \frac{-J_2 \frac{\delta J_1}{J_1} \frac{x}{\delta x} / \frac{\delta J_1}{J_1} \frac{x}{\delta x}}{\left(\frac{J_1 \frac{\delta J_1}{J_1} \frac{x}{\delta x}}{\frac{\delta J_1}{J_1} \frac{x}{\delta x}} \right) + \left(\frac{J_2 \frac{\delta J_2}{J_2} \frac{x}{\delta x}}{\frac{\delta J_1}{J_1} \frac{x}{\delta x}} \right) + \left(\frac{J_3 \frac{\delta J_3}{J_3} \frac{x}{\delta x}}{\frac{\delta J_1}{J_1} \frac{x}{\delta x}} \right)}$$

General Equation A₁

All terms containing the intermediate (x) and each of the absolute fluxes are cancelled where possible and the expression rearranged to give general Equation 1 (Quant, 1993). This equation enables the first group flux control coefficient in series 1 (Table A1.1) to be calculated from flux data alone:

$$*C_{Block2}^{J_1} = \frac{-J_2 / J_1}{1 + \left(\frac{\delta J_2^{(3)}}{\delta J_1^{(3)}} \right) + \left(\frac{\delta J_3^{(2)}}{\delta J_1^{(2)}} \right)}$$

General Equation 1

In general equation 1, the numbers in brackets represent the two independent experimental manipulations of the system. For example, $\delta J_2^{(3)}$ indicates the change in flux J_2 brought about by the experimental manipulation of system block 3.

As seen for Equation A, Equation B can be modified by expressing all group elasticities ($*\varepsilon_x^{Block}$, Section 1.4.4) as a function of fluxes (J) and intermediate levels (x), and dividing all terms by the expanded form of the ($*\varepsilon_x^{Block}$), thus general equation B₁ can be derived:

$$*C_{Block1}^{J_1} = \frac{\left(\frac{J_2 \cdot \frac{\delta J_2 \cdot x}{J_2 \cdot \delta x}}{\frac{\delta J_1 \cdot x}{J_1 \cdot \delta x}} \right) + \left(\frac{J_3 \cdot \frac{\delta J_3 \cdot x}{J_3 \cdot \delta x}}{\frac{\delta J_1 \cdot x}{J_1 \cdot \delta x}} \right)}{\left(\frac{J_1 \cdot \frac{\delta J_1 \cdot x}{J_1 \cdot \delta x}}{\frac{\delta J_1 \cdot x}{J_1 \cdot \delta x}} \right) + \left(\frac{J_2 \cdot \frac{\delta J_2 \cdot x}{J_2 \cdot \delta x}}{\frac{\delta J_1 \cdot x}{J_1 \cdot \delta x}} \right) + \left(\frac{J_3 \cdot \frac{\delta J_3 \cdot x}{J_3 \cdot \delta x}}{\frac{\delta J_1 \cdot x}{J_1 \cdot \delta x}} \right)}$$

 Equation B₁

Cancelling all x –terms (i.e. terms relating to the intermediate) in Equation B₁, dividing each term by J_1 and rearranging the expression, enables general equation 2 to be derived. As before, superscripts in brackets indicate two independent experimental manipulations of two separate blocks of reactions.

General Equation 2

$$*C_{Block1}^{J_1} = \frac{\left(\frac{\delta J_{2(3)}}{\delta J_{1(3)}} \right) + \left(\frac{\delta J_{3(2)}}{\delta J_{1(2)}} \right)}{1 + \left(\frac{\delta J_{2(3)}}{\delta J_{1(3)}} \right) + \left(\frac{\delta J_{3(2)}}{\delta J_{1(2)}} \right)}$$

Equation 2

The final group flux control coefficient in the first series (Table A1.1) can be calculated by application of the summation theorem (Kacser and Burns, 1979). This states that the sum of all the flux control coefficients in a pathway is generally one (Section 1.4.3) and can be arranged to obtain the remaining group flux control coefficient, giving general Equation 3:

$$*C_{Block3}^{J_1} = 1 - \left(*C_{Block1}^{J_1} + *C_{Block2}^{J_1} \right)$$

General Equation 3

Hence a complete series of group flux control coefficients for each block over J_1 can be calculated from flux data alone and without measuring the intermediate, using general equations 1, 2 and 3.

A1.5 Specific equations for the calculation of the first series of group flux control coefficients as a function of fluxes alone

The first series of group flux control coefficients (Chapter 4, Table 4.1) may be calculated using the general equations described previously. To form the specific equations needed for TDCA in this hepatocyte system from the generalised equations, block 1 from the generalised equations can be said to represent the reactions of the HMG-CoA cycle (and J_{KB} represents ketogenic flux), block 2 represents the β -oxidation block of reactions (and $J_{\beta OX}$ represents total carbon flux), and block 3 represents the reactions of the Krebs cycle (and J_{CO_2} represents the flux to CO_2). Thus the specific equations for this hepatocyte system become:

$$*C_{\beta OX}^{J_{KB}} = \frac{-J_{\beta OX} / J_{KB}}{1 + \left(\frac{\delta J_{\beta OX} (CO_2)}{\delta J_{KB} (CO_2)} \right) + \left(\frac{\delta J_{CO_2} (\beta OX)}{\delta J_{KB} (\beta OX)} \right)}$$

Specific Equation 1

$$*C_{KB}^{J_{KB}} = \frac{\left(\frac{\delta J_{\beta OX} (CO_2)}{\delta J_{KB} (CO_2)} \right) + \left(\frac{\delta J_{CO_2} (\beta OX)}{\delta J_{KB} (\beta OX)} \right)}{1 + \left(\frac{\delta J_{\beta OX} (CO_2)}{\delta J_{KB} (CO_2)} \right) + \left(\frac{\delta J_{CO_2} (\beta OX)}{\delta J_{KB} (\beta OX)} \right)}$$

Specific Equation 2

As in the general equations, the superscript terms in brackets represent the blocks of reactions being manipulated when the changes in fluxes are calculated, thus in these specific equations (CO_2) indicates that the Krebs cycle block of reactions has been manipulated.

$$*C_{CO_2}^{J_{KB}} = 1 - (*C_{KB}^{J_{KB}} + *C_{\beta OX}^{J_{KB}})$$

Specific Equation 3:

Thus, using these three specific equations, all three group flux control coefficients for flux through the KB block (Series 1, Table 4.1) may be calculated by substitution of flux data into the appropriate equation.

However, application of the rearranged equations to obtain group flux control coefficients for J_{CO_2} and $J_{\beta OX}$ would require the experimental manipulation of the HMG-CoA cycle block of reactions. At present, there is no specific inhibitor of this block (or other means of independently manipulating its activity). Therefore, whilst the specific equations in this section may be used to calculate the $*C^{J_{KB}}$ series of flux control coefficients, it is not appropriate to use these equations to calculate either of the other two series of flux control coefficients (Table 4.1). In order to calculate the remaining series of flux control coefficients, relative elasticities may be used, as described in the following section.

A1.6 Calculation of relative elasticities

Elasticities describe how the potential of an enzyme (or *block* of reactions) to control flux is related to the kinetic properties of the enzyme (or *block* of reactions) (Section 1.4.4). In the hepatocyte system being used for TDCA in Chapter 4, three group elasticities can be considered: $*\mathcal{E}_x^{\beta OX}$, $*\mathcal{E}_x^{CO_2}$ and $*\mathcal{E}_x^{KB}$. Elasticities may be measured experimentally, using data on fluxes and intermediates. However, in the system described in Chapter 4, the intermediate is not measured, therefore group elasticities cannot be obtained using this approach. Instead, in this system, since it is the *relative proportions*, rather than *absolute elasticity* that is of interest, *relative elasticities* may be used

Thus it is appropriate to assign an arbitrary value of 1 to an elasticity and let the other elasticities be considered relative to this term:

$$*\mathcal{E}_X^{BOX} = 1 \qquad \text{Equation C}$$

The second group elasticity, $*\mathcal{E}_x^{CO_2}$, may be calculated by application of the Connectivity theorem (Kacser and Burns, 1973, Section 1.4.5) which relates elasticities to flux control coefficients and which has been shown to hold for group

elasticities (Brown *et al.*, 1990; Quant, 1993, Brand, 1996):

$$\left(*C_{\beta OX}^{JKB} \cdot * \mathcal{E}_x^{\beta OX}\right) + \left(*C_{KB}^{JKB} \cdot * \mathcal{E}_x^{KB}\right) + \left(*C_{CO2}^{JKB} \cdot * \mathcal{E}_x^{CO2}\right) = 0$$

Equation D

This can be rearranged to derive Equation D₁:

$$\left(*C_{KB}^{JKB} \cdot * \mathcal{E}_x^{KB}\right) = -\left(*C_{\beta OX}^{JKB} \cdot * \mathcal{E}_x^{\beta OX}\right) - \left(*C_{CO2}^{JKB} \cdot * \mathcal{E}_x^{CO2}\right)$$

Equation D₁

Which may also be rearranged, deriving Equation D₂:

$$* \mathcal{E}_x^{KB} = -\frac{*C_{\beta OX}^{JKB} \cdot * \mathcal{E}_x^{\beta OX}}{*C_{KB}^{JKB}} - \frac{*C_{CO2}^{JKB} \cdot * \mathcal{E}_x^{CO2}}{*C_{KB}^{JKB}}$$

Equation D₂

Equation D₃ can be derived by dividing Equation D₂ throughout by $\frac{1}{* \mathcal{E}_x^{CO2}}$ and cancel terms where appropriate:

$$\frac{* \mathcal{E}_x^{KB}}{* \mathcal{E}_x^{CO2}} = -\frac{*C_{\beta OX}^{JKB} \cdot * \mathcal{E}_x^{\beta OX}}{*C_{KB}^{JKB} \cdot * \mathcal{E}_x^{CO2}} - \frac{*C_{CO2}^{JKB}}{*C_{KB}^{JKB}}$$

Equation D₃

By describing the elasticities shown on the left hand side of equation in terms of fluxes and intermediate, Equation D₄ may be derived:

$$\frac{\frac{\delta J_{KB}}{J_{KB}} \cdot \frac{x}{\delta x}}{\frac{\delta J_{CO2}}{J_{CO2}} \cdot \frac{x}{\delta x}} = -\frac{*C_{\beta OX}^{JKB} \cdot * \mathcal{E}_x^{\beta OX}}{*C_{KB}^{JKB} \cdot * \mathcal{E}_x^{CO2}} - \frac{*C_{CO2}^{JKB}}{*C_{KB}^{JKB}}$$

Equation D₄

After terms are cancelled where appropriate, this then forms Equation D₅:

$$\frac{\frac{\delta J_{KB}}{J_{KB}}}{\frac{\delta J_{CO2}}{J_{CO2}}} = - \frac{*C_{\beta OX}^{J_{KB}} \cdot *E_x^{\beta OX}}{*C_{KB}^{J_{KB}} \cdot *E_x^{CO2}} - \frac{*C_{CO2}^{J_{KB}}}{*C_{KB}^{J_{KB}}}$$

Equation D₅

'Flip' left hand side of equation, deriving Equation D₆:

$$\frac{\delta J_{KB}}{J_{KB}} \cdot \frac{J_{CO2}}{\delta J_{CO2}} = - \frac{*C_{\beta OX}^{J_{KB}} \cdot *E_x^{\beta OX}}{*C_{KB}^{J_{KB}} \cdot *E_x^{CO2}} - \frac{*C_{CO2}^{J_{KB}}}{*C_{KB}^{J_{KB}}}$$

Equation D₆

Finally, this can be rearranged, forming Equation E:

$$\frac{*C_{\beta OX}^{J_{KB}} \cdot *E_x^{\beta OX}}{*C_{KB}^{J_{KB}} \cdot *E_x^{CO2}} = - \frac{\delta J_{KB}}{J_{KB}} \cdot \frac{J_{CO2}}{\delta J_{CO2}} - \frac{*C_{CO2}^{J_{KB}}}{*C_{KB}^{J_{KB}}}$$

Equation E

Since this section describes *relative* elasticities and $*E_x^{\beta OX}$ has been defined = 1, there is only one unknown in Equation E, $*E_x^{CO2}$. Thus, by substitution of appropriate flux data, the second elasticity coefficient, $*E_x^{CO2}$, may be obtained.

The final elasticity, $*E_x^{KB}$, may be calculated by application of connectivity once more, multiplying by $*E_x^{CO2}$ to get $*E_x^{KB}$ on its own, forming Equation F:

$$*E_x^{KB} = - \left(\left(\frac{*C_{\beta OX}^{J_{KB}} \cdot *E_x^{\beta OX}}{*C_{KB}^{J_{KB}} \cdot *E_x^{CO2}} \right) - \frac{*C_{CO2}^{J_{KB}}}{*C_{KB}^{J_{KB}}} \right) *E_x^{CO2}$$

Equation F

Thus, substitution of flux data and the values for the first series of group flux control coefficients obtained using Equations 1, 2 and 3, into these expressions, enables all the relative elasticities to be calculated. Once these relative elasticities have been calculated from flux data, the remaining six flux control coefficients, Series 2 and 3 (Table 4.1), may be calculated.

A1.7 Calculation of the remaining series of group flux control coefficients

As values for elasticity coefficients have been calculated, it is possible to use

Equation A to obtain values for $*C^{J\beta OX}$ series of group flux control coefficients, deriving Equation 4:

$$*C_{KB}^{J\beta OX} = \frac{-J_{KB} \cdot * \mathcal{E}_X^{\beta OX}}{(J_{\beta OX} \cdot * \mathcal{E}_X^{\beta OX}) + (J_{CO_2} \cdot * \mathcal{E}_X^{CO_2}) + (J_{KB} \cdot * \mathcal{E}_X^{KB})}$$

Equation 4

Then Equation B, can be used to derive an expression for specific to the $*C^{J\beta OX}$ series, forming Equation 5:

$$*C_{\beta OX}^{J\beta OX} = \frac{(J_{KB} \cdot * \mathcal{E}_x^{KB}) + (J_{CO_2} \cdot * \mathcal{E}_x^{CO_2})}{(J_{\beta OX} \cdot * \mathcal{E}_x^{\beta OX}) + (J_{KB} \cdot * \mathcal{E}_x^{KB}) + (J_{CO_2} \cdot * \mathcal{E}_x^{CO_2})}$$

Equation 5

Application of the summation theorem gives the final flux control coefficient for the second series:

$$*C_{CO_2}^{J\beta OX} = 1 - (*C_{KB}^{J\beta OX} + *C_{\beta OX}^{J\beta OX})$$

Equation 6

Similarly, for the final series of flux control coefficients, $*C^{J_{CO_2}}$:

$$*C_{CO_2}^{J_{CO_2}} = \frac{(J_{KB} \cdot \epsilon_x^{KB}) + (J_{\beta OX} \cdot \epsilon_x^{\beta OX})}{(J_{CO_2} \cdot \epsilon_x^{CO_2}) + (J_{KB} \cdot \epsilon_x^{KB}) + (J_{\beta OX} \cdot \epsilon_x^{\beta OX})}$$

Equation 7

$$*C_{KB}^{J_{CO_2}} = \frac{-J_{KB} \cdot \epsilon_x^{CO_2}}{(J_{\beta OX} \cdot \epsilon_x^{\beta OX}) + (J_{KB} \cdot \epsilon_x^{KB}) + (J_{CO_2} \cdot \epsilon_x^{CO_2})}$$

Equation 8

$$*C_{\beta OX}^{J_{CO_2}} = 1 - (*C_{KB}^{J_{CO_2}} + *C_{CO_2}^{J_{CO_2}})$$

Equation 9

A1.8 Summary of key equations for calculation of each group flux control coefficient

For convenience, the key equations derived in this Appendix and which are used in Chapter 4, are summarised in the following tables:

Group flux control coefficient	Specific equation
$*C_{KB}^{J_{KB}}$	$*C_{KB}^{J_{KB}} = \frac{\left(\frac{\delta J_{\beta OX}(CO_2)}{\delta J_{KB}(CO_2)}\right) + \left(\frac{\delta J_{CO_2}(\beta OX)}{\delta J_{KB}(\beta OX)}\right)}{1 + \left(\frac{\delta J_{\beta OX}(CO_2)}{\delta J_{KB}(CO_2)}\right) + \left(\frac{\delta J_{CO_2}(\beta OX)}{\delta J_{KB}(\beta OX)}\right)}$
$*C_{\beta OX}^{J_{KB}}$	$*C_{\beta OX}^{J_{KB}} = \frac{-J_{\beta OX} / J_{KB}}{1 + \left(\frac{\delta J_{\beta OX}(CO_2)}{\delta J_{KB}(CO_2)}\right) + \left(\frac{\delta J_{CO_2}(\beta OX)}{\delta J_{KB}(\beta OX)}\right)}$
$*C_{CO_2}^{J_{KB}}$	$*C_{CO_2}^{J_{KB}} = 1 - (*C_{KB}^{J_{KB}} + *C_{\beta OX}^{J_{KB}})$

Table A1.2 (a) Equations used for series 1 flux control coefficients

Group flux control coefficient	Specific equation
$*C_{KB}^{J\beta OX}$	$*C_{KB}^{J\beta OX} = \frac{-J_{KB} \cdot \varepsilon_x^{\beta OX}}{(J_{\beta OX} \cdot \varepsilon_x^{\beta OX}) + (J_{CO_2} \cdot \varepsilon_x^{CO_2}) + (J_{KB} \cdot \varepsilon_x^{KB})}$
$*C_{\beta OX}^{J\beta OX}$	$*C_{\beta OX}^{J\beta OX} = \frac{(J_{KB} \cdot \varepsilon_x^{KB}) + (J_{CO_2} \cdot \varepsilon_x^{CO_2})}{(J_{\beta OX} \cdot \varepsilon_x^{\beta OX}) + (J_{KB} \cdot \varepsilon_x^{KB}) + (J_{CO_2} \cdot \varepsilon_x^{CO_2})}$
$*C_{CO_2}^{J\beta OX}$	$*C_{CO_2}^{J\beta OX} = 1 - (*C_{KB}^{J\beta OX} + *C_{\beta OX}^{J\beta OX})$

Table A1.2 (b) Equations used for series 2 flux control coefficients

Group flux control coefficient	Specific equation
$*C_{KB}^{JCO_2}$	$*C_{KB}^{JCO_2} = \frac{-J_{KB} \cdot \varepsilon_x^{CO_2}}{(J_{\beta OX} \cdot \varepsilon_x^{\beta OX}) + (J_{KB} \cdot \varepsilon_x^{KB}) + (J_{CO_2} \cdot \varepsilon_x^{CO_2})}$
$*C_{\beta OX}^{JCO_2}$	$*C_{\beta OX}^{JCO_2} = 1 - (*C_{KB}^{JCO_2} + *C_{CO_2}^{JCO_2})$
$*C_{CO_2}^{JCO_2}$	$*C_{CO_2}^{JCO_2} = \frac{(J_{KB} \cdot \varepsilon_x^{KB}) + (J_{\beta OX} \cdot \varepsilon_x^{\beta OX})}{(J_{CO_2} \cdot \varepsilon_x^{CO_2}) + (J_{KB} \cdot \varepsilon_x^{KB}) + (J_{\beta OX} \cdot \varepsilon_x^{\beta OX})}$

Table A1.2 (c) Equations used for series 3 flux control coefficients

Reference list

- Abo-Hashema KAH, Cake M, Lucas MA and Knusden J. Evaluation of the affinity and turnover number of both hepatic mitochondrial and microsomal carnitine acyltransferases: relevance to intracellular partitioning of Acyl-CoAs. *Biochemistry*. **38**, 15840-15847. 1999.
- Agius L, Meredith E and Sherratt HSA. Stereospecificity of the inhibition by etomoxir of fatty acid and cholesterol synthesis in isolated hepatocytes. *Biochem Pharmacol*. **42**, 1717-1720. 1991(a).
- Agius L, Peak M and Sherratt HSA. Differences between human, rat and guinea pig hepatocyte cultures - a comparative study of their rates of beta-oxidation and esterification of palmitate and their sensitivity to R-etomoxir. *Biochem Pharmacol* **42**, 1711-1715. 1991(b).
- Aldoretta PW and Hay WW. Fetal nutrition. *Nutri Res*. **14**, 929-965. 1994.
- Anderson MR and Blumer JL. Advances in the therapy for sepsis in children. *Ped Clinics*. **44**(1), 179-205. 1997.
- Anderson RC, Balestra M, Bell PA, Deems RO, Fillers WS, Foley JE, Fraser JD, Mann WR, Rudin M and Villhauer EB. Antidiabetic agents: a new class of reversible carnitine palmitoyltransferase I inhibitors. *J Med Chem*. **38**, 3448-3450. 1995.
- Aprille JR. Perinatal development of mitochondria in rat liver. In *Mitochondrial Physiology and Pathology*. Fiskum G (Ed) New York. Von Nostrand Reinhold 66-99. 1986.
- Arias G, Asins G, Hegardt FG and Serra D. The effect of fasting/refeeding and insulin treatment on the expression of the regulatory genes of ketogenesis in intestine and liver of suckling rats. *Arch Biochem Biophys*. **340**, 287-298. 1997.
- Asins G, Serra D, Arias G and Hegardt FG. Developmental changes in carnitine palmitoyltransferases I and II gene expression in intestine and liver of suckling rats. *Biochem J*. **306**, 379-384. 1995.
- Astiz M, Rackow EC, Weil MH, Schumer W. Early impairment of oxidative metabolism and energy production in severe sepsis. *Circ Shock*. **26**, 311-320. 1988.
- Augenfeld J and Fritz IB. Carnitine palmitoyltransferase activity and fatty acid oxidation by livers from fetal and neonatal rats. *Can J Biochem*. **48**, 288-294. 1970.
- Aw TY and Grigor MR. Digestion and absorption of milk triacylglycerols in 14 day old suckling rats. *J Nutr*. **110**, 2133-2140. 1980.
- Ayala A, Evans TA and Chaudry IH. Does hepatocellular injury in sepsis involve apoptosis? *J Surg Res*. **76**, 165-173. 1998.
- Aynsley-Green A, Hawdon JM, Deshpande S, Platt MW, Lindley K and Lucas A. Neonatal insulin secretion: implications for the programming of metabolic homeostasis. *Acta Paed Jpn*. **39**, S21-5. 1997.

- Bailey E and Lockwood EA. Some aspects of fatty acid oxidation and ketone body formation and utilization during development of the rat. *Enzyme*. **15**, 239-253. 1973.
- Balasse EO and Fery F. Ketone body production and disposal: effects of fasting, diabetes and exercise. *Diabetes Metab Rev*. **5**, 247-270. 1989.
- Ballard FJ and Oliver IT. Glycogen metabolism in embryonic chick and neonatal rat liver. *Biochem Biophys Acta*. **71**, 578-588. 1963.
- Bardsley WG and Prasad N. Using ASCII text files in post fit notation (reverse polish) to define mathematical models and systems of differential equations for simulation and non-linear regression. *Computers Chem*. **21**, 71-82. 1997.
- Barke RA, Brady PS and Brady LJ. The effect of peritoneal sepsis on hepatic gene expression and mitochondrial fat oxidation. *Surg Forum*. **XLII**, 62. 1991.
- Barke RA, Birklid S, Chaplin RB, Roy S, Brady PS and Brady LJ. The effect of surgical treatment following peritoneal sepsis on hepatic gene expression. *J Surg Res*. **60**, 101-106. 1996.
- Barker DJ. Outcome of low-birth-weight. *Hormone Res*. **42**, 223-230. 1994.
- Bartlett K, Bhuiyan AK, Aynsley-Green A, Butler PC and Alberti KG. Human forearm arteriovenous differences of carnitine, short-chain acylcarnitine and long-chain acylcarnitine. *Clin Sci*. **77**, 413-416. 1989.
- Battaglia FC and Meschia G. Principal substrates of fetal metabolism. *Physiol Rev*. **58**, 499-527. 1978.
- Battaglia FC and Meschia G. An introduction to fetal physiology. New York. Academic. 1986.
- Bazzoni F and Beutler B. The tumour necrosis factor ligand and receptor families. *Seminars in Medicine*. 1717-1725. 1996.
- Beard A, Cornblath M, Gentz F, Kellium M, Persson B, Zetterstrom K and Haworth JC. *J Pediatr*. **79**, 314-324. 1971.
- Becker WF, von Jagow G, Anke T and Steglich W. Oudemansin, Strobilurin A, Strobilurin B and myxothiazol: new inhibitors of the bc1 segment of the respiratory chain with an E methoxyacrylate system as the common structural element. *FEBS Letts*. **132**, 329-333. 1981.
- Benito M, Whitelaw E and Williamson DH. Regulation of ketogenesis during the suckling-weaning transition in the rat. *Biochem J*. **180**, 137-144. 1979.
- Berry MN and Friend DS. High yield preparation of isolated rat liver parenchymal cells. *J Cell Biol*. **43**, 506-520. 1969.
- Berry MN, Farrington C, Gay S, Grivell AR and Wallace PG. In *Isolation, characterisation and use of hepatocytes*. Harris RA and Gornell NW (eds). Elsevier. 7. 1983.
- Berry MN, Edwards AM and Barritt GJ. Laboratory techniques in biochemistry and molecular biology. Burdon RH and Van Knippenberg PH (eds). Elsevier. 1991.

- Berry MN and Phillips J. The isolated hepatocyte preparation: 30 years on. *B Soc Trans* **28** 131-135. 2000.
- Beylot M, Guiraud M, Grau G and Bouletreau P. Regulation of ketone body flux in septic patients. *Am J Physiol.* **257**, E665-E674. 1989.
- Beylot M, Vidal H, Mithieux G, Odeon M, and Martin C. Inhibition of hepatic ketogenesis by tumour necrosis factor in rats. *Am J Physiol.* E897-E902. 1992.
- Bhuiyan AKMJ, Pande SV. Unexpected stimulation of carnitine palmitoyltransferase (CPT) activities by bovine serum albumin with octanoyl-CoA as substrate. *FASEB Journal.* **5**, A593. 1991.
- Bhuiyan AKMJ, Pande SV. Carnitine palmitoyltransferase activities effects of serum albumin, acyl-CoA-binding protein and fatty acid binding protein. *Mol Cell Biol.* **139**, 109-116. 1994.
- Bitman J, Wood DL, Hamosh M, Hamosh P and Mehta NR. Comparison of the lipid composition of breast milk from mothers of term and preterm infants. *Am J Clin Nutr.* **38**, 300-312. 1983.
- Blackman FF. Optima and limiting factors. *Ann Bot.* **19**, 281. 1905.
- Blazquez E, Sugase M and Blazquez M. Neonatal changes in the concentration of liver c-amp and of serum glucose, FFA, insulin, pancreatic and total glucagons in man and in the rat. *J Lab Clin Med.* **83**, 957-967. 1974.
- Bonnefont JP, Jaroni F, Cavadini P, Capanec C, Brovet M and Saudubray JM *et al.*, Molecular analysis of CPTII deficiency with hepatocardiomyocardial expression. *Am J Hum Genet.* **58**, 971-978. 1996.
- Bonnefont JP, Demaugre F, Prip-Buus C, Saudubray JM, Brivet M, Abadi N and Thuillier L. Carnitine palmitoyltransferase deficiencies. *Mol Genetics Met.* **68**. 424-440. 1999.
- Brand MD, Hafner RP and Brown GC. Control of respiration in non-phosphorylating mitochondria is shared between the proton leak and the respiratory chain. *Biochem J.* **255**, 535-539. 1988.
- Brand MD, Vallis BPS and Kessler A. The sum of flux control coefficients for the electron-transport chain of mitochondria. *Eur J Biochem.* **226**, 819-829. 1994.
- Brand MD and Kessler A. Control analysis of energy metabolism in mitochondria. *B Soc Trans.* **37**. 1995.
- Brand MD. Top down metabolic control analysis. *J Theor Biol.* **182**, 351-360. 1996.
- Bremer J and Norum KR. Palmitoyl CoA:carnitine o-palmitoyltransferase in the mitochondrial oxidation of palmitoyl CoA. *Eur J Biochem.* **1**, 427-433. 1967(a).
- Bremer J and Norum KR. The mechanism of substrate inhibition of palmitoyl Co enzyme A: carnitine palmitoyltransferase by palmitoyl Co enzyme A. *J Biol Chem.* **242**, 1744-1748. 1967(b).

- Bremer J and Osmundsen H. Fatty acid oxidation and its regulation. In *Fatty acid metabolism and its regulation*. Numa S (ed). Amsterdam: Elsevier. 7, 113-154. 1984
- Brivet M, Boutron A, Slama A, Costa C, Thuillier L, Demaugre F, Rabier D, Saudubray JM and Bonnefont JP. Defects in activation and transport of fatty acids. *J Inher Met Dis*. 22, 428-441. 1999.
- Brosnan JT and Qian D. Endotoxin-induced increase in liver mass and hepatocyte volume. *B Soc Trans*. 22, 529-532. 1994.
- Brown G, Larkin-Thomas PL and Brand MD. Control of respiration and oxidative phosphorylation in isolated rat liver cells. *Eur J Biochem*. 192, 355-362. 1990.
- Brown GC, Hafner RP and Brand MD. A top down approach to the determination of control coefficients in metabolic control theory. *Eur J Biochem*. 188, 321-325. 1990.
- Carcillo JA and Cunnion RE. Septic shock. *Crit Care Clin*. 13, 553-574. 1997.
- Carpenter K, Pollitt RJ and Middleton B. Human liver long-chain 3-hydroxyacyl-Coenzyme-A dehydrogenase is a multifunctional membrane-bound beta-oxidation enzyme of mitochondria. *Biochem Biophys Res Comm*. 183, 443-448. 1992.
- Carroll JE, McGuire BS, Chancey VF and Harrison KB. Acyl-CoA dehydrogenase enzymes during early postnatal development in the rat. *Biol Neonate*. 55, 185-190. 1989.
- Castell JV, Gomez-Lechon MJ, David M, Andus T, Geiger T, Trullenque R, Fabra R and Heinrich PC. Interleukin 6 is the major regulator of acute phase protein synthesis in adult human hepatocytes. *FEBS Letts*. 242, 237-239. 1989.
- Chalk PA, Higham FC, Caswell AM and Bailey E. Hepatic mitochondrial fatty acid oxidation during the perinatal period in the rat. *Int J Biochem*. 15, 531-538. 1983.
- Chan SI and Li PM. Cytochrome c oxidase: understanding nature's design of a proton pump. *Biochemistry*. 29, 1-12. 1990.
- Chattergee B, Song CS, Kim JM and Roy AY. Cloning, sequencing and regulation of rat liver carnitine octanoyltransferase: transcriptional stimulation of the enzyme during peroxisomes proliferation. *Biochemistry*. 27, 9000-9006. 1988.
- Chioléro R, Revely JP and Tappy L. Energy metabolism in sepsis and injury. *Nutrition*. 13, S45-S51. 1997.
- Christiansen RZ. Regulation of palmitate metabolism by carnitine and glucagons in hepatocytes isolated from fasted and carbohydrate refeed rats. *Biochem Biophys Acta*. 488, 249-262. 1977.
- Clarke SD and Armstrong MK. Cellular lipid binding proteins: expression, function and nutritional regulation. *FASEB*. 3, 2480-2487. 1989.

- Clark JB, Bates TE, Cullingford T and Land JM. Development of enzymes of energy-metabolism in the neonatal mammalian brain. *Dev Neurosci.* **15** 174-180. 1993.
- Clouet P, Niot I, Gresti J, Demarquoy J, Boichot J, Durand G and Bezard J. Polyunsaturated n-3 and n-6 fatty-acids at a low-level in the diet alter mitochondrial outer-membrane parameters in wistar rat-liver. *J Nutr Biochem.* **6**, 11, 626-634. 1995.
- Cohen I, Kohl C, McGarry JD, Girard J and Prip-Buus C. The N-terminal domain of rat liver carnitine palmitoyltransferase I mediates impart into the outer mitochondrial membrane and is essential for activity and malonyl-CoA sensitivity. *J Biol Chem.* **273**, 29896-904. 1998.
- Cook GA, Otto DA and Cornell NW. Differential inhibition of ketogenesis by malonyl-CoA in mitochondria from fed and starved rats. *Biochem J.* **192**, 955-8. 1980.
- Cooperstock MS, Tucker RP and Baubles JV. Possible pathogenic role of endotoxin in Reye's Syndrome. *Lancet.* **1**, 1272-1274. 1975.
- Corkey BE, Hale DE, Glennon MC, Kelley R, Coates PM and Kilpatrick L. Relationship between unusual hepatic acyl coenzyme-A profiles and the pathogenesis of Reye's Syndrome. *J Clin Invest.* **82**, 782-788. 1988.
- Crane F and Beinert H. *J Biol Chem.* **218**, 717-731. 1956.
- Cryer A and Jones HM. Changes in the lipoprotein lipase (clearing-factor lipase) activity of white adipose tissue during development of the rat. *Biochem J.* **172**, 319-325. 1978.
- Cullingford T, Bhakoo KK, Dolphin CT, Peuchen S, Patel R and Clark JB. Ketogenic enzymes in the developing brain. *J Neurochem.* **69**, S262. 1997.
- Cullingford TE, Bhakoo KK, Peuchen S, Dolphin CT and Clark JB. Regulation of the ketogenic enzyme mitochondrial 3-hydroxy-3-methylglutaryl-CoA synthase in astrocytes and meningeal fibroblasts. In *Current Views of fatty acid oxidation and ketogenesis: from organelles to point mutations*. Quant PA & Eaton S (Eds). Plenum Press. 241-251. 1999.
- Dahn MS, Mitchell RA, Lange P, Smith S and Jacobs LA. Hepatic metabolic response to injury and sepsis. *Surgery.* **117**, 520-530. 1995.
- Damas P, Ledoux D, Nys M, Vrindts Y, de Groote D, Franchimont P and Lamy M. Cytokine serum level during severe sepsis in human Il-6 as a marker of severity. *Ann Surg.* **215**(4), 356-362. 1991.
- Davis AT. Fractional contributions to total carnitine in the neonatal rat. *J Nutr.* **119**, 262-267. 1989.
- Dawkins MJR. Glycogen synthesis and breakdown in fetal and neonatal rat liver. *Ann NY Acad Sci.* **111**, 203-211. 1963.
- Dawson TL, Gores GJ, Nieminen AL, Herman B and Lemasters JJ. Mitochondria as a source of reactive oxygen species during reductive stress in rat hepatocytes. *Am J Physiol.* **264**, 961-967. 1993.

- de Duve C and Baudhuin P. Peroxisomes (microbodies and related particles). *Physiol Rev.* **46**, 323-357. 1966.
- Decaux JF, Robin D, Robin P, Ferré P and Girard J. Intramitochondrial factors controlling hepatic fatty acid oxidation at weaning in the rat. *FEBS Letts.* **232**, 156-158. 1988.
- Declercq PE, Falck JR, Kuwajima M, Tyminski H, Foster DW and McGarry JD. Characterization of the mitochondrial carnitine palmitoyltransferase enzyme-system: 1 Use of inhibitors. *J Biol Chem.* **262**, 9812-21. 1987.
- Demarne Y, Lhuilery C, Pihet J, Martinet L and Flanzy J. Comparative study of triacylglycerol fatty acids in milk from two Leporidae species: rabbit (*Oryctolagus cuniculus*) and hare (*Lepus europaeus*). *Comp Biochem Physiol.* **61**, 223-226. 1978.
- Desia M, Crowther NJ, Ozanne SE, Lucas A and Hales CN. Adult glucose and lipid metabolism may be programmed during fetal life. *B Soc Trans.* **23**, 331-335. 1995.
- di Marco PN, Ghisalberti AV, Pearce PH and Oliver IT. Postnatal changes in blood glucose, phosphopyruvate carboxylase and tyrosine aminotransferase after normal birth and premature delivery in the rat. *Biol Neonate.* **30**, 205-215. 1976.
- Dodson WE, Prensky AL, Devivo DC, Goldring S and Dodge PR. Management of seizure disorders: selected aspects. *J Pediatr.* **89**, 695-703. 1976.
- Drahota Z, Hahn P, Kleinzeller A and Kostolanska A. Acetoacetate formation by liver slices from adult and infant rats. *Biochem J.* **93**, 61-65. 1964.
- Drynan L, Quant PA and Zammit VA. Flux control exerted by mitochondrial outer membrane carnitine palmitoyltransferase over beta-oxidation, ketogenesis and tricarboxylic acid cycle activity in hepatocytes isolated from rats in different metabolic states. *Biochem J.* **317**, 791-795. 1996.
- Drynan L, Quant PA and Zammit VA. The role of changes in the sensitivity of hepatic mitochondrial overt carnitine palmitoyltransferase in determining the onset of the ketosis of starvation in the rat. *Biochem J.* **318**, 767-770. 1996.
- Duée PH, Pégorier J-P, El Manoubi L, Herbin C, Kohl C and Girard J. Hepatic triglyceride hydrolysis and development of ketogenesis in rabbits. *Am J Physiol.* **12**, E478-E484. 1985.
- Duran M, Hofkamp M, Rhead WJ, Saudubray JM, Wadman SK. Sudden child-death and healthy affected family members with medium-chain acyl-coenzyme-a dehydrogenase-deficiency. *Pediatrics.* **78**, 1052-1057. 1986.
- Duszynski J, Groen AK, Wanders RJA, Vervoorn RC and Tager JM. Quantification of the role of the adenine-nucleotide translocator in the control of mitochondrial respiration in isolated rat-liver cells. *FEBS Letts.* **146**, 262-266. 1982.
- Eaton S, Bartlett K and Pourfarzam M. Mammalian mitochondrial beta-oxidation. *Biochem J.* **320**, 345-357. 1996.
- Eaton S, Bartlett K, Pourfarzam, Markley M, New KJ and Quant PA. Production and export of acyl-carnitine esters by neonatal rat hepatocytes. In *Current Views of*

- fatty acid oxidation and ketogenesis: from organelles to point mutations*. Quant PA & Eaton S (Eds). Plenum Press. 241-251. 1999(a).
- Eaton S, Middleton B, Sherratt HAS, Pourfarzam M, Quant PA and Bartlett K. Control of mitochondrial β -oxidation at the levels of [NAD⁺]/[NADH] and Coa acylation. In *Current Views of fatty acid oxidation and ketogenesis: from organelles to point mutations*. Quant PA & Eaton S (Eds). Plenum Press. 145-154. 1999(b).
- Ebeling P and Koivisto VA. Non-esterified fatty acids regulate lipid and glucose oxidation and glycogen synthesis in healthy man. *Diabetologia*. **37**, 202-209. 1994.
- Edmond J, Auestad N, Robbins RA and Bergstrom J D. Ketone body metabolism in the neonate: development and the effect of diet. *Fed Proceedings*. **44**(4), 2359-2363. 1985.
- Emery JL, Variend S, Howart AJ and Vawter GF. Investigation of inborn-errors of metabolism in unexpected infant deaths. *Lancet*. **8601**, 29-31. 1988.
- Esser V, Britton CH, Weis, BC, Foster DW and McGarry JD. Cloning, sequencing and expression of a cDNA encoding rat liver carnitine palmitoyltransferase I: direct evidence that a single polypeptide is involved in inhibitor interaction and catalytic function. *J Biol Chem*. **268**, 5817-5822. 1993(a).
- Esser V, Kuwajima M, Britton CH, Krishnan K, Foster DW and McGarry JD. Inhibitors of mitochondrial carnitine palmitoyltransferase I limit the action of proteases on the enzyme: isolation and partial amino acid analysis of a truncated form of the rat liver isozyme. *J Biol Chem*. **268**, 5810-5816. 1993(b).
- Færgeman NJ and Knusden J. Role of long-chain fatty acyl-CoA esters in the regulation of metabolism and cell signalling. *Biochem J*. **323** 1-12. 1997.
- Fell DA and Snell K. Control analysis of mammalian serine biosynthesis: feedback on the final step. *Biochem J*. **256**, 97-101. 1988.
- Fell DA and Thomas S. Physiological control of metabolic flux - the requirement for multi-site modulation. *Biochem J*. **311**, 35-39. 1995
- Fell DA. Metabolic control analysis: a survey of its theoretical and experimental development. *Biochem J* **286**, 313-330. 1992
- Fell DA. Understanding the control of metabolism. Snell K (Ed). Portland Press, London 1997
- Fell DA. Increasing the flux in metabolic pathways: A metabolic control analysis perspective. *Biotech bioeng*. **58**, 121-124. 1998.
- Fernandez E, Valcarce C, Cuezva JM and Medina JM. Postnatal hypoglycaemia and gluconeogenesis in the newborn rat: delayed onset of gluconeogenesis in prematurely delivered newborns. *Biochem J*. **214**, 525-532. 1983.
- Fernando-Warnakulasurya GJP, Staggers JE, Frost SC and Wells MA. Studies on fat digestion, absorption and transport in the suckling rat. *J lipid Res*. **22**, 668-674. 1981.

- Ferré P, Pégorier J-P and Girard J. The effects of inhibition of gluconeogenesis in suckling newborn rats. *Biochem J.* **162**, 209-212. 1977.
- Ferré P, Pégorier J-P, Williamson DH and Girard J. The development of ketogenesis at birth in the rat. *Biochem J.* **176**, 759-765. 1978.
- Ferré P, Satabin O, El Manoubi L, Callikan S and Girard J. Relationship between ketogenesis and gluconeogenesis in isolated hepatocytes from newborn rats. *Biochem J.* **200**, 429-433. 1981.
- Fink MP and Heard SO. Laboratory models of sepsis and septic shock. *J Surg Res.* **49**, 186-196. 1990.
- Finocchiaro G, Ito K and Tanaka K. Purification and properties of short chain acyl-CoA, medium chain acyl-CoA, and isovaleryl-CoA dehydrogenases from human-liver. *J Biol Chem.* **262**, 7982-7989. 1987.
- Foley JE. Rationale and application of fatty acid oxidation inhibitors in treatment of diabetes mellitus. *Diabetes Care.* **15**, 773-784. 1992.
- Foster PC and Bailey E. Changes in the activities of the enzymes of hepatic fatty acid oxidation during development of the rat. *Biochem J.* **154**, 49-56. 1976.
- Fraser F, Corstorphine CG and Zammit VA. Topology of carnitine palmitoyltransferase I in the mitochondrial membrane. *Biochem J.* **323**, 711-718. 1997.
- Fraser F and Zammit VA. Enrichment of carnitine palmitoyltransferases I and II in the contact sites of rat liver mitochondria. *Biochem J.* **329**, 225-229. 1998.
- Fromenty B, Freneaux E, Labbe G, des Champs D, Larrey D, Letteron P and Pessayre D. Tianeptine, a new tricyclic antidepressant metabolized by beta-oxidation of its heptanoic side-chain, inhibits the mitochondrial oxidation of medium and short-chain fatty acids. *Biochem Pharm.* **38**, 3743-3751. 1989.
- Frost SC and Wells MA. Comparison of the utilization of medium and long chain fatty acids for oxidation and ketogenesis in the suckling rat: *in vivo* and *in vitro* studies. *Arch Biochem Biophys.* **2**, 537-546. 1981.
- Furuta S, Miyazawa S and Hashimoto T. Purification and properties of rat-liver acyl-CoA dehydrogenases and electron-transfer flavoprotein. *J Biochem (Tokyo).* **90**, 1739-50. 1981.
- Galanos C, Rietschel ET, Luderitz O and Westphal O. Biological activities of lipid A complexed with bovine-serum albumin. *Eur J Biochem.* **31**, 230-233. 1972.
- Gallop DM, Seifter S and Meilman E. *J Biol Chem.* **227**, 891. 1957.
- Garland PB, Shepherd D, Nicholls DG and Ontko J. Energy dependent control of TCA cycle by fatty acid oxidation in rat liver mitochondria. *Adv Enzyme Reg.* **6**, 3-30. 1968.
- Geelmuyden HC. *Z. Physiol Chem.* **23**, 431-475. 1897.
- Gehring U and Riepertinger C. Dissoziation und reconstitution der thiolase. *Eur J Biochem.* **6**, 281-292. 1968.

- Genzel-Boroviczényi O, Wahle J and Koletzko B. Fatty acid composition of human milk during the first month after term and pre-term delivery. *Eur J Pediatrics*. **156**, 142-147. 1997.
- Gibson RA and Kneebone GM. Fatty acid composition of human colostrums and mature breast milk. *Am J Clin Nutr*. **34**, 252-257. 1981.
- Giovanni M, Riva E and Agostoni C. Fatty acids in pediatric nutrition. *Pediatric Nutrition*. **42**(4), 861-873. 1995.
- Girard J, Cuendet GS, Marliss EB, Kervran A, Rieutort M and Assan R. Fuels, hormones and liver metabolism at term and during the early postnatal period in the rat. *J Clin Invest*. **52**, 3190-3200. 1973.
- Girard J and Ferré P. Metabolic and hormonal changes around birth. In *Biochemical development of the fetus and neonate*. Jones CT (Ed). Amsterdam Elsevier. 517-551. 1982.
- Girard J, Duée P-H, Ferré P, Pégorier J-P, Escriva F and Decaux JF. Fatty acid oxidation and ketogenesis during development. *Reprod Nutri Dev*. **25**, 303-319. 1985.
- Girard J, Ferré P, Pégorier J-P and Duée P-H. Adaptations of glucose and fatty acid metabolism during perinatal period and suckling-weaning transition. *Physiol Rev*. **72**, 507-562. 1992.
- Glatz JFC and Veerkamp JH. Intracellular fatty acid binding proteins. *Int J Biochem*. **17**, 13-22. 1985.
- Gordon JI, Elshourbagy N, Lowe JB, Liao WS and Alpers DH. Tissue specific expression and developmental regulation of two genes coding for the rat fatty acid binding proteins. *J Biol Chem*. **260**, 1995-1998. 1985.
- Grantham BD and Zammit VA. Role of carnitine palmitoyltransferase I in the regulation of hepatic ketogenesis during the onset and reversal of chronic diabetes. *Biochem J*. **249**, 409-414. 1988.
- Green A and Hall SM. Investigation of metabolic disorders resembling Reyes Syndrome. *Arch Dis Child*. **67**, 1313-1317. 1992.
- Grenville GD and Tubbs PK. The catabolism of long-chain fatty acids in mammalian tissues. *Essays in biochemistry*. **4**, 155-212. 1968.
- Groen AK, Wanders RJA, Westerhoff HV, van der Meer R and Tager JM. Quantification of the contribution of various steps to the control of mitochondrial respiration. *J Biol Chem*. **257**, 2754-2757. 1982.
- Groop LC, Bonadonna RC, Shank M, Petrides AS and DeFronzo RA. Role of fatty acids and insulin in determining free fatty acid and lipid oxidation in man. *J Clin Invest*. **87**, 83-89. 1991.
- Grunfeld C and Palladino Jr MA. Tumour necrosis factor: antitumour, metabolic and cardiovascular activities. *Adv Int Med*. **35**, 45-72. 1990.
- Grunfeld C and Feingold KR. The metabolic effects of tumour necrosis factor and other cytokines. *Biotherapy*. **3**, 143-158. 1991.

- Guthrie JP and Jordan F. Amine-catalysed decarboxylation of acetoacetic acid. The rate constant for decarboxylation of beta-immino acid. *J Am Chem Soc.* **94**, 9136-9141. 1972.
- Gutknecht J. Aspirin, acetaminophen and proton transport through phospholipid bilayers and mitochondrial membranes. *Mol Cell Biochem.* **114**, 3-8. 1992.
- Guzmán M and Geelen MJH. Short-term regulation of carnitine palmitoyltransferase activity in isolated rat hepatocytes. *Biochem Biophys Res.* **151**(2), 781-787. 1988.
- Guzmán M and Geelen MJH. Activity of carnitine palmitoyltransferase in mitochondrial outer membranes and peroxisomes in digitonin-permeabilized hepatocytes. *Biochem J.* **287**, 487-492. 1992.
- Guzmán M and Geelan MJH. Regulation of fatty acid oxidation in mammalian liver. *Biochem Biophys Acta.* **1167**, 227-241. 1993.
- Guzmán M, Kolodziej MP, Caldwell A, Corstorphine CG and Zammit VA. Evidence against direct involvement of phosphorylation in the activation of carnitine palmitoyltransferase by okadaic acid in rat hepatocytes. *Biochem J.* **300**, 693-699. 1994.
- Guzmán M, Velasco G, Castro J and Zammit, VA. Inhibition of carnitine palmitoyltransferase I by hepatocyte swelling. *FEBS Letts.* **344**, 239-241. 1994.
- Guzmán M, Klein W, del Pulgar TG and Geelen MJH. Metabolism of trans fatty acids by hepatocytes. *Lipids.* **34**, 381-386. 1999.
- Guzmán M, Velasco G and Geelen MJH. Do cytoskeletal components control fatty acid translocation into liver mitochondria? *Trends Endocrinology and metabolism.* **11**, 49-53. 2000.
- Hafner RP, Brown GC and Brand MD. Analysis of the control of respiration rate, phosphorylation rate, proton leak rate and proton motive force in isolated mitochondria using the 'top-down' approach of metabolic control theory. *Eur J Biochem.* **188**, 313-319. 1990.
- Hahn P and Novak M. Development of brown and white adipose tissue. *J Lipid Res.* **16**, 79-91. 1975.
- Halestrap AP. Pyruvate and ketone body transport across the mitochondrial membrane: exchange properties, pH dependence and mechanism of carrier. *Biochem J.* **172**, 377-387. 1978.
- Hamosh M. Fat digestion in the newborn: the role of lingual lipase and periduodenal digestion. *Pediatric Research.* **13**, 615-622. 1979.
- Hamosh M and Hamosh P. Lingual and gastric lipases during development. *In Human gastrointestinal development.* Lebenthal E (Ed). Raven. 251-276. 1989.
- Hamosh M. Lipid metabolism. *In Neonatal nutrition and metabolism.* Hay M (Ed). Mosby Year Book Inc. St Louis USA. 1991.

- Hamosh M. Lipid metabolism in pediatric nutrition. *Pediatric Nutrition*. **42**(4), 839-855. 1995.
- Hardie D. Regulation of fatty-acid and cholesterol-metabolism by the AMP-activated protein-kinase. *Biochim Biophys Acta*. **1123**, 231-238. 1992.
- Hargrove DM, Bagby GJ, Lang CH and Spitzer JJ. Adrenergic blockade prevents endotoxin-induced increases in glucose metabolism. *Am J Physiol*. **255**, E629-E635. 1983.
- Harpey JP, Charpentier C and Patumeau-Jouas M. Sudden infant death syndrome and inherited disorders of fatty acid β -oxidation. *Biol Neonate*. **58**, 70-80. 1990.
- Harrison J, Hodson AW, Skillen AW and Stappenbeck R. Blood glucose, lactate, pyruvate, glycerol, β -hydroxybutyrate and acetoacetate measurements in man using a centrifugal analyser with a fluorometer attachment. *J Clin Chem Biochem*. **26**, 141-146. 1988.
- Harzer G, Hang M, Dieterich I and Gentner PR. Changing patterns of human milk lipids in the course of the lactation and during the day. *Am J Clin Nutr*. **37**, 612-621. 1983.
- Hass GM and Hill RL. The subunit structure of crotonase. *J Biol Chem*. **244**, 6080-6086. 1969.
- Hatefi Y. The mitochondrial electron transport and oxidative phosphorylation system. *Ann Rev Biochem*. **54**, 1015-1069. 1985.
- Hawdon JM, Ward Platt MP and Aynsley-Green A. Patterns of metabolic adaptation for preterm and term infants in the first neonatal week. *Arch Dis Child*. **67**, 357-365. 1992.
- Hawdon JM, Weddell A, Aynsley-Green A and Ward Platt MP. Hormonal and metabolic response to hypoglycaemia in small for gestational age infants. *Arch Dis Child*. **68**, 269-273. 1993.
- Hawdon JM and Ward Platt MP. Metabolic adaptation in small for gestational age infants. *Arch Dis Child*. **68**, 262-268. 1993.
- Hawdon JM, Aynsley-Green A and Ward Platt MP. Neonatal blood glucose concentrations: metabolic effects of intravenous glucagon and intragastric medium chain triglyceride. *Arch Dis Child*. **68**, 255-261. 1993.
- Hawdon JM, Ward Platt MP and Aynsley-Green A. Prevention and management of neonatal hypoglycaemia. *Arch Dis Child*. **70**, F60-F64. 1994.
- Hawdon JM. Hypoglycaemia of the neonatal brain. *Eur J Ped*. **158**, S9-S12. 1999.
- Hawkins RA, Williamson DH and Krebs HA. Ketone body utilization by adult and suckling rat brain *in vivo*. *Biochem J*. **122**, 13-18. 1971.
- Hay W. Fetal and neonatal glucose homeostasis and their relation to the small for gestational age infant. *Semin Perinatol*. **8**, 101-116. 1984.
- Hegardt FG. Regulation of mitochondrial 3-hydroxy-3-methylglutaryl-CoA synthase gene expression in liver and intestine from the rat. *B Soc Trans* **23**. 1995.

- Hegardt FG. Mitochondrial 3-hydroxy-3-methylglutaryl-CoA synthase: a control enzyme in ketogenesis. *Biochem J.* **338**, 569-582. 1999.
- Heim T. How to meet the lipid requirements of the premature infant. *Ped Clin Nrth Am.* **32**, 289-317. 1985.
- Heimberg M, Weinstein J and Kohout M. The effects of glucagons dibutyryl cyclic adenosine 3'5'monophosphate and concentration of free fatty acids on hepatic lipid metabolism. **244**, 5131-5139. 1969.
- Heinisch J. Isolation and characterization of the two structural genes coding for phosphofructokinase in yeast. *Mol Gen Genet.* **194**, 75-82. 1986.
- Heinrich PC, Castell JV, Andus T. Interleukin-6 and the acute phase response. *Biochem J.* **265**, 621-636. 1990.
- Heinrich R and Rapoport TA. A linear steady-state treatment of enzymatic chains. General properties, control and effector strength. *Eur J Biochem.* **42**, 89-95. 1974(a).
- Heinrich R and Rapoport TA. A linear steady-state treatment of enzymatic chains. Critique of the crossover theorem and a general procedure to identify interaction sites with an effector. *Eur J Biochem.* **42**, 97-105. 1974(b).
- Helander HF and Olivecrona T. Lipolysis and lipid absorption in the stomach of the suckling rat. *Gastroenterology.* **59**, 22-35. 1970.
- Helle M, Brakenhoff JPJ, De Groot ER and Aarden LA. Interleukin 6 is involved in interleukin 1 induced activity. *Eur J Immunol.* **18**, 957-959. 1988.
- Henning SJ. Postnatal development: coordination of feeding, digestion and metabolism. *Am J Physiol.* **241**, G199-G214. 1981.
- Herbin C, Pégrier JP, Duée PH, Kohl C and Girard J. Regulation of fatty acid oxidation in isolated hepatocytes and liver mitochondria from newborn rabbit. *Eur J Biochem.* **165**, 201-207. 1987.
- Herzfeld A, Federman M and Greengard O. Subcellular morphometric and biochemical analysis of developing rat hepatocytes. *J Cell Biol.* **57**, 475-493. 1973.
- Hesler CB, Olymbios C and Haldar D. Transverse-plane topography of long-chain acyl-CoA synthetase in the mitochondrial outer-membrane. *J Biol Chem.* **265**, 6600-6605. 1990.
- Horan MA, Little RA, Rothwell NJ and Strijbos PJ. Comparison of the effects of several endotoxin preparations and body temperature and metabolic rate in the rat. *Can J Phys Pharm.* **67**, 1011-1014. 1989.
- Horie S, Ishii H and Suga T. Developmental changes in the characteristics of peroxisomal fatty acid oxidation system in rat liver. *Life Sci.* **29**, 1649-1656. 1981.
- Hull S. *E Coli* lipopolysaccharide in pathogenesis and virulence. In: *Mechanism of virulence*. Susman M (Ed). CUP, 145-165. 1997.

- Idell-Wenger JA. Carnitine - acyl-carnitine translocase of rat-heart mitochondria - competition for carnitine uptake by carnitine esters. *J Biol Chem.* **256**, 5597-5603. 1981
- Ikeda Y, Dabrowski C and Tanaka K. Separation and properties of 5 distinct acyl-CoA dehydrogenases from rat liver mitochondria: identification of a new 2-methyl branched chain acyl-CoA dehydrogenase. *J Biol Chem.* **258**, 1066-1076. 1985.
- Indiveri C, Tonazzi A and Palmieri F. Identification and purification of the carnitine carrier from rat liver mitochondria. *Biochim Biophys Acta.* **1020**, 81-86. 1990.
- Indiveri C, Tonazzi A and Palmieri F. Characterisation of the unidirectional transport of carnitine catalysed by the reconstituted carnitine carrier from rat liver mitochondria. *Biochim Biophys Acta.* **1069**, 110-116. 1991.
- Izai K, Uchida Y, Orii T, Yamamoto S and Hashimoto T. Novel fatty-acid beta-oxidation enzymes in rat-liver mitochondria(1): Purification and properties of very-long-chain acyl-coenzyme-a dehydrogenase. *J Biol Chem.* **267**, 1027-1033. 1992.
- Jackson S, Kler RS, Bartlett K, Briggs H, Bindoff LA, Pourfarzam M, Gardner-Medwin D and Turnbull DM. Combined enzyme defect of mitochondrial fatty-acid oxidation. *J Clin Invest.* **90**, 1219-1225. 1992.
- Jackson VN, Cameron JM, Zammit VA and Price NT. Sequencing and functional expression of the malonyl-CoA sensitive carnitine palmitoyltransferase from *Drosophila melanogaster*. *Biochem J.* **341**, 483-489. 1999.
- Jenness R. Biosynthesis and composition of milk. *J Invest Dermatol.* **63**, 109-118. 1974.
- Jepson MM, Pell JM, Bates PC and Millward DJ. The effects of endotoxaemia on protein metabolism in skeletal muscle and liver of fed and fasted rats. *Biochem J.* **235**, 329-336. 1986.
- Kacser H and Burns JA. The control of flux. *Symp Soc Exp Biol.* **27**, 65-104. 1973.
- Kacser H and Burns JA. Molecular democracy: who shares the controls? *B Soc Trans.* **7**, 1149-1160. 1979.
- Kacser H and Acerenza L. A universal method for achieving increases in metabolite production. *Eur J Biochem.* **216**, 361-367. 1993.
- Kacser H and Burns JA. The control of flux: 21 years on. *B Soc Trans.* **23**, 341-364. 1995.
- Kacser H. Recent developments beyond metabolic control analysis. *B Soc Trans.* **23**, 387-391. 1995
- Kaminski MV, Neufeld HA and Pace JG. Effect of inflammatory and non-inflammatory stress on plasma ketone bodies and free fatty acids and on glucagon and insulin in peripheral and portal blood. *Inflammation.* **3**, 289-294. 1979.

- Kantrow SP, Taylor DE, Carraway MS and Piantadosi CA. Oxidative metabolism in rat hepatocytes and mitochondria during sepsis. *Arch Biochem Biophys*. **345**(2), 278-288. 1997.
- Kashfi K, Weakley J and Cook GA. Effects of diabetes on the carnitine palmitoyltransferase of isolated hepatic mitochondrial outer membranes. *B Soc Trans*. **16**, 1010-1011. 1988.
- Kell DB and Mendes P. Snapshots of systems - metabolic control analysis and biotechnology in the post-genomic era. <http://gepasi.dbs.aber.ac.uk/dbk/mca99bio.htm> 1999;
- Killenbergh PG, Davidson ED and Webster Jr L. Evidence for a medium chain fatty acid:CoA ligase (AMP) that activates salicylate. *Mol Pharmacol*. **7**, 260-268. 1971.
- Kilpatrick L, Polin RA, Douglas SD and Corkey BE. Hepatic metabolic alterations in rats treated with low-dose endotoxin and aspirin: an animal model of Reyes Syndrome. *Metabolism*. **38**, 73-77. 1989.
- Kliegman RM and Sparks JW. Perinatal galactose metabolism. *J Pediatr*. **107**, 831-841. 1985.
- Knoop F. *Beitr Chem Physiol Path*. **6**, 150-162. 1905.
- Koeslag JH, Noakes TD and Sloan AW. Post exercise ketosis. *J Physiol*. **301**, 79-90. 1980.
- Kolodziej MP and Zammit VA. Re-evaluation of the interaction of malonyl-CoA with the rat liver mitochondrial carnitine palmitoyltransferase system by using purified outer membranes. *Biochem J*. **267**, 85-90. 1990.
- Kolodziej MP, Crilly PJ, Corstophine CG and Zammit VA. Development and characterisation of a polyclonal antibody against rat liver overt carnitine palmitoyltransferase (CPT I). *Biochem J*. **282**, 415-421. 1992.
- Kolodziej MP and Zammit VA. Mature carnitine palmitoyltransferase-I retains the N-terminus of the nascent protein in rat-liver. *FEBS Letts*. **327**, 294-296. 1993.
- Koren Z and Shafir E. *Proc Soc Exp Biol Med*. **116**, 411-414. 1964.
- Kossodo S, Houba V, Grau GE and WHO. Assaying tumour necrosis factor concentrations in human serum - A WHO International Collaborative Study. *J Imm Methods*. **182**, 107-114. 1995.
- Krahling JB, Gee R, Gauger JA and Tolbert NE. Postnatal development of peroxisomal and mitochondrial enzymes in rat liver. *J Cell Physiol*. **101**, 375-390. 1979.
- Krauss S and Quant PA. Regulation and control in complex, dynamic metabolic systems - experimental application of the top-down approaches of metabolic control analysis to fatty acid oxidation and ketogenesis. *J Theor Biol*. **182**, 381-388. 1996

- Krauss S, Lascelles CV, Zammit VA and Quant PA. Flux control exerted by overt carnitine palmitoyltransferase over palmitoyl-CoA oxidation and ketogenesis is lower in suckling than in adult rats. *Biochem J.* **319**, 427-433. 1996.
- Krebs H. The role of citric acid in intermediate metabolism in animal tissues. *Enzymologia.* **4**, 148-156. 1937.
- Krisans SK, Mortensen RM and Lazarow PB. Acyl-CoA synthetase in rat liver peroxisomes: computer assisted analysis of cell fractionization experiments. *J Biol Chem.* **255**, 9599-9607. 1980.
- Kunz WS. Application of the theory of steady-state flux control to mitochondrial beta-oxidation. *Biomed Biochem Acta.* **50**, 1143-1157. 1991.
- Kuratsune H, Watanabe Y, Yamaguti K, Jacobson G, Takahshi M, Machii T, Onoe K, Matsumara K, Valind S, Kitani T and Langstom B. High uptake of [2-¹¹C]acetyl-carnitine into the brain: a PET study. *Biochem Biophys Res Comm.* **231**, 488-493. 1997.
- Kuzawa CW. Adipose tissue in human infancy and childhood: an evolutionary perspective. *Am J Physiol.* **27**, 177-209. 1998.
- Kuznetsov AV, Clark JF, Winkler K and Kunz WS. Change in flux control coefficient of cytochrome *c* oxidase in copper deficient mottled brindled mice. In *What is controlling life? Modern Trends in BioThermokinetics.* Gnaiger E, Gellerich FN and Wyss M (Eds). 275-277. 1994.
- Kuzin MI, Shimkevich LL, Istratov VG and Amiraslanov IUA. Diagnostic role of determination of plasma free fatty acid spectrum in patients with suppurative surgical infection. *Vestn Khir.* **132**, 3-8. 1984.
- Labadaridis J, Mavridou I, Sarafidou G, Alexiou N, Costalos C and Michelakakis H. Carnitine supplementation and ketogenesis by small-for-date neonates on medium- and long-chain fatty acid formulae. *Biology Neonate.* **77**. 25-28. 2000.
- Lanza-Jacobs S, Rosato E, Braccia G and Tabares A. Altered ketone body metabolism during gram-negative sepsis in the rat. *Metabolism.* **11**, 1151-1157. 1990.
- Larrick JW and Kunkel SL. Is Reye's Syndrome caused by augmented release of tumour necrosis factor? *Lancet.* **2**, 132-133. 1986.
- Lascelles CV and Quant PA. Investigation of human hepatic mitochondrial 3-hydroxy-3-methylglutaryl-coenzyme A synthase in post mortem or biopsy tissue. *Clinica Chimica Acta.* **260**, 85-96. 1997.
- Lascelles CV and Quant PA. Gestational and neonatal expression and activity of human HMG-CoA synthase. *B Soc Trans.* **26**, S89. 1998.
- Lazarow PB and De Duve C. A fatty acyl-CoA oxidizing system in rat liver peroxisomes: enhancement by clofibrate, a hypolipidemic drug. *Proc Natl Acad Sci.* **73**, 2043-2046. 1976.
- Lazarow PB. The role of peroxisomes in mammalian cellular metabolism. *J Inher Metab Dis.* **10**, 11-22. 1987.

- Lee LPK and Fritz IB. Hepatic ketogenesis during development. *Can J Biochem.* **49**, 599-605. 1971.
- Lefevre G, Dhainaut FJ, Tallet F, *et al.*, Individual free fatty acid and lactate uptake in the human heart during severe sepsis. *Ann Clin Biochem.* **25**, 546-551. 1988.
- Lennox WG. Ketogenic diet in the treatment of epilepsy. *New Eng J Med.* **199**, 74-75. 1928.
- Lettellier T, Malgat M, Rossignol R and Mazat JP. Metabolic control analysis and mitochondrial pathologies. *Mol Cell Biochem.* **184**, 409-417. 1998.
- Lewis DB. Host defense mechanism against bacteria, fungi, viruses and normal intracellular pathogens. In *Fetal and neonatal physiology*. Polin RA and Fox WW (Eds) Philadelphia PA Saunders. 1869-1919. 1998.
- Lilly K, Bugaisky GE, Umeda PK and Bieber LL. The medium-chain carnitine acyltransferase activity associated with rat liver is malonyl-CoA sensitive. *Arch Biochem Biophys.* **280**, 167-174. 1990.
- Lilly K, Chung C, Kerner J, Van Renterghem R and Bieber LL. Effect of etomoxirylyl-CoA on different carnitine acyltransferases. *Biochem Pharmacol.* **43**, 353-361. 1992.
- Linz DN, Garcia VF, Arya G, Hug G, Tombragel E, Landrigan E, Chuck G, Tsoras M and Ziegler MM. Weanling and adult rats differ in fatty acid and carnitine metabolism during sepsis. *J Paed Surgery.* **30**, 959-965. 1995.
- Lionetti L, Iossa S, Liverini G and Brand M. Changes in the hepatic mitochondrial respiratory system in the transition from weaning to adulthood in rats. *Arch Biochem Biophys.* **352**, 240-246. 1998.
- Lipmann F. On the chemistry and function of coenzyme A. *Bacteriol Rev.* **17**, 1-16. 1953.
- Lockwood EA and Bailey E. Fatty acid utilization during development of the rat. *Biochem J.* **120**, 49-54. 1970.
- Lockwood EA and Bailey E. The time course of ketosis and the activity of key enzymes of ketogenesis and ketone body utilization during development of the postnatal rat. *Biochem J.* **124**, 249-254. 1971.
- Lorenzo M, Roncero C and Benito M. The role of prolactin and progesterone in the regulation of lipogenesis in maternal and foetal rat liver in vivo and in isolated hepatocytes during the last day of gestation. *Biochem J.* **239**, 135-139. 1986.
- Lu A. *Pharm Rev.* **31**, 277-295. 1980.
- Lubchenco LO and Bard H. Incidence of hypoglycemia in newborn infants classified by birth weight and gestational age. *Pediatrics.* **47**, 831-838. 1971.
- Luckey TD, Mende TJ and Pleasant J. The physical and chemical characterization of rats milk. *J Nutr.* **54**, 345-359. 1954.

- Luo MJ, He XY, Sprecher H and Schultz H. Purification and characterization of the trifunctional beta-oxidation complex from pig-heart mitochondria. *Arch Biochem Biophys.* **304**, 266-271. 1993.
- Maclaren DM. Soft tissue infection and septicaemia. In *Escherichia Coli: mechanisms of virulence*. Sussman M (Ed). Cam University Press. 469-481. 1997.
- Makins R and Quant PA. Metabolic control analysis of hepatic oxidation: the top down approach. *B Soc Trans.* **22**, 441-446. 1994.
- Makins R, Drynan L, Zammit VA and Quant PA. Top-down regulation analysis of palmitoyl-CoA oxidation and ketogenesis in isolated rat liver mitochondria. *B Soc Trans.* **23**, 288S. 1995.
- Mannaerts GP, Debeer LJ, Thomas J and De Schepper PJ. Mitochondrial and peroxisomal fatty acid oxidation in liver homogenates and isolated hepatocytes from control and clofibrate-treated rats. *J Biol Chem.* **11**, 4585-4595. 1979.
- Markley, MA, Eaton, S and Pierro, A. Effects of endotoxemia on neonatal hepatic oxidative metabolism. *Proc Nutr Soc.* 2000.
- Matsushashi M, Matsushashi S and Lynen F. *Biochem Z.* 263-289. 1964.
- Matsushashi M, Matsushashi S, Numa S and Lynen F. *Fed Proc.* **21**, 288. 1962.
- Mattson FH and Volpenhein RA. The digestion and absorption of triglycerides. *J Biol Chem.* **239**, 2772-2777. 1964.
- Mazat J-P, Letellier T, Malgat M, Jouaville S and Morkuniene R. Application of control analysis to the study of metabolic disease in mitochondria. Metabolic expression of mitochondrial DNA mutations. In *What is controlling life? Modern Trends in BioThermokinetics*. Gnaiger E, Gellerich FN and Wyss M (Eds). 272-274. 1994.
- Mazat J-P, Reder C and Letellier T. Why are most flux control coefficients so small? *J Theor Biol.* **182**, 253-258. 1996.
- Mazat J-P, Letellier T, Malgat M, Rossignol R, Korzeniewski B, Demaugre F and Leroux J-P. Inborn errors of metabolism in the light of metabolic control analysis. *B Soc Trans.* **26**, 141-145. 1998.
- McAndrew HF, Lloyd DA, Rintala R and van Saene HKF. Intravenous glutamine or short-chain fatty acids reduce central venous catheter infection in a model of total parenteral nutrition. *J Ped Surg.* **34**. 281-285. 1999.
- McCance RA and Widdowson EM. Fat. *Pediatr Res.* **11**, 1081-1083. 1977.
- McGarry JD and Foster DW. The regulation of ketogenesis from octanoic acid. *J Biol Chem.* **295**, 1149-1159. 1971.
- McGarry JD and Foster DW. The metabolism of (-)octanoylcarnitine in perfused livers from fed and fasted rats. *J Biol Chem.* **249**, 7984-7990. 1974.

- McGarry JD, Mannaerts GP and Foster DW. A possible role for malonyl-CoA in the regulation of hepatic fatty acid oxidation and ketogenesis. *J Clin Invest.* **60**, 265-270. 1977.
- McGarry JD, Leatherman GF and Foster DW. CPT I, the site of inhibition of hepatic fatty acid oxidation by malonyl-CoA. *Biol Chem.* **253**, 4128-4136. 1978.
- McGarry JD and Foster DW. Regulation of hepatic fatty acid oxidation and ketone body production. *Annu Rev Biochem.* **49**, 395-420. 1980.
- McGarry JD, Woeltje KF, Kuwajima M and Foster DW. Regulation of ketogenesis and the renaissance of carnitine palmitoyltransferase. *Diabetes Metab Rev.* **5**, 271-284. 1989.
- McGarry JD, Sen A, Esser V, Woeltje KF, Weiss B and Foster DW. New insights into the mitochondrial carnitine palmitoyltransferase enzyme system. *Biochimie (Paris)* **73**, 77-84. 1991.
- McGarry JD, Brown NF, Inthanousay PP, Park DI, Cook BA and Foster DW. Insights into the topography of mitochondrial carnitine palmitoyltransferase gained from the use of proteases. In *New Developments in fatty acid oxidation*. Coates PM, Tanaka K (Eds). 47-61. Wiley-Leiss Inc New York. 1992.
- McGarry JD. Ketogenesis and lipogenesis: metabolic integration in health and disease. *B Soc Trans.* **23**, 481-485. 1995.
- McGarry JD and Brown NF. The mitochondrial carnitine palmitoyltransferase system: From concept to molecular analysis. *Eur J Biochem.* **244**, 1-14. 1997.
- McIntosh JK, Jablons DM, Mule JJ, Nordan RP, Rudenoff S, Lotze MT and Rosenberg SA. In vivo induction of IL6 by administration of exogenous cytokines and detection of de novo serum levels of IL6 in tumour bearing mice. *J Immunol.* **143**, 162-167. 1989.
- Medina JM, Tabernero A, Tovar JA and MartinBarrientos J. Metabolic fuel utilization and pyruvate oxidation during the perinatal period. *J Inher Met Dis.* **19**, 432-442. 1996.
- Mela-Riker L, Bartos D, Vlessis AA, Widener L, Muller P and Trunkey DD. Chronic hyperdynamic sepsis in the rat. *Circ Shock.* **36**, 83-92. 1992.
- Meléndez-Hevia E and Torres NV. Determination of control coefficients by shortening and enzyme titration of metabolic pathways. In: *Control of metabolic processes*. Cornish-Bowden A, Cardenas ML. (Eds). Plenum Press, New York. 231-237. 1990.
- Memon RA, Feingold KR, Moser AH, Doerrler W, Adi S, Dinarello CA and Grunfeld C. Differential effects of interleukin-1 and tumour necrosis factor on ketogenesis. *Am J Physiol.* **263**, 301-309. 1992.
- Memon RA, Fuller J, Moser AH, Smith PJ, Feingold KR and Grunfeld C. In vivo regulation of acyl-CoA synthetase mRNA and activity by endotoxin and cytokines. *Am J Physiol.* **38**, E64-E72. 1998.

- Memon RA, Feingold KR, Moser AH, Fuller J and Grunfeld C. Regulation of fatty acid transport protein and fatty acid translocase mRNA levels by endotoxin and cytokines. *Am J Physiol.* **37**, E210-E217. 1998.
- Memon RA, Bass NM, Moser AH, Fuller J, Appel R, Grunfeld C and Feingold KR. Down-regulation of liver and heart specific fatty acid binding proteins by endotoxin and cytokines in vivo. *Biochim Biophys Acta.* **1440**, 118-126. 1999.
- Miller LL, Bly CG, Watson ML and Bale WF. *J Exp Med.* **94**, 431-453. 1951.
- Mitchell GA, Kassovska-Bratinova S, Boukaftane Y, Robert MF, Wang SP, Ashmarina L, Lambert M, Lapierre P and Potier E. Medical aspects of ketone body metabolism. *Clin Invest Med.* **18**, 193-216. 1995.
- Mitchell G, Wang SP, Ashmarina L, Robert MF, Bouchard G, Laurin N, Kassovska-Bratinova S and Boukaftane Y. Inborn errors of ketogenesis. *B Soc Trans.* **26**, 136-140. 1998.
- Mitchell P. Chemiosmotic coupling in oxidative and photosynthetic phosphorylation. *Biol Rev.* **41**, 445-502, 1966.
- Mitchell P. Possible molecular mechanisms of the proton motive function of cytochrome systems. *J Theor Biol.* **62**, 327-367. 1976.
- Moir MB and Zammit VA. Insulin independent and extremely rapid switch in the partitioning of hepatic fatty acids from oxidation to esterification in starved-refed diabetic rats: possible roles for changes in cell pH and volume. *Biochem J.* **305**, 953-958. 1995.
- Mollica MP, Iossa S, Liverini G and Soboll S. Oxygen consumption and biosynthetic function in perfused liver from rats at different stages of development. *Cell Mol Life Sci.* **54**, 1277-1282. 1998.
- Morris AAM, Lascelles CV, Olpin SE, Leonard JV and Quant PA. Hepatic mitochondrial 3-hydroxy-3-methylglutaryl-CoA synthase deficiency. *J Inherit Metab Dis.* **20** (Sup 1) 40. 1997.
- Morris AAM, Lascelles CV, Olpin SE, Lake BD, Leonard JV and Quant PA. Hepatic mitochondrial 3-hydroxy-3-methylglutaryl-CoA synthase deficiency. *Ped Res.* 1998.
- Moshage H. Cytokines and the hepatic acute phase response. *J Pathology.* **181**, 257-266. 1997.
- Moss GS, Erve PP and Schumer W. Effect of endotoxin on mitochondria respiration. *Surg Forum.* **20**, 24-26. 1969.
- Moynagh PN. Contact sites and transport in mitochondria. *Essays in Biochemistry.* Apps D and Tipton KF (Eds) **30**, 1-14. 1995.
- Murthy MS and Pande SV. Malonyl-CoA binding site and the overt carnitine palmitoyltransferase activity reside on the opposite sides of the outer mitochondrial membrane. *Proc Natl Acad Sci USA.* **84**, 378-382. 1987.

- Nachiappan V, Curtiss D, Corkey BE and Kilpatrick L. Cytokines inhibit fatty acid oxidation in isolated rat hepatocytes: synergy among TNF, IL-6 and IL-1. *Shock*. **1**(2), 123-129. 1994.
- Nanbo A, Nishimura H, Muta T and Nagasawa S. Lipopolysaccharide stimulates HepG2 human hepatoma cells in the presence of lipopolysaccharide-binding protein via CD14. *Eur J Biochem*. **260**, 183-191. 1999.
- Nanni G, Siegel JH, Coleman B, Fader P and Castiglione R. Increased lipid fuel dependence in the critically ill septic patient. *J Trauma*. **24**, 14-30. 1984.
- Nebert DW, Nelson DR, Coon MJ, Estabrook RW, Feyereisen R, *et al.*, The P450 superfamily: update on new sequences, gene mapping and recommended nomenclature. *DNA and Cell Biol*. **10**, 1-14. 1991.
- Nehlig A and Pereira de Vasconcelos A. Glucose and ketone-body utilization by the brain of neonatal rats. *Prog Neurobiol*. **40**, 163-221. 1993.
- Nehlig A. Respective roles of glucose and ketone-bodies as substrates for cerebral energy-metabolism in the suckling rat. *Developmental Neuroscience*. **18**, 426-433. 1996.
- Neufeld HA, Pace JA and White FE. The effect of bacterial infections on ketone concentrations in rat liver and blood and on free fatty acid concentrations in rat blood. *Metabolism*. **25**, 877-884. 1976.
- Neufeld HA, Pace JA, Kaminski MV, George DT, Jahrling PB, Wannemacher RW and Beisel WR. A probable endocrine basis for the depression of ketone bodies during infectious or inflammatory state in rats. *Endocrinology*. **107**, 596-601. 1980.
- Neufeld HA, Pace JA, Kaminski MV, Sobocinski P and Crawford DJ. Unique effects of infectious or inflammatory stress on fat metabolism in rats. *J Parent Nutr*. **6**, 511-521. 1982.
- New KJ, Elliott KRF and Quant PA. Quantitative analysis of control exerted by mitochondrial outer membrane carnitine palmitoyltransferase over carbon fluxes from palmitate in hepatocytes isolated from suckling rats. *B Soc Trans*. **25**, 418S. 1997.
- New KJ, Elliott KRF and Quant PA. Flux control exerted by mitochondrial outer membrane carnitine palmitoyltransferase over ketogenic flux in hepatocytes isolated from suckling rats *B Soc Trans*. **26**, S88. 1998(a).
- New KJ, Eaton S, Elliott KRF and Quant PA. CPT I: a reassessment of its role in control over ketogenic flux. In *BioThermoKinetics in the Post Genomic Era*. Larsson, Pålman & Gustafsson (Eds). **8**. 113-116. 1998(b).
- New KJ, Elliott KRF and Quant PA. Is it time to reconsider the role of CPT I in control over ketogenesis? In *Current Views of fatty acid oxidation and ketogenesis: from organelles to point mutations*. Quant PA & Eaton S (Eds). Plenum Press. 227-232. 1999(a).
- New KJ, Krauss S, Elliott KRF and Quant PA. Comparisons of flux control exerted by mitochondrial outer-membrane carnitine palmitoyltransferase over ketogenesis

- in hepatocytes and mitochondria isolated from suckling or adult rats. *Eur J Biochem.* **259**, 684-691. 1999(b).
- New KJ, Eaton S, Spitz L, Elliott KRF and Quant PA. Analysis of control exerted by CPT I over ketogenic flux in *in vitro* hepatocyte models designed to mimic the early stages of neonatal sepsis. *Eur J Med Research.* **5** 46-47. 2000.
- Nobes CD, Brown GC, Olive PN and Brand MD. Non-ohmic proton conductance of the mitochondrial inner membrane in hepatocytes. *J Biol Chem.* **265**(22), 12903-12909. 1990.
- Noel H and Pande SV. An essential requirement of cardiolipin for mitochondrial carnitine acylcarnitine translocase activity – lipid requirement of carnitine acylcarnitine translocase. *Eur J Biochem.* **155**, 99-102. 1986.
- Nordenström J, Carpentier YA, Askanazi J, *et al.*, Free fatty acid mobilization and oxidation during total parenteral nutrition in trauma and infection. *Ann Surg.* **198**, 725-735. 1983.
- Novak M, Melichar V and Hahn P. Postnatal changes in the blood serum content of glycerol and free fatty acids in human infants. *Biol Neonate.* **7**, 179-184. 1964.
- O'Neil S, Hunt J, Filkins J and Gamelli R. Obstructive jaundice in rats results in exaggerated hepatic production of tumour necrosis factor-alpha and systemic and tissue tumour necrosis factor-alpha levels after endotoxin. *Surgery.* **122**, 281-287. 1997.
- Ockner RK, Weisiger RA and Gollan JL. Hepatic uptake of albumin bound substances: albumin receptor concept. *Am J Physiol.* **245**, G13-G18. 1983.
- Ockner RK, Kaikaus RM and Bass NM. Fatty acid binding proteins: recent concepts of regulation and function. In *New developments in fatty acid oxidation*. Coates P and Tanaka K (Eds). Wiley-Liss Inc New York. 189-204. 1992.
- Old LJ. Tumour necrosis factor. *Science.* **230**, 630-632. 1985.
- Ontko JA and Johns ML. Evaluation of malonyl-CoA in the regulation of long-chain fatty acid oxidation in the liver: evidence of an unidentified regulatory component of the system. *Biochem J.* **192**, 959-962. 1980.
- Owen OE, Morgan AP, Kemp HG, Sullivan JM, Herrera MG and Cahill GF Jr. Brain metabolism during fasting. *J Clin Invest.* **46**, 1589-1595. 1967.
- Pagani R, Portolés MT and Municio AM. The binding of *E Coli* endotoxin to isolated rat hepatocytes. *FEBS Letts.* **131**, 103-107. 1981.
- Pagani R, Portolés MT, Bosch MA, Diaz-Laviada I and Municio AM. Direct and mediated *Escherichia Coli* lipopolysaccharide action in primary hepatocyte cultures. *Eur J Cell Biol.* **43**, 243-246. 1987.
- Pagani R, Portolés MT, Vina S, Melzner I and Vergani G. Alterations induced on cytoskeleton by *E. Coli* endotoxin in different types of liver cells. *International conference on endotoxins*. Amsterdam IV. Amsterdam. Abstract. 1993.

- Pailla K, Lim S-K, de Bandt J-P, et al. TNF-alpha and IL6 synergistically inhibit ketogenesis from fatty acids and alpha-ketoisocaproate in isolated rat hepatocytes. *J Paren Ent Nutr.* **22**, 286-290. 1998.
- Palmieri F, Bisaccia F, Capobianco L, Dolce V, Fiermonte G, Iacobazzi, V, Indiveri C and Palmieri L. Mitochondrial metabolic transporters. *Biochim Biophys Acta.* **1275**, 127-132. 1996.
- Pande SV and Parvin R. Carnitine-acylcarnitine translocase catalyses an equilibrating unidirectional transport as well. *J Biol Chem.* **255**, 2994-3001. 1980.
- Pande SV. Reversal by CoA of palmitylCoA inhibition of long-chain acyl-CoA synthetase activity. *Biochim Biophys Acta.* **306**, 15-20. 1973.
- Pande SV. A mitochondrial carnitine acylcarnitine translocase system. *Proc Natl Acad Sci. USA* **72**, 883-887. 1975.
- Parent JB. Membrane receptors on rat hepatocytes for the inner core region of bacterial lipopolysaccharides. *J Biol Chem.* **265**, 3455-3461. 1990.
- Patel MS, Johnson CA, Rajan R and Owen OE. The metabolism of ketone bodies in developing human brain: development of ketone-body-utilizing enzymes and ketone bodies as precursors for lipid synthesis. *J Neurochemistry.* **25**, 905-908. 1975.
- Patil KK, Eaton S and Quant PA. Effect of pathological levels of hydrogen peroxide on control of ketogenic flux in hepatocytes isolated from neonatal rats. in *BioThermoKinetics in the Post Genomic Era*. Larsson, Pålman & Gustafsson(Eds). **8**. 287-290. 1998
- Paterson P, Sheath J, Taft P and Wood C. Maternal and foetal ketone concentrations in plasma and urine. *Lancet.* **1**, 862-865. 1967.
- Paulussen RJA, Jansen PM and Veerkamp JH. Fatty-acid binding capacity of cytosolic proteins of various rat tissues: effect of postnatal development, starvation, sex, clofibrate feeding and light cycle. *Biochim Biophys Acta.* **877**, 342-349. 1986.
- Paulussen RJA, Geelen MJH, Beynen AC and Veerkamp JH. Immunochemical quantitation of fatty acid binding proteins (1) Tissue and intracellular distribution, postnatal development and influence of physiological conditions on the heart and liver FABP. *Biochim Biophys Acta.* **1001**, 201-209. 1989.
- Pedersen PV, Warner BW, Bjomson HS, Hiyama DT, Li S, Rigel DF, Hasselgren P-O and Fischer JE. Hemodynamic and metabolic alterations during experimental sepsis in young and adult rats. *Surg Gyne & Obs.* 148-155. 1989.
- Pégorier J-P, Ferré P and Girard J. The effects of inhibition of fatty acid oxidation in suckling newborn rats. *Biochem J.* **166**, 631-634. 1977.
- Pégorier J-P, Duée P-H, Assan, R Peret J and Girard J. Changes in circulating fuels, pancreatic hormones and liver glycogen concentration in fasting or suckling pig. *J Dev Physiol.* **3**, 203-217. 1981.

- Pégorier J-P, Duée P-H, Clouet P, Kohl C, Herbin C and Girard J. Octanoate metabolism in isolated hepatocytes and mitochondria from fetal, newborn and adult rabbit. *FEBS Letts.* **184**, 681-686. 1989.
- Péquignot-Planche E, De Gasquet P, Boulangé A and Tonnu NT. Lipoprotein lipase activity at onset of development of white adipose tissue in newborn rats. *Biochem J.* **162**, 461-463. 1977.
- Persson B and Gentz J. The pattern of blood lipids, glycerol and ketone bodies during the neonatal period, infancy and childhood. *Acta Paediatrici Scand.* **55**, 353-362. 1966.
- Pettersson G. Errors associated with experimental determinations of enzyme flux control coefficients. *J Theor Biol* **179**, 191-197. 1996.
- Pierro A, van Saene HKF and Donnell SC *et al.*, Microbial translocation in neonates and infants on long-term parenteral nutrition. *Arch Surg.* **131**, 176-179. 1996.
- Pierro A, van Saene HKF and Jones MO *et al.*, Clinical impact of abnormal gut flora in infants receiving parenteral nutrition. *Ann Surg.* **227**, 547-552. 1998
- Pinsky MR, Vincent JL, Deviere J, Alegre M, Kahn RJ and Dupont E. Serum cytokine levels in human septic shock: relation to multiple-system organ failure and mortality. *Chest.* **103**, 565-575. 1993.
- Plank LD Connolly AB and Hill GI. Sequential changes in the metabolic response in severely septic patients during the first 23 days after the onset of peritonitis. *Ann Surg.* **228**(2), 146-158. 1998.
- Playhoust MR and Isselbacher KJ. Studies on the intestinal absorption and intramucosal lipolysis of medium-chain triglycerides. *J Clin Invest.* **43**, 878-885. 1964.
- Porter RK and Brand MD. Body mass dependence of H⁺ leak in mitochondria and its relevance to metabolic rate. *Nature.* **362**, 628-630. 1993.
- Portolés MT, Ainaga MJ and Pagani R. The induction of lipid peroxidation by E.coli lipopolysaccharide on rat hepatocytes as an important factor in the etiology of endotoxic liver damage. *Biochim Biophys Acta.* **1158**, 287-292. 1993.
- Power GW, Yaqoob P, Harvey DJ, Newsholme EA and Calder PC. The effect of dietary lipid manipulation on hepatic mitochondrial phospholipid fatty acid composition and carnitine palmitoyltransferase I activity. *Biochem Mol Biol Int.* **34**(4), 671-684. 1994.
- Power GW, Cake MH and Newsholme EA. Influence of diet on the kinetic behaviour of hepatic carnitine palmitoyltransferase I toward different acyl CoA esters. *Lipids.* **32**(1), 31-36. 1997.
- Powis, MR, Smith K, Rennie M, Halliday D and Pierro A. Effect of major operations on energy and protein metabolism in infants and children. *J Ped Surg.* **33**, 49-53. 1997.
- Prip-Buus C, Thumelin S, Chatelain F, Pégorier J-P and Girard J. Hormonal and nutritional control of liver fatty acid oxidation and ketogenesis during development. *B Soc Trans.* **23**, 500-505. 1995.

- Quant PA, Tubbs PK and Brand MD. Treatment of rats with glucagon or mannoheptulose increases mitochondrial 3-hydroxy-3-methylglutaryl-CoA synthase activity and decreases succinyl-CoA content in liver. *Biochem J.* **262**, 159-164. 1989.
- Quant PA, Tubbs PK and Brand MD. Glucagon activates mitochondrial 3-hydroxy-3-methylglutaryl-CoA synthase in vivo by decreasing the extent of succinylation of the enzyme. *Eur J Biochem.* **187**, 169-174. 1990.
- Quant PA, Robin D, Robin P, Ferré P, Brand MD and Girard J. Control of hepatic mitochondrial 3-hydroxy-3-methylglutaryl-CoA synthase during the foetal/neonatal transition, suckling and weaning in the rat. *Eur J Biochem.* **195**, 449-454. 1991.
- Quant PA, Henson JN, Williams AF, Jeffrey I, Taylor P and Carter ND. Does reduced expression of mitochondrial 3-hydroxy-3-methylglutaryl-coa synthase in preterm human infants explain lack of stimulation of ketogenesis following birth? *J Phys.* **467**, 367. 1993.
- Quant PA, Robin D, Robin P, Girard J and Brand MD. A top-down control analysis in isolated rat liver mitochondria: can the 3-hydroxy-3-methylglutaryl-CoA pathway be rate-controlling for ketogenesis? *Biochim Biophys Acta.* **1156**, 135-143. 1993.
- Quant PA. Experimental application of top-down control analysis to metabolic systems. *Trends Biochem Sci.* **18**, 26-30. 1993.
- Quant PA. The role of mitochondrial HMG-CoA synthase in regulation of ketogenesis. *Essays in Biochem.* **28**, 13-25. 1994.
- Quant PA and Krauss S. Regulation and control in complex, dynamic metabolic systems: experimental application of the top-down approaches of metabolic control analysis to fatty acid oxidation and ketogenesis. *J Theor Biol.* **182**, 381-388. 1996.
- Quant PA, Lascelles CV, New KJ, Patil KK, Azzouzi N, Eaton S and Elliott KRF. Impaired neonatal hepatic ketogenesis. *B Soc Trans.* **26**, 125-130. 1998.
- Rackow EC and Astiz ME. Pathophysiology and treatment of septic shock. *J Am Med Assoc.* **266**, 548-554. 1991.
- Ramsay RR and Tubbs PK. The mechanism of fatty acid uptake by heart mitochondria: an acyl-carnitine – carnitine exchange. *FEBS Letts.* **54**, 21-25. 1975.
- Ramsay RR and Tubbs PK. The effects of temperature and some inhibitors on the carnitine exchange system of heart mitochondria. *Eur J Biochem.* **69**, 299-303. 1976.
- Ramsay RR, Steenkamp DJ and Husain M. Reactions of electron-transfer flavoprotein and electron-transfer flavoprotein:ubiquinone oxidoreductase. *Biochem J.* **241**, 883-892. 1987.
- Ramsay RR. A comparison of the malonyl-CoA sensitive carnitine palmitoyltransferase activities acting on cytoplasmic substrates and their

- distribution in mitochondria, peroxisomes and microsomes. *Biochem (Life Sci Adv)*. **12**, 23-29. 1993.
- Ramsay RR. Carnitine and its role in acyl-group metabolism. *Essays in Biochem*. **28**, 47-60. 1994.
- Rasmussen JT, Rosendal J and Knudsen J. Interaction of acyl-CoA binding protein ACBP on processes for which acyl-CoA is a substrate, product or inhibitor. *Biochem J*. **292**, 907-913. 1993.
- Rebouche CJ and Engel AG. Tissue distribution of carnitine biosynthesis enzymes in man. *Biochim Biophys Acta*. **630**, 22-29. 1980.
- Robinson AM and Williamson DH. Physiological roles of ketone bodies as substrates and signals in mammalian tissues. *Physiol Rev*. **60**(1), 143-177. 1980.
- Robinson IN and Zammit VA. Sensitivity of carnitine acyltransferase-I to malonyl-CoA inhibition in isolated rat-liver mitochondria is quantitatively related to hepatic malonyl-CoA concentration in vivo. *Biochem J*. **206**, 177-9. 1982.
- Robles-Valdes C, McGarry JD, Foster DW. Maternal-fetal carnitine relationships and neonatal ketosis in the rat. *J Biol Chem*. **251**, 6007-6012. 1976.
- Rofe AM, Conyers RAJ, Bais R, Gamble JR and Vadas MA. The effects of recombinant tumour necrosis factor (cachetin) on metabolism in isolated rat adipocyte, hepatocyte and muscle preparations. *Biochem J*. **247**, 789-792. 1987.
- Rohr HP, Wirz A, Henning LC, Riede UN and Bianchi L. Morphometric analysis of the rat liver cell in the perinatal period. *Lab Invest*. **24**, 128-139. 1971.
- Rolfe DFS, Newman JMB, Buckingham JA, Clarke MG and Brand MD. Contribution of mitochondrial proton leak to respiration rate in working skeletal muscle and liver and to SMR. *Am J Physiol*. **45**, 692-699. 1999.
- Romanosky AJ, Bagby GJ, Bockman GL and Spitzer JJ. Free fatty acid utilization by skeletal muscle after endotoxin administration. *Am J Physiol*. **239**. E391-E395. 1980.
- Romeo C, Eaton S, Quant PA, Spitz L and Pierro A. Neonatal oxidative liver metabolism: effects of hydrogen peroxide, a putative mediator of septic damage. *J Paed Surgery*. **34**, 1107-1111. 1999.
- Romeo C, Eaton S, Spitz L and Pierro A. Nitric oxide inhibits neonatal hepatocyte oxidative metabolism. *J Paed Surgery*. **35**, 44-48. 2000.
- Rosser DM, Stidwill RP, Jacobson DJ and Singer M. Cardiorespiratory and tissue oxygen dose response to rat endotoxemia. *Am J Physiol*. **271**, 891-895. 1996.
- Rosser DM, Manji M, Cooksley H and Bellingan G. Endotoxin reduces maximal oxygen consumption in hepatocytes independent of any hypoxic insult. *Intensive Care Med*. **24**, 725-729. 1998.
- Roumen RMH, Hendriks T, Ven-Jongekrijg J, Nieuwenhuijzen GAP, Sauerwein RW, van der Meer JWM and Goris RJA. Cytokine patterns in patients after major

- vascular surgery, hemorrhagic shock and severe blunt trauma. *Ann Surg.* **218**(6), 769-776. 1993.
- Rowe PC, Valle D and Brusilow SW. Inborn errors of metabolism in children referred with Reyes syndrome. *JAMA.* **260**, 3167-3170. 1988.
- Saggerson ED and Carpenter CA. Effects of fasting, adrenalectomy and streptozotocin-diabetes on sensitivity of hepatic carnitine acyltransferase to malonyl CoA. *FEBS Letts.* **129**, 225-228. 1981(a).
- Saggerson ED and Carpenter CA. Carnitine palmitoyltransferase and carnitine octanoyltransferase activities in liver, kidney cortex, adipocyte, lactating mammary gland, skeletal muscle and heart. *FEBS Letts.* **129**, 229-232. 1981(b).
- Saggerson ED and Carpenter CA. Effects of fasting and malonyl CoA on the kinetics of carnitine palmitoyltransferase and carnitine octanoyltransferase in intact rat liver mitochondria. *FEBS Letts.* **132**, 166-168. 1981(c).
- Saggerson ED and Carpenter CA. Regulation of hepatic carnitine palmitoyltransferase activity during the foetal-neonatal transition. *FEBS Letts.* **150**, 177-180. 1982.
- Salter M, Knowles RG and Pogson CI. *Essays in Biochemistry.* Tipton KJ (Ed). **28**, 1-12 Portland Press London. 1994.
- Samra JS, Summers LKM and Frayn KN. Sepsis and fat metabolism. *British J Surgery.* **83**, 1186-1196. 1996.
- Saudubray JM, Mitchell GA, Bonnefont JP, Schwartz G, Nuttin C, Munnich A, Brivet M, Vassault A, Demaugre F, Rabier D and Charpentier C. Approach to the patient with a fatty acid oxidation disorder. In *New developments in fatty acid oxidation.* Coates PM, Tanaka K (Eds). New York, Wiley-Liss Inc. 271-288. 1992.
- Sauer PJ, Camielli VP, Sulkers EJ and Vangoudoever JB. Substrate utilization during the first weeks of life. *Acta Paed.* **83**, 49-53. 1994.
- Schofield PS, French TJ and Sugden MC. Ketone body metabolism after surgical stress or partial hepatectomy. *Biochem J.* **241**, 475-481. 1987.
- Schulz H. Beta-oxidation of fatty-acids. *Biochem Biophys Acta.* **1081**, 109-120. 1991.
- Schulze-Osthoff K, Bakker AC, Vanhaesebroeck B, Beyaert R, Jacobs WA and Fiers W. Cytotoxic activity of tumour necrosis factor is mediated by early damage of mitochondrial functions: evidence for the involvement of mitochondrial radical generation. *J Biol Chem.* **267**, 5317-5323. 1992.
- Schumann RR, Leong SR, Flaggs, GW, Gray PW, Wright SD, Mathison JC, Tobias PS and Ulevitch RJ. Structure and function of lipopolysaccharide binding protein. *Science.* **249**, 1429-1431. 1990.
- Schuster S, Kahn D and Westerhoff D. Modular analysis of the control of complex metabolic pathways. *Biophys Chem.* **48**. 1. 1993.

- Senior JR. In *Medium chain triglycerides*. Senior JR, Van Itallie TB and Greenberger NJ (Eds). 1-7, University of Pennsylvania Press, Philadelphia. 1968.
- Shai Y. Molecular recognition between membrane spanning polypeptides. *Trends Biochem Sci.* **20**, 460-464. 1995.
- Shelley HJ. Glycogen reserves and their changes at birth and in anoxia. *Br Med Bull.* **17**, 137-143. 1961.
- Sherratt HSA and Spurway T. Regulation of fatty acid oxidation in cells. *B Soc Trans.* **22**, 423-426. 1994.
- Shi J, Zhu H, Arvidson DN, Cregg JM and Woldegiorgis G. Deletion of the conserved first 18 N-terminal amino acid residues in rat liver carnitine palmitoyltransferase I abolishes malonyl-CoA sensitivity and binding. *Biochem J.* **37**, 11033-8. 1998.
- Shi JY, Zhu HF, Arvidson DN, Woldegiorgi G, Shi JY, Zhu HF, Arvidson DN and Woldegiorgis G. The first 28 N-terminal amino acid residues of human heart muscle carnitine palmitoyltransferase I are essential for malonyl CoA sensitivity and high-affinity binding. *Biochemistry.* **39**, 712-717. 2000.
- Shindo Y and Hashimoto T. Acyl-coenzyme A synthetase and fatty acid oxidation in rat liver peroxisomes. *J Biochem (Tokyo).* **84**, 1177-1181. 1978.
- Shug AP, Lerner E, Elson C and Shrago E. The inhibition of adenine nucleotide translocase activity by oleoyl CoA and its reversal in rat liver mitochondria. *Biochem Biophys Res Comm.* **43**, 557-63. 1971.
- Simpson KJ, Lukacs NW, Colletti L, Strieter RM and Kunkel SL. Cytokines and the liver. *J Hepatology.* **27**, 1120-1132. 1997.
- Singer M and Brealey D. Mitochondrial dysfunction in sepsis. *Biochem Soc Symp.* **66**, 149-166. 1999.
- Singh I, Singh R, Bhushan A and Singh AK. Lignoceroyl-CoA ligase activity in rat brain microsomal fraction: topographical localization and effect of detergents on α -cyclodextrin. *Arch Biochem Biophys.* **236**, 418-426. 1985.
- Skehel JM, Fearnley IM and Walker JE. NADH:ubiquinone oxidoreductase from bovine heart mitochondria: sequence of a novel 17.2-kDa subunit. *FEBS Letts.* **438**, 305-305. 1998.
- Skorin C, Necochea C, Johow V, Soto U, Grau AM, Bremer J and Leighton F. Peroxisomal fatty acid oxidation and inhibitors of the mitochondrial carnitine palmitoyltransferase I in isolated rat hepatocytes. *Biochem J.* **281**, 561-567. 1992.
- Sly MR and Walker DG. A comparison of lipid metabolism in hepatocytes isolated from fed and starved neonatal and adult rats. *Comp Biochem Physiol B Comp Biochem.* **61**, 501-506. 1978.
- Small JR and Kacser H. Responses of metabolic systems to large changes in enzyme activities and effectors - linear treatment of branched pathways and metabolite concentrations - assessment of the general non-linear case. *Eur J Biochem.* **213**, 625-640. 1993.

- Small JR. Flux control coefficients determined by inhibitor titration: the design and analysis of experiments to minimize errors. *Biochem J.* **296**, 423-433. 1993.
- Smith S, Watts R and Dils R. Quantitative gas-liquid chromatographic analysis of rodent milk-triglycerides. *J Lipid Res.* **9**, 52-57. 1968.
- Spector R. Fatty acid transport through the blood-brain barrier. *J Neurochem.* **50**, 639-642. 1975.
- Spitzer JJ, Bagby GJ, Mesazaros K and Lang CH. Alterations in lipid and carbohydrate metabolism in sepsis. *J Parenter Enteral Nutr.* **12**, S53-S58. 1988.
- Spurway TD, Sherratt HSA, Pogson CI and Agius L. The flux control coefficient of carnitine palmitoyltransferase I on palmitate β -oxidation in rat hepatocytes. *Biochem J.* **323**, 119-122. 1997.
- Spurway TD. Control of hepatic fatty acid oxidation. PhD Thesis. Newcastle upon Tyne. G2b. 45-11042. 1995.
- Stadler J, Bentz BG, Harbrecht BG, et al. Tumour necrosis factor alpha inhibits hepatocyte mitochondrial respiration. *Ann Surg.* 539-546. 1991.
- Stanley KK and Tubbs PK. The role of intermediates in mitochondrial fatty acid oxidation. *Biochem J.* **150**, 77-88. 1975.
- Stephens TW, Cook GA and Harris RA. Effect of pH on malonyl-CoA inhibition of carnitine palmitoyltransferase I. *Biochem J.* **212**, 521-524. 1983.
- Stoner HB, Little RA, Frayn KN, Elebute AE, Tresadem J and Gross E. The effect of sepsis on the oxidation of carbohydrate and fat. *Br J Surg.* **70**, 32-35. 1983.
- Sullivan JS, Kilpatrick L, Costarino AT, Lee SC and Harris MC. Correlation of plasma cytokine elevations with mortality rate in children with sepsis. *J Pediatrics.* **120**(4), 510-515. 1992.
- Swanson ST, Foster DW, McGarry JD and Brown NF. Roles of the N- and C-terminal domains of Carnitine palmitoyltransferase I isoforms in malonyl-CoA sensitivity of the enzymes: insights from expression of chimaeric proteins and mutation of conserved histidine residues. *Biochem J.* **335**, 513-519. 1998.
- Swink TD, Vining EPG and Freeman JM. The ketogenic diet: 1997. In: *Advances in pediatrics*. Mosby-Year Book, Inc, **44**, 297-329. 1997.
- Takeyama N, Takagi D, Matsuo N, Kitazawa Y and Tanaka T. Altered hepatic fatty acid metabolism in endotoxemia: effect of L-carnitine on survival. *Am J Physiol.* **256**, 31-37. 1989.
- Takeyama N, Itoh Y, Kitazawa Y and Tanaka T. Altered hepatic mitochondrial fatty acid oxidation and ketogenesis in endotoxic rats. *Am J Physiol.* **4**, E498-E505. 1990.
- Taylor DE, Ghio AJ and Piantadosi CA. Reactive oxygen species produced by liver mitochondria of rats in sepsis. *Arch Biochem Biophys.* **316**, 70-76. 1995.
- Taylor RW, Birchmachin MA, Bartlett K, Lowerson SA and Turnbull DM. The control of mitochondrial oxidations by complex-III in rat muscle and liver-mitochondria -

- implications for our understanding of mitochondrial cytopathies in man. *J Biol Chem.* **269**, 5, 3523-3528. 1994.
- Thiemermann C, Ruetten H, Wu C-C and Vane JR. The multiple organ dysfunction syndrome caused by endotoxin in the rat: attenuation of liver dysfunction by inhibitors of nitric oxide synthase. *Br J Pharm.* **116**, 2845-2851. 1995.
- Thierbach G and Reichenbach H. Myxothiazol, a new inhibitor of the cytochrome b-c segment of the respiratory chain. *Biochim Biophys Acta.* **638**, 282-289. 1981.
- Thomas S and Fell DA. A control analysis exploration of the role of ATP utilisation in glycolytic flux control and glycolytic metabolite concentration regulation. *Eur J Biochem.* **258**, 956-967. 1998(a).
- Thomas S and Fell DA. The role of multiple enzyme activation in metabolic flux control. *Adv Enz Reg.* **38**, 65-85. 1998(b).
- Thumelin S, Esser V, Charvy D, Kolodziej M, Zammit VA, McGarry D, Girard J and Pégrier J-P. Expression of liver carnitine palmitoyltransferase I and II genes during development in the rat. *Biochem J.* **300**, 583-587. 1994.
- Thumelin S, Forestier M, Girard J and Pégrier J-P. Developmental changes in mitochondrial 3-hydroxy-3-methylglutaryl-Coa synthase gene expression in rat liver, intestine and kidney. *Biochem J.* **292**, 493-496. 1993.
- Tonsgard JH. Effect of Reyes Syndrome serum on the ultrastructure of isolated liver mitochondria. *Lab Invest.* **60**, 568-573. 1989.
- Townsend MC, Gauderer MWL, Yokum MD and Fry DE. Alterations of hepatic mitochondrial function in a model of peritonitis in immature rats. *J Paed Surgery.* **21**, 521-524. 1986.
- Uchida Y, Izai K, Orii T and Hashimoto T. Novel fatty-acid beta-oxidation enzymes in rat-liver mitochondria(2): Purification and properties of enoyl-coenzyme-A (CoA) hydratase/3-hydroxyacyl-coa dehydrogenase/3-ketoacyl-CoA thiolase trifunctional protein. *J Biol Chem* **267**, 1034-1041. 1992.
- Urao M, Fujimoto T, Lane GJ, Seo G-I and Miyano T. Does probiotics administration decrease serum endotoxin levels in infants?. *J Paed Surg.* **34**, 273-276. 1999.
- Valcarce C, Navarrete RM, Encabo P, Loeches E, Satrustegui J and Cuezva JM. Postnatal development of rat liver mitochondrial functions. The role of protein synthesis and of adenine nucleotides. *J Biol Chem.* **263**, 7767-7775. 1988.
- Van der Leij FR, Kram AM, Bartelds B, Roelofsen H, Smid, GB, Takens, J, Zammit VA and Kuipers JRG. Cytological evidence that the C-terminus of carnitine palmitoyltransferase I is on the cytosolic face of the mitochondrial outer membrane. *Biochem J.* **341**, 777-784. 1999.
- Vandenbosch H, Schutgens RBH, Wanders RJA and Tager JM. Biochemistry of peroxisomes. *Ann Rev Biochem.* **61**, 157-197. 1992.
- Van Veldhoven PP and Mannaerts GP. Role and organization of peroxisomal β -oxidation. In *Current Views of fatty acid oxidation and ketogenesis: from organelles to point mutations*. Quant PA & Eaton S (Eds). Plenum Press. 261-272. 1999.

- Vary TC, Siegel JH, Nakatani T, Sato T and Aoyama H. A biochemical basis for depressed ketogenesis in sepsis. *J Trauma*. **26**, 419-425. 1986.
- Vasconcelos PRL, Kettlewell MGW and Williamson DH. Time course of changes in hepatic metabolism in response to sepsis in the rat: impairment of gluconeogenesis and ketogenesis *in vitro*. *Clinical Science*. **72**, 683-691. 1987.
- Veerkamp JH, van Moerkerk HTB, Glatz JFC, Zuurveld JGEM, Jacobs AEM and Wagenmakers AJM. $^{14}\text{CO}_2$ Production is no adequate measure of [^{14}C]fatty acid oxidation. *Biochem Med Metab Bio*. **35**, 248-259. 1986.
- Velasco G, Sanchez C, Geelen MJH and Guzmán M. Are cytoskeleton components involved in the control of hepatic carnitine palmitoyltransferase I activity? *Biochem Biophys Acta*. **224**, 754-759. 1996.
- Vergani G, Portoles MT and Pagani R. E Coli lipopolysaccharide effects on proliferating rat liver cells in culture: a morphological and functional study. *Tissue & Cell*. **31**, 1-7. 1999.
- Vilcek J. The cytokines: an overview. *The cytokine Handbook*. Thomson A (Ed). AP. 1998.
- Vllessis AA, Goldman RK and Trunkey DD. New concepts in the parapsiology of oxygen metabolism during sepsis. *British J Surgery*. **82**, 870-876. 1995.
- Wahlig TM and Georgieff MK. The effects of illness on neonatal metabolism and nutritional management. *Clinics in Perinatology*. **22**(1), 77-93. 1995.
- Wanders RJA, Ijlst L, Poggi F, Bonnefont JP, Munnich A, Brivet M, Rabier D and Saudubray JM. Human trifunctional protein-deficiency - a new disorder of mitochondrial fatty-acid beta-oxidation. *Biochem Biophys Res Comm*. **188**, 3, 1139-1145. 1992.
- Wanders RJA. Functions and disfunctions of peroxisomes in fatty acid α - and β -oxidation: new insights. In *Current Views of fatty acid oxidation and ketogenesis: from organelles to point mutations*. Quant PA & Eaton S (Eds). Plenum Press. 283-300. 1999.
- Wang P, Ayala A, Zheng F, Zhou M, Perrin M and Chaudry IH. Tumour necrosis factor-alpha produces hepatocellular dysfunction despite normal cardiac output and hepatic microcirculation. *Am J Physiol*. **265**, 126-132. 1993
- Wannemacher RW, Pace JG, Beall FA, Dinterman RE, Petrella VJ and Neufeld HA. Role of the liver in regulation of ketone body production during sepsis. *J Clin Invest*. **64**, 1565-1572. 1979.
- Warshaw JB. Cellular energy metabolism during fetal development IV Fatty acid activation, acyl transfer and fatty acid oxidation during development of the chick and rat. *Dev Biol*. **28**, 537-544. 1972.
- Weisiger RA, Gollan JL and Ockner RK. Receptor for albumin on the liver cell surface may mediate uptake of fatty acids and other albumin bound substances. *Scienc., Wash*. **211**, 1048-1051. 1981.
- Westerhoff HV, Groen AK and Wanders RJA. Modern theories of metabolic control and their applications. *Biosci Rep*. **4**, 1-22. 1984.

- Whitelaw E and Williamson DH. Effects of lactation on ketogenesis from oleate or butyrate in rat hepatocytes. *Biochem J* **164**, 521-528. 1977.
- Widdowson EM. Chemical composition of newly born mammals. *Nature Lond.* **166**, 626-628. 1950.
- Widdowson EM. Growth of the body and its components and the influence of nutrition. In *Biology of normal human growth*. Ritzen M (Ed). New York Raven. 253-263. 1981.
- Wieser T. Genetics of carnitine palmitoyltransferase II deficiencies. In *Current Views of fatty acid oxidation and ketogenesis: from organelles to point mutations*. Quant PA & Eaton S (Eds). Plenum Press. 339-346. 1999.
- Williamson DH, Bates BW and Krebs HA. Activity and intracellular distribution of enzymes of ketone body metabolism in rat liver. *Biochem J.* **108**, 353-361. 1968.
- Williamson DH. The production and utilization of ketone bodies in the neonate. In *The biochemical development of the fetus*. Jones CT (Ed). Elsevier. Amsterdam. 621-650. 1982.
- Williamson DH. Ketone body metabolism during development. *Fed Proceedings.* **44**(7), 2342-2346. 1985.
- Williamson DH. Ketone body production and metabolism in the fetus and newborn. In *Fetal and neonatal physiology*. Polin RA and Fox WW (Eds). Philadelphia WB Saunders Co. 330-340. 1992.
- Witters LA, Watts TD, Daniels DL and Evans JL. Insulin stimulates the dephosphorylation and activation of acetyl-CoA carboxylase. *Proc Natl Acad Sci.* **85**, 5473-5477. 1988.
- Woeltje KF, Kuwajima M, Foster DW and McGarry JD. Characterisation of the mitochondrial carnitine palmitoyltransferase enzyme system II Use of detergents and antibodies. *J Biol Chem.* **262**, 9822-9827. 1987.
- Woeltje KF, Esser V, Weis BC, Cox WF, Schroeder JG, Liao S-T, Foster DW and McGarry JD. Inter-tissue and inter-species characteristics of the mitochondrial carnitine palmitoyltransferase enzyme system. *J Biol Chem.* **265**, 10714-10719. 1990.
- Wolfe RR, Herndon DN, Jahoor F, Miyoshi H and Wolfe M. Effect of severe burn injury on substrate cycling by glucose and fatty acids. *N Eng J Med.* **317**, 403-408. 1987.
- Wolfe RR, Herndon DN, Peters EJ *et al.*, Regulation of lipolysis in severely burned children. *Ann of Surgery.* **206**, 214-221. 1987.
- Wolfe RR. Assessment of substrate cycling in humans using tracer methodology. In *Energy metabolism: tissue determinants and cellular correlates*. Kinney JM (Ed). New York. Raven Press. 495-524. 1991.
- Wolfe RR. Substrate utilization/insulin resistance in sepsis/trauma. *B Clin End Metab.* **11**, 645-657. 1998.

- Yamazaki N, Shinohara Y, Shima A and Terada H. High expression of a novel carnitine palmitoyltransferase I like protein in rat brown adipose tissue and heart: isolation and characterization of its cDNA clone. *FEBS Letts.* **363**, 41-45. 1995.
- Yeh Y-Y and Sheehan PM. Preferential utilization of ketone bodies in the brain and lung of newborn rats. *Fed Proceedings.* **44(4)**, 2352-2357. 1985.
- Yeung C-Y, Lee H-C, Huang F-Y and Wang C-S. Sepsis during TPN: exploration of risk factors and determination of the effectiveness of peripherally inserted central venous catheters. *Pediatr Infect Dis J.* **17**, 135-142. 1998.
- Young RSK, Woods C and Towfighi J. Hepatic damage in neonatal rat due to *E Coli* endotoxin. *Dig Dis and Sciences.* **31(6)**, 651-656. 1986.
- Yu GS, Lu Y-C and Gulick T. Expression of novel isoforms of Carnitine palmitoyltransferase I (CPTI) generated by alternative splicing of the CPTI β gene. *Biochem J.* **334**, 225-231. 1998.
- Zammit VA. Regulation of hepatic fatty acid metabolism. The activities of mitochondrial and microsomal acyl-CoA:sn-glycerol 3-phosphate O-acyltransferase and the concentrations of malonyl-CoA, non-esterified and esterified carnitine, glycerol 3-phosphate, ketone bodies and long-chain acyl-CoA esters in livers of fed or starved pregnant, lactating and weaned rats. *Biochem J.* **198**, 75-83. 1981.
- Zammit VA and Boon MR. Use of a selectively permeabilized isolated rat hepatocyte preparation to study changes in the properties of CPT I. *Biochem J.* **249**, 645-652. 1988.
- Zammit VA, Corstophine CG, Kolodziej M and Fraser F. Lipid molecular order in liver mitochondrial outer membranes, and sensitivity of carnitine palmitoyltransferase I to malonyl-CoA. *Lipids.* **33**, 371-376. 1998.
- Zammit VA, Fraser F and Corstophine CG. Regulation of mitochondrial outer-membrane carnitine palmitoyltransferase (CPT I): Role of membrane-topology. *Adv Enzyme Regul.* **37**, 295-317
- Zammit VA. Carnitine acyltransferases: functional significance of subcellular distribution and membrane topology. *Prog Lipid Res.* **38**, 199-224. 1999.
- Zammit VA. Mechanisms of regulation of the partition of fatty-acids between oxidation and esterification in the liver. *Prog Lipid Res.* **23**, 39-67. 1984.
- Zammit VA. Regulation of ketone body metabolism – a cellular perspective. *Diabetes Rev.* **2**, 132-155. 1994.
- Zammit VA. Role of insulin in hepatic fatty acid partitioning: emerging concepts. *Biochem J.* **314**, 1-14. 1996.
- Zammit VA. Time-dependence of inhibition of carnitine palmitoyltransferase-I by malonyl-CoA in mitochondria isolated from livers of fed or starved rats - evidence for transition of the enzyme between states of low and high-affinity for malonyl-CoA. *Biochem J.* **218**, 379-86. 1984.

Zamparelli M, Eaton S, Quant PA, McEwan A, Spitz L and Pierro A. Analgesic doses of fentanyl impair oxidative metabolism of neonatal hepatocytes. *J Ped Surg.* **34.** 260-263. 1999.

Zensor TV, DeRubertis FR, George DT and Rayfield EJ. Infection-induced hyperglucagonemia and altered hepatic response to glucagon in the rat. *Am J Physiol.* **227,** 1299-1305. 1974.